Function of Fra1 in mesenchymal stromal cell differentiation & the potential immune modulatory role of Fra1

Dissertation

zur Erlangung des akademischen Grades doctor rerum naturalium

(Dr. rer. nat.)

im Fach Biologie

Eingereicht an der

Mathematisch-Naturwissenschaftlichen Fakultät I

Humboldt-Universität zu Berlin

Von Diplom – Biologe

Frank Drießler

geboren am 18.11.1975 in Bad Langensalza

Präsident der Humboldt-Universität zu Berlin:

Prof. Dr. Christoph Markschies

Dekan der Mathematisch-Naturwissenschaftlichen Fakultät I:

Prof. Dr. Christian Limberg

Gutachter: 1.   Prof. Saumweber

2.   Prof. Lauster

3.   Prof. Manz

Eingereicht am: 09.04.2008

Tag der mündlichen Prüfung: 15.07.2008

Für mich.

Summary

AP-1 transcription factor is a general name for multiple dimers formed by the association of Fos (or ATF) and Jun proteins. AP-1 acts as a sensor of changes in the cellular environment and thus, it is implicated in the modulation of cell proliferation, differentiation, transformation and cell death. Besides the well-documented role of c-Fos protein in oncogenesis, where this gene can function as a tumor promoter, AP-1 proteins are being recognized as regulators for mesenchymal stromal cell development and as regulators of immune cells. The mesenchymal stromal cells are the common progenitors for various mesenchymal lineages such as adipocytes, osteoblasts, chondrocytes, myocytes and fibroblasts. AP-1 seems to play a key role in the control of mesenchymal cell fate decision and differentiation. This is suggested by phenotypes of mice with a genetic modifications in either the Jun or the Fos component of AP-1. In particular, mice overexpressing the Fos-related antigen-1 (Fra1) or the short isoform of FosB (delta[Δ]FosB) have been found to develop osteosclerosis due to an accelerated differentiation of osteoblasts. Interestingly, mice overexpressing ΔFosB also developed less fat tissue. The activity of Fos proteins can be regulated by post-transcriptional modification. Based on knockout mouse model, a role for the growth factor regulated kinase Rsk2 was proposed in the differentiation of mesenchymal stromal cells to osteoblasts as well as in fat tissue development. Goal in this study was to identify the molecular mechanisms explaining the differences between the *wild type*, *fra1*-tg, *rsk2*-deficient and *fra1*-tg/*rsk2*-deficient phenotypes.

The comparison of the bones of the different mice genotypes revealed, that Fra1 and Rsk2 were independently regulating bone metabolism. Quantitative analysis of adipocyte markers expressions, like PPARγ and C/EBPα, revealed, that Fra1 overexpression was blocking adipocyte maturation *in vivo and in vitro*. Moreover, the *in vivo* results show that the *fra1*-tg/*rsk2$^{-/y}$* mice develop a severe lipodystrophy. A milder phenotype was observed in the parental *fra1*-tg strain but not in the *Rsk2* knockout strain. Additionally, it was been observed, that mesenchymal cells overexpressing Fra1 were resistant to glucocorticoid-induced growth inhibition. This effect can most likely be explained by Fra1-mediated downregulation of the glucocorticoid receptor. Furthermore, Fra1 overexpression influenced spleen development. Liver and heart analyses showed that Fra1 overexpression induced collagen tissue. Diseases like cholangitis and fibrosis were the outcome.

_____

Zusammenfassung

Aktivator Protein-1 (AP-1) ist ein kollektiver Terminus für dimerische Transkriptionsfaktoren, die sich aus Fos- und Jun- Proteinen zusammensetzen. Diese Untereinheiten binden an eine gemeinsame, spezifische DNA-Sequenz, die AP-1 Bindungsstelle. Zusätzlich zu der gut dokumentierten Rolle des c-Fos Proteins in der Tumorgenese, wo dieses Gen als ein Aktivator beschrieben ist, übt AP-1 einen Einfluss auf mesenchymale Stromazellen und Immunzellen aus. Mesenchymale Knochenmarkszellen sind die Vorläuferzellen für Adipozyten, Osteoblasten, Chondrozyten, Myozyten und Fibroblasten. Die molekularen Mechanismen, welche die Differenzierungen regeln, sind noch weitgehend unerforscht. Der heterodimere Transkriptionsfaktor AP-1 übt eine wichtige Rolle in der Kontrolle der Zelldifferenzierung aus. Verschieden genetisch veränderte Mausmodelle untermauerten dies. Mäuse, welche das Fos-related antigen-1 (Fra1) oder eine kürzere Protein-Isoform von FosB (delta[Δ]FosB) überexpremieren, entwickelten, durch eine beschleunigte Differenzierung der Osteoblasten, eine Osteosklerose. Interessanterweise konnte gezeigt werden, dass die transgenen ΔFosB Mäuse weniger Fett haben. Die Stabilität und Aktivität von Fos Proteinen kann durch post-transkriptionale Modifizierungen geregelt werden. Basierend auf knockout Mausmodellen, wurde eine tragende Rolle für das wachstumsregulierende Enzym Rsk2 postuliert. Rsk2 spielt eine mögliche Rolle bei der Ausdifferenzierung von mesenchymalen Vorläuferzellen zu Osteoblasten und Adipozyten. Das Ziel dieser Arbeit war es molekulare Mechanismen zu finden, welche die unterschiedlichen Phänotypen (_wild typ_, _fra1_-tg, _rsk2_-defizient und _fra1_-tg/_rsk2_-defizient) charakterisieren.

Die Knochenuntersuchungen der verschiedenen Genotypen zeigten, dass Fra1 und Rsk2, unabhängig voneinander, tragende Rollen im Knochenmetabolismus spielen. Quantitative Analysen von Adipozytenmarker, wie PPARγ und C/EBPα, zeigten, dass das Protein Fra1 die Adipozytenreifung _in vivo_ und _in vitro_ reguliert. Zusätzlich entwickelten die „doppel-mutierten" _fra1_-tg/_rsk2$^{-/y}$_ Mäuse einen Lipodystrophy. Ein milderer Phänotyp wurde in den _fra1_-tg Tieren beobachtet, jedoch nicht in den Rsk2-knockout Mäusen. Zusätzlich wurde beobachtet, dass mesenchymale Zellen, welche Fra1 überexpremieren, gegen Glucocorticoid-induzierte Wachstumshemmung resistent waren. Diese Wirkung kann am wahrscheinlichsten durch die Fra1-vermittelte Suppression des Glucocorticoidrezeptors erklärt werden. Außerdem beeinflusste die Überexpression von Fra1 die Milzentwicklung. Leber und Herzanalysen zeigten, dass Fra1 collagenhaltiges Gewebe induziert. Krankheiten wie Cholangitis und Fibrosen waren die Folge.

8

Table of Contents

14

Abbreviation

Ab	Antibody
Ag	Antigen
ag. bidest´	aqua bidest´
AIDS	Acquired immunodeficiency syndrome
AP-1	Activator protein-1
APC	Antigen-presenting cell
APS	Ammoniumperoxydisufat
ATF	Activating transcription factor
ATP	Adenosine triphosphate
BAT	Brown adipose tissue
BCA	Bicinchoninic acid
BMP	Bone morphogenetic protein
bp	Base pair
BSA	Bovine serum albumin
C region	constant region of Ig
cAMP	cyclic AMP
CBP	CREB-binding protein
CD	cluster of differentiation/ determination
$CD4^+$ T cell	cytotoxic T cells
$CD8^+$ T cell	cytotoxic T cells
cDNA	complementary DNA
C/EBP	CCAAT/enhancer binding protein
CF	Cystic Fibrosis
CNS	Central nervous system
CoA	Coenzyme A
cpm	Counts per minute
CREB	cAMP response element binding protein
cRNA	complementary RNA
CSF	Colony-stimulating factor
d	deoxy; distilled (as in dH_2O)
DMSO	Dimethylsulfoxide
DNA	Deoxyribonucleic acid
DNase	Deoxyribonuclease
DNP	Dinitrophenyl
dNTP	2´-Deoxynucleoside 5´-triphosphate
ds	double-stranded
DTT	1,4- Dithiothreitol
EBV	Epstein-Barr virus
ECL	Enhanced Chemiluminescence

EDTA	Ethylenediaminetetraacetic acid
EGTA	Ethyleneglycol-bis(b-aminoethylester)-N,N,N´,N´-tetraacetic acid
ELISA	Enzyme-linked immunosorbent assay
EMSA	Electrophoetic mobility shift assay
FCS	Fetal calf serum
Fos	Immediate early response gene, TF, SRF-induced
Fra1, Fra2	Fos-related anigen -1, -2, TF
G-CSF	Granulocyte CSF
GM-CSF	Granulocyte-macrophage CSF
GLUT	Glucose transporter, seven membrane proteins
h	Hour
HEPES	N-2-hydroxyethylpiperazine-N´-2-ethanesulfonic acid
HIV	Human immunodeficiency virus
IBMX	Isobutyl methylxanthine
ICAM	Intercellular adhesion molecule
Ig	Immunoglobulin
IKK	Inhibitor of nuclear factor kappa B kinase
IL	Interleukin
INF-γ	Interferon γ
IP	Immunoprecipitation/kinase assay
IκB	Inhibitory NF-κB
kb	Kilobase
kDa	kilo-Dalton
LPS	Lipopolysaccharide
mAb	monoclonal antibody
MAP	Mitogen-acivated protein
MAPK	Mitogen-activated protein kinase; syn. ERK, JNK/SAPK, CSBP, Mxi2, p38RK/HOG1 ident. to p38/SAPK2
MAPKAPK2	Mitogen-activated protein kinase 2
MAPKK	MAPK kinase, syn.: MKK1-6, MEK, SEK1-2
MAPKKK	MAPKK kinase, syn.: raf, mos, tpl-2, MEKK1,2
MCS	Mesenchymal stromal/ stem cell
MEM	Minimal essential medium
MHC	Major histocompatibility complex
min	Minute
MIP	Macrophage inflammatory protein
ml	Milliliter
mRNA	messenger RNA
µg	Microgram
µl	Microliter
n	Number in study or group
NF-AT	Nuclear factor of activated T cells

NF-κB	Nuclear factor kappa B
NK	Natural killer cell
NO	Nitric oxide
NOD	Nonobese diabetic
NP-40	Nonidet P-40
OCT	Octamer-binding factor
P	Phosphorylation
PAGE	Polyacrylamide gel electrophoresis
PBMC	Peripheral blood mononuclear cell
PBS	Phosphate-buffered saline
r	recombinant
RANTES	regulated upon activation, normal T cell expressed and secreted
RNA	Ribonucleic acid
RNase	Ribonuclease
rpm	Revolutions per minute
RPMI 1640	synthetic cell culture medium
rRNA	ribosomal RNA
RT	Roomtemperature (20 - 24 °C)
SCID	Severe combined immunodeficiency
SD	Standard deviation
SDS	Sodium dodecyl sulfate
SE	Standard error
STAT	Signal transducer and activator of transcription
TBS	Tris-buffered saline
TBST	TBS with Tween 20
T_H	T helper cell
TNF	Tumor necrosis factor
Tris	Tris(hydroxylmethyl)aminomethane
tRNA	transfer RNA
U	Unit
UV	Ultraviolet
WAT	White adipose tissue
WB	Western blot analysis

1. Introduction

1.1 Activator protein 1 (AP-1)

In order to survive, all organisms must be able to respond rapidly and effectively to changes in their environment. These changes might include externally applied stresses [e.g. radiation, ultraviolet (UV) light, shear stress], the presence of infectious agents (e.g. viruses, bacteria, parasites and their cellular by-products) or increased concentrations of signalling molecules (e.g. hormones, cytokines or growth factors). Most types of signalling molecules induce cellular responses by binding to specific cell-surface receptors that respond to occupancy by undergoing structural or biochemical changes that can be transmitted to the interior of the cell. One of the most common responses to receptor ligation is the synthesis of new proteins through alteration of the pattern of gene expression. Consequently, the relatively few transcription factors that regulate inducible gene expression can be the targets for many distinct signal transduction pathways triggered by a wide variety of stimuli.

One important and widely used transcription factor that plays a pivotal role in many cellular responses to environmental changes is activator protein-1 (AP-1). Although AP-1 was initially discovered and characterized as a transcription factor encoded by viruses causing tumours, subsequent studies demonstrated that it is ubiquitously expressed and serves as a critical regulator of the inducible expression of many genes.

1.1.1. AP-1 transcription factor family

Transcription factor AP-1 is a dimer composed by DNA-binding proteins. The main AP-1 proteins in mammalian cells are the Fos family members and the Jun family members. All AP-1 proteins are characterised by a basic leucine zipper region (bZIP). They dimerize through the leucine zipper motif and contain a basic domain for interaction with the DNA backbone [1, 2]. AP-1 were originally known as a 12-O-tetradecanoylphorbyl-13-acetate (TPA) inducible transcription factor, since the TPA response element (TRE: TGACTCA) was identified as a binding site for AP-1 in many cellular and viral genes [3]. This element was identified in the promoters and enhancers of the metallothionein I gene and Simian Virus 40 (SV40). AP-1 recognition sequences were found in many other promoters and enhancers of cellular and viral genes, including collagenase, stromelysin, metallothionein-2a (MT-2a), interleukin-2 (IL-2), transforming growth factor β (TGFβ), polyomavirus and papillomavirus.
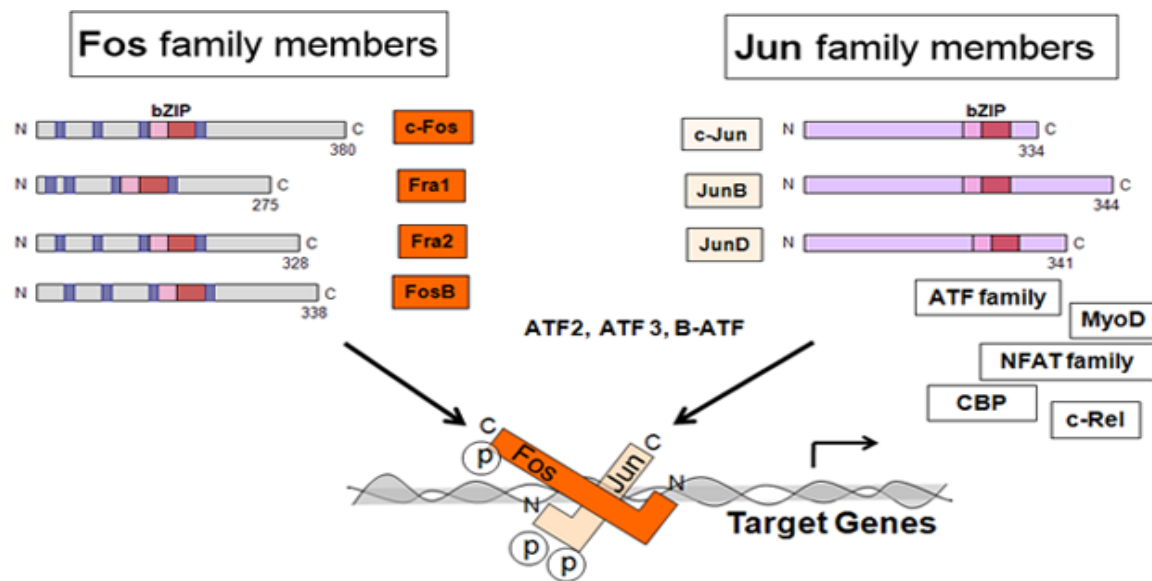
Figure1.1.AP-family

Fos proteins do not form homodimers but can heterodimerize with members of the Jun family, the Jun proteins can both homodimerize and heterodimerize ass well with other transcription factors (e.g. ATF or MyoD).

While the Fos proteins (c-Fos, FosB, Fra1, and Fra2) do not form homodimers but can heterodimerize with members of the Jun family, the Jun proteins (c-Jun, JunB, and JunD) can both homodimerize and heterodimerize with other Jun or Fos members to form transcriptionally active complexes [4]. In addition to Fos proteins, Jun proteins can also heterodimerize efficiently with other transcription factors, such as members of the activator transcription factor family (ATF) and other basic zipper containing transcription factors such as calcium binding protein (CBP), myoblast differentiation factor (MyoD), nuclear factor of activated T-cells (NFAT) or c-Rel [5, 6] (possible interactions are summarized in Figure 1.1). Fos–Jun heterodimers are more stable than Jun homodimers, and are believed to be the prevalent, and biologically most relevant, forms of Jun in vivo [7, 8, and 9]. Whereas four Fos-like genes have been identified in mammals, Drosophila seems to possess only one Fos homologue, D-Fos (also referred to as D-Fra) [4, 10]. Drosophila Jun and Fos have been characterized biochemically, and have been shown to act similarly to their mammalian counterparts [11, 12, 13, and 14].

AP-1 mediates cell response to growth factors, cytokines, neurotransmitters and other intercellular signalling molecules. G-proteins, adapter proteins, MAP kinases and other elements of cellular signalling systems mediate AP-1 activity (Figure 1.2). AP-1 dependent genes play a pivotal role in regulation of cell proliferation, morphogenesis, apoptosis, and differentiation.
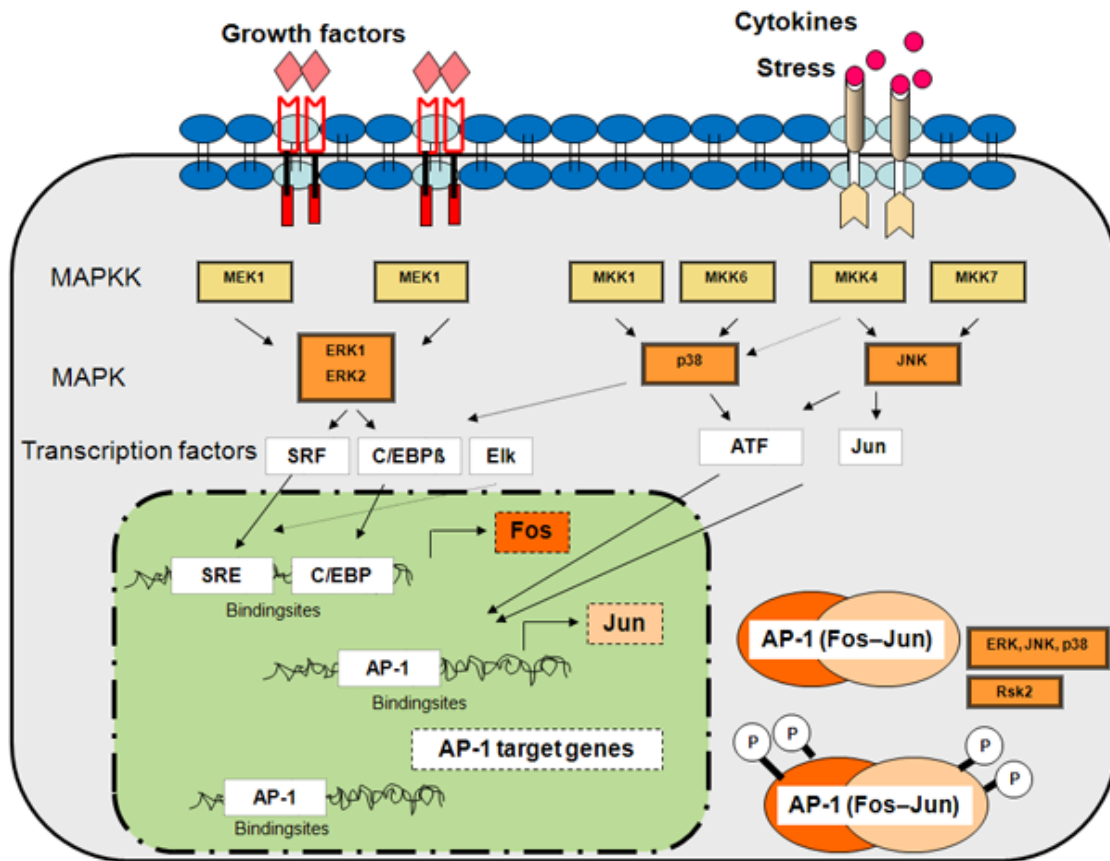
Figure1.2.NetworkofAP-1field

Overview of signal transduction pathways affecting AP-1 activity. AP-1 cell signalling pathways leading to apoptosis, survival and proliferation. ERK1/2, p38 and JNK have been shown to activate transcription factor like SRF, C/EBPß or Elk and AP-1 by itself, which control the transcription of the Fos and Jun members. AP-1 dimers are phosphorylated and stabilised by kinase, e.g. ERK, JNK, p38 and Rsk2 (Refer to text for explanation).

Transcription from both the Fos and Jun promoters is rapidly and transiently induced in cells that are treated with serum or peptidic growth factors via oncogene-mediated signal transduction networks [15]. Growth factor-induced signal transduction cascades also regulate the activity of pre-existing AP-1 dimers. Both Fos and Jun are phosphorylated and activated by the MAPK, RSK and JNK kinase system [16, 17, 18, and 19] (Figure 1.2). This ubiquitous response to extra cellular signals highlights a role for AP-1 in converting transient biochemical signals into permanent changes in gene expression that effect a cellular response to external stimuli. Numerous in vitro studies have suggested that the different AP-1 dimers may act as tissue-specific and signal-specific transcriptional activators. Indeed, each individual targeted deletion of an AP-1 gene reported so far leads to specific phenotype, especially the c-Fos family, indicating that the different AP-1 subunits, although highly homologous, are not fully redundant in vivo.

1.1.2. Characteristics of Fos family members and related mice models

The cytogenetic locations of three of the human Fos genes are known: c-Fos maps to 14q24.3 (5), FosB to 19q13.3 (11), and Fra1 to 11q13 (17) and Fra2 to 2p22–p23 [20].

1.1.2.1. Structure and function of c-Fos

An important step in defining the AP-1 transcription factor came with the discovery that the viral oncoprotein v-Fos binds to the same DNA sequence as c-Jun [21]. c-Fos was originally identified in the FBJ (Finkel, Biskis, Jinkins) and FBR (Finkel, Biskis, Reilly) murine sarcoma viruses [22]. c-Fos is an immediate-early proto-oncogene with rapid and transient transcriptional activation following mitogenic stimuli and is involved in numerous cellular processes such as proliferation, differentiation, transformation, and apoptosis [23].

The 4 kb mammalian c-Fos gene has four exons and transcribes a 2.2 kb mRNA. The protein is composed of 381 amino acids and contains a more recently discovered ERK-docking site or DEF domain in the C-terminus [18] (Figure 1.3) . The c-Fos mRNA and protein are very unstable. Stabilisation and regulation by kinases like Rsk2 playing an important biological role in some diseases, e.g. osteosarcoma. David and colleagues (2005) could show that in the absence of Rsk2, c-Fos-dependent osteosarcoma formation is impaired [19]. The lack of c-Fos phosphorylation leads to reduced c-Fos protein levels, which are thought to be responsible for decreased proliferation and increased apoptosis of transformed osteoblasts. Therefore, Rsk2-dependent stabilization of c-Fos was essential for osteosarcoma formation. In addition, the protein is degraded by ubiquitination, but also by ubiquitin-independent mechanisms through two distinct regions in the C- and N-terminus, called destabilizers [24, 25, and 26].
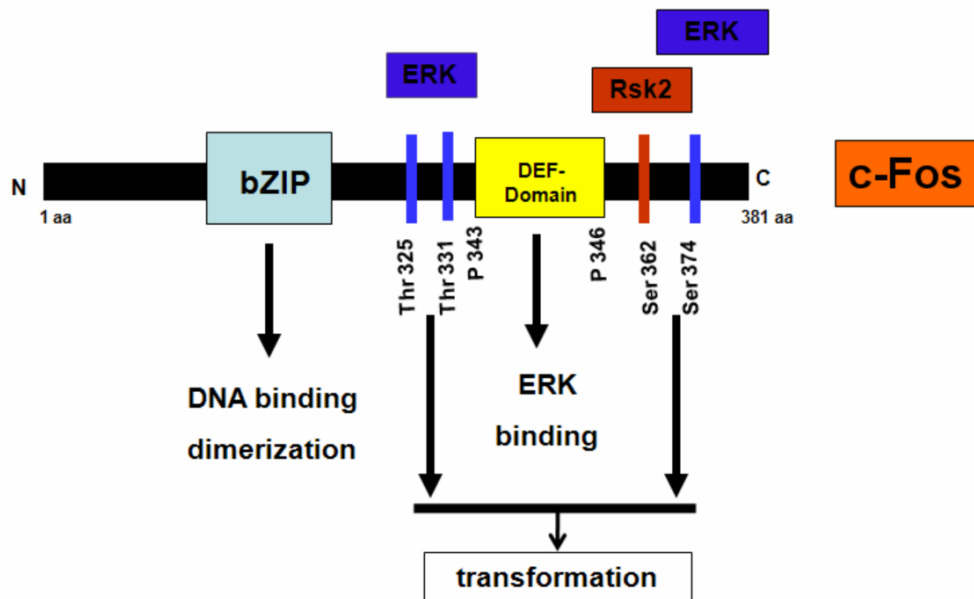
Figure1.3 Phosphorylation sites for the stabilisation and regulation of c-Fos protein

The c-Fos protein is composed of 381 amino acids and contains an ERK-docking site, Rsk2-docking site, and the DEF domain, in the C-terminus. c-Fos is phosphorylated at Ser (serine) 374, Thr (threonine) 325 and Thr 332 by ERK1/2 and at Ser 362 by its downstream kinase, Rsk2, and that phosphorylation of c-Fos by these kinases bring about its stabilization.

The c-Fos protein is expressed at low or undetectable levels in most cell types, but is rapidly and transiently induced in response to various stimuli, such as growth factors, and environmental and physical stress. Furthermore, c-Fos is associated with a variety of biological processes, from cell-cycle progression and cell differentiation to cell transformation and tumorigenesis [27].

The c-Fos-deficient mice are viable, fertile but develop osteopetrosis and are lacking teeth due to a block in osteoclast differentiation [28, 29]. High levels of c-Fos can be found in developing bone, the central nervous system, and in some haematopoietic cells, such as megakaryocytes [30, 31, 32, and 33]. Tumorigenic properties of c-Fos have been demonstrated by overexpression, which causes osteosarcoma by transforming chondroblasts and osteoblasts [34].

1.1.2.2. Structure and Function of Fra1

Fos-related antigen-1 or Fra1 is an immediate-early gene and a constituent of the AP-1 complex discovered by Cohen and Curran in 1988. Fra1 appear as a candidate for

central regulatory functions that will in turn modulate the expression of other genes. The protein lacks the C-terminal transactivation domain and has therefore been proposed to be a negative regulator of AP-1 activity (Figure 1.4). However, the Ras-induced stabilisation and activation of Fra1 is well understood but nothing is known about Rsk2-dependend regulation of this AP-1 member. Therefore, Fra1 can either increase or decrease total AP-1 activity depending on the status of the other Fos and Jun proteins in the cell and on its phosphorylation, and has been proposed to function as a negative-feedback regulator of AP-1 [35, 36, 37, 38, 39, 40, and 41].

Overexpression of Fra1 has a growth inhibitory effect and induces apoptosis in glioma cells [42]. The oncogenic potential of Fra1 is significantly weaker than that of c-Fos. Nevertheless, overexpression of Fra1 in established rat fibroblasts leads to anchorage-independent growth and tumour development in nude mice [44]. Furthermore, neoplastic transformation of rat thyroid cells requires induction of Fra1 and JunB [43]. Fra1 expression is subject to positive control by AP-1 in several cell types [34, 37, 44, and 45]. Fra1 is involved in Ras-induced transformation of NIH 3T3 cells, and it stimulates transformation, and increases invasiveness and motility of epithelioid adenocarcinoma cells, reflecting cases where Fra1 does not act as a negative regulator of AP-1 [46, 47].
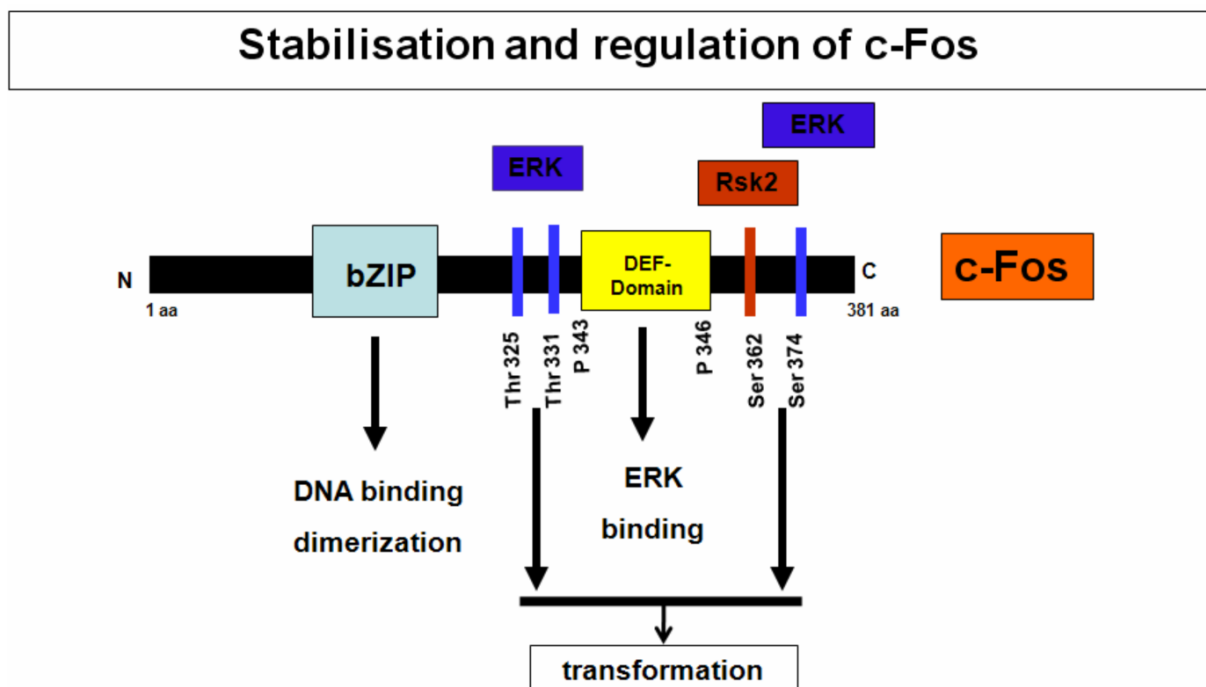
Figure 1.4 Phosphorylation sites for the stabilisation and regulation of Fra1 protein

The Fra1 protein is composed of 274 amino acids and contains an ERK-docking site, the DEF domain, but no transactivation domain. Following ERK1/2 phosphorylation (at Ser 209 and Ser269, Thr 231 and Thr 244) Fra1 is stabilized in cells and interacts with AP-1 family partners.

The mouse Fra1 gene, which consists of four exons and three introns at positions also found in the other members of the Fos gene family. Fra1 is expressed rather highly in the brain and testes of adult mice, and at low levels in most other tissues. Absence of c-Fos leads to significantly reduced serum stimulation of fra1 expression in gene targeted mouse fibroblasts, demonstrating that mitogen induction of Fra1 is partially mediated by c-Fos/ AP-1. As Fra1 expression appears to be at least in part controlled by c-Fos, it is conceivable that Fra1 might contribute to the phenotypic effects of overexpression or deletion of c-Fos. Overexpression of Fra1 can substitute for c-Fos, in overcoming the differentiation block of osteoclasts lacking c-Fos in in vitro co-culture assays [48]. Fra1-deficient mice die at E 9.5 due to defects in the placenta and yolk sac. Mutated placentas display morphologic alterations, have reduced size and lack of vascularization. The embryonic lethality can be overcome by crossing conditional Fra1 knockout mice with the MORE-cre mouse. MORE-cre mice express Cre ubiquitously except in extraembryonal tissues [49]. These mice are viable and fertile and develop osteopenia due to decreased osteoblast differentiation [50]. Ectopic Fra1 expression can also rescue the embryonic lethality of Fra1 knockout mice [51]. Similar to ΔFosB, overexpression of Fra1 from a ubiquitous promoter result in osteosclerosis due to accelerated osteoblast differentiation with splenomegaly as secondary effect [52]. Therefore, Fra1 plays an important role in skeletogenesis and is proposed to influence mesenchymal stromal cell and myeloid linage differentiation.

1.1.2.3. Structure and Function of Fra2

The Fos-related AP-1 transcription factor Fra2 (encoded by Fosl2) was originally identified as a chicken gene whose product was recognized by a c-Fos antiserum [53]. cDNA sequences, covering the protein coding parts only, have been reported for the human and rat Fra2 genes [54]. For the chicken and mouse homologs, the genomic structure has been determined, showing that the overall organization (four exons and three introns) is conserved between c-Fos and Fra2 [53]. However, both the Fra2 introns and the untranslated parts of the mRNA are considerably larger than those of other Fos family members. Fra2 is expressed at high levels in ovary, stomach, intestine, brain, lung and heart and in differentiating epithelia, the central nervous system and developing cartilage [64, 65, and 66]. Overexpression of Fra2 induces tumour formation in pancreas, thymus and lung. Transgenic overexpression from the CMV promoter results in ocular malformations [67]. The absence of Fra2 in embryos and newborns leads to reduced zones of hypertrophic chondrocytes and impaired matrix deposition in femoral and tibial

growth plates, probably owing to impaired differentiation into hypertrophic chondrocytes. In addition, hypertrophic differentiation and ossification of primordial arches of the developing vertebrae are delayed in Fra2-deficient embryos. Primary Fosl2–/– chondrocytes exhibit decreased hypertrophic differentiation and remain in a proliferative state longer than wild-type cells. Pups lacking Fra2 die shortly after birth. The coll2a1-Cre, Fosl2f/f mice die between 10 and 25 days after birth, are growth retarded and display smaller growth plates similar to Fosl2–/– embryos. In addition, these mice suffer from a kyphosis-like phenotype, an abnormal bending of the spine. Hence, Fra2 is a transcription factor important for skeletogenesis by affecting chondrocyte differentiation [68].

1.1.2.4. Structure and Function FosB and delta(Δ)-FosB

Zerial and colleagues identified FosB, encoding a nuclear protein of 338 amino acids presenting a 70 % homology with c-Fos, whose expression is activated during G0 / G1 transition, in 1989. Growth factor stimulation of quiescent cells leads to a rapid and transient accumulation of FosB mRNA, with kinetics similar to those of c-Fos. The induction of FosB mRNA levels is in part due to a dramatic increase in the transcription of the gene. The half-life of FosB mRNA is in the order of 10 - 15 min. Both transcriptional activation and mRNA stability are substantially increased in the presence of protein synthesis inhibitors. FosB forms a complex with c-Jun and JunB in vitro [59]. The expression of FosB has been localized to neuronal tissue and bone during embryonic development, although no known essential function during embryonic development has been identified [60]. FosB-deficient mice develop normally but have a nurturing defect [61].

ΔFosB, first identified in cultured cells, is a truncated product of the fosB gene, which lacks the C-terminal 101 amino acids of the full-length FosB protein [61, 62, 63, and 64]. ΔFosB triggers one round of proliferation in quiescent rat embryo cell lines, followed by a different cell fate such as morphological alteration or delayed cell death. Interestingly, transgenic mice over-expressing ΔFosB, under the control of the neuron-specific enolase (NSE) promoter show markedly increased bone formation and decreased adipogenesis but OG2-ΔFosB mice [ΔFosB is under the control of the osteocalcin (OG2) promoter] demonstrated increased osteoblast numbers and an osteosclerotic phenotype but normal adipocyte differentiation. This result firmly establishes that the skeletal phenotype in OG2-ΔFosB mice is cell autonomous to the osteoblast lineage and independent of adipocyte formation. Although the increased bone formation in the NSE-ΔFosB mice was

shown to be due, at least in part, to a cell autonomous effect on cells of the osteoblast lineage. The dramatic decrease in adipogenesis observed in these mice, as revealed by decreased abdominal fat, low leptin levels in serum, and reduced number of adipocytes in the bone marrow, could be independently cell autonomous to the adipocyte lineage or secondary to the alteration in osteoblast differentiation. This uncertainty is due to the fact that the NSE promoter directs ΔFosB transgene expression in several tissues in addition to the brain, including bone and white adipose tissue [65, 66].

1.2   From mesenchymal stromal cell to a tissue forming organ

Bone marrow (BM) was for many years primarily regarded as the source of haematopoietic stem cells (HSCs). Today it is known that BM contains not only haematopoietic but also heterogeneous non-haematopoietic stem cells. It is likely that similar or overlapping populations of primitive non-haematopoietic stem cells in BM were detected by different investigators using different experimental strategies and hence were assigned different names (e.g. mesenchymal stromal cells, multipotent adult progenitor cells, or marrow-isolated adult multilineage inducible cells). Mesenchymal stromal cells (MSCs) — a mixed cell population that generates bone, cartilage, fat, fibrous connective tissue, and the reticular network that supports blood cell formation— were described shortly after the discovery of HSCs [67, 68, and 69]. The biology and properties of mesenchymal stromal cells has expanded dramatically over the last years. The notion that tissue repair with mesenchymal stromal cells is related to transdifferentiation has been re-evaluated. Mesenchymal stromal cells are a biologically important cell population that are able to support haematopoiesis, can differentiate along mesenchymal and non-mesenchymal lineages in vitro, are capable of suppressing alloresponses and appear to be non-immunogenic. These properties underline the potential roles for mesenchymal stromal cells in cell therapy.

1.2.1. Historical background of MSCs

Ernest A. McCulloch and James E. Till first revealed the clonal nature of marrow cells in the 1960s [70, 71]. An ex vivo assay for examining the clonogenic potential of multipotent marrow cells was later reported in the 1970s by Friedenstein and colleagues [72, 73]. In this assay system, stromal cells were referred to as colony-forming unit-fibroblasts (CFU-f). Subsequent experimentation revealed the plasticity of marrow cells and how their fate could be determined by environmental cues. Culturing marrow stromal

cells in the presence of osteogenic stimuli such as ascorbic acid, inorganic phosphate, and Dexamethasone could promote their differentiation into osteoblasts. In contrast, the addition of TGFβ could induce chondrogenic markers. Today it is clear that MSCs are multipotent stem cells that can differentiate into a variety of cell types. Cell types that MSCs have been shown to differentiate into in vitro or in vivo include osteoblasts, chondrocytes, myocytes, adipocytes, and, as described lately, into beta-pancreatic islets cells. They can also transdifferentiate into neuronal cells [74].

1.2.2. Differentiation markers for mesenchymal stromal cells

MSCs are less well characterized and their functional role in the bone marrow is not as well understood as that of HSCs. They comprise a heterogeneous group of cells thought to be crucial to maintenance of an environment conducive to survival and maturation of HSCs. Several groups have isolated MSCs by exploiting their capacity to adhere to plastic tissue culture dishes and proliferate in response to serum [75, 76]. Unfortunately, there is currently no clear consensus on how many individual cell types constitute MSCs, how MSCs should be isolated and purified, or even which MSCs are actually stem cells capable of asymmetric division. The mesenchymal stromal progenitor cells are committed to the differentiation into different lineages by the activation of a set of transcription factors. These factors are often used as markers for the different lineages (Figure 1.5). MSCs are typically described as expressing no lineage-specific markers and they are c-kit-negative, but do moderately express Sca-1, and highly Stro-1, on their surface. Individual cells from the stromal population can differentiate into other cell types such as bone, adipose and muscle and bone [77, 78, and 79].

Mesenchymal stromal cells differentiation
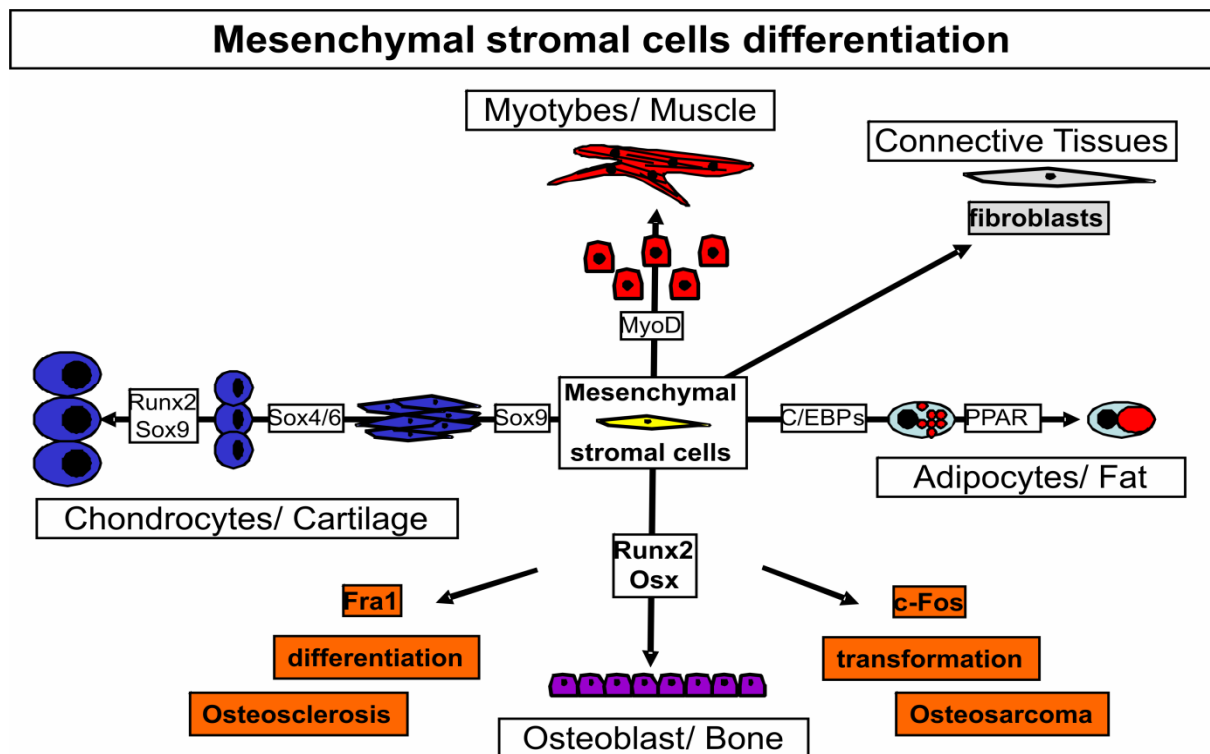
Figure 1.5 Transcriptional controls of osteoblastic, chondrocytic, adipocytic and myocytic differentiation

MSCs are a heterogeneous group of adherent cells that can be cultured from bone marrow aspirates. These cells are believed to contribute to the HSC niche in bone marrow, but can also differentiate to express markers typical of osteoblasts, chondrocytes, adipocytes and myocytes. Osteoblasts differentiate from mesenchymal progenitor cells that also give rise to myocytes, under the control of MyoD, to adipocytes under the control of C/EBPα, β, δ and PPARγ, and to chondrocytes, under the control of Sox4, -6 and -9 and STAT1. Runx2 is essential for osteoblast differentiation and is involved in chondrocyte maturation. Osterix (Osx) acts downstream of Runx2 to induce mature osteoblasts that express osteoblast markers, including osteocalcin.

1.2.2.1. Markers of osteoblast differentiation

Osteoblasts (OB) are the bone-forming cells. The osteoblasts are cell types of mesenchymal origin that are responsible for bone matrix deposition, or bone formation. They synthesize and secrete most of the proteins of the bone matrix, including type I collagen and non-collagenous proteins. They express high levels of alkaline phosphatase (AP), which participates in mineralization. Proteins, produced by osteoblasts and secreted into the blood, are used as indicators of bone formation. In addition to the matrix-forming ability, cells of the osteoblastic family (osteocytes, lining cells, and maybe other cells) participate in the regulation of bone turnover. They respond to Parathyroid hormone (PH), glucocorticoids (GC), vitamin D (VD3), sex steroids, Insulin, prostaglandins, and growth factors (GF) [79, 80, 81, and 82].

There are two stages in the development of osteoblasts. In the first step, mesenchymal progenitor become pre-osteoblasts and in the second step pre-osteoblasts become mature osteoblasts (i.e. mineralizing cells). Molecular markers of the first step are Type I Collagen, alkaline phosphatase and above all the transcriptions factor Runx2 that is absolutely require for osteoblast commitment. Osteocalcin and high expression of Osterix (Osx), a zinc finger containing transcription factor, downstream of Runx2, serves as markers for the second step of osteoblast differentiation [83, 84].

A central regulator of bone formation is the Runx2 transcription factor. It is a master regulatory switch through unique properties for mediating the temporal activation and/or repression of cell growth and phenotypic genes as osteoblasts progress through stages of differentiation. Runx2 is a transcription factor that belongs to the runt-domain gene family. Three runt-domain genes (Cbfa1/ Pebp2αA, Cbfa2/ Pebp2αB, and Cbfa3/ Pebp2αC) have been identified [85, 86, and 87]. They have a DNA binding domain, runt, which is homologous with the Drosophila pair-rule gene runt, and form heterodimers with co-transcription factor Cbfb/Pebp2β and acquire enhanced DNA-binding capacity in vitro [88, 89, and 90]. In recent studies, Cbfa-related factors were shown to interact with the promoter region of the Osteocalcin gene [91, 92, and 93]. Genetic inhibition of the Runx2/ Cbfa1 gene causes developmental defects in osteogenesis and hereditary mutations in this gene are linked to specific ossification defects as observed in cleidocranial dysplasia. Runx2-deficient mice showed multiple defects in bone formation, by affecting the three major cellular components of the bone: osteoblasts, chondrocytes, and osteoclasts. The mutanted mice completely lacked both endochondral and intramembranous ossification, and mature osteoblasts were absent throughout the body. Runx2 functions as a "platform protein" that interacts with a spectrum of co-regulatory proteins to provide a combinatorial mechanism for integrating cell signalling pathways required for osteoblast differentiation and the tissue-specific regulation of gene expression [94, 95, 96, and 97].

Osterix (Osx) is a transcription factor that was identified in a subtractive hybridization screen in extracts of C2C12 cells treated with bone morphogenetic protein-2 (BMP-2) [98]. Milona and colleagues (2003), recently isolated two cDNAs for human homologues of Osx, referred to as Sp7 alpha and beta isoforms [99, 100]. A phenotype similar to the Runx2 knockout was observed with knockout of Osx. Osx-deficient mice do not form a bony skeleton, forming only cartilage. In addition, Osx induces OB differentiation of dispersed embryonic stem cells. Runx2 is expressed in Osx knockouts, suggesting that Osx functions downstream of Runx2 in the differentiation pathway. Therefore, Osx may be involved in the segregation of osteoblast and chondrocyte

lineages where Runx2 is expressed by bi-potential precursor cells where expression of Osx would suppress chondrocyte lineage.

Besides Runx2 and Osx, transcription factors of the AP-1 complex are involved in osteoblast differentiation and transformation. Overexpression of Fra1 and ΔFosB, the truncated version of FosB, results in enhanced differentiation of osteoblasts possibly caused by altered progenitor cell differentiation and increased osteoblast activity [96, 101, 102, and 103]. In contrast, c-Fos overexpression results in osteoblast transformation and osteosarcoma development [104].

1.2.2.2. Markers of chondrocyte differentiation

Chondrocytes (from Greek chondros cartilage + kytos cell) are the only cells found in cartilage. They produce and maintain the cartilaginous matrix, which consists mainly of collagen and proteoglycans. Although chondroblast is still commonly used to describe an immature chondrocyte, use of the term is discouraged since the progenitor of chondrocytes (which are MSCs) can also differentiate into osteoblasts. Chondrocyte differentiation is a precisely regulated process that involves proliferation, hypertrophic differentiation, mineralization and apoptosis. Disruption of these events can result in various skeletal diseases and growth disorders [105]. The control of chondrocyte differentiation involves multiple extra cellular and intracellular signalling molecules [106, 107, 108, and 109]. The key transcription factor requires for the mesenchymal condensation necessary for chondrocyte commitment is Sox9. It is expressed in all chondrocyte progenitors and is required for cartilage formation [110]. Sox9, together with Sox5 and Sox6, regulates differentiation of chondrocytes Maturation of chondrocytes to hypertrophy is controlled positively by Runx2 and negatively by Sox9 [111, 112].

1.2.2.3. Markers of adipocyte differentiation

Adipocyte is the fat cell, which has differentiated and become specialized in the synthesis and storage of fat. The adipocyte is important to maintain proper energy balance, to store calories in the form of lipids, to mobilize energy sources in response to hormonal stimulation, and to command changes by signal secretions. Under the microscope, the adipocyte appears bloated with triglycerides. The nucleus of the cell is displaced to one side by the fat. The cytoplasm of the cell looks like a thin line surrounding the pool of fat. Studies of mesenchymal adipocyte precursor have shown that the expression of markers for mature adipocytes is elevated when they are cultured

in adipocyte differentiation medium composed of Insulin, Dexamethasone and IBMX [113, 114, 115, 116, 117, 118, and 119] (Figure 1.6).

Pref-1 (Preadipocyte factor-1) and PPARγ (peroxisome proliferator activated receptor gamma) are key regulators in the early stage of preadipocyte differentiation. Pref-1 is an inhibitor of adipocyte differentiation and is synthesized as a plasma membrane protein containing six epidermal growth factor (EGF)-repeats in the extracellular domain. Pref-1 is highly expressed in 3T3-L1 preadipocytes, but is not detectable in mature fat cells.

PPARγ regulate storage and catabolism of fats and carbohydrates. PPARγ is regarded as a "master regulator" of adipocyte differentiation and is abundantly expressed in adipose [120, 121, 122, 123, 124, and 125]. Furthermore, C/EBPα/ β/ δ (CCAAT-enhancer binding protein alpha, beta, and delta) are members of a family of transcription factors that are integral to adipogenesis. C/EBPα regulates terminal adipocyte differentiation, turning on the battery of fat-specific genes required for the synthesis, uptake, and storage of long chain fatty acids [126, 127, 128, 129, 130, 131, 132, and 133]. There are evidences that C/EBPδ and C/EBPβ plays early catalytic roles in the differentiation pathway, relaying the effects of the hormonal stimulant Dexamethasone in a cascade-like fashion, leading to the activation of the gene encoding C/EBPα [134, 135, 136, 137, 138 and 139]. C/EBP and other C/EBP-like proteins play a critical role in regulating the transcription of the fat-specific gene [140, 141, 142, and 143]. C/EBP binding sequences are present in genes regulated during adipocyte differentiation that can directly be regulated by C/EBPs [144].

The aP2 (adipocyte lipid-binding protein) belongs to a family of intracellular lipid-binding proteins involved in the transport and storage of lipids. The aP2 protein has important effects on Insulin and lipid metabolism. The aP2-deficient mice developed dietary obesity but, they did not develop Insulin resistance or diabetes. Rather it seems to in a way such as, that aP2 is central to the pathways that links obesity to Insulin resistance, possibly by linking fatty acid metabolism [145, 146, 147, and 148]. The blood glucose homeostasis can be controlled, in part, by a family of structurally related glucose transporter proteins (Glut) composed of at least five isoforms [149, 150]. One of these isoforms, Glut4 is of particular importance because it is a major Insuline-regulated glucose transporter. Glut4 is selectively expressed in Insuline-sensitive tissue such as adipose cells [151]. Therefore, the impairment of Glut4 expression, Glut4 translocation, and/ or Insuline signalling in adipocytes may affect basal and Insulin-stimulated glucose uptake. Both, Glut4 and aP2 are important markers for adipocytes differentiation.

Enzymes are also important in a wide variety of cellular processes, including intracellular trafficking, organization of the cytoskeleton, cell growth and transformation, and prevention of apoptosis [152, 153]. The Raf/ MEK/ extracellular signal-regulated kinase (ERK) kinase cascade is a pathway involved in the determination of cell fate [154, 155]. In mammalian cells, signaling through the Raf/ MEK/ ERK/ RSK kinase cascade has been implicated in multiple aspects of cell fate determination, including the regulation of senescence, proliferation, transformation, differentiation, and apoptosis [156]. While a positive role for ERK signaling is well established in proliferation, transformation, and oncogene-induced senescence [155, 157, 158, and 159], its role in cell differentiation programs remains controversial. In adipogenic conversion of 3T3-L1 preadipocytes, inhibition its activity reveals a positive role for ERKs [160, 161, and 162], whereas constitutive activation of the pathway suggests a negative role for ERKs [163, 164]. Phosphorylation and activation of the ERK downstream of ERK kinase Rsk2 plays an important role in Insuline and lipid metabolism. However, the role of Rsk2 in adipocyte differentiation and, more specifically, at which level in the differentiation process it might act during adipogenesis remain largely unknown.
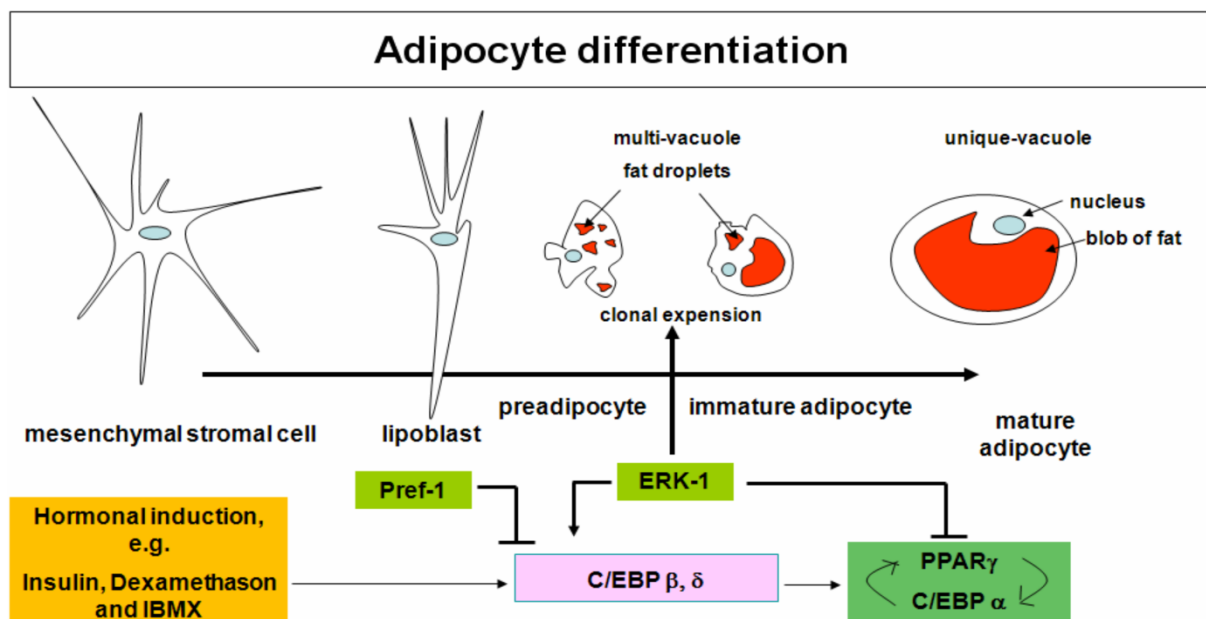
Figure1.6Adipocytedifferentiation

Preadipocyte differentiation is influenced by endocrine and autocrine factors that promote or constrain adipogenesis by intracellular mechanisms that induce the synthesis and activation of adipogenic transcription factors. Upon treatment of mesenchymal stromal cells with an adipocyte cocktail of methylisobutylxanthine, Dexamethasone, and Insulin(AD), there is a rapid induction of C/EBPβ and C/EBPδ (1 to 2 h) lasting 2 to 3 days. With the expression of C/EBPβ/δ, postconfluent, growth-arrested preadipocytes reenter the cell cycle and undergo multiple rounds of cellular division, a process termed mitotic clonal expansion (MCE). C/EBPβ/δ then induce the expression of C/EBPα and peroxisome proliferator-activated receptor gamma (PPARγ). C/EBPα and PPARγ terminate MCE and together induce the expression of genes involved in triglyceride storage and metabolism that lead to formation of a mature adipocyte.

Growth of the adipose tissue results from both the enlargement of mature adipocytes and the formation of new adipocytes from adipocyte precursor cells (mitotic clonal expansion) [138, 162]. The differentiation process of adipocyte precursor cells is controlled by a variety of hormones. Leptin is one of the main hormones, which play a role in adipocyte differentiation. Leptin is synthesized and secreted primarily by adipocytes, and is present in serum in direct proportion to the amount of adipose tissue and involved in the central control of body weight, energy homeostasis, sexual maturation and exerts its action on hypothalamus, modifying eating behavior and inhibiting the lust for food consumption [165, 166, 167, and 168].

1.2.2.4. Markers of myocyte differentiation

A muscle fiber, also known as a myocyte, is a single cell of a muscle. Muscle fibers contain many myofibrils, the contractile unit of muscles. Muscle fibers can be grouped according to what kind of tissue they are found in skeletal muscle, smooth muscle, and cardiac muscle. The formation of skeletal muscle in vertebrates involves a family of myogenic regulatory genes encoding the basic-helixloop-helix (bHLH) transcription factors Myf-5, myogenin, MyoD, and MRF-4. Each of these genes can activate myogenesis in a variety of transfected tissue culture cells in vitro, suggesting that they may play an important role in muscle cell determination and differentiation. Interestingly, all established muscle cell lines express MyoD in committed myoblasts and activate transcription of myogenin only when induced to differentiation. This interpretation of these was that MyoD might define the myoblasts stage [169, 170, and 171].

1.3   Bone or fat development – is that the question?

Bones are rigid organs that form part of the endoskeleton of vertebrates. Bones function to move, support, and protect internal organs, such as the skull protecting the brain or the ribs protecting the heart and lungs. Bone also serves as a storage site for minerals, most notably calcium and phosphorus and provides the medium - marrow - for the development and storage of blood cells. Blood production located within the medullary cavity of long bones and the interstices of cancellous bone is a process called haematopoiesis [172, 173, and 174].

Bones come in a variety of shapes and have a complex internal and external structure, allowing them to be lightweight yet strong and hard, while fulfilling their many other functions. Other types of tissue found in bones include marrow, endosteum and periosteum, nerves, blood vessels and cartilage. Bone buffers the blood against excessive pH changes by absorbing or releasing alkaline salts. Bones are important in the mechanical aspect of hearing.

The primary tissue of bone, osseous tissue, is a relatively hard and lightweight composite material, formed mostly of calcium phosphate in the chemical arrangement termed calcium hydroxylapatite (this is the osseous tissue that gives bones their rigidity). It has relatively high compressive strength but poor tensile strength, meaning it resists well to pushing forces, but not pulling forces. While bone is essentially brittle, it does have a significant degree of elasticity mainly contributed by collagen. All bones consist of living cells embedded in the mineralised organic matrix that makes up the osseous tissue [175].

1.3.1. Cellular structure of bone: osteoblast, osteocytes, osteoclast and chondrocytes

Two different tissues form most of the skeletal elements, bone and cartilage, and each of these two tissues have its own specific cell types: the osteoblasts, osteocytes and osteoclasts in bone; the chondrocytes in cartilage. Finally, each of these cell types has its own differentiation pathway, physiological functions, and therefore pathological conditions. Bone at the tissue level undergoes remodelling: it is continuously being resorbed and rebuilt (or formed).

1.3.1.1. Osteblast - the bone forming cell

Osteoblasts are responsible for bone formation. Osteoblasts are specialized mesenchymal cells that undergo a process of maturation where genes like core-binding factor alpha1 (Cbfa1/ Runx2) and osterix (Osx) play an important role. There are important pathways which are closely related to the osteoblast environment. Recently, both human genetic and animal studies have pointed to the role of the Wnt/ LRP5 pathway as a major regulator of bone mass formation. Wnts are a family of 19 secreted glycoproteins that bind to receptor complexes including low-density lipoprotein receptor-related protein (LRP)-5/ 6 as well as frizzled proteins. A subsequent intracellular cascade of events stabilizes β-catenin, leading to its translocation into the nucleus where,

associated with Tcf/ Lef transcription factors, it triggers gene expression. During the last decade, canonical Wnt signaling has been shown to play a significant role in the control of osteoblastogenesis and bone formation. In several clinical cases, mutations have been found in the Wnt receptor complexes that are associated with changes in bone mineral density and fractures. Loss-of-function mutations in LRP5 receptors cause, osteoporosis-pseudoglioma syndrome, while gain-of-function mutations lead to high bone mass phenotypes. Furthermore, osteocytes secrete proteins such as sclerostin, which blocks the membrane complex activation by Wnt, resulting in inhibition of bone formation. Studies of knockout and transgenic mouse models for Wnt pathway components have demonstrated that canonical signaling regulates most aspects of osteoblast physiology including commitment, differentiation, bone matrix formation/mineralization and apoptosis as well as coupling to osteoclastogenesis and bone resorption.

Osteoblast have also a role in regulating bone resorption through the production of receptor activator of nuclear factor-kappa (RANK) ligand (RANKL), that binds to its receptor, RANK, on the surface of pre-osteoclast cells, inducing their differentiation and fusion. On the other hand, osteoblasts secrete a soluble decoy receptor (osteoprotegerin, OPG) that blocks RANK/ RANKL interaction by binding to RANKL and, thus, prevents osteoclast differentiation and activation. Therefore, the balance between RANKL and OPG determines the formation and activity of osteoclasts [176, 177, and 178]. Another factor that influences bone mass is leptin, a hormone produced by adipocytes that have a dual effect. It can act through the central nervous system and diminish osteoblasts activity, or can have an osteogenic effect by binding directly to its receptors on the surface of osteoblast cells.

1.3.1.2. Osteocyte

Osteocyte is the most abundant cell found in bone. Many individuals view the osteocyte as being a passive, inactive cell that merely acts as a 'place holder' in bone. It has been proposed decades ago that the osteocyte is not a passive cell, but has several potential functions [179, 180, 181, and 182]. The proposed functions of osteocytes include the translation of mechanical strain into signals of bone formation or of bone resorption, as modifiers of their microenvironment thereby modifying the properties of bone and the magnitude of shear stress in the bone fluid, as regulators of mineralization and as regulators of phosphate homeostasis. Osteocytes, with their distribution throughout the bone matrix and their high degree of interconnectivity, are ideally positioned within the

bone matrix to sense mechanical strain and translate that strain into biochemical signals of resorption or formation related to the intensity and distribution of the strain signals [183]. Although osteocytes have reduced synthetic activity and, like osteoblasts are not capable of mitotic division, they are actively involved in the maintenance of bony matrix, through various mechanosensory mechanisms.

1.3.1.3. Osteoclast - the bone resorbing cell

Osteoclasts, first named by Kölliker (1873), are multinucleated cells (1 - 50 nuclei per cell depending of the species). Their function is to resorb and remove unwanted bone. Bone resorption takes place at a specialized area of the osteoclast cell membrane called "ruffled border," which comprises a sealed lysosomal compartment where the acidic pH solubilizes the mineral and the proteolytic enzymes digest the matpic characteristics with circulating monocytes and tissue macrophages [184, 185]. rix [187, 188, 189, 190, and 191]. Osteoclasts are derived from haematopoietic stem cells (CFU-GM) and share phenotyThe osteoclast belongs to the monocyte/ macrophage cell lineage [186]. The PU.1 transcription factor increases as macrophages assume an osteoclastic phenotype. Factors that induce the formation of osteoclasts (Dexamethasone and 1, 25-Dihydroxyvitamin D3) also cause the increase in PU.1. Mice born with homozygous deficiency of the PU.1 genes lack both macrophages and osteoclasts. They die (of infection due to the lack of macrophages) shortly after birth, and autopsies show that their bones have an osteopetrotic phenotype.

The presence of stromal cells or pre-osteoblasts within the bone microenvironment appears to be essential for the differentiation and subsequent functional activation of osteoclasts. These cells respond to osteotrophic factors such as Vitamin D3, Parathyroid hormone (PTH), and Parathyroid hormone related protein (PTHrP) and are responsible for the production of M-CSF (macrophage colony stimulating factor) and RANKL, factors that play direct roles in osteoclast proliferation, survival, and differentiation. Thus, the osteoblast precursors help the differentiation of the osteoclasts. The binding of RANKL to its receptor on the osteoclast leads to the activation of the transcription factor NF-κB, which is involved in increasing the expression of genes that play a role in the differentiation and/or function of the osteoclast. The expression of other important transcription factors involved in osteoclast differentiation includes at least one of the c-Fos family members [192, 193, 194 and 195].

1.3.1.4. Chondrocyte and chondrogenesis

The formation of the skeleton in vertebrates involves the differentiation of mesenchymal cells to cartilage. This process, called chondrogenesis, is a tightly regulated event involving multiple steps, including condensation of the precartilagineous mesenchyme, commitment to the chondrogenic lineage, and differentiation into chondroblasts and, eventually, into chondrocytes. All these events are regulated by the concerted action of extracellular and intracellular cues, including extracellular factors specific for cartilage differentiation (e.g. type IIa1 Collagen and Aggrecan). Other pathways that, while not being exclusively specific to this process, play an important role at various stages of chondrogenesis are for example the bone morphogenetic protein (BMP), Hedgehog, Wnt and fibroblast growth factor pathways. The intracellular events elicited by the activation of these and other pathways lead to the transcriptional regulation of chondrogenesis-specific genes (e.g. the gene for Sox9), enabling the differentiation of mesenchymal cells towards chondrocytes.

Chondrogenesis or the development of a cartilage template is essential for proper formation of endochondral bones. The intermediary cartilage anlagen, which result from chondrogenesis, provide the template on which bone is laid down [196]. The control of chondrogenesis is best understood in the context of the long bones of the limbs. In the developing limbs, cells originating from the lateral plate mesoderm are stimulated to aggregate ('condense') without an increase in proliferation, creating increased cell density and cell–cell interactions [197]. These interactions are most likely involved in propagating signal transduction events.

1.3.2. How does bone formation work?

The skeleton is established by two different ways (Figure 1.7): intra-membranous ossification, whereby mesenchymal cells differentiate directly into osteoblasts, and endochondral ossification (intracartilage ossification), during which a cartilage template is replaced by bone.

The process called intra-membranous ossification generates most bones of the skull and flat bones, and cartilage is not involved or present in this process. The condensations of mesenchymal cells assemble at the site of the future bone. These mesenchymal cells directly differentiate into osteoblasts, which in turn depose the mineralized bone matrix.

The steps in intra-membranous ossification are:

1. Development of ossification center
2. Calcification
3. Formation of trabeculae
4. Development of periosteum

On the other hand, long bones and most of the other skeletal elements are formed by endochondral ossification. Endochondral ossification requires the formation of a transient cartilage template. Chondrocytes in the most central region of the template differentiate to the terminal stage of the hypertrophic chondrocyte. Chondrocytes located between the resting/ reserve zone and the hypertrophic zone proliferate in an unidirectional manner, resulting in characteristic columns. Hypertrophic chondrocytes mineralize the matrix surrounding them, undergo apoptosis, and are invaded by blood vessels. The mineralized cartilage is degraded by osteoclasts and replaced with bone tissue through the activity of osteoblasts. The regions on either side of the bone tissue are termed the growth plates and responsible for longitudinal growth. This developmental process, which requires the orchestrated interaction of all bone cells, will be reviewed in Figure 1.7.

The steps in endochondral ossification are:

1. Development of cartilage model (anlagen)
2. Growth of cartilage model (anlagen)
3. Development of the primary ossification center
4. Development of medullary cavity
5. Development of the secondary ossification center
6. Formation of articular cartilage and epiphyseal plate (growth plate)
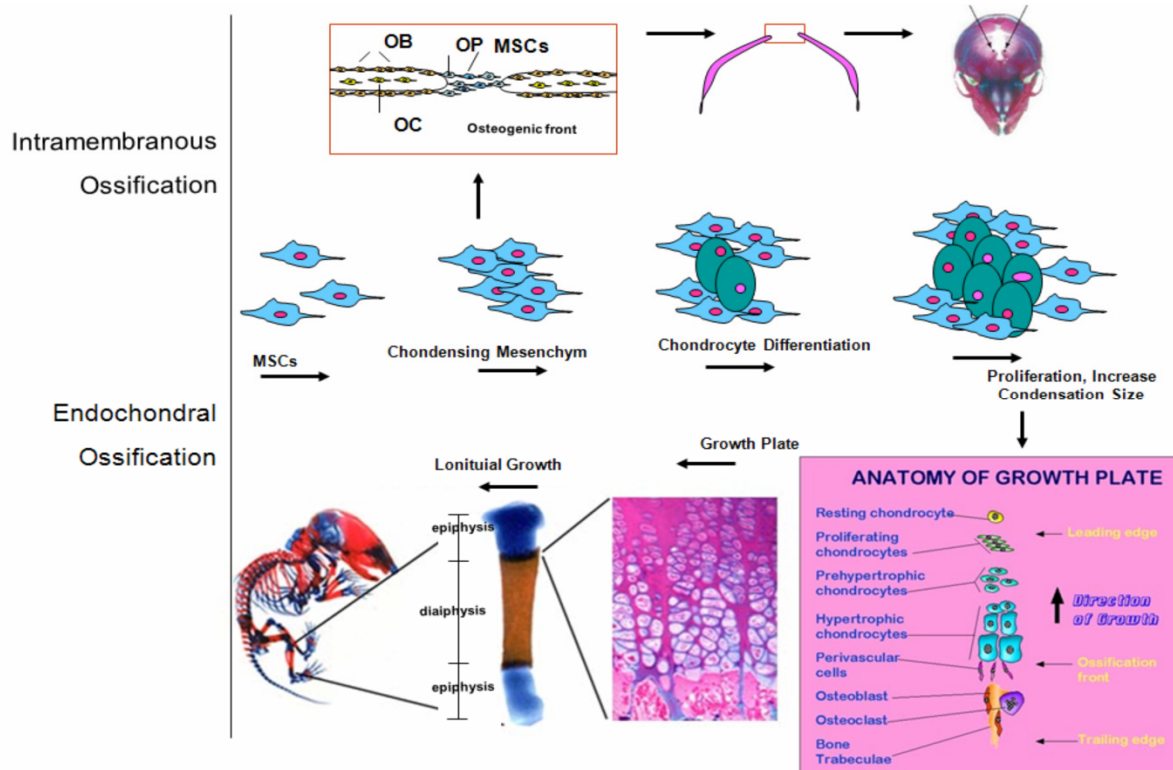
Figure 1.7 Skeleton developments through intramembranous or endochondral ossification

Endochondral ossification begins with points in the cartilage called "primary ossification centres". They mostly appear during fetal development. They mostly appear during fetal development, though a few short bones begin their primary ossification after birth. They are responsible for the formation of the diaphyses of long bones, short bones and certain parts of irregular bones. Secondary ossification occurs after birth, and forms the epiphyses of long bones and the extremities of irregular and flat bones. The diaphysis and both epiphyses of a long bone are separated by a growing zone of cartilage (the epiphyseal plate). When the child reaches skeletal maturity (18 to 25 years of age), all of the cartilage is replaced by bone, fusing the diaphysis and both epiphyses together (epiphyseal closure).

1.3.3. Function and characteristics of adipocytes tissue – BAT and WAT

Mammals have two types of adipocyte, the brown and the white adipocyte. Brown adipocytes (BAT) store less lipids and have more mitochondria than white adipocytes. Brown adipocytes express almost all the genes that are expressed in white adipocytes, but they also express some distinctive one, including uncoupling protein-1 (UCP-1), which allows energy to be dissipated as heat without generating ATP. Most brown

adipose tissue in rodents is localized to the interscapular region. Humans have large depots of brown adipose tissue in infancy, but only small amounts that are dispersed throughout depots of white adipose tissue persist in adults. Brown adipogenesis is similar to white adipogenesis as both cell types require PPARγ and CCAAT-enhancer-binding proteins (C/EBPs). However, although ablation of C/EBPα blocks the development of most of the white adipose tissue, effects on brown-adipose tissue are less marked, with delayed expression of UCP1. Conversely, the loss of both C/EBPβ and C/EBPδ results in significantly reduced amounts of UCP1 in brown adipose tissue despite the normal amounts of C/EBPα. Unlike white adipocyte differentiation, most of which occurs in the postnatal period in mice, brown adipocyte differentiation occurs before birth. This temporal sequence has led to speculation that brown adipocytes represent a partially differentiated form of white adipocytes, but this proven not to be true [226].

White adipocytes tissue (WAT) occurs in virtually all vertebrates and the physiological basis for its presence has never been investigated thoroughly. Conversely, because of its diverse nature, WAT had been considered to occur almost universally in the animal body and had not been fully recognized as an anatomically organized tissue with site-specific properties until the past few decades. Although large variability in relative masses of depots and large individual and taxonomical differences are evident, a common pattern of a dozen or so adipose tissue depots can be found in all eutherian and metatherian mammals. Unilocular white adipocytes are simple by their structure, store large amounts of triacylglycerols (TAGs) during periods of energy excess and deliver fatty acids to other tissues as required. Despite of its simple structure, WAT performs numerous functions in the body that are related with its anatomical locations, such as the provision for lactation [205].

The recently discovered secretory product of white adipocytes, leptin, has been proposed to play a role in the regulation of body weight and the total amount of adipose tissue in the body [206, 207]. Leptin is expressed by the ob gene, which has extensive homology among vertebrates [206]. The original 'lipostatic' concept states that leptin is a hormonal substance that circulates in the blood and provides the brain with a signal about the amount of stored adipose tissue, thereby acting as a satiety factor [208]. Fasting and weight loss decrease the level of leptin in circulation, and weight gain and overfeeding increase it [206, 207, and 208]. The sympathetic nervous system plays a key role in the regulation of leptin levels, possibly by down-regulating leptin production via β3-adrenoceptors [209]. Reduced blood leptin and Insulin levels presumably increase the activity of anabolic neural pathways in the brain to boost appetite and feed intake, and thereby aim to restore energy homeostasis. Although WAT seems to be the main site of

leptin production, leptin is also produced in other tissues, including BAT and placenta, and may have versatile functions in the body.

Besides leptin, WAT also secretes a large number of other signals that affect energy homeostasis. These include pro-inflammatory cytokines, regulators of lipoprotein metabolism and growth factors, among others. Catecholamines, Insuline and the sympathetic nervous system that modulate the adipocyte function also influence efferent signalling of adipose tissue. WAT is thus increasingly being recognised as an active endocrine and paracrine organ, which closely interacts with other organs and tissues, and enables the organism to adapt to a wide range of metabolic challenges [209].

The relationship between bone and fat formation within the bone marrow microenvironment is complex and remains an area of active investigation. Classical in vitro and in vivo studies strongly support an inverse relationship between the commitment of bone marrow-derived mesenchymal stromal cells to the adipocyte and osteoblast lineage pathways [210, 211, 212, and 213]. The clinical fact that a decrease in bone volume (BV) of age-related osteoporosis is accompanied by an increase in marrow adipose tissue also implies the possible reciprocal relationship that is postulated to exist between the two differentiation pathways [214, 215, 216, and 217]. Several key transcription factors that function in the complex transcriptional cascade during adipocyte differentiation have been identified, including PPARγ and CCAAT enhancer-binding proteins (C/EBPs). PPARγ plays requisite and sufficient roles in the regulation of adipocyte differentiation, because its overexpression in fibroblast cell lines initiates adipogenesis and ES cells and embryonic fibroblastic cells from mice lacking PPARγ were unable to differentiate into adipocytes [218, 219, 220, 221, and 222].

Today it is supposed, that the amount of adipocytes and the amount of osteoblasts in the body are regulated in a reciprocal manner. The first evidence of this came from the analysis of the effect of leptin on bone and fat formation. The amounts of Leptin in the blood have been reported to correlate with the total amount of fat in the body. Recently it has been shown that leptin is mediating the protective effects of fat on bone tissue. Indeed, mice lacking leptin develop obesity and are protected against bone loss. How leptin is controlling bone metabolism is still controversial. On the one hand, a direct stimulation of osteoblast function by the leptin secreted by the adipocytes present in the bone marrow has been proposed. On the other hand it was suggested that Leptin decreases bone remodelling in the mature skeleton by establishing a negative feedback loop involving the hypothalamus [223, 224].

In addition to Leptin, other pathways have been shown to co-regulate adipogenesis and ostoegenesis. One example of this is that activation of the mitogen-

activated protein kinase (ERK) cascade has been shown to stimulate osteoblast differentiation but also the phosphorylation of PPARγ that inhibits adipogenesis [225]. The lineage determination of mesenchymal stromal cells can be regulated by a transcription factor named TAZ (transcription activator with PDZ binding motif). Both, Runx2 and PPARγ are reported to be regulated by TAZ [226].

An other potential candidate is Rsk2. Rsk2, also named p90 ribosomal S6 kinase 2 or mitogen-activated protein (MAP) kinase-activated protein kinase 1 (MAPKAP-K1b) is a serine theronine kinase. Rsk2 is composed of two kinase domains which are activated by ERK and by PI3K-dependent kinase PDK1 [19]. Mutations that inactivate Rsk2 are the cause of an X-linked mental retardation disease in humans called Coffin-Lowry Syndrome (CLS). The Coffin-Lowry Syndrome is associated with abnormalities in the skeleton which leads to the conclusion, that Rsk2 may be playing an important role in bone development. Indeed, Rsk2 was recently identified as a positive regulator of bone. Mice lacking Rsk2 develop osteopenia, due to impaired function of osteoblasts. The absence of Rsk2 also reduced the formation of c-Fos induced osteosarcoma. While, Rsk2 effect on tumour formation was attributed to a lack of phosphorylation of c-Fos, the osteopenia seemed to be independent on AP-1 protein c-Fos [19]. Rsk2 phosphorylation sites are also present in Fra1 suggesting that Fra1 could be a substrate of Rsk2 in bone. Interestingly, Rsk2 is highly expressed in adipose tissue. One of the Rsk2 knockout mice line, was shown to waste weight with age, a phenotype proposed to be caused by a loss of adipose tissue associated with reduced levels of Leptin. Rsk2 knockout mice have also decreased Insuline sensitivity. It was therefore concluded that Rsk2 would play a role in the regulation of the mass of adipose tissue by regulating the response to Insulin.

The signal transduction pathways implicated in osteogenic and adipogenic processes are therefore evaluated as potential targets for therapeutic intervention of bone diseases (e.g. osteoporose or osteosclerose) and metabolic diseases (e.g. diabetes, obesity and lipodystrophy). The molecular mechanisms underlying the reciprocal relationships are not yet well understood. This work was aimed to providing better understanding in the role of Rsk2 in the control of Fra1 osteogenic/ adipogenic function.

44

2. Aims and Plan

2.1 Aims

Bone integrity depends on the proper coupling between the activity of the bone forming cells, osteoblast and the activity of the bone resorbing cells, osteoclast. Osteoclasts are specialized bone polynuclear macrophages, which differentiate from bone morrow macrophage precursors, while osteoblasts differentiate from the bone marrow stromal stem cells. The bone marrow stromal stem cells are common progenitors for many mesenchymal lineages including fibroblasts, chondrocytes, myoblasts and adipocytes. Genetic studies in mouse, have demonstrated the central role of the family of transcription factors AP-1 in controlling decision fate of mesenchymal cells. The functional differences between AP-1 members are well illustrated by the analysis of bone phenotypes, e.g. mice overexpressing c-Fos develop osteosarcoma, tumours affecting the osteoblasts while the mice overexpressing Fra1 develop osteosclerosis, a bone disease characterized by an increase bone formation due to an acceleration of osteoblast differentiation. David and colleagues could show how import AP-1 transcriptional activity is, in part regulated by post-transcriptional modifications of c-Fos. Phosphorylation of c-Fos by ERK1/2 and ERK/ PI3-kinase dependent kinase Rsk2 can stimulate its transcriptional activity and thereby modulating c-Fos-induced cell transformation. Reported was that c-Fos-dependent osteosarcoma formation is impaired in absence of Rsk2. The lack of c-Fos phosphorylation leads to reduced c-Fos proteins levels, decreased proliferation and increased apoptosis of transformed osteoblasts. Therefore, Rsk2-dependent stabilisation of c-Fos was essential for osteosarcoma formation [19]. Thus, c-Fos is most likely not the only substrate mediating Rsk2 function in osteoblasts. Indeed, it has been suggested that some of the skeletal phenotypes observed in Coffin-Lowry Syndrome (CLS) are caused by the lack of phosphorylation of the transcription factor ATF4 by Rsk2 [35]. Moreover, several arguments suggest that Fra1 could also be a substrate for RSk2 in bone. First, the two-phosphorylation sites in the c-terminal domain of c-fos (Ser 362 and Ser 374) are also present in Fra1. Second, similar to c-Fos, Fra1 stability and activity is known to be post-transcriptional regulated in an ERK-dependent manner [36, 37]. Finally, while increased osteoblast activity was observed in *fra1* transgenic mice [52], *Fra1*-deficiency was leading to osteopenia due to a decreased osteoblast function [50]. Therefore, it is important to investigate the role of Fra1 phosphorylation by Rsk2 in the development of Fra1-induced osteosclerosis.

2.2   Plan

a) Role of Rsk2 in Fra1-induced osteosclerosis

To determine whether Fra1 could be a substrate of Rsk2 in bone, fra1 transgenic mice were intercrossed with Rsk2-deficent mice. Since Rsk2 is an X-linked gene, F1 males were used to analyse the bone phenotypes.

b) Role of Rsk2 and Fra1 in controlling decision fate of mesenchymal cells

Fra1 and ΔFosB that are sharing common features, such as the absence of transactivation domain are both positively regulating bone formation. In addition, ΔFosB overexpressing mice have shown markedly decreased adipogenesis, suggesting that the increased osteoblasts differentiation occurred at the expense of adipogenesis. Based on these observations, I analysed the role of Rsk2 and Fra1 in adipogenesis in vivo. In addition, in vitro culture conditions to differentiate primary osteoblasts into adipocytes were set up and the differentiation properties of cells overexpressing Fra1 were analysed.

c) Role of Rsk2 in Fra1-induced splenomegaly

Spenomegaly is often associated with osteosclerotic conditions including in Fra1 overexpressing mice. I analysed the spleen phenotype of Fra1 transgenic mice.

d) Role of Fra1 overexpression in organs such as heart and liver

Little is known about the role of Fra1 overexpression in organs such as heart and liver. I additionally analysed these organs to look if AP-1 member Fra1 can influences cell populations where precursor cells are mesenchymal stromal cells.

_____

3. Material

3.1 Mice animals

C57/Bl6	wild type (wt) mice for male and female
Rsk2-/y	Rsk2-deficient or knockout mice for male; rsk2 is a X-linked gene
Rsk2-/x	Rsk2-deficient heterozygote mice, female
Rsk2-/-	Rsk2-deficient or knockout homozygote mice, female
H2-fra1-LTR	fra1-tg (fra1 transgenic) mice for male and female; Fra1 transgene is expressed under the control of the H2Kb promoter, and Fra1 is therefore widely expressed in various cell types in these mice
H2-fra1-LTR/rsk2-/y	fra1-tg mice deficient for rsk2 (duple muted mice for male)
H2-fra1-LTR/rsk2-/x	fra1-tg mice heterozygote for rsk2 (duple muted mice for female)

All mice are on a C57Bl/6 background and were maintained under specific pathogen-free conditions. All experiments were performed in accordance with the guidelines for the care and use of laboratory animals of Humboldt - University zu Berlin and LAGetSi.

3.2 Cell material for ex vivo and in vitro experiments

mPOBswt	primary wild type osteoblasts were isolated from mice calvarias; cells were used for ex vivo experiments
mPOBsrsk2-/y	primary Rsk2-deficient osteoblasts were cells isolated from mouse calvarias; cells were used for ex vivo experiments
mPOBsfra1-tg	primary fra1-tg osteoblasts were cells isolated from mouse calvarias; cells were used for ex vivo experiments
mOBsrsk2-/y	murine OBs cell line derived from rsk2-/y mice by sequentially passaging mPOBs for at least 12 passages; cells were used for in vitro experiments

_____

mOBsrsk2-/y - pBabe-empty	infected mOBsrsk2-/y cell line with pBabe-empty (Puro-2) vector (control vector)
mOBsrsk2-/y - pBabe-fra1	infected mOBsrsk2-/y cell line with pBabe-fra1 retrovirus vector overexpressing Fra1
mOBsrsk2-/y - pMSCV-Neo	infected mOBsrsk2-/y cell line with pMCSV-Neo retrovirus vector (control vector)
mOBsrsk2-/y - pMSCV-FraER	infected mOBsrsk2-/y cell line with retrovirus vector overexpressing the fusion protein estradiol receptor ligand binding domain with Fra1
Phoenix cells	packaging cell line used to produce the retrovirus particles

3.3   Cell culture media and supplements

Culture or α-MEM medium

500 ml	α-MEM (PAA Laboratories GmbH)
10 %	FCS (PAN)
1%	Penicillin/ Streptomycin (Gibco BRL)
2 mM	L-Glutamin (Gibco BRL)

Adipocyte medium

500 ml	α-MEM (PAA Laboratories GmbH)
10 %	FCS (PAN)
1 %	Penicillin/ Streptomycin (Gibco BRL)
2 mM	L-Glutamin (Gibco BRL)
10 µg/ ml	Insulin (Sigma)
1 µM	Dexamethasone (Sigma)
0.5 mM	IBMX (Sigma)

Calvaria isolation medium

500 ml	α-MEM (PAA Laboratories GmbH)
0.1 %	Collagenase (Sigma)
0.2 %	Dispase (Boehringer Mannheim)

_____

3.4   Buffer

Tail preparation Buffer

50 ml	10 % SDS
25 ml	Tris-HCL, pH 8.0 [1M]
100 ml	EDTA [0.5 M]
10 ml	NaCl [5 M]
315 ml	dH$_2$O

SDS Sample Buffer

600 µl	Tris-HCL, pH 7.2 [1 M]
4 ml	20 % SDS
4.8 g	Glycerol
510 µl	ß-Mercaptoethanol
1 %	Bromophenol blue

Frakelton Buffer

5 ml	Tris-HCL, pH 7.5 [1 M]
5 ml	NaCl [5 M]
6.69 g	Na-Pyrophosphate
450 ml	dH$_2$O
	set pH to 7.05
5 ml	Triton X 100

Before use, Frakelton buffer is completed with:
    1 mM PMSF or 1x protease inhibitor cocktail
    100 mM Na3 VO4
    100 nM Okadaic Acid

Buffer A for cytosolic extraction

500 µl	HEPES pH 7.6 [1 M]
250 µl	KCl [2 M]
25 µl	EDTA [0.2 M]
50 µl	EGTA [0.1 M]
37.5 µl	Spermidine [1 M]
15 µl	Spermine [0.5 M]
0.4 %	IGEPAL
48.92 m	dH$_2$O

Before use, the Buffer A is completed with:
    1 M DTT (10 µl/ 10ml)
    100x Protease inhibitor cocktail (100 µl/ 10ml)
    100 mM PMSF (100 µl/ 10ml)
    1M Na3 MoO4 (100 µl/ 10ml)
    10 % NonidetP-40 (NP-40)

_____

Buffer B for nuclear extraction

1 ml	HEPES pH 7.6 [1 M]
4 ml	NaCl [5 M]
250 µl	EDTA [0.2 M]
500 µl	EGTA [0.1 M]
44.25 ml	dH$_2$O

Before use, the Buffer B is completed with:

1 M DTT (10 µl/ 10ml)
100x Protease inhibitor cocktail (100 µl/ 10ml)
100 mM PMSF (100 µl/ 10ml)
1M Na3 MoO4 (100 µl/ 10ml)
10 % NonidetP-40 (NP-40)

Upper - Tris Buffer (4x)

15.1 g	Tris-HCl, pH 6.8
10 ml	10 % SDS
250 ml	dH$_2$0

Lower - Tris Buffer (4x)

90.8 g	Tris-HCl, pH 8.8
20 ml	10 % SDS
500 ml	dH$_2$O

4 % Stacking gel

2.0 ml	Upper-Tris-Buffer (4 x)
800 µl	40 % Acrylamid
10 µl	TEMED
50 µl	10 % APS
5.14 ml	dH$_2$O

8 % Running ge l

3.0 ml	Lower – Tris Buffer (4 x)
2.40 ml	40 % Acrylamid
10 µl	TEMED
120 µl 1	0 % APS
6.47 ml	dH$_2$O

Loading - Buffer (1x)

2.5 ml	Upper – Tris Buffer (4 x)
2.3 ml	87 % Glycerol
4.0 ml	10 % SDS
1.0 ml	2-Mercapto-ethanol
5.0 mg	Bromophenol blue
20 ml	dH$_2$O

Running - Buffer (10x)

30.25 g	Tris
144 g	Glycine
10 g	SDS
1000 ml	dH$_2$O

_____

Blotting - Buffer (10x)

30.25 g	Tris
144 g	Glycine
1000 ml	dH_2O

TBS - Buffer (20x)

121 g	Tris-HCl, pH 7.4
175.3 g	NaCl
1000 ml	dH_2O

TBS - 0.1 % Tween (TBS-T)

50 ml	TBS - Buffer (20x)
1 ml	Tween 20
950 ml	dH_2O

Stripping - Buffe r

3.85 g	DTT
10 g	SDS
3.78 g	Tris-HCl, pH 6.7
500 ml	dH_2O

3.5   Staining solutions

Eosin solution

25 g   Eosin in
600 ml dH_2O
Add 1400 ml absolut ethanol
Directly prior usage: 3 – 5 ml pure acetic acid
per 300 ml Eosin solution

Mayer´s Hematoxylin

8 g	Hematoxylin
1 g	Sodiumiodat
250 g	Aluminiumkalisulfat
250 g	Chloralhydrat

_____

Oil Red O

      0.5 g   Oil Red O
      100 ml   Isopropanol

Ponceau S solution

      0.1 %   Ponceau S in 5 % acetic acid

3.6   Oligonucleotide

All primers were ordered from TIB Molbiol Syntheselabor GmbH. The primers were diluted in dH_2O to a stock solution of 100 µM. The stock solution was applied as a 10fold dilution for PCR reaction mixes.

Genotyping

RSK2-/y	WL112	5´ TTG TTG GTT TAC TTT CTT TCG GTC TG 3´
	WL113	5´ AAG ATG ATT GCT TTG CTT AGT TTA 3´
H2K-fra 1-LTR	CE4	5´ GGG ATT AAA TGC ATG CCA AGC T 3´
	H2kB	5´ CGA TCA CCA GAG ACC AAT CAG 3´

qPCR and QRT - PCR

HPRT	forward	5´ GTT AAG CAG TAC AGC CCC AAA 3´
	reverse	5´ AGG GCA TAT CCA ACA ACA AAC TT 3´
PPARγ	forward	5´ CAT AAA GTC CTT CCC GCT GA 3´
	reverse	5´ GAA ACT GGC ACC CTT GAA AA 3´
Pref-1	forward	5´ CTG GAG AAA GGC CAG TAC GA 3´
	reverse	5´ GG GGT ACA GCT GTT GGT TG 3´
Fra1	forward	5´ GAG ACG CGA GCG GAA CAA G 3´
	reverse	5´ CTT CCA GCA CCA GCT CAA GG 3´
Runx2	forward	5´ TGT TCT CTG ATC GCC TCA GTG 3´
	reverse	5´ CCT GGG ATC TGT AAT CTG ACT CT 3´
Sox9	forward	5´ CTG AAG GGC TAC GAC TGG AC 3´
	reverse	5´ TAC TGG TCT GCC AGC TTC CT 3´
Pref-1	forward	5´ CTG GAG AAA GGC CAG TAC GA 3´
	reverse	5´ AGG GGT ACA GCT GTT GGT TG 3´
C/EBPα	forward	5´ CCT ACC GAG TAG GGG GAG CA 3´

_____

	reverse	5´ TGT AGC TGG GGG TGA GGA CA 3´
MyoD	forward	5´ GGT TCT TCA CGC CCA AAA G 3´
	reverse	5´ GGT GCA GCC AGA GTG CAA GT 3´
aP2	forward	5´ TGC AGC TTC CTT CTC ACC TGA 3´
	reverse	5´ TCC TGG CCC AGT ATG AAG GAA ATC 3´
Glut4	forward	5´ GAA CAG CCT GGG GAA CT 3´
	reverse	5´ GAG TCT GGG AGG GGC AGG A 3´

Antibodies

Fra1 (rabbit), sc-605	Santa Cruz Biotechnology
PPARγ (rabbit), 2492	Cell Signalling Technology
GR (rabbit), sc-1004	Santa Cruz Biotechnology
β – Actin (mouse), AC-15	Sigma
Mouse IgG HRP (goat)	Promega
Rabbit IgG HRP (goat)	Promega
B 220 : Alexa 488	DRFZ
B 220 : dig	DRFZ
CD 41	Dako
FDC - M2 : bio	ImmunoKontakt
MOMA-1	Southern Biotech
SA - Rhodamin	Moleculare Probes
SA - Alexa 488	Moleculare Probes
Anti-dig – cy5	DRFZ
Anti-dig – Alexa 546	DRFZ
DAPI	Moleculare Probes
BP3	Present by Max Cooper
SA - Alkalic phosphatase	Sigma

_____

3.7 Molecular weight marker

RainbowTM coloured protein molecular weight marker (Code RPN 755)

Amersham Pharmacia Biotech

peqGOLD Prestained Protein Marker (27-1110)

peqLab Biotechnologie GmbH

peqGOLD 1 kp DNA-Leiter (25-2030)

peqLab Biotechnologie GmbH

3.8 Kits and enzymes

Trizol ® Reagent	Invitrogen
ECL® Western Blot	Amersham Biosciences
TaqMan® Kit	Roche
LightCycler® 480 SYBR	Roche
LSAB+ System - HRP	DakoCytomation
HistoRed AP – Kit	Linaris

3.9 Chemicals

Acrylamid 40 %	Biozym Diagnostics
APS	Roth
Brome-phenol blue	Promega
DMSO	Sigma
EDTA	Roth
Eisen-Haematoxylin A + B	Chroma
Ethanol	Merck
Ethidiumbromid	Merck
Eosin	Sigma
Flouromount – G	SouthernBiotech
Formalin	Wako Pure Chemical

Glycerine	Roth
Glycerol	Merck
HCL	Merck
Isopropanol	Merck
KCl	Roth
KH2PO4	Merck
Kaisers Glyceringelatine	Merck
Lichtgrün	Chroma
MgCl2	Roth
Mercaptoethanol	Bio-Rad
Methanol	Roth
Milk Powder	Heirler
NaCl	Sigma
Orange G	Chroma
Okadaic acid	Merck
Parafin	Sigma
PMSF	Sigma
Pikro - Fuchsin van Gieson	Chroma
Ponceau S	Sigma
Proteinkinase K	Roth
Resorcin-Fuchsin "Elastica"	Chroma
SDS	Serva Electrophoresis GmbH
Sodium vanadate	Sigma
TEMED	Roth
Tris	Roth
Triton X 100	Sigma
Trypsin	PAA Laboratories GmbH
Tween 20	Sigma
Xylol	Merck

_____

3.10 Consumables

0.2 ml Thermo – Strip	ABgene
1.8 ml CryoTubeTM vials	Nunc
Cell lifter	Costar
0.2 µm Filtropur S 0.2	Sarstedt
Microtube EASY CAP	Sarstedt
Safe Seal Tips 10 - 1000µl	Biozym
Flasks, dishes and plates	Greiner Bio One
Slides (76 x 26 mm)	Roth
Trans-blot®, 0.2 µm	Bio-Rad
X-OMAT LS	Kodak

3.11 Laboratory Instruments

Agilent 2001	Bionalyzer
Autoklave 2540 EL	Tuttnauer
Blotting machine	Pharmacia Biotech, Nava Blot, Multiphor II
Centrifuge type 5403	Eppendorf
Centrifuge type 5415 C	Eppendorf
Centrifuge type Biofuge	Heraeus Instruments
Bench type HeraSafe	Hereaus Instruments
Colour digital camera	Scion Corporation
Optimax 2010	Protec
Gel Dryer Model 583	Bio-Rad
Gel Wrap®*	C.B.S. Scientific
Imaging caption computer	Cybertech
Incubator Hereaus 6000	Hereaus Instruments
Microscope Diaphot 300	Nikon
Large White Spring Clamp	C.B.S. Scientific
Light Cycler® 2.0 System	Roche
Microplate reader Max 190	Molecular devices
Microscope type ID 03	Zeiss

Microscope type IX50	Olympus
Minishaker MS2	IKA
NanoDrop® ND-1000	NanoDrop
pH - Meter 761	Calimatic Knick
Photometer Spectra Fluor	Tecan
T3 Themocycler	Biometra
Thermo Block DRI DB2A	Techne
Transfer Chamber Multiphor	Pharmacia Biotech

_____

4. Methods

4.1 Cell culture

4.1.1. Splitting cells and cell density

Cells were grown in flasks or 6-well culture plates at 37 °C in an atmosphere of 5 % CO_2 and an atmospheric humidity of 95 %. The cells were trypsined and replated in new flasks or dishes when reaching a confluence of 80 %. For this, the old α-MEM media was removed, the cells were washed two times with PBS without Ca2+ and Mg2+) and coated with pre-warmed with a 0.25 % Trypsin/ EDTA - solution. After an incubation of 2 min at 37 °C the cells were collected and carefully resuspended to get a single cell suspension. After centrifugation (5 min, 1000 rpm), the pellet was resuspended in new α-MEM media and the cells were counted in a Neubauer haemocytometer. 1 x 10^5 cells per 6-well culture plates were used for differentiation experiments.

4.1.2. Freezing and thawing of cells

Cells were harvested, washed in ice cold medium and resuspended in pre-cooled freezing medium [20 % (v/v) FCS, 10 % (v/v) DMSO]. The resuspended cells were aliquotted in screw-top tubes and cooled in a freezing box to - 70 °C. The aliquots were stored in liquid nitrogen. To thaw one of these aliquots, the screw-top of the tube was loosened and the cell suspension was thawed by holding the tube in a 37 °C water bath. The cells were then transferred into a 15 ml Falcon tube and slowly resuspended in medium. The cells were then washed once and plated on cell plates.

4.1.3. Isolation of murine primary osteoblast cells (mPOBs)

Five calvariae from newborn mice (up to six days of age) were dissected, cleaned in 70 % Ethanol and in PBS. They were subsequently transferred into a solution for bone digestion containing 0.1 % Collagenase and 0.2 % Dispase II α-MEM without FCS and were shaken for 10 min at 37 °C. After incubation the liquid phase, the fraction 1, was

discard. To the calvaria were added again 1 ml of digestion medium. The calvaria were incubated again, but this time the liquid phase (fraction 2) was recovered and collected. This step was repeated 4 times. The cells from the combined fraction 2 to 5 were polled by centrifugation (5 min, 2000 rpm). The supernatant was discarded and the pellet was resuspended in 1 ml α-MEM. The cells were seeded and cultured in 6-well plates. 1.5 ml of α-MEM culture medium containing 10 % FCS and antibiotics (P/ S) was added to each well before 1 ml of cell suspension was added. The cells were grown at 37 °C in an atmosphere of 5 % CO_2 in air. The medium was replaced every 3 day. The medium was pre-warmed to 37 °C before changing. The cells were grown until sub-confluences, trypsinized and replaced from 1 dish into 5 new dishes. The cells were grown again until sub-confluences, trypsinized and plated in 6-well cell culture plates with a density of 1x 105 cells per well to conduct adipocyte differentiation experiments.

4.1.4. Differentiation and analysis of mPOBswt and mPOBsfra1-tg to adipogenic cells (ex vivo analysis)

Adipocyte differentiation ex vivo was performed as follow: after genotyping, the cells were seeded in 6-well tissue culture plates with a cell number of 1x 105 cells per well. One 6-well plate per genotype was used for RNA isolation and another 6-well plate for Oil Red O staining for every time point when the adipocyte differentiation had to be analyzed (day 0 and day 21). The cells were cultured in 2 ml culture media for mPOBs per well. The culture media was changed every 2 to 3 days. At confluence that is referred as day 0 the cells were treated with the adipogenic cocktail (IBMX, Dexamethasone and Insulin). In the experiments samples made from mPOBs, mRNA and Oil Red O staining was conduct at day 0 and day 21 post-stimulation.

4.1.5. Differentiation of mPOBs to an immortalized murine osteoblast cell line (mOBs)

Murine primary osteoblast cells (mPOBs passage 1 – 4/ ex vivo) were cultured and trypsinated when sub-confluent. First, the cells were washed with 5 – 10 ml PBS according to the culture vessel size. 2.5 – 5 ml Trypsin/ EDTA (1x) was added followed by an incubation at 37 °C / 5 % CO_2 until all cells were detached. 2.5 – 5 ml culture media was put to neutralize the Trypsin. The solution was put in a centrifuge tube with a conic end (cells of same genotype and passage coming from different flasks were

merged). The solution was spun down for 5 min at 500 g (centrifuge type 5403 - Eppendorf). The supernatant was taken off and the pellet was resuspended in 1 ml of culture media. 200 µl of the suspension was shared to a new flask splitting the cell number 1: 5. Cells were cultured and trypsinated again and experiments were done with mOBs on passage 27 (in vitro).

4.1.6. Retrovirus infection of mOBs with constitutive overexpression of Fra1

The system for constitutive over-expression of Fra1 in mesenchymal cells used in this work consists of the vector pBabe with a cDNA insert of the gene encoding rat Fra1 (pBabe-fra1) and the empty vector (pBabe-empty) as control. The vector pBabe based on the Moloney Murine Leukaemia Virus (MoMuLV). It is a system for transfer and express exogenous genes in mammalian cells. The pBabe retroviral vector expresses inserted genes from the Mo MuLV Long Terminal Repeat (LTR). Moreover, the vector includes a gene for Ampicillin resistance for selection in bacteria culture and a gene encoding for Puromycin resistance for selection in cell culture. The expression of the Puromycin resistance gene is driven by a Simian virus 40 promoter (SV40) (Morgenstern and Land, 1990).

4.1.7. Retrovirus infection of mOBs with inducible overexpression of Fra1

In the following work the empty vector pMSCV-Neo was used as control for cells that are infected with the vector pMSCV-Fra1Er. The LTR used in these vectors is derived from the murine stem cell virus PCMV. A gene of interest can be cloned in the multiple cloning site (MSCV) which is downstream of the LTR. To construct the vector pMSCV-Fra1Er (a gift from Dr. M. Busslinger, IMP, Vienna, Austria), a 1900 bp long HindIII EcoRI partial of the vector pRK-fra1-er was cloned into the vector pMV-8 which contains the same LTR and resistance gene that the pMSCV-Neo. The fragment which was cloned in pMV-8 consists of the coding part of cDNA of the rat fra1 gene fused to the coding part of the hormone binding domain of the human oestrogen receptor. The advantage of this Fra1 system of over-expression, which is inducible by Estradiol treatment, is that Fra1 activity can be switched on or off in the infected cell line. This system was used in the following work as an additional tool to investigate the effect of Fra1 over-expression at particular times in mesenchymal cell differentiation.

4.1.8. Production of vector containing virus particles by transfection of Phoenix cells

Phoenix cells were cultured in a 75 cm2 cell culture flask until confluence, trypsinized and counted using a Neubauer haemocytometer. 8x 10 5 cells were seeded in a 6 wells tissue culture plate per well. The cells were cultured until confluence. Two wells of the six wells plate were used for the transfection of each vector construct. For the transfection, 5 µg of plasmid DNA were mixed with 20 µl MetafectenTM and 100 µl α-MEM Eagle media without additives to get a total volume of 200 µl per vector construct. The solution was mixed well and left at RT for 20 min. Subsequently, the 200 µl mix was added to the culture media in the chosen well of the six well plate. The Phoenix cells were cultured in this mix at 5 % CO2 and 37 ºC for one day. The culture media was changed on the next day and replaced by 2 ml of α-MEM Eagle culture media containing 10 % FCS and 1 x Penicillin/ Streptomycin. After 24 h incubation at 5 % CO2 and 37 ºC, the culture media was filtered with a filter of a pore size of 45 µm diameter allowing the virus particles to go through but not the cells. These virus supernatants were collected each in a sterile 15 ml tube and frozen at -80 ºC until their use.

4.1.9. Retrovirus infection of mOBsrsk2-/y

Murine osteoblast cells derived from rsk2-/y mice were cultured in a 75 cm2 cell culture flasks until confluence. Subsequently, the cells were trypsinized and counted using a Neubauer haemocytometer. The cells were plated at 2 different densities, 2.5 x105 and 5x 105 cells in 100 mm diameter tissue culture. The cells were then cultured at 5 % CO2 and 37 ºC in 10 ml α-MEM Eagle culture media containing 10 % FCS and 1x Penicillin/ Streptomycin. After 24 hours, 5 ml of the culture media was removed. 1ml of defrosted virus supernatant was added. To increase the efficiency of the retrovirus infection, 10 µg/ ml Polybrene were added (stock solution: 10 mg/ ml stored at –20 °C). Eventually, one cell culture plate containing 2.5x 105 cell and one cell culture plate containing 5x 105 was infected with retroviruses containing either the vector constructs pBabe-empty, pBabe-Fra1, pMSCV-Neo or pMSCV-Fra1Er. The culture media was changed on the next day. The cells were now cultured in 10 ml α-MEM Eagle culture media containing 10 % FCS and 1x Penicillin/ Streptomycin until confluence.

4.1.10. Selection of infected cells

The infected cells were harvested and counted. Two 100 mm diameter tissue culture dishes were plated using 6x 105 cells each per vector construct. Non-infected cells of the same genotype and passage number as the infected ones were cultured in parallel. These cells were harvested, counted and plated with the same cell number to serve as control in the following selection step. To select the cells successfully infected by the vector constructs pBabe-empty or pBabe-Fra1, the cells were cultured in 10 ml α-MEM Eagle culture media containing 10 % FCS, 1x Penicillin/ Streptomycin and 2.5 µg/ ml Puromycin. To select for the cells successfully infected by the vector constructs pMSCV-Neo or pMSCV-Fra1Er that also encoded for Neomycin resistance, the cells were cultured in 10 ml α-MEM Eagle cell culture media containing 50 µg/ ml G418 antibiotic. As control for the efficiency of the selection, non infected cells of the same genotype and passage number were treated with the antibiotics, i.e. one culture dish containing the same cell number was treated with 2.5 µg/ ml Puromycin or 50 µg/ ml G418, respectively. In parallel, one tissue culture dish was cultured without the used antibiotics to determine the specificity of the effect of the antibiotic on the control. The cells were cultured in 10 ml selection culture media until all cells in the non-infected control dishes died. Subsequently, every two culture dishes containing the cells infected with the same vector construct were merged in the following passage of the cells. The cells were then plated in two 175cm2 cell culture flasks, were cultured under selective condition until confluence and detached by trypsinisation. Cells from the two flasks were merged and samples of each cell line containing the different vectors were frozen and stored at -80 ºC.

4.1.11. Differentiation and analysis of mOBsrsk2-/y-pBabe-empty and mOBsrsk2-/y-pBabe-fra1 to adipogenic cells (in vitro analysis)

Adipocyte differentiation in vitro was performed as follow: at passage 27, the cells were seeded in 6-well plates with a cell number of 1x 105 cells per well. One 6-well plate per genotype was used for RNA isolation and another 6-well plate for Oil Red O staining for every time point when the adipocyte differentiation had to be analyzed. In the experiments conducted with the generated cell lines with either pBabe-empty (Puro-2) or pBabe-fra1 the cells were treated with adipocyte differentiation culture media or control culture media, the samples were isolated on day 0 and day 21 post-stimulation. From day 0 the half the wells were cultured in 2 ml adipocyte differentiation culture media. The

_____

other half part served as control and was treated with control culture media. RNA isolation and Oil Red O staining were conducted at day 15 or day 21 of treatment with adipocyte differentiation media or control media.

4.1.12. Differentiation and analysis of mOBsrsk2-/y-pMSCV-Neo and mOBsrsk2-/y-pMSCV-FraER to adipogenic cells (in vitro analysis)

In experiments comparing cells infected with the vector constructs pMSCV-Neo and pMSCV-FraER, four different treatments were compared: culture of cells in control culture media containing 0.099 % Ethanol, culture medium containing 1 μM β-Estradiol, adipocyte differentiation culture media or adipocyte differentiation culture media containing 1 μM β-Estradiol. Adipocyte differentiation in vitro was performed as follow: at passage 27, the cells were seeded in 6-well plates with a cell number of 1×10^5 cells per well. One six well plate per genotype was used for RNA isolation and another six well plate for Oil Red O staining for every time point when the adipocyte differentiation had to be analyzed.

4.2 Isolation, quantification and characterisation of nucleic acid

4.2.1. Isolation of genomic mouse DNA

A small piece of tail (~ 2 mm) was cut and incubated overnight at 55 °C in 750 μl tail preparation buffer containing 0.5 mg/ ml Proteinase K. After complete digestion 250 μl of saturated NaCl was added and tubes were shaken vigorously for 5 min. Samples were centrifuged at full speed in a table centrifuge (Heraeus Biofuge) for 20 min, the supernatant was transferred to a new tube and DNA was precipitated with 500 μl Isopropanol. DNA was harvested at full speed, supernatant was discarded and DNA dissolved in 500 μl Tris - EDTA (10 mM Tris, 1 mM EDTA).

4.2.2. Isolation of RNA

To get RNA, cells were harvested at day 0, day 15 and/ or day 21 during adipocyte differentiation. Total RNA was isolated from cultured cells by using Trizol® Reagent. Homogenized samples in Trizol® Reagent were separated by adding 0.5 ml chloroform. After centrifugation, the aqueous phase contain RNA was removes, and the RNA was precipitated with 1 ml Isopropanol. After washing the RNA pellet with 2 ml 75 % Ethanol and centrifugation, the RNA was solubilised in diethylpyrocarbonate-treated water (DEPC-water). Furthermore, total RNA was also isolated from mice fat pads. The tissue samples were homogenized in 2 ml of Trizol® Reagent by using a power homogenizer. After an incubation of the homogenized samples of 5 min, 0.4 ml Chloroform was added and probes were centrifuged for 35 min with 5000 rpm. The aqueous phase was mixed with 1 ml Isopropanol and centrifuged again for 35 min, 5000 rpm. The RNA pellet was washed with 2 ml 75 % Ethanol. At the end the pellet was dried on air and resuspended in DEPC-water.

4.2.3. Quantification of RNA

The RNA quality was analysed using UV absorbance: 260/ 280 ratios ranged from 1.8 - 2.0. The RNA concentration in the isolated RNA samples was measured using a Spectrophotometer type NanoDrop® ND-1000.

4.2.4. Digestion of DNA

The digestion of the DNA was reached by a treatment of the 1 µg RNA with 1 µl DNAse and 1 µl buffer. The reaction mixture was incubated 30 min at 37 °C. The inactivation of the DNAse was reached by incubation with 1 µl EDTA at 65 °C for 15 min.

_____

4.2.5. Reverse Transcription (RT-PCR)

cDNA synthesis was performed with the Reverse Transcription Kit from Roche as follow:

4 µl RNA [100 ng/ µl]
2 µl TaqMan 10x buffer
4.4 µl MgCl2 [25 mM]
4 µl dNTP [10 mM]
0.5 µl Random hexamer [50 µM]
0.5 µl Oligo dT [50 µM]
0.5 µl RNase inhibitor [20 U/ µl]
0.5 µl Reverse Transcriptase [50 U/ µl]
3.6 µl dH$_2$O

The samples were incubated for 10 min at 25 °C, followed by 40 min at 48 °C and a final step at 95 °C for 5 min.

4.2.6. PCR - Analysis of mouse genotype

All Polymerase chain reactions were carried out in 0.2 ml Thermo stripe reaction tubes using a Themocycler Type T3 (Biometra) and according to the following temperature profile:

Rsk2-/y PCR: initial denaturation, 94 °C, 2 min→ 35 cycles of PCR amplification: denaturation, 94 °C, 30 s → annealing, 60 °C, 45 s → elongation, 65 °C, 2.5 min → final elongation, 65 °C, 15 min → cool off, 4°C, ∞

Fra1-tg PCR: initial denaturation, 94 °C, 2 min → 35 cycles of PCR amplification: denaturation, 94 °C, 30 s → annealing, 58 °C, 45 s → elongation, 65 °C, 2.5 min → final elongation, 65 °C, 15 min → cool off, 4°C, ∞

Genotyping for rsk2-/y mice was carried out using the primers WL 112 and WL113:

2.5 µl 10x GenTherm buffer without MgCl2 (Rapidozym)
0.5 µl dNTPs [10 mM]
0.75 µl MgCl2 [50 mM]
2.5 µl WL 112 [100 µM]
2.5 µl WL 113 [100 µM]
0.25 µl 50 U/ µl Taq DNA Polymerase GenTherm (Rapidozym)
2.6 µl dH$_2$O
1 µl DNA

The DNA fragments amplified by this PCR have the size 230 bp or 320 bp. The 230 bp DNA fragment will be amplified if at least one allele of the genome in the analyzed DNA corresponds to a wild type Rsk2 gene. In case that at least one of the alleles corresponds to a knockout rsk2 genotype, the 320 bp fragment will be amplified. The amplified PCR products were analyzed by electrophoresis using a 2 % agarose gel.

Genotyping for fra1-tg mice was carried out using the primers primers CE4 and H2kB:

2.5 µl 10x GenTherm buffer without MgCl2 (Rapidozym)
0.5 µl dNTPs [10 mM]
0.75 µl MgCl2 [50 mM]
2.5 µl CE4 [100 µM]
2.5 µl H2kB [100 µM]
0.25 µl 50 U/ µl Taq DNA Polymerase GenTherm (Rapidozym)
1 µl DNA
10 µl dH$_2$O

The use of the primers CE4 and H2kB leads to the amplification of a DNA fragment with the size of 1200 bp in case the DNA derives from a fra1-tg mouse. The amplified PCR Products were analyzed by electrophoresis using a 1 % agarose gel.

4.2.7. PCR - Semi-quantitative PCR (qPCR)

Semi-quantitative PCR (qPCR) was utilized to analyze the cDNA obtained from reverse transcription of RNA isolated during adipocyte differentiation experiments or isolated from mouse fat pads. The analyzed cDNA samples were diluted to obtain a dilution series consisting of a 0, 10^1, 10^2, 10^3, 10^4 and 10^5 fold dilutions, respectively. The cDNA was diluted in autoclaved and distilled water. Subsequently, a mastermix was prepared consisting of the same volumes for a reaction mix of one sample as described for the PCR used for genotyping. For the analysis of HPRT, PPARγ, C/EBPα and Fra1 a forward and a reverse primer were used at a time for the PCR analysis of one single gene per PCR reaction. 19 µl of the mastermix were transferred into a 0.2 ml reaction tube for use in PCR and 1 µl of each cDNA dilution was added on top. The polymerase chain reaction for HPRT, PPARγ, C/EBPα and Fra1 was conducted under following conditions:

qPCR: initial denaturation, 94 °C, 2.5 min → 35 cycles of PCR amplification: denaturation, 94 °C, 30 s → annealing, 62 °C, 40 s → elongation, 72 °C, 1 min → final elongation, 72 °C, 10 min → cool off, 4°C, ∞

The PCR products were loaded according to the dilution step from left to right onto a 2 % agarose gel beginning with undiluted sample and ending with the most diluted sample. To analyze the expression level of PPARγ, C/EBPα and Fra1 the last dilution step that shows a visible band in the gel in the dilution series for HPRT was compared with the last dilution step that shows a visible band in the gel in the dilution series for the analyzed gene. It is therefore possible to compare in two samples the relative expression level of a given gene compared to the housekeeping gene HPRT.

4.2.8. Agarose gel electrophoresis

To prepare a 1 % agarose gel 1 g agarose were dissolved in 100 ml 1x TAE buffer. The solution was boiled using a microwave until it got clear. The solution was left to cool down for several min and 3.5 µl Ethidiumbromid were added. The solution was mixed and subsequently filled into an agarose gel tray. Finally, combs with 20 teeth each were put into the liquid gel solution. 2 µl of an Orange G loading buffer were added to each sample and the agarose gel was loaded with 20 µl of this mix. 1x TAE buffer was used as separation buffer per gel tank. The gels were run at 120 V and 90 mA for approximately 20 min or longer depending on the size of the PCR product and the pore size of the agarose gel. After the PCR products were separated in the agarose gel, intercalated Ethidiumbromid was visualized by UV light using a gel documentation system consisting of a camera, an imaging caption computer (Cybertech) and an UV light table (PeqLab). A print of the gel pictures was taken with a Type P90 printer (Mitsubischi).

4.2.9. PCR - Quantitative Real-Time PCR (QRT - PCR)

To determine the expression of HPRT, PPARγ, C/EBPα, Pref-1, Sox9, Runx2, Osx1, aP2, Glut4 and MyoD in more detail, QRT-PCR were conducted using a Roche LightCycler® 2.0 System. The kit LightCycler® 480 SYBR Green I Master was used for this method. It comprises of a ready to use master mix containing FastStart TaqDNA

polymerase, reaction buffer, dNTPmix (with dUTP instead of dTTP), SYBR Green I dye and MgCl$_2$. The used primers (TIB Molbiol Syntheselabor GmbH) were applied as 100 µM stock solution and diluted 40 fold in the reaction mix to a final concentration of 2.5 µM. Reaction mix for one sample using QRT-PCR:

> 5 µl ready to use master mix
> 0.25 µl forward primer [100 µM]
> 0.25 µl reverse primer [100 µM]
> 1 µl cDNA sample
> 3.5 µl H$_2$O PCR grade

The ready to use mastermix and the water of the kit as well as the primers were mixed together according to the number of samples. Every sample was measured with one replicate. The required numbers of LightCycler capillaries (Roche) were put into centrifuge adapters on an aluminium cooling block (Roche). 9 µl of the previous prepared reaction mix solution was transferred into each capillary 1 µl cDNA sample was added on top. For the negative control 1 µl of PCR grade water was added instead of cDNA. The capillaries were closed with appropriate lids and transferred into a centrifuge type Biofuge Fresco (Hereaus). The reaction mixes were spun down at 2000 g for 1 min. and measured in the LightCycler. The QRT-PCR for HPRT, PPARγ, C/EBPα, Pref-1, Sox9, Runx2, Osx1, aP2, Glut4 and MyoD was conducted under the following conditions using the software LightCycler 3 (Roche):

QRT-PCR: Initial denaturation: 95 °C; hold time 10 min; slope 20 °C/ sec, amplification: 45 cycles comprised of denaturation step 95 °C; hold time 10 sec; slope 20 °C/ sec, primer annealing step: 64 °C; 10 sec; slope 20 °C/ sec; elongation step: 72 °C; 10 min, melting of PCR products: 1 cycle comprised of 2 steps first 95 °C 10 sec; slope 20 °C/ sec and second 50°C 20 sec; slope 20 °C/ sec, cooling step: 40 °C for 30 sec; slope 20 °C/ sec.

Primer sequences for the analysis of the genes PPARγ, C/EBPα, Pref-1, Glut4 and MyoD using the described LightCycler protocol were generated using the NCBI Nucleotide database and the online program Primer 3 created by Steve Rozen and Helen Skaletsky from Whitehead Institute for Biomedical Research.

4.3 Protein chemistry

4.3.1. Isolation of total protein using SDS Sample buffer

The cells were cultured in 100 mm tissue culture dishes. 6 x 105 cells were seeded per dish and cultured until confluence. The culture media was sucked off and the cells were washed twice with cold PBS. 0.5 ml SDS sample buffer was added, the cell were scraped with a cell lifter and transferred into a 1.5 ml reaction tube. The samples were boiled while shaking at 95 oC for 10 min. Subsequently, the samples were spun down at room temperature at 13000 g for 1 min. 40 µl of the total extract were separated by means of SDS PAGE each time. The samples were loaded on SDS gel and Western Blot analysis was carried out. The supernatant can also be stored at - 20 °C.

4.3.2. Isolation of total protein with Frakelton Buffer

The cells were cultured in 100 mm tissue culture dishes. 6 x 105 cells were seeded per dish and cultured until confluence. The culture media was removed and the cells were washed twice with cold PBS. 0.75 ml of complemented Frakelton Buffer was put onto the cells. The cells were scraped using a cell lifter and the suspension was transferred into a 1.5 ml reaction tube. After 30 min incubation on ice at 4 °C room temperature, the suspension was spun down for 20 min at 13000 g and 4 °C. The supernatant was transferred into a fresh 1.5 ml reaction tube and stored at - 20 °C until measurement of protein concentration and Western Blot analysis were carried out. 40 µl of the total extract were separated by means of SDS Page each time.

4.3.3. Extraction of cytoslic and nuclear proteins

The necessary volume of Buffer A and Buffer B was calculated and the supplements PMSF, Protease inhibitor cocktail, Sodium vanadate, Okadaic acid, Spermine and Spermidine were added. The cells were cultured in 100 mm tissue culture dishes. 6x 10^5 cells were seeded per dish and cultured until confluence. The culture media was sucked off and the cells were washed twice with cold PBS. The cells were scraped using a cell lifter and transferred to a 1.5 ml reaction tube. Afterwards, the cells were spun down shortly at 4 oC and the supernatant was removed. Cells were

resuspended in 450 µl Buffer A and incubated on ice at 4 °C for 15 min. Afterwards, 25 µl of 10 % NP-40 were added to each tube. The tubes were mixed using a vortex mixer for 10 sec and spun down for 30 sec at 12000 g and 4 °C (centrifuge 5415 C, Eppendorf). The supernatant that contains the cytosolic fraction was transferred into another tube. The remaining pellet was resuspended in 50 µl Buffer B, vortexed for 15 min at 4 °C and spun down with 12000 g at 4 °C for 5 min using the same centrifuge. The supernatant that contains the nuclear fraction was transferred to a new tube. All protein extracts were stored at -80 °C until their analysis. 40 µl of the cytosolic and nuclear extract were separated by means of SDS Page each time.

4.3.4. Measurement of protein concentration with Micro BCA™- working reagent

The following formula was used to specify the total volume of working reagent required: (Number of standards + number of unknown samples) × (number of replicates) × (150 µl of working reagent per sample) = total volume working reagent required. Two replicates of each standard dilution and of each sample were measured. The working reagent was prepared by mixing 25 parts of Micro BCA™ Reagent MA and 24 parts Reagent MB with 1 part of Reagent MC (25:24:1, Reagent MA:MB:MC). The working reagent is stable for one day when stored in a closed container at room temperature. 150 µl of each standard or unknown sample were pipette into 96 wells microplate. Altogether two replicates were measured of each sample. 150 µl of the working reagent were added to each well and mixed thoroughly on a plate shaker for 30 seconds. Subsequently, the plate was covered and incubated at 37 °C for 2 hours. The plate was cooled down to room temperature and the absorbance was measured at 562 nm using a microplate reader type Spectra Max 190 (Molecular devices). The average 562 nm absorbance reading of the Blank standard replicates were subtracted from the 562 nm reading of all other individual standard and unknown sample replicates. A standard curve was prepared by plotting the average Blank-corrected 562 nm reading for each BSA standard vs. its concentration in µg/ ml.

4.3.5. Preparation of SDS Page

The glass plates were cleaned with 70 % Ethanol. The slab gel unit of the used Gel Wrap® Casting System (C.B.S. Scientific) was assembled with the glass sandwich

set in the casting mode using 1.5 mm spacers. The ingredients for an 8.5 % or 10 % running gel were put together, mixed and transferred into the gel casting chamber using a glass pipette. The glass chamber was gently filled with the solution by allowing the solution to run down the side of one of the spacers without introducing air bubbles. To equalize the surface and remove bubbles on the top of the gel, water was added at the side of the chamber. A comb was added to prevent oxygen reaching the gel. The solution was left to polymerize for 30 min and the water was poured off and left to dry for 15 min. A 4 % stacking gel was prepared using the ingredients listed in the materials part and added on top of the running gel. A comb was added to form sample wells and the gel was left to polymerize for another 30 min. A comb with 15 teeth forming sample wells of 80 µl volume was used.

4.3.6. SDS Page electrophoresis

The silicone gasket and the comb were removed from the used gel casting chamber. The SDS PAGE slab gel system (C.B.S. Scientific) was assembled fixing the gel casting chamber to the slab unit with the designated clamps following the manufacturer's directions for assembly. 1x SDS running buffer was filled in the two chambers above and below the fixed slab gel. To prepare protein samples, the volume of the protein extract to load a given amount of protein was calculated. This volume was transferred into 1.5 ml reaction tubes and topped up with protein extraction buffer and 10 µl of 6x loading buffer to a final volume of 70 µl. The samples were then boiled at 95 °C for 5 min and spun down shortly and loaded into the wells of the stacking gel as well as 8 µl Molecular weight marker pre stained protein. 10 µl 6x loading buffer were transferred into the 2 wells at each extremity of the gels in order to get a regular running of the samples. The separation of the samples was conducted over night at 32 V. The application of the current was continued until the tracking dye reached the bottom of the running gel. The stacking gel was cut off as well as the band of the tracking dye. The gel was transferred to a container filled with distilled water and was subsequently used for western blot.

4.3.7. Semi-dry transfer of SDS Page

The separated proteins transferred from the SDS Page onto a nitrocellulose membrane using a transfer chamber for Western Blot type Multiphor II (Pharmacia Biotech). The electrodes were gently cleaned with a water soaked tissue. The gel was washed in water while four layers of Whatman filter papers grade 1F/ 200 x 250 were soaked in transfer buffer and put on the anode electrode. The nitrocellulose membrane was soaked with water, afterwards with Transfer Buffer and was put on the stack of soaked filter paper. The gel was put on top. Another four layers of filter papers were soaked in transfer buffer and put on the gel. A little amount of transfer buffer was poured onto the stack. The device was closed by putting the cathode electrode on the top and closing the lid. The transfer chamber was connected to the power supply and the transfer was conducted using a constant current of 110 mA for 2 hours.

4.3.8. Western Blot

After the semi-dry transfer, the membrane was washed gently in distilled water to get rid of the SDS. The marker bands were marked with a pen. The proteins on the membrane were then visualized by incubation in Ponceau S (0.2 % in 3 % TCA) solution for 5 min in order to detect any defect in the quality of the transfer (bubbles or irregular transfer). The Ponceau S solution was washed off in distilled water. The membrane was then incubated in 50 ml TBS-T washing solution containing 10 % milk powder (blocking solution) for one hour to saturate unspecific binding sites on the membrane. The membrane was washed in TBS-T washing solution for 15min and subsequently incubated with the primary antibody diluted in TBS-T solution over night at 4 °C, under mild agitation. The primary polyclonal Fra1 antibody was used in a 1000 fold dilution; the primary monoclonal β-Actin antibody was used in a 5000 fold dilution and the primary polyclonal antibody to detect Glucocorticoid receptor proteins was used in a 500 fold dilution. After the incubation with the primary antibody, the membrane was washed in TBS-T for 30 min. Followed by incubation with the appropriate secondary antibody diluted in TBS-T for one hour at room temperature. For the detection of the polyclonal Anti-Fra1 and Anti-Glucocorticoid receptor antibodies, an Anti Rabbit IgG HRP Conjugate was used as a 20000 fold dilution. For the detection of the monoclonal β-Actin antibody, an Anti-Mouse IgG HRP Conjugate was used as a 10000-fold dilution. This step was followed by three washing steps in TBS-T, the first one for about 1 hour and the

other times for 15 min. The identification of the proteins the primary antibody reacted with was carried out using the ECL Western Blot Detection Reagent Kit (Amersham Biosciences). 1 ml of Reagent 1 and Reagent 2 was pipette on a piece of cling film and mixed. The membrane was put on the solution the proteins facing the ECL. The solution was equally distributed by capillarity between the cling film and the membrane. After an incubation of 1 min the excess of ECL was quickly removed, the membrane was enwrapped in dry cling film and transferred to a Hypercassette TM for Western Blot detection (Amersham). The chemiluminescence is stable for about 30 min. In a darkroom a Scientific Imaging Film X-OMATTM 18x24cm was exposed for 1 min on the membrane while in the closed HypercassetteTM. The film was processed using a film processing device type Optimax 2010 (Protec). Depending on the determined signal strength, another film was exposed for longer or shorter time until the wished intensity of the protein band was reached. The bands of the molecular weight marker were copied onto the exposed film for the analysis of the molecular weight of the detected protein bands. The membrane was enwrapped in cling foil to prevent it from running dry. It was stored at 4 °C.

4.3.9. Stripping of the Western Blot

The amount of the protein β-Actin served as loading control in the Western Blot analysis. For the detection of β-Actin it was necessary to get rid of the antibodies of the previous protein detection by stripping them off. The stripping was carried out with a pre-warmed Stripping Buffer to 50 °C in a water bath. The nitrocellulose membrane was incubated in the warm stripping buffer for 5 min shaking. After this step the Western Blot detection protocol was preceded starting from the blocking step.

4.4 Histology

4.4.1. Bone and tissue collection

The mice were sacrificed by cervical dislocation and subsequently the fat pads, the spleens, the hearts and the livers were dissected. Bone and organ tissues were fixed in 3.7 % formaldehyde/ PBS at 4 °C. After fixation, the bone samples were decalcified with 5 % EDTA (pH 7.25) for 10 days at room temperature. Decalcified sampled were

dehydrated according standard protocols in increasing alcohol gradients and Xylol and finally embedded in paraffin. Samples were cut with a microtome (Leica) to obtain 2 - 4 µm thick sections.

4.4.2. Bone histomorphometry

For bone histomorphometry vertebral bodies were fixed overnight at 4 °C in 3.7 % formaldehyde. Samples were dehydrated as mentioned above and subsequently treated with infiltration solution. Acrylatpolymerization was performed overnight at 4 °C. Sections of 3 - 12 µM thickness were obtained by using a microtome. Prior staining, sections were incubated 3x 10 min with 2-(Methoxyethy)-acetate (Sigma) and afterwards re-hydrated. Von Kossa staining was performed according the following protocol:

> 5 min in Silvernitrate (3 %)
> 10 min in dH20
> 5 min in Sodaformol
> 10 min in tap water
> 5 min in Sodiumthiosulfate (5 %)
> 10 min in tap water
> 20 min in van Gieson solution
> Dehydration in alcohol gradients with final step in Xylol
> Mounting in DPX (Sigma)

Bone mineral density and trabecular thickness were quantified according standardized protocols with the OsteoMeasure histomorphometry system (OSTEOMETRICS Inc.),

4.4.3. Oil Red O staining

Oil Red O staining dissolved in Isopropanol was kept overnight at room temperature, filtered, mixed with distilled water, kept overnight in the cold, and finally filtered twice before use. The final staining solution was 0.2 % Oil Red O in 60 % Isopropanol (working solution). Cells were washed twice with PBS and fixed with 10 % neutral formalin for at least 1 h at room temperature. The cells were washed twice with water, and then stained for 2 h with the Oil Red O working solution. The cells were washed, counterstained with Mayer's Hematoxylin solution, washed exhaustively with water, and the excess water was evaporated by placing the stained culture at room

temperature. The stained cells were observed under a microscope and photographed using phase contrast microscopy.

4.4.4. Hematoxylin and Eosin (H&E) staining of paraffin sections

The prepared paraffin sections were dried in a 70 °C incubator for 15 min. The paraffin was unhinged in Xylol for 5 min and the sections were washed in Xylol. After that, the sections were washed in absolute Ethanol, then in 95 % and 70 % Ethanol and finally twice in aqua dest. The sections were covered with Mayer´s Hematoxylin staining solution for 4 min. After the staining the sections were washed in warm tap water for 4 min. Following, they were stained in Eosin for 4 min and washed again in warm tap water. In conclusion, the sections were washed twice in aqua dest, in alcohol (70 % and 95 % absolute) and in Xylol. The sections were mounted before taking a photo.

4.4.5. Masson–Goldner–Tricolor (MGT) staining

The prepared parafin sections were dried in a 70 °C incubator for 15 min. The paraffin was unhinged in Xylol for 5 min and the sections were washed in Xylol. After that, the sections were washed in absolute Ethanol, then in 96 % and 70 % Ethanol and finally twice in aqua dest. The sections were covered with Weigert staining solution (Chroma; Eisenhematoxylin nach Weigert) for 1 min and differentiate in 0.5 % HCl - Ethanol. After the staining the sections were washed in warm tap water. Following, sections were stained in Ponceau S for 15 min and twice in 1 % Acetic acid. Followed by Orange G 5 min, twice in 1 % Acetic acid, Lichtgruen (Chroma) 1 – 2 min, twice in 1 % Acetic acid and fixed with a brief wash 96 % Ethanol. The tissue was cleared by incubation in Xylol and coverslipping with Kanadabalsam.

4.4.6. Elastica van Gieson (EvG) staining

The prepared parafin sections were dried in a 70 °C incubator for 15 min. The paraffin was unhinged in Xylol for 5 min and the sections were washed in Xylol. After that, the sections were washed in absolute Ethanol and 80 % Ethanol. The sections were covered with Resorcin - Fuchsin staining solution (Chroma) for 30 min and destained with 0.5 % HCl in ethanol. After the staining the sections were washed in warm tap water. Following, they were stained in Weigert´s staining solution (Chroma) for 1 min and destained with 0.5 % HCl in ethanol. Sections were washed for 5 min in tap water and

_____

stained in Pikrofuchsin (Chroma) for 2 min. In conclusion, the sections were washed twice in 96 % Ethanol, twice in absolute Ethanol and in Xylol. The sections were mounted with Kanadabalsam.

4.4.7. Cryosection of spleen tissue

Cryosection was performed applying a Microm HM 500 OM cryostat adjusted to a box temperature of - 20 °C and an object temperature of - 17 °C. Frozen tissue samples were first allowed to adjust to the box temperature by leaving them untouched in the box for about fifteen minutes. Cryosections of a thickness of 7 – 9 µm were cut and picked up onto Superfrost Plus glass slides (Roth). Tissue sections were air-dried for about one hour at room temperature and subsequently fixed in fresh cold acetone for ten minutes. After complete evaporation of acetone, slides were stored at - 70 °C.

4.4.8. Standard protocol for immunofluorescence staining

Splenic cryosections were allowed to thaw at room temperature for about five to 10 minutes before they were encircled with a grease pen (Dako pen, Dako). Prior to staining with various antibody combinations (Table 3.1), unspecific binding was prevented by blocking the sections in PBS/ 3 % BSA. Likewise, all antibodies were diluted in PBS/ 3 % BSA. For direct immunofluorescence staining sections were incubated with diluted fluorescent dye conjugated primary antibodies for about 30 min, extensively washed in PBS and then mounted with Fluoromount-G (Southern Biotech). In case of indirect immunofluorescence staining, un-conjugated antibodies were detected using fluorescent dye conjugated secondary antibodies and incubated in the dark for another 30 min. Sections were washed in PBS and coverslips were mounted with Fluoromount-G (Southern Biotech). Before examination mounted sections were allowed to air-dry for at least two hours.

Specificity	Source	Dilution
B 220 : Alexa 488	rat, clone RA3.6 B2 (DRFZ)x	1:50
B 220 : dig	rat, clone RA3.6 B2 (DRFZ)x	1:100
CD 41	rat (Dako)	1:50
FDC - M2 : bio	rat, clone FDC-M2 (ImmunoK)	1:200
MOMA-1	rat (Southern Biotech)	1:100
SA-Rhodamin	Moleculare Probes	1:500
SA-Alexa 488	Moleculare Probes	1:500
Anti-dig – cy5	DRFZ	1:500
Anti-dig – Alexa 546	DRFZ	1:300
DAPI	Moleculare Probes	1:10000

_____

Survey of antibodies applied for immunofluorescence staining. The x labelled antibodies were purified from B cell hybridoma culture supernatants and conjugated to fluorescent dyes in the DRFZ.

4.4.9. Standard protocol for immunohistochemistry

For immunohistochemistry staining with the DakoCytomation LSAB+System-HRP, sections were re-hydrated in decreasing alcohol gradients. Epitopes were unmasked by boiling the samples in citrate buffer (10 mM, pH 6.0) for 10 min. After cooling down, samples were blocked in 3 % hydrogen peroxide for 5 min at room temperature. Sections were washed in PBS and incubated with primary antibody in PBS/ 0.1 % Triton X 100 + 1 % FCS for 30 min at room temperature. After 3 times washing in PBS, linker solution was added and incubated for 15 min at room temperature. Sections were washed 3 times with PBS and incubate with substrate solution for 5 min. Negative controls included omission of primary antibodies. The samples were coverslipped in Kaisers Glyceringelatine (Merck) and examined by microscopy at 400x magnification.

Specificity	Source	Dilution
Fra1 (R-20)	rabbit, sc-605 (Santa Cruz)	1:10
BP3	Present by Max Cooper	1:50
B 220 : bio	rat, clone RA3.6 B2 (DRFZ)	1:200
FDC - M2 : bio	rat, clone FDC-M2 (ImmunoK)	1:400
MOMA-1	rat (Southern Biotech)	1:200
SA-alkalic phosphatase	Sigma	1:500
HistoRed AP - Substrate Kit	Linaris	

4.5 Statistics

The statistical significance of the difference between different data sets was tested using an unpaired two tailed t-test with a threshold chosen for statistical significance of $p = 0.05$. Statistical significance is indicated by asterisks using one asterisk for low significance and three asterisks for high significance. All listed data are derived from three independent experiments and are expressed as mean + SD unless otherwise noted.

5.   Results

Several genetic studies in mice have demonstrated the central role of the transcription factor AP-1 in the control of both osteoblast and osteoclast differentiation. Thus, the various components of transcription factor AP-1 play specific roles in bone cells differentiation. In particular, mice overexpressing the Fos-related protein-1 (Fra1) develop osteosclerosis due to accelerated osteoblast differentiation. Furthermore, specific posttranscriptional modifications like phosphorylation through kinases modulate the activities of each AP-1 member. As already shown by David et al., 2005, in c-Fos overexpressing mice the kinase Rsk2 plays an essential role in c-Fos-dependent osteosarcoma development [19]. In addition, Rsk2 is an important regulator of osteoblast biology [19, 35]. To analyze the role of Rsk2 in regulating Fra1 functions in bone cells, mice overexpressing Fra1 and Rsk2-deficient mice were crossed.

5.1   Mice nomenclature

In the following text, the C57/Bl6 control wild type mice are designated wt for both males and females. Mice with genetic inactivation of the Rsk2, which is located on X-chromosome, are designated rsk2-/y for rsk2 knockout males and rsk2-/x for heterozygote deletion of Rsk2 in females; the fra1 transgenic mice (H2-fra1-LTR) are designated fra1-tg for males and females. The double mutated mice produced from the crossing between fra1-tg males and rsk2-/x females with are designated fra1-tg/rsk2-/y for the males or fra1-tg/rsk2-/x for the females.

5.2   Vital parameter analysis: body growth, body weight and lifespan

5.2.1.   Decreased genotype frequency of fra1-tg mice lacking Rsk2

In order to analyse the role of Rsk2 in the development of Fra1-induced osteosclerosis, mice overexpressing Fra1 and rsk2-/x mice were crossed. The distribution of the genders was well balanced. From a total off 248 littermates were born 137 males and 111 females. That makes a ratio of 55 % off males and 45 % off females. The various genotypes (wt, rsk2-/y, rsk2-/x, fra1-tg, fra1-tg/rsk2-/y and fra1-tg/rsk2-/x)

resulting from the crossing were born with different frequency. A mild discrepancy appeared between the frequencies of the female genotypes. Clear differences were observed when male offspring were compared. A mild reduction for fra1-tg male and female newborns, but mice carrying the double mutation, fra1-tg/rsk2-/y or fra1-tg/rsk2-/x, were born in a clear decreased frequency. This phenomenon was pronounced in fra1-tg/rsk2-/y male (Table 5.1).

Table 5.1 Statistical distribution from crossing fra1-tg males with rsk2-/x females

male	wild type	rsk2-/y	fra1-tg	fra1-tg/rsk2-/y	total
littermate	42	51	26	18	137
%	31%	37%	19%	13%	100%

female	wild type	rsk2-/x	fra1-tg	fra1-tg/rsk2-/x	total
littermate	29	38	23	21	111
%	26%	34%	21%	19%	100%

5.2.2. Rsk2 modulates Fra1-dependent suppression of body growth

Figure 5.1 A shows representative pictures of wt, rsk2-/y, fra1-tg and fra1-tg/rsk2-/y males at the age of 7 weeks. The growth of fra1-tg/rsk2-/y mice was severely retarded. To analyze the growth retardation of fra1-tg/rsk2-/y mice the vertebral body size was employed as a measurement of the longitudinal growth. The size study was based on the analysis of 6 wt, 5 rsk2-/y, 8 fra1-tg and 4 fra1-tg/rsk2-/y littermates. Significantly smaller vertebral bodies were observed in fra1-tg/rsk2-/y mice in comparison to all the other genotypes, indicating a decrease in longitudinal growth of the body: wt vs. fra1-tg/rsk2-/y **$P=0.0018$, rsk2-/y vs. fra1-tg/rsk2-/y **$P=0.0022$ and fra1-tg vs. fra1-tg/rsk2-/y ***$P=0.0006$ (Figure 5.1 B).

These data show that the absence of Rsk2 combined to Fra1 overexpression causes a drastic decrease of the longitudinal growth of the body in mice.

5.2.3. Rsk2 modulates Fra1-dependent suppression of body weight

The body weight was measured as an evaluation of the growth of the mice. The body weight study of 7 weeks old males was based on the analysis of 24 wt, 39 rsk2-/y, 22 fra1-tg and 19 fra1-tg/rsk2-/y mice. While no significant difference was found between wt and rsk2-/y mice at this age, a mild but significant reduction in the body weight was observed in the fra1-tg mice confirming previous published observations [19, 52]. At seven weeks of age, the weight of fra1-tg/rsk2-/y mice was approximately half of the weight of the wt littermates and so significantly reduced (Figure 5.1 C).
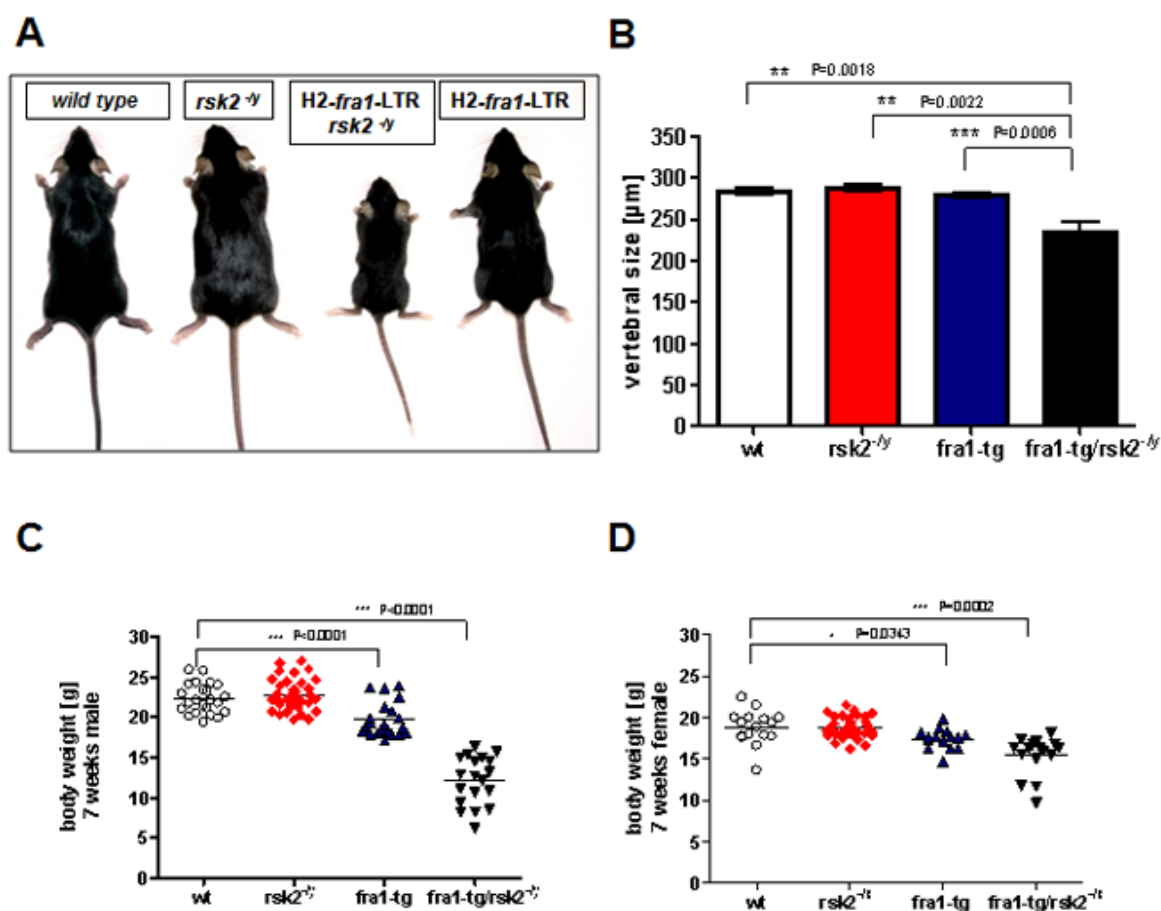
Figure 5.1 Decreased body growth and body weight and in mice overexpressing Fra1

Picture of 7 weeks old male wt, rsk2-/y, fra1-tg and fra1-tg/rsk2-/y mice; B) Measurement of vertebral size of 7 weeks old male wt, rsk2-/y, fra1-tg and fra1-tg/rsk2-/y mice; C) Body weight measurement of 7 weeks old male wt, rsk2-/y, fra1-tg and fra1-tg/rsk2-/y mice; D) Body weight measurement of 7 weeks old female wt, rsk2-/x, fra1-tg and fra1-tg/rsk2-/x mice; Results represent the mean value and error bars indicate standard deviations. Asterisks indicate statistically significant differences.

Figure 5.1 D shows body weight analysis off females based on the analysis of 15 wt, 37 rsk2-/x, 15 fra1-tg and 16 fra1-tg/rsk2-/x 7 weeks old mice. When compared to the wt, the rsk2-/x females showed no difference in body weight. In contrary, the weight of fra1-tg and fra1-tg/rsk2-/x mice were significantly decreased in comparison to the weight of the wt littermates.

These data confirmed that the growth of Fra1 overexpressing mice was retarded. Furthermore, this effect was enhanced in the absence of Rsk2.

5.2.4. Fra1 overexpression induced weight loss and decreased lifespan

To get a more complete picture of the effect of deleting Rsk2 on the body weight of fra1-tg mice, mice were weighted after weaning (3 weeks old) once a week until the age of 63 weeks. The weight curves and the survival curves were drawn and compared between the different genotypes. The weight and survival data are based on the analysis of 9 wt, 27 rsk2-/y, 12 fra1-tg and 17 fra1-tg/rsk2-/y males and 9 wt, 30 rsk2-/x, 11 fra1-tg and 13 fra1-tg/rsk2-/x females.

In Figure 5.2 A and Figure 5.2 B the weight curves of the male and female parental lines were compared. A slightly but not significant decreased of body weight could be observed in rsk2-/y mice when compared to wt males. Males overexpressing Fra1 displayed a mild but significant reduction in their body weight during their lifespan. In addition, they stopped growing and began to lose weight at the age of 17 to 18 weeks. Males overexpressing Fra1 survived until 28 weeks, and their half-life was approximately 26 weeks (Figure 5.2 C). A mild but not significant mortality was also observed in rsk2-/y mice, whose half-life could not be deduced from the period studied.

The reduction of body weight was more pronounced in fra1-tg/rsk2-/y mice. Their weight was, all along their life, significantly less than all other genotypes. After 12 weeks, the body weight of the fra1-tg/rsk2-/y was drastically dropping until death. Analysing the survival curve of the different strains indicated that none of the fra1-tg/rsk2-/y mice survived more than 20 weeks (Figure 5.2 C). These mice died in three distinct time intervals, the early interval between 3 to 5 weeks of age (25 % of mortality), the second one between 5 to 7 weeks (35 % of mortality) and a late one after 17 weeks of age. The half-life of fra1-tg/rsk2-/y (i.e. the time when 50 % of the mice are dead) was around 9 weeks.

Comparable data were obtained when analysing the wt, rsk2-/x, fra1-tg and fra1-tg/rsk2-/x survival curves of the different female strains in Figure 5.2 D. The females

rsk2-/x weight curve was indistinguishable from the weight curve of the wt (Figure 5.2 B). Similar to the males, Fra1 overexpressing females displayed a mild but significant reduction in their body weight during all their lifespan. Mice stopped growing and began to lose weight at the age of 14 to 16 weeks and their half-life was around 21 weeks. No fra1-tg females survived after 26 weeks. Based on the survival curve of the female fra1-tg/rsk2-/x strains, these mice were comparable to the fra1-tg females. Fra1-tg/rsk2-/x mice did not survived more than 23 weeks and there half-life was 20 weeks.
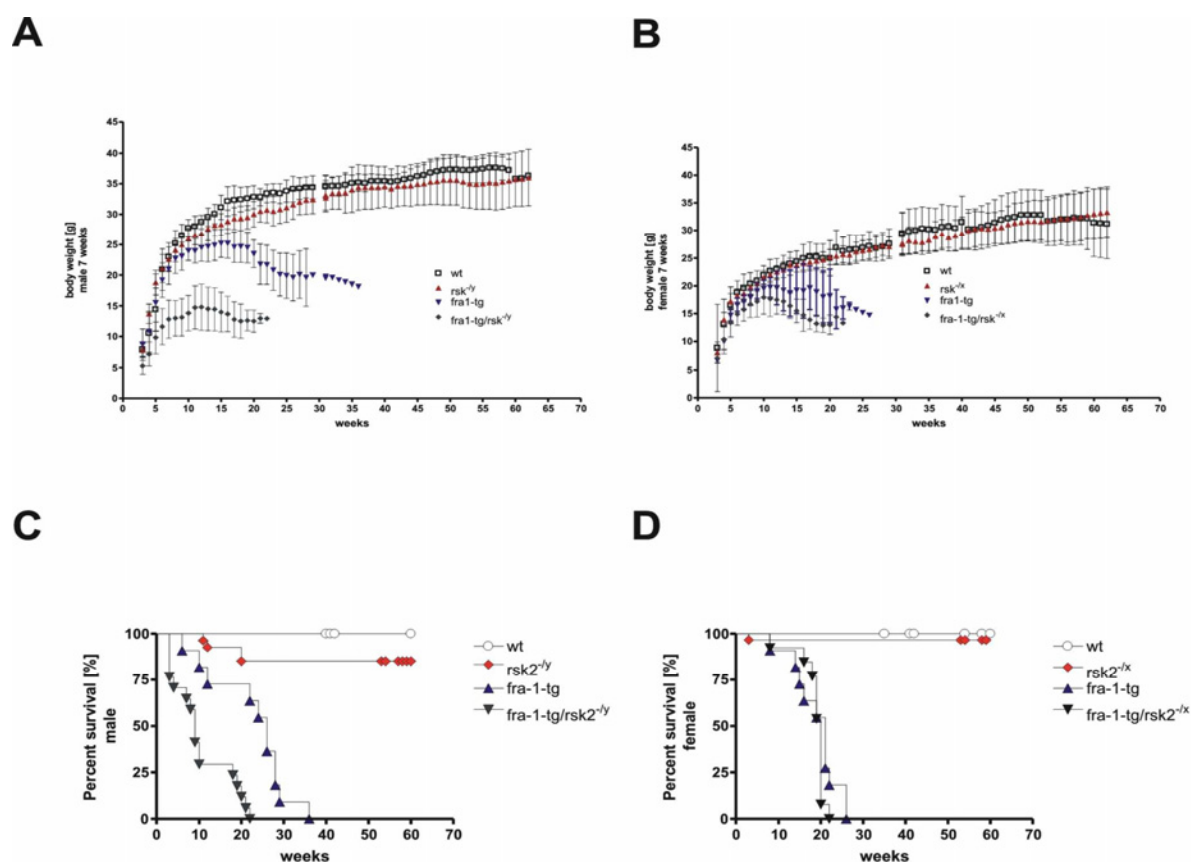
Figure 5.2 Body weight analyses of wt, rsk2-deficient, fra1-tg and fra1-tg/rsk2-deficient mice through lifespan of 63 weeks

A) Body weight analysis of male wt, rsk2-/y, fra1-tg and fra1-tg/rsk2-/y mice; B) Body weight analysis of female wt, rsk2-/x (n=30), fra1-tg (n=11) and fra1-tg/rsk2-/x (n=13) mice; C) Mean survival of male wt (n=9), rsk2-/y (n=27), fra1-tg (n=12) and fra1-tg/rsk2-/y (n=17) littermate mice; D) Mean survival of male wt (n=9), rsk2-/x (n=30), fra1-tg (n=11) and fra1-tg/rsk2-/x (n=13) littermate mice. Error bars indicate standard deviations.

Absence of Rsk2 in fra1-tg/rsk2-/y mice or mosaic expression in some fra1-tg/rsk2-/x littermates affected the body weight, body growth and the survival rate. Thus, Rsk2-deficient mice, which are fra1 transgenic, were severely growth-retarded and succumbed prematurely. Mosaic expression of Rsk2 in fra1-tg/rsk2-/x littermates seemed to affect the weight and growth rate but not survival. The phenotype was already present in the fra1-tg mice albeit milder and not observed in wt or rsk2-/y mice.

These data are indicating that Fra1 overexpression resulted in weight loss and a decreased lifespan, two Fra1-dependet phenomenons (events) that may be regulated by Rsk2.

5.3 Bone and fat analyses

The separates roles of Fra1 and Rsk2 in bone cell differentiation and development has been established. Therefore, further question aroused as to whether Fra1 and Rsk2 could regulate the function of each other in bone. The opposite bone phenotypes between the two mice models, whereby fra1 transgenic mice develop osteosclerosis [52] and Rsk2-deficient mice develop osteopenia [19], supported a potential interaction between Fra1 and Rsk2.

5.3.1. Fra1 induced osteosclerosis is independent of Rsk2

The histology of the bones of 7 weeks old mice were analyzed by Von Kossa staining of un-decalcified sections of spine (upper panel) and tibia (lower panel) (Figure 5.3 A). In this method, the mineralized bone matrix was stained in black, whereas the not yet mineralized osteoid was stained in pink using counterstaining with Hematoxylin. More mineralized matrix could be observed in sections of spine and tibia of bones isolated from fra1-tg mice or fra1-tg/rsk2-/y compared to wt or rsk2-/y mice. No clear difference could be observed when wt and rsk2-/y or when fra1-tg and fra1-tg/rsk2-/y mice were compared, respectively. Histomorphometric analysis for bone volume/total volume (Figure 5.3 B) and osteoid volume/bone volume (Figure 5.3 C) were performed to get a quantitative measurement of the phenotypes. Mild but not significant reductions in rsk2-/y mice BV/TV (15.4±2.0 %) were found compare to wt mice (18.4±1.7 %). The drastic increase of fra1-tg BV/TV (47.4±3.4 %) confirmed the previously published data [52] and

illustrated the strong osteosclerosis that developed in fra1-tg mice. The BV/TV of fra1-tg/rsk2-/y mice (47.4±3.3 %) indicated that Rsk2 inactivation did not correct the increase in bone mass induced by Fra1 overexpression. The OV/BV levels of wt (1.85±1.70 %) and fra1-tg (2.34±0.32 %) were similar. In rsk2-/y mice, the OV/BV levels (3.28±1.45 %) were increased confirming the mineralization defect that was previously described (David et al., 2005). Furthermore, Fra1 overexpression did not correct but rather increased the mineralization defect induced by Rsk2-deficiency (OV/BVrsk2-/y 3.28±1.45 % vs. OV/BVfra1-tg/rsk2-/y 6.87±2.30 %) (Figure 5.3 C) as shown by the increased osteoid areas in fra1-tg/rsk2-/y mice (Figure 5.3 D).

The results show that Fra1 induced osteosclerosis is independent of Rsk2 activity and suggest that Rsk2 and Fra1 are acting independently in bone.

A

wild type   *rsk2* ^{-/y}   H2-*fra1*-LTR   H2-*fra1*-LTR/ *rsk2* ^{-/y}

B

C
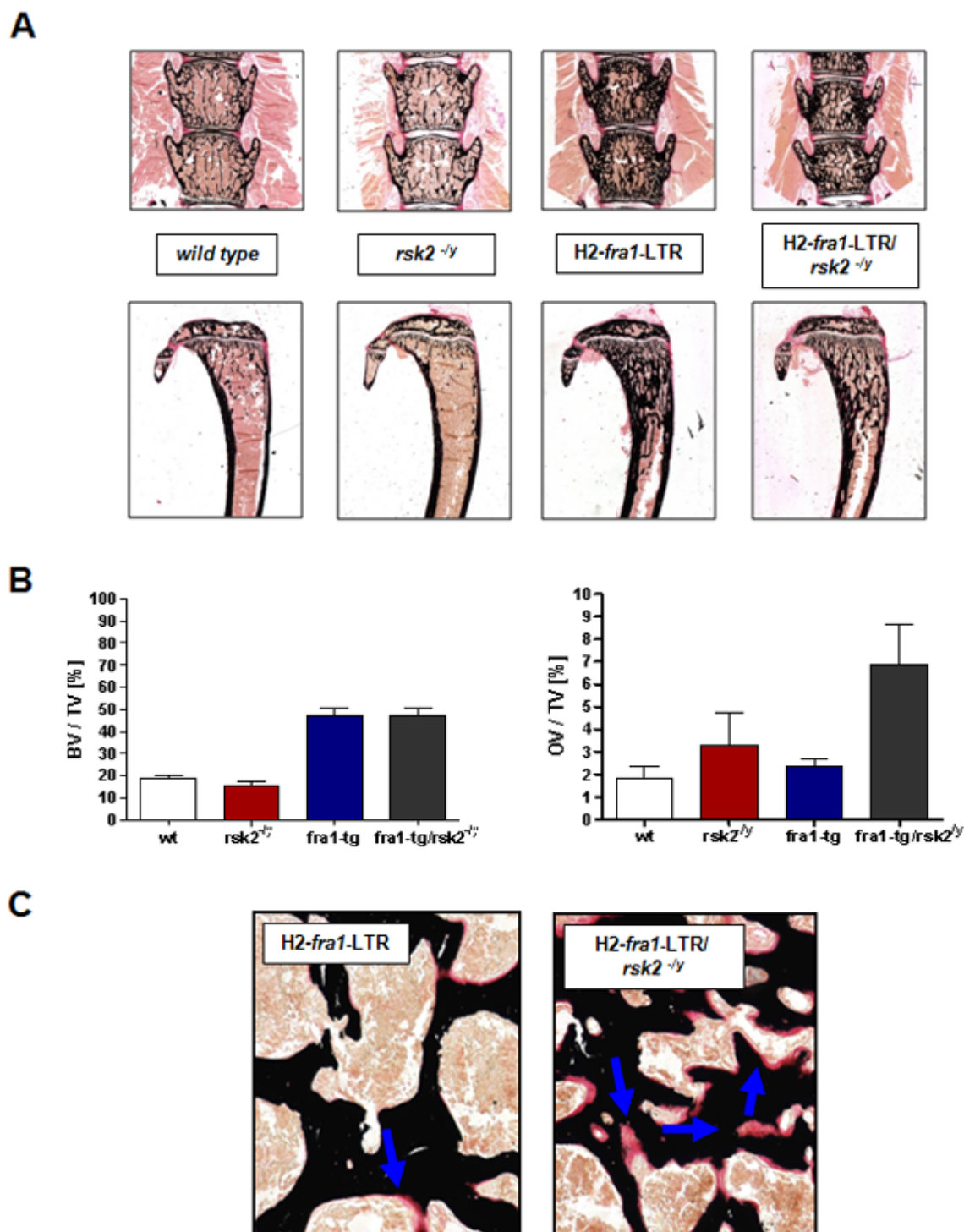
Figure 5.3 Fra1 induced osteosclerosis in bone is Rsk2 independent

Picture of Von Kossa stained bone sections of 7 weeks old male wt, rsk2-/y, fra1-tg and fra1-tg/rsk2-/y mice, mineralized bone is stained in black, top: sections of the spine, bottom: section of the tibia; B) Histomorphological analysis of the bones: index of bone volume (BV) (stained black) rapport to the total volume (TV) and index of osteoid volume (OV) (non mineralized bone matrix) rapport to bone volume (BV); C) Picture of trabecular bone sections, osteoids stained in pink are indicated by the blue arrows; Error bars indicate standard deviations. Asterisks indicate statistically significant differences.

5.3.2. Mice overexpressing Fra1 developed a progressive lipodystrophy

In order to gain insight about the origin of the growth defect and lethality, mice were sacrificed and dissected at 7 weeks or at 18 weeks of age. Surprisingly, the abdominal fat pads were completely absent in 7 weeks old male fra1-tg/rsk2-/y mice. This phenotype was not observed in all of the other age-matched males (Figure 5.4 A). Interestingly, a complete absence of fat pads could also be observed but not in all sacrificed fra1-tg female mice at age of 18 weeks (Figure 5.4 B). These observations indicate that Fra1 overexpression was leading to progressive lipodystrophy, again the phenotype was seen earlier in the absence of Rsk2.

To study the effect Fra1 overexpression and the absence of Rsk2 on the development of fat in more detail, the fat weight/ body weight ratio were calculated in both males and females at 7 weeks and at 18 weeks of age. The fat to body weight comparison data were based on the analysis of 16 wt, 15 rsk2-/y, 12 fra1-tg and 8 fra1-tg/rsk2-/y males at age of 7 weeks; 11 wt, 6 rsk2-/y and 7 fra1-tg males at age of 18 weeks. The female data were generated by analyses of 7 wt, 8 rsk2-/x, 4 fra1-tg and 3 fra1-tg/rsk2-/x females at age of 7 weeks and 12 wt, 5 rsk2-/x, 5 fra1-tg and 2 fra1-tg/rsk2-/x females at age of 18 weeks.

No significant difference in this ratio was observed when 7 weeks wt, rsk2-/y and fra1-tg males were compared (wt: 0.0101 ± 0.0018; rsk2-/y: 0.0110 ± 0.0036; fra1-tg: 0.0089 ± 0.0028; Figure 5.4 C, left panel). A total absence of abdominal fat pad was found in all of the fra1-tg/rsk2-/y mice and, therefore, the fat weight/ body weight ratio could not be calculated and was set to 0 (Figure 5.4 A). At 18 weeks of age, no significant difference could be observed between wt and rsk2-/y males (wt: 0.0174 ± 0.0063; rsk2-/y: 0.0126 ± 0.0067; Figure 5.4 C, right panel). However, a significant difference could be measured between the fat pad weight/ body weight ratio of wt vs. fra1-tg males (wt: 0.0174 ± 0.0063; fra1-tg: 0.0045 ± 0.0038, ***$P<0.0001$).

Similar analyses have been done with females at different ages. No significant difference in this ratio was observed when 7 weeks or 18 weeks old wt and rsk2-/x females were compared (7 weeks/ wt: 0.0090 ± 0.0012; rsk2-/x: 0.0091 ± 0.0034; 18 weeks/ wt: 0.0119 ± 0.0033; rsk2-/x: 0.0120 ± 0.0045; Figure 5.4 D). Nevertheless, the wide dispersion of the measurement data was remarkable in 18 weeks of age rsk2-/x offspring mice. This may be due to the mosaic expression of Rsk2 in the heterozygote females. When fra1-tg females were analyzed, a significant decrease in fat weight/body weight ratio was observed in the 7 weeks old fra1-tg mice (fra1-tg: 0.0056 ± 0.0004, ***$P<0.0001$). When compared to female wt, this difference drastically increased with

age. Indeed, most of the sacrificed fra1-tg females did not have any analyzable fat pads at age of 18 weeks (fra1-tg: 0.0000±0.0000, ***P<0.0001; Figure 5.4 D, right panel). 7 and 18 weeks old fra1-tg/rsk2-/x mice (7 weeks/ fra1-tg/rsk2-/x: 0.0063±0.0072; 18 weeks/ fra1-tg/rsk2-/x: 0.0027) showed the same trend as the fra1-tg females (Figure 5.4 D). Fat pads were drastically reduced or absent in the analyzed mice.

These data indicate that the mice overexpressing Fra1 develop a progressive lipodystrophy, which is more pronounced in females.
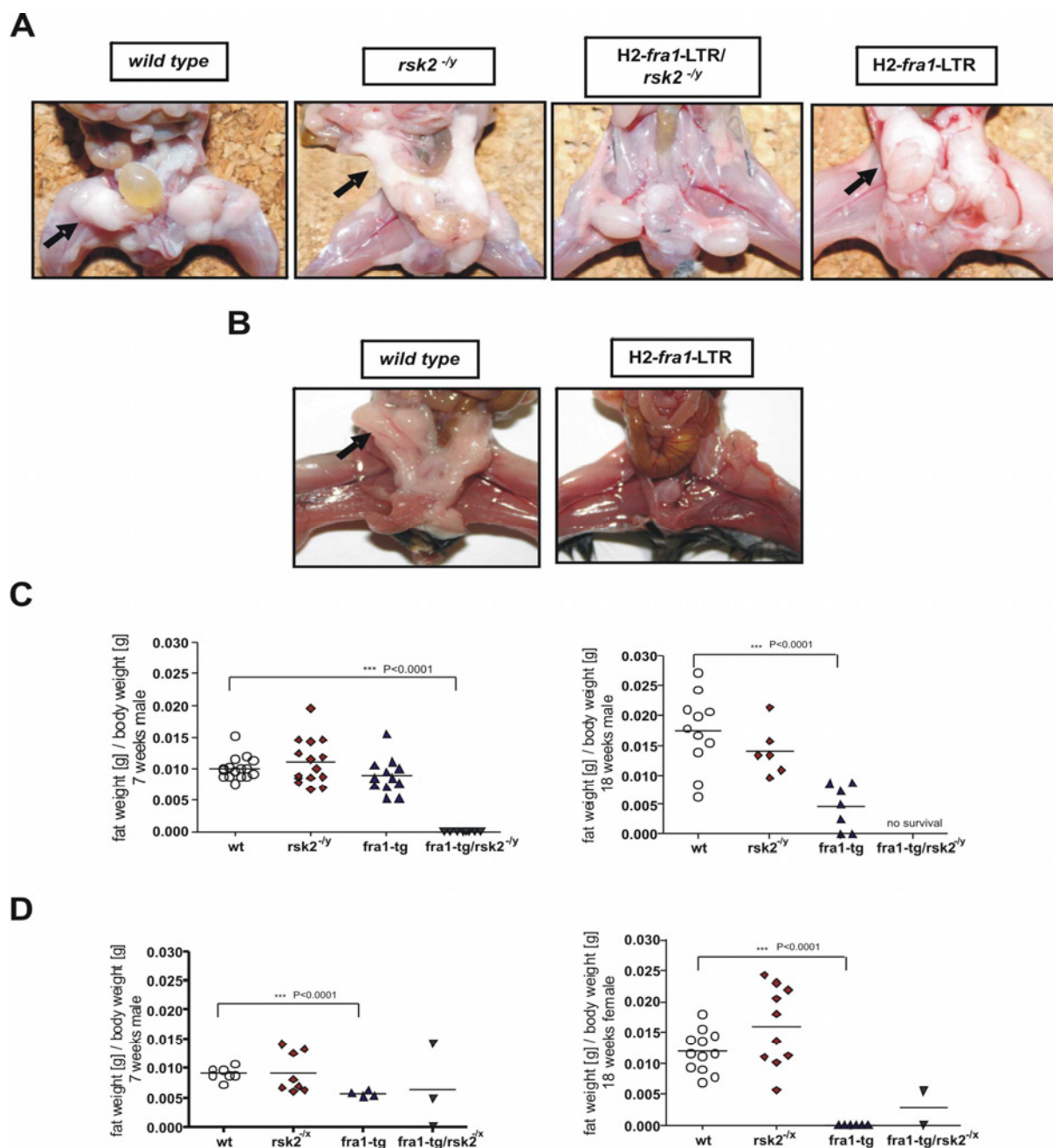
Figure 5.4 Absence of fat pad in Fra1 overexpressing mice lacking Rsk2

A)Dissected abdomen of 7 weeks old male wt, rsk2-/y, fra1-tg and fra1-tg/rsk2-/y mice, arrow indicated white fat pad; B) Abdomen of 18 weeks old females wt and fra1-tg littermates, arrow indicated white fat pad; C) Ration between fat weight and body weight of 7 weeks old and 18 weeks old males wt, rsk2-/y, fra1-tg and fra1-tg/rsk2-/y mice; D) Ratio between fat weight and body weight of 7 weeks old and 18 weeks old females wt, rsk2-/x, fra1-tg and fra1-tg/rsk2-/x mice; Asterisks indicate statistically significant differences.

5.4 Adipocytes analyses in vivo, ex vivo and in vitro

Mesenchymal cells can differentiate in osteoblast, myocytes, chondrocytes and adipocytes. Fra1 overexpressing mice developed progressive lipodystrophy. To determine the cause of the lipodistrophy, the role of Fra1 in adipogenesis was analyzed by in vivo, ex vivo and in vitro experiments. Adipogenesis is a process by which pluripotent mesenchymal cells are differentiating into mature adipocytes. This process involves several steps including an increase in the size of the adipocytes in function of the stage of maturity.

5.4.1. Adipocytes analyses in vivo

5.4.1.1. In vivo: Effect of Fra1 overexpression and absence of Rsk2 on adipocytes size

Histological analyses of cell sizes are an indication of phenotypes that could affect maturity of the cells. To analyze the cell size Hematoxylin and Eosin (H&E) stains of paraffin embedded fat pad sections of 7 weeks and 18 weeks old male and female littermates were done. The following genotypes where analyzed wt mice, rsk2-deficent mice, fra1 overexpressing mice and fra1-tg mice lacking Rsk2.

Figure 5.5 A shows sections of fat pads from males of the various genotypes. While no obvious differences in the size of H&E stained adipocytes were seen between 7 and 18 weeks old wt and rsk2-/y males, a clear decrease in the cell size of 7 weeks old fra1-tg male mice could be observed (Figure 5.5 A). Fra1-tg mice lacking Rsk2 did not have any fat pad that could be analysed. No changes in cell dimensions could be ascertained in 18 weeks old wt and Rsk2-deficient male mice optically. However, the reduction induced by Fra1 was significantly more pronounced in 18 weeks old Fra1 overexpressing mice (Figure 5.5 A).

The cell density was calculated to quantify the decrease of the size of the adipocytes in fra1-tg fat pads. For this, cells contained in define surface were counted (Figure 5.5). The cell densities reported to the wt were expressed in percent (wt = 100 %). No significant differences between 7 weeks old wt fat pads and rsk2-/y fat pads were measured (rsk2-/y = 108.36 %) and between the fat pads of wt and rsk2-/y at 18 weeks of age (rsk2-/y = 88.64 %). A significant increase of 52.60 % at age of 7 weeks and of

107.11 % at age of 18 weeks in the cell densities were observed for fra1-tg males (Figure 5.5 B).

A
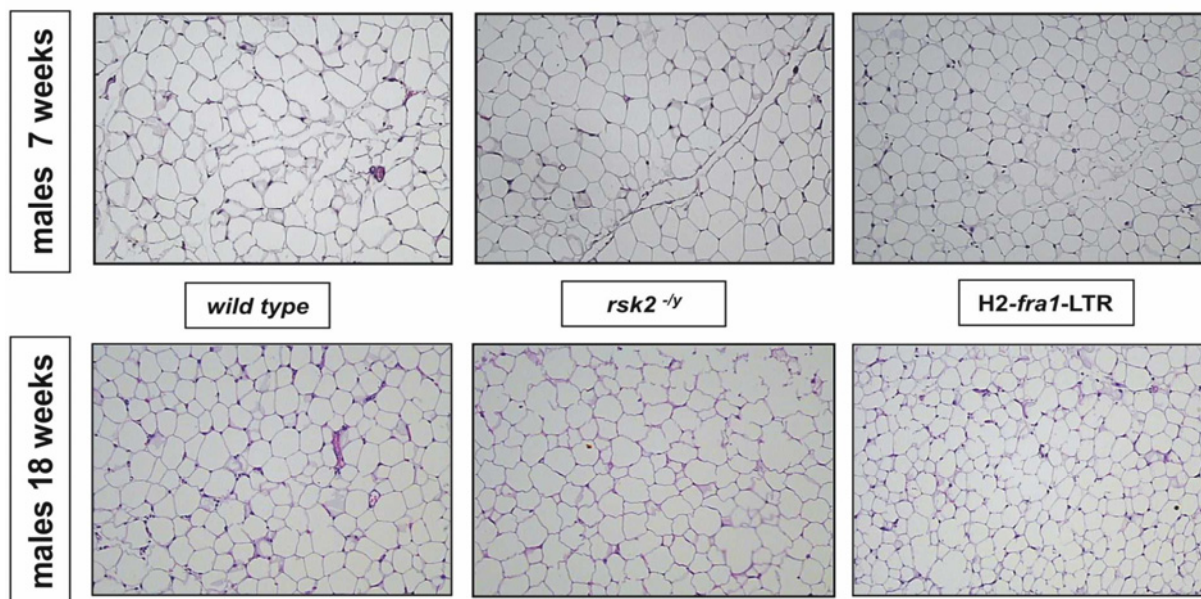
B

Figure 5.5 Fra1 overexpression reduced adipocyte size and cell density in fat pad of male mice

A) Hematoxylin & Eosin (H&E) staining of paraffin embedded fat pad sections of 7 and 18 weeks old male wt, rsk2-/y and fra1-tg mice (phase contrast microscopy, 100x magnifications); B) Cell density in fat tissue of 7 weeks and 18 weeks old male wt , rsk2-/y, fra1-tg and fra1-tg/rsk2-/y (7 weeks = no fat pads; 18 weeks = no survival) mice; Asterisks indicate statistically significant differences.

The adipocytes were also analysed in females at age of 7 and 18 week. The wt, rsk2-/x, fra1-tg and fra1-tg/rsk2-/x mice were compared. In wt and rsk2-/x mice, no differences were visible in the H&E staining but adipocytes also appeared smaller in 7 weeks females fat pad mice of fra1-tg mice (Figure 5.6 A). Analysis of fat pad sections of 18 weeks old females overexpressing Fra1 were not possible, because of a complete absence of fat pads in the ageing fra1-tg females (Figure 5.6 A).

The cell density was calculated in 7 and 18 weeks old females. No significant changes in the density of the cells were measured when wt and rsk2-/x were compared

_____

(wt = 100 %; rsk2-/x = 108.36 %). A significantly increased density was calculated in 7 weeks old fra1-tg females (fra1-tg = 152.60 %; Figure 5.6 B). The data derived from fra1-tg/rsk2-/x mice indicates substantial difference between the littermates (7 weeks = 152.60 % and 18 weeks = 59.77 %). From two 18 weeks old fra1-tg/rsk2-/x mice which were analyzed only one owned fat pads.

These data suggested that Fra1 overexpression in male and female mice led to progressive lipodystrophy most likely due to a block in adipocyte maturation.
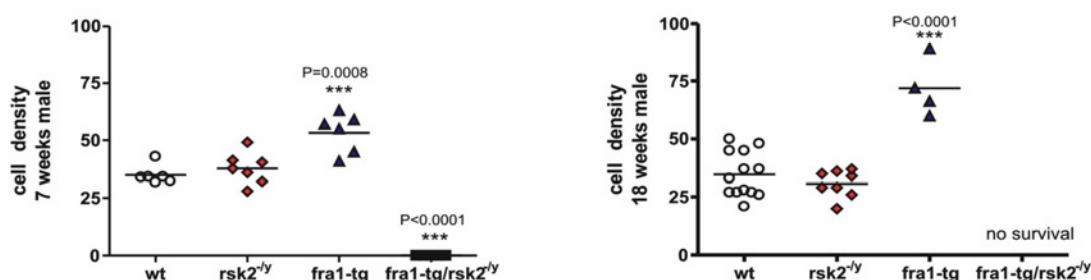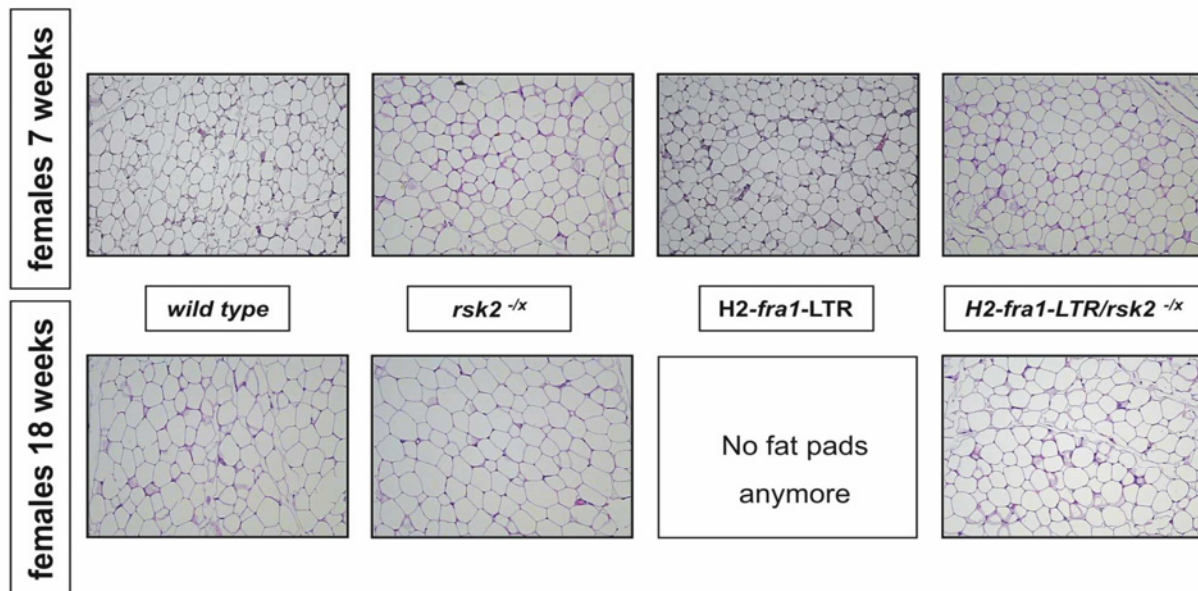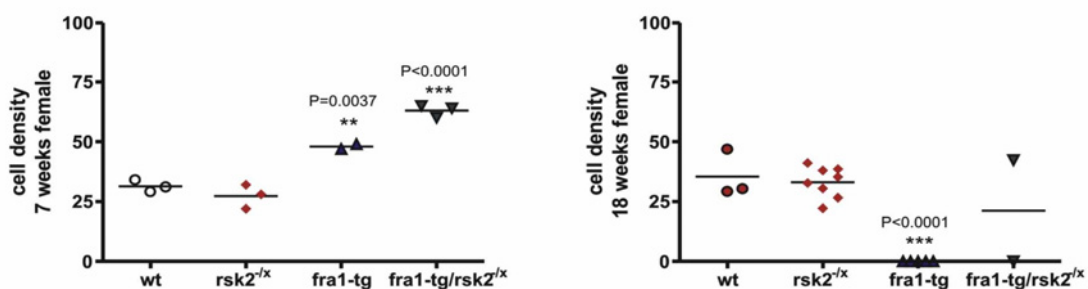

Figure 5.6 Fra1 overexpression reduced adipocyte size and cell density in the fat pad of female mice

A) Hematoxylin & Eosin (H&E) stains of paraffin embedded fat pad sections of 7 and 18 weeks old female wt, rsk2-/x, fra1-tg and fra1-tg/rsk2-/x mice (phase contrast microscopy, 100x magnifications); B) Cell density in fat tissue of 7 weeks and 18 weeks old female wt, rsk2-/x, fra1-tg and fra1-tg/rsk2-/x mice; Asterisks indicate statistically significant differences.

5.4.1.2. In vivo: Fra1 overexpression in abdominal fat pad affects adipogenesis

To determine the cause of the phenotype (fra1-induced inhibition of adipogenesis), markers for fat cell differentiation were analysed by Polymerase Chain Reaction (PCR). The mRNAs were isolated and amplified to cDNA in order to look at Fra1 expression in abdominal fat pads isolated from wt and fra1-tg mice (Figure 5.7 A). Reverse Transcription - PCR (RT-PCR) in fat tissue of 7 weeks old male mice evaluated the expression of endogenous (endo) and exogenous (exo) Fra1 genes. Fra1 (endo) was found to be expressed in the fat pad of wt mice. Fra1 expression was increased in the fat pad of fra1-tg mice due to the expression of the transgenic (exo) gene as revealed by the use of primers specifically amplifying the transgene (Figure 5.7 A).

Expression of adipocyte markers were analysed using mRNAs from abdominal fat pads isolated from 7 weeks, 9 weeks and 18 weeks old wt and fra1-tg mice. Figure 5.7 B show the relative expression of total Fra1 cDNA levels of 7 weeks, 9 weeks and 18 weeks old wt and fra1-tg mice. Very low levels of Fra1 were detected in 18 weeks old wt fat pad, a highest cDNA level was found in 18 weeks old fra1-tg fat pad. Thus, Fra1 expression was increasing with age.

Adipocyte differentiation is associated with expression of several adipocyte-specific genes including Glut4 and aP2. The levels of expression of Glut4 and aP2 were determined in the fat pad of fra1-tg mice compared to wt mice. The expression of both was found to be decreased in fra1-tg mice (Figure 5.7 C) confirming that Fra1 overexpression was decreasing fat maturation.
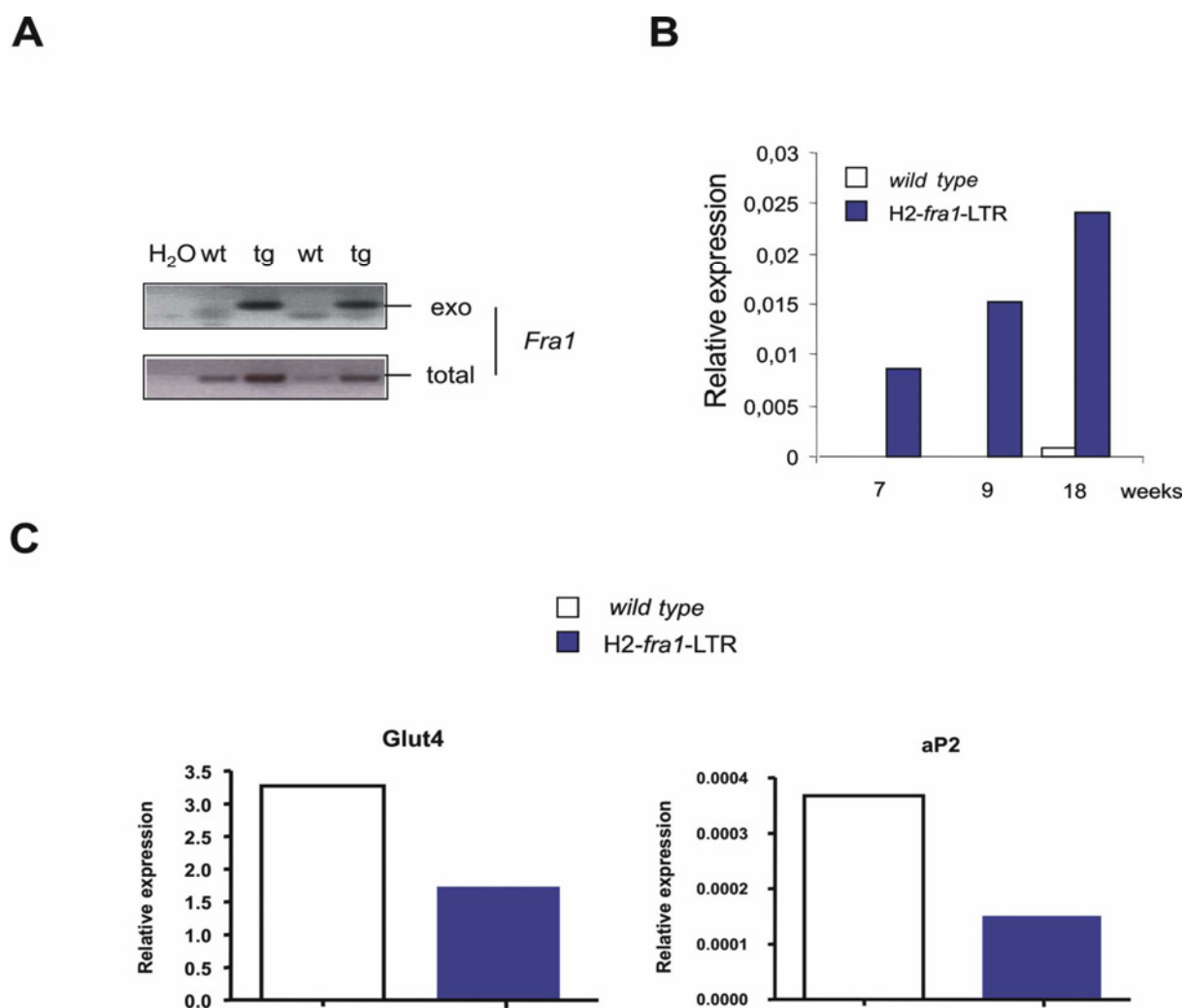
Figure 5.7 Increased expression of Fra1 in the fat of fra1-tg mice and reduced expression of adipocyte differentiation markers

A) Expression of the Fra1 transgene (exo) and expression of total Fra1 (transgene and endogen) in 7 weeks old male wt and fra1-tg mice; B) Relative expression of total Fra1 related to HPRT in 7, 9 and 18 weeks old wt and fra1-tg mice measured by real time PCR; C) Relative expression of the adipocyte markers Glut4 and aP2 related to HPRT in 18 weeks old littermates measured by real time PCR; Results represent one animal experiment.

5.4.1.3. In vivo: Fra1 overexpression decreased C/EBPα mRNA and PPARγ mRNA expression

The potential inhibitory actions of Fra1 on adipocyte differentiation were further characterized by determining its effect on expression of genes known to control adipocytes maturation such as PPARγ and C/EBPα. Their expression was quantified by semi-quantitative PCR analysis of samples derived from the fat pads of 7 weeks and 18 weeks old male wt and fra1-tg mice.

Figure 5.8 A shows cDNA analysis from 7 weeks old fra1-tg and wt males. In the fat pad of fra1-tg overexpressing mice PPARγ cDNA band were visible until the dilution 3 (1:100) compare to bands from wt, that could be followed until the dilation 4 (1:1000) (panel 1). The limiting dilution of the cDNA to detect HPRT were found to be 1:10 for 7 weeks old fra1-tg mice and 1:100 for 7 weeks old wt mice (panel 2). Thus, PPARγ mRNA expression was decreased in fra1-tg fat pads compare to the wt.

At 18 weeks, the expression of Fra1 transgene was analyzed. Figure 5.8 B panel 1 shows that Fra1 (exo) was as expected only detectable in the fat pad of fra1-tg mice. The limiting dilution to detect PPARγ and C/EBPα was 1:10. Both adipocytes markers were increased in these fra1-tg samples compared to wt PPARγ at 1:100 and C/EBPα at 1:100 (panel 2 and 3). The limiting dilutions of the cDNA to detect HPRT were found to be 1:100 fold or both mice phenotypes (panel 4). These results indicate that Fra1 overexpression resulted in a decreased expression of C/EBPα and PPARγ in the fat pad of mature mice.
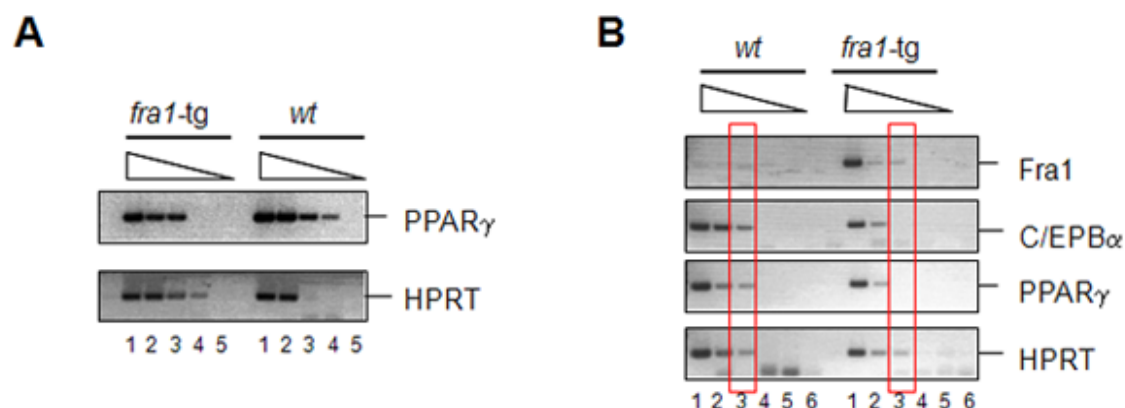
Figure 5.8 Fra1 overexpression reduced marker genes of mature adipocytes

Expression of PPARγ related to HPRT in the fat pad of wt and fra1-tg mice analyzed by semi-quantitative PCR; B) Expression of PPARγ, C/EBPα and Fra1 related to HPRT in the fat pad wt and fra1-tg mice analyzed by semi-quantitative PCR; PPARγ, C/EBPα, Fra1 and HPRT cDNA were amplified with PCR program described in methods. Probes for each amplified were diluted in followed steps: 1 = 1μl of original cDNA amplified, 2 = 1:10 of original cDNA amplified, 3 = 1:100 of original cDNA amplified, 4 = 1:1000 of original cDNA amplified, 5 = 1:10000 of original cDNA amplified and 6 = H_2O.

5.4.2. Adipocytes analyses ex vivo

The data obtained from in vivo experiments by histology and the decreased expression of markers for mature adipocytes, such as C/EBPα and PPARγ indicated that the phenotype observed could be due to a decreased differentiation of adipocytes in fra1-tg mice. The question arose whether Fra1 could directly interfere in a cell autonomous manner with adipocyte differentiation.

5.4.2.1. Ex vivo: Fra1 overexpression reduces adipocytes differentiation

Ex vivo experiment with isolated murine primary osteoblast cells (mPOBs) obtained by digestion of calvarias from newborn mice can be use as an adipocyte differentiation model. To investigate the effect of Fra1 overexpression on adipocyte differentiation, mPOBs were isolated from wt and fra1-tg littermates and their capacity to differentiate into adipocytes was compared ex vivo. The cells were grown until confluence and then induced to differentiate by adding an adipogenic cocktail (AD). The adipocyte solution includes Insulin, Dexamethasone and IBMX. The differentiation was monitored by Oil Red O staining that revealed the adipose content of vacuoles included in adipocytes, as well as by measuring the expression of adipocyte markers by Quantitative Real-Time PCR (QRT-PCR).

Adipocyte differentiation was efficiently induced by the treatment of wt mPOBs (mPOBswt) by the adipogenic cocktail confirming that the cell preparation contained adipogenic progenitor cells (Figure 5.9). A clear inhibition of adipocyte differentiation was observed when mPOBsfra1-tg isolated from fra1-tg mice were used (Figure 5.9).

A

B
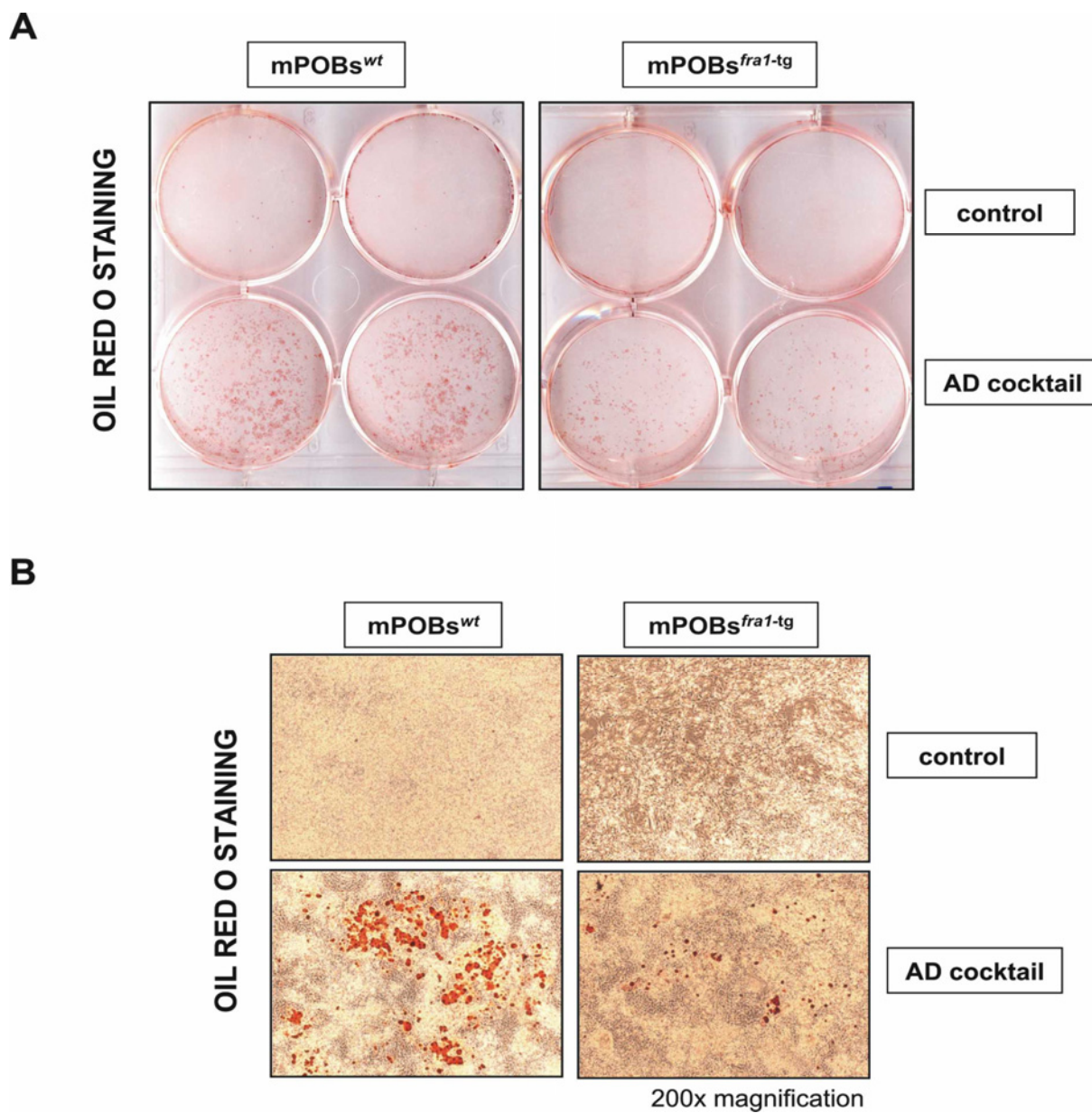
Figure 5.9 Fra1 overexpression decreased lipid filling of mPOBs cultured in the absence or presence of an adipogenic cocktail

A) wt and fra1-tg mPOBs where cultured over 15 days in absence or presence of Insulin, Dexamethasone and IBMX (AD cocktail) in six-well plates. Cells were fixed and cellular lipids were stained with Oil Red O. B) 200x magnification of Oil Red O stained mPOBswt and mPOBsfra1-tg. Experiments were repeated three times.

5.4.2.2. Ex vivo: Fra1 overexpression reduces the expression of adipogenic markers

Early mesenchymal progenitor cells are pluripotent cells, which are expressing all key genes involved in mesenchymal cell fate decision, i.e. Runx2 and its target Osx1 for osteoblastogenesis, MyoD for myocytes differentiation, Sox9 for chondrocytes, PPARγ and C/EBPα for adipocytes as well as Pref-1, a secreted protein that can block both adipogenesis and osteoblastogenesis.

To determine whether the block in adipocyte differentiation observed in Fra1 overexpressing cells could be caused by a change in the expression of these key genes, Quantitative Real-Time PCR (QRT-PCR) were performed at day 0 (when the cells are reaching confluence) of the cultures and after day 15 where wt cells are fully differentiate to adipocytes. The levels of expression of mRNA coding for proteins that characterized fully mature adipocytes were quantified in two independent experiments.

Quantitative Real-Time PCR analysis – day 0

QRT-PCR analysis confirmed that Fra1 was expressed in wt and fra1-tg mPOBs (Figure 5.10 diagram 1). The level of expression was greatly increased and stable in the mPOBs isolated from fra1-tg mice.

Expressions of Runx2, Osx1, MyoD, PPARγ, Pref-1 and Sox9 were not clearly affected by Fra1 overexpression (Figure 5.10 diagram 2, 3, 4, 5, 6 and 7). Only C/EBPα was found to be downregulated (Figure 5.10 diagram 8).

This data suggested that Fra1 overexpression had no influence on Runx2 or Osx1 expression and therefore no effect on the commitment to osteoblast. Furthermore, myogenesis and chondrogenesis were not favoured in fra1-tg mPOBs. However, Fra1 may be able to impair adipogenesis by blocking C/EBPα expression.
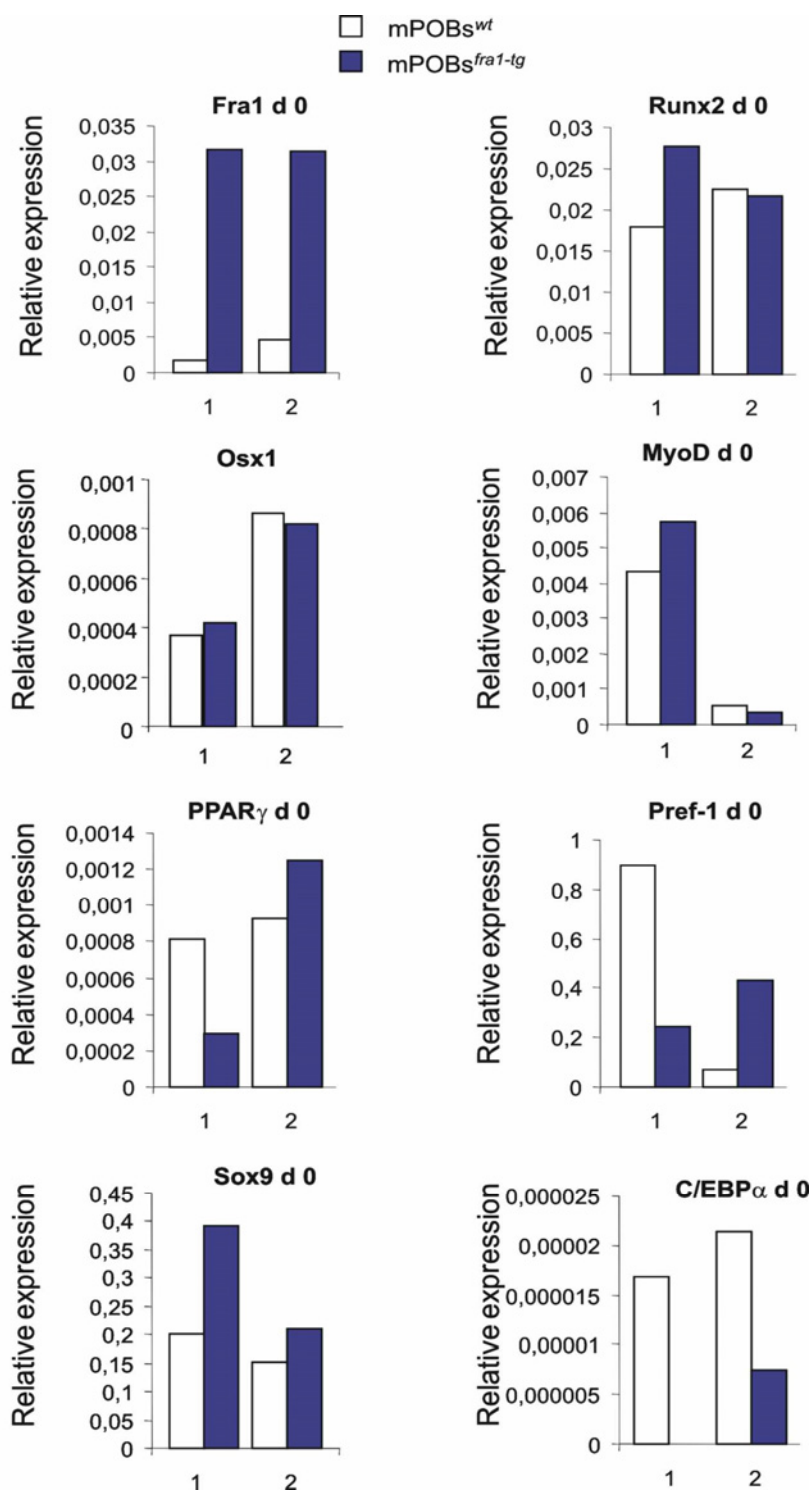
Figure 5.10 Effect of Fra1 overexpression on cell fate decision in mPOBs at day 0

Expression of total Fra1, Runx2, Osx1, MyoD, PPARγ, Pref-1, Sox9 and C/EBPα, related to HPRT in mPOBs analyzed by Quantitative Real-Time PCR; The samples were taken when the mPOBswt and mPOBsfra1-tg reached confluence (day 0 of the treatment). The graph shows the data of two experiments indicated by 1 and 2.

_____

Quantitative Real-Time PCR analysis – day 15

The relative expression levels of the Fra1 (total), Sox9, Runx2, Pref-1, PPARγ and C/EBPα were also measured by QRT-PCR on samples isolated on day 15 of the culture in the absence (minus) or the presence (plus) of the adipogenic cocktail.

Low levels of Fra1 RNA expression were found in untreated mOBswt. Fra1 expression was found to be slightly increased in response to adipogenic stimulation in treated mOBswt (Figure 5.11 diagram 1). High levels of Fra1 expression were found in cells isolated from fra1-tg mice in both untreated and treated experiments.

In wt and fra1-tg mPOBs expression of Sox9 and Runx2 were not effected in absence or presence of adipocytes differentiation cocktail (Figure 5.11 diagram 2 and diagram 3).

Although, in the first experiment, Pref-1 was found to be highly upregulated in Fra1 overexpressing cells after 15 days AD stimulation, the second experiments did not confirm these data. In both experiments, a highest level of Pref-1 expression was found in the un-treated control group of fra1-tg cells compared to the wt control group (Figure 5.11 diagram 4).

In vivo results showed decreased PPARγ expression in fra1-tg fat pad. Ex vivo contradictory data were obtained when comparing the two experiments. The AD treatment could strongly induced PPARγ expression in wt mPOBs in both experiments. While, a similar effect was seen in one of the experiment using fra1-tg mPOBs, a decreased expression for PPARγ was observed in the second experiment (Figure 5.11 diagram 5).

A decreased expression of C/EBPα was found in the fat pad of wt and fra1-tg mice. Ex vivo, the expression of C/EBPα RNA was found to be increased in response to AD stimulation of mPOBswt. While an increased C/EBPα expression was also found in stimulated cells overexpressing Fra1, the effect was greatly reduced. Thus, a clear change in the expression level of C/EBPα could be measured in cells overexpressing Fra1 induced to differentiate to adipocytes. These data suggest that downregulation of C/EBPα may be the mechanism by which Fra1 impairs adipogenesis of mPOBs (Figure 5.11 diagram 6).
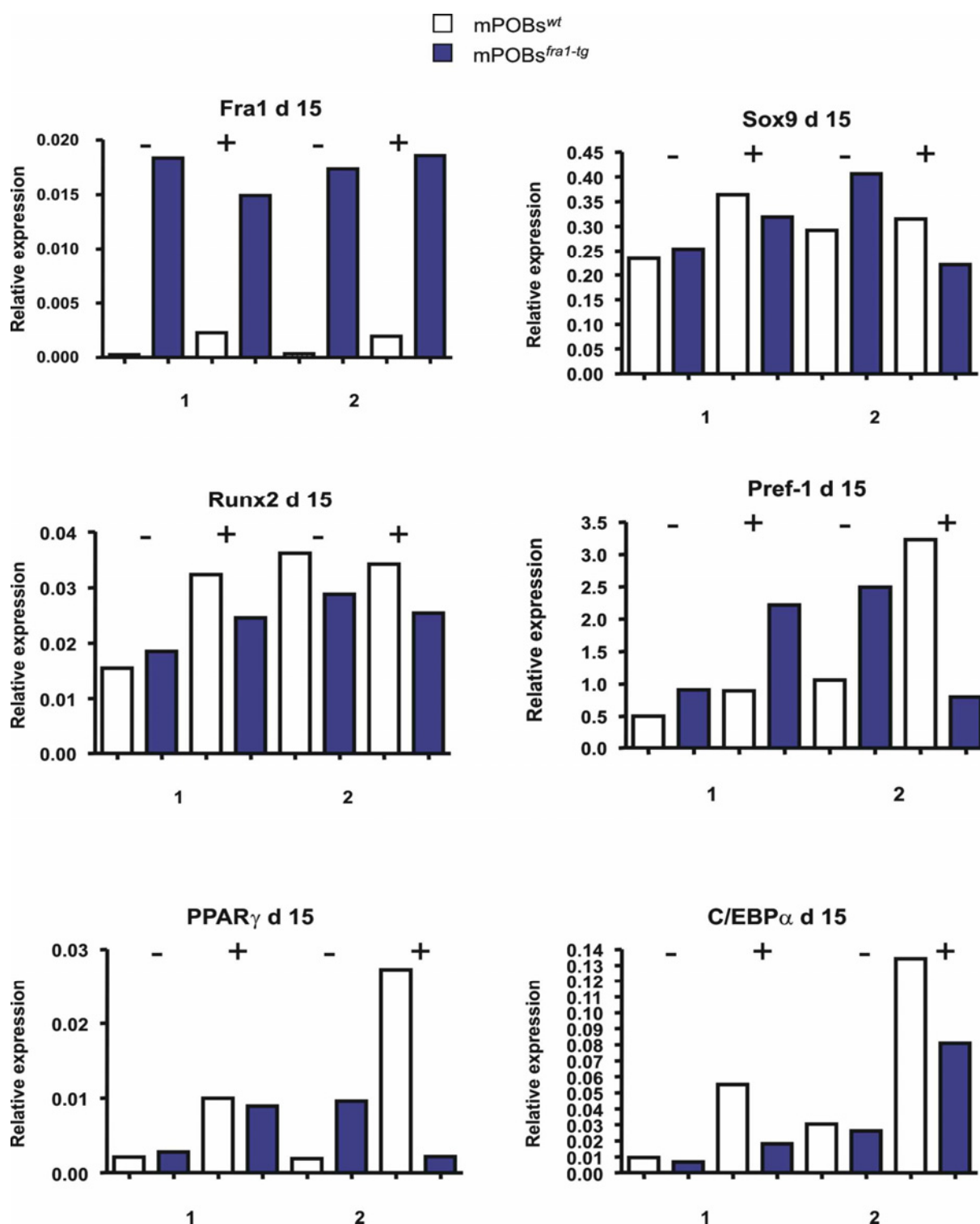
Figure 5.11 Effect of Fra1 overexpression on cell fate decision in absence or presence of adipocyte cocktail AD at day 15

Expression of total Fra1, Sox9, Runx2, Pref-1, PPARγ, C/EBPα, and related to HPRT in mPOBs analyzed by Quantitative Real-Time PCR; The samples were taken when the mPOBswt and mPOBsfra1-tg reached adipogenic character (day 15 of the treatment). The graph shows the data of two experiments indicated by 1 and 2.

5.4.3. Adipocytes analyses in vitro

5.4.3.1. In vitro: Derivation of adipogenic cell line used for retrovirus infection

A cell line with adipogenic potential was derived by successive passage of murine mesenchymal cells isolated from rsk2-/y mouse calvaria. The isolated cells, derived from three calvarias of rsk2-/y mice, were merged and cultured until passage 27 to obtain an immortalised mesenchymal cell line that are called mOBsrsk2-/y (described in methods). Before infecting the cells with different vectors for Fra1 overexpression, their capacity to differentiate to adipocytes was tested in vitro. Adipocyte differentiation experiments were conducted which have shown by Oil Red O staining that these mPOBsrsk2-/y were able to differentiate into adipocytes (Figure 5.12). Thus, the retrovirus infection could be carried out using this cell line.
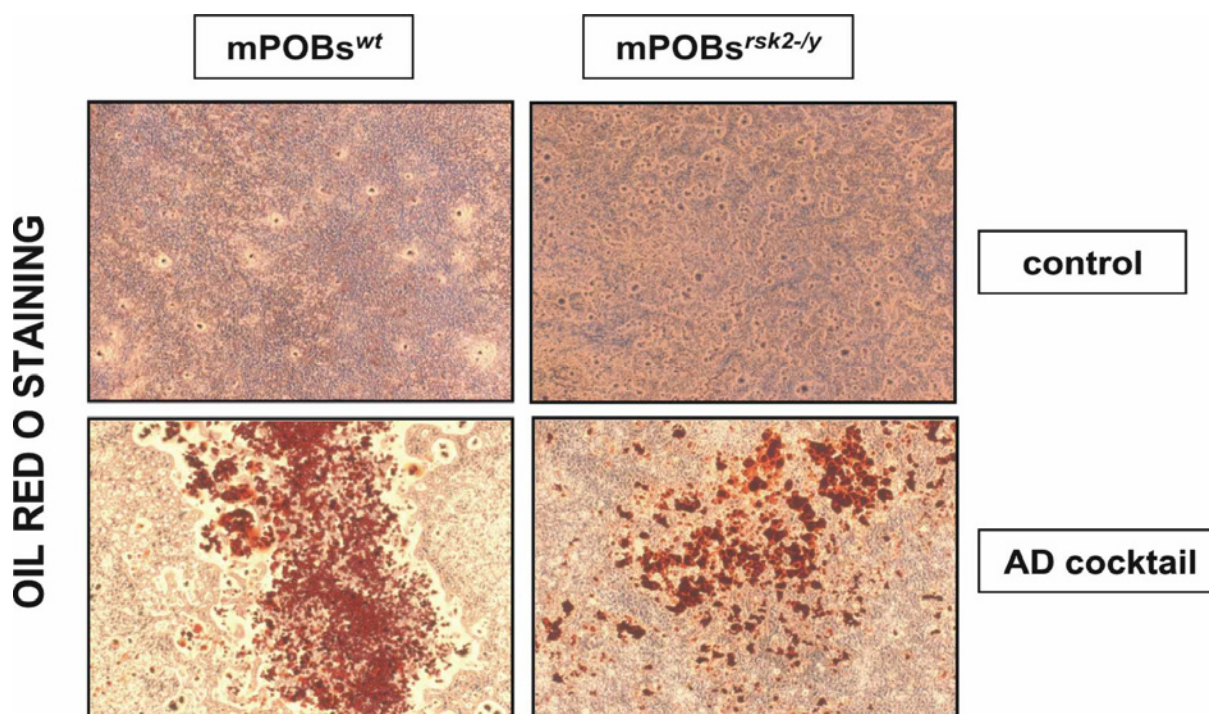
Figure 5.12 Equal lipids filling of mPOBswt vs. mPOBsrsk2-/y cultured in the absence or presence of adipogenic cocktail

wt and rsk2-/y mPOBs where cultured over 15 days in absence or presence of Insulin, Dexamethasone and IBMX (AD cocktail) in six-well plates. Cells were fixed and cellular lipid was stained with Oil Red O. 200x magnification. Experiments were repeated three times.

Two different strategies were used to generate mOBsrsk2-/y overexpressing Fra1. First, mOBsrsk2-/y were infected with an empty vector as control called pBabe-empty and a vector pBabe, which contains fra1 cDNA (pBabe-Fra1) (gift from M. Bussilinger´s laboratory, IMP Vienna, Austria). After puromycine selection, a population of cells that may constitutively expressing Fra1 were isolated and further characterised by comparison with selected cells infected with the empty vector. Successful expression of Fra1 from the constructs could be observed in pBabe-Fra1 transfect mOBsrsk2-/y cells (Figure 5.13 A and B).

In the second study, a retroviral vector was used to express a hybrid protein consisting of the fusion of the rat Fra1 with the oestrogen receptor ligand-binding domain. The expression of the fusion protein was under the control of the Moloney murine sarcoma virus long terminal repeat (MSCV). The vector includes a neomycin phosphotransferase gene driven by the Simian virus 40 early promoter enabling selection for transduced cells. This virus vector (pMSCV-FraER) should produce a form of Fra1, which was kept into the cytoplasm and was therefore transcriptional inactive. Upon addition of estradiol (E2), the fusion protein was transferred into the nucleus and was now becoming transcriptional active. This setting would allow to tightly controlling the time when Fra1 was activated. After selection, a population of cells that may express FraER were isolated and further characterised by comparison with selected cells infected with the control vector pMSCV-Neo. Successful expression of Fra1 can be observed in Figure 5.13 A and Figure 5.13 B.

5.4.3.2. In vitro: Fra1 expression in transfect mOBsrsk2-/y

The mOBsrsk2-/y were infected with the various vectors and cultured under selection pressure until resistant population of cells could be expanded. Subsequently, the level of expression of Fra1 was controlled in the selected populations. An increase level of Fra1 was detected by PCR in cells infected with pBabe-Fra1 (Figure 5.13 A) as well as pMSCV-FraER (Figure 5.13 A) when compared to the empty vector.

Western blot analyses were performed to determine whether the increased amounts of RNA were resulting in increased expression of the protein. An increase in the amount of a 45 kDa protein was detected in the nuclear extract from mOBsrsk2-/y-pBabe-Fra1 when compared to mOBsrsk2-/y-pBabe-empty (5.13 B). Thus, Fra1 was expressed at low level in mOBsrsk2-/y and a clear increase in Fra1 expression was seen in nuclear extract (NE) isolated from mOBsrsk-2/y infected with pBabe-Fra1. Detection of ß-Actin was used as loading control.

_____

The estradiol-inducible expression of Fra1 was clearly seen in nuclear extracts (NE) isolated from mOBsrsk2-/y infected with pMSCV-FraER stimulated with E2 over a time of 3 hours (Figure 5.13 B). A band of 70 kDa corresponding to the size of the fusion protein was detected in the nuclear extracts of the cells infected with the pMSCV-FraER even in the absence of estradiol, but not in the control vector pMSCV-Neo. In addition, the intensity of the band was increasing upon addition of estradiol (Figure 5.13 B). To better characterize the kinetic of induction of the fusion protein nuclerar extracts were isolated from mOBsrsk2-/y - pMSCV-Neo and mOBsrsk2-/y-pMSCV-FraER following treatment with 1µM β-estradiol (E2) for an increasing time between 0 and 30 minutes. The expression of Fra1 was analysed by Western blot. The nuclear accumulation of Fra1-ER fusion protein was first seen after five minutes of treatment with β-estradiol in mOBsrsk2-/y-pMSCV-FraER but not in mOBsrsk2-/y-pMSCV-Neo (Figure 5.13 C). The nuclear accumulation of Fra1-ER fusion protein was increasing with time after 10 min, 15 and 30 min of 1µM β-estradiol treatment.

The data demonstrated that Fra1 was overexpressed in mOBsrsk2-/y-pBabe-Fra1. Furthermore, the infection with the retrovirus vectors encoding Fra1 resulted in efficient increase in Fra1 expression in mOBsrsk2-/y-pMSCV-FraER treated with estradiol. Some leakiness was also observed when the Fra1-ER system was used most likely due to the presence of an oestrogen agonists in the media or serum complementing the media.
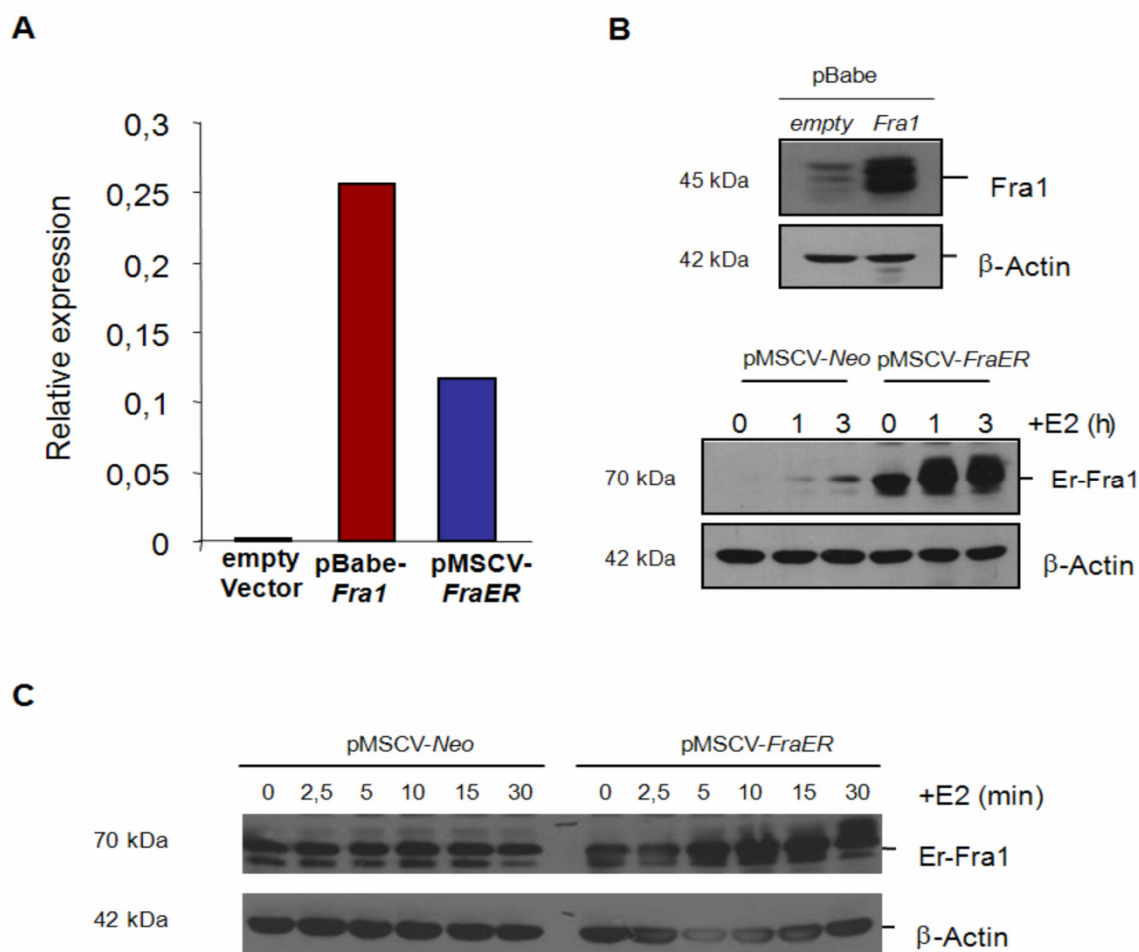
Figure 5.13 Constitutive and estradiol-inducible overexpression of Fra1 in mOBsrsk2-/y

A) Expression of total Fra1 relative to HPRT in mOBsrsk2-/y infected with vectors pBabe-Fra1, pMSCV-FraER and mean of the relative Fra1 expression in mOBsrsk2-/y infected with pBabe-empty (V) and pMSCV-Neo (V), relative expression measured using PCR; B) Fra1 detection by Western blot analysis in nuclear extracts of mOBsrsk2-/y infected with pBabe-empty and pBabe-Fra1; bottom: expression of nuclear Fra-1-estradiol receptor fusion protein (Er-Fra1) measured by Western Blot analysis in mOBsrsk2-/y infected with pMSCV-Neo and pMSCV-FraER, cells were treated for 0, 1 and 3 hours with 1µM β-estradiol (E2); loading control: β-Actin; C) Kinetic of induction of ER-Fra1 in mOBsrsk2-/y infected with pMSCV-FraER, Western Blotting of nuclear extracts isolated from mOBsrsk2-/y infected with pMSCV-Neo or mOBsrsk2-/y infected with pMSCV-FraER after stimulation with 1µM β-estradiol (E2) for the indicating time, loading control: β-Actin.

5.4.3.3. In vitro: Characterisation of growth and shape differences in transfected mOBsrsk2-/y cell lines

The growth properties of the transfected mOBsrsk2-/y with pBabe-empty, pBabe-Fra1, pMSCV-Neo and pMSCV-FraEr were compared. The cells were plated in six-well plates and counted once per day over a period of 8 days. Three phases could be distinguished in the growth curves, in the first one (from day 1 to 3), the cells were growing very slowly, in the second one, and (between day 3 and day 5) a typical log phase was observed. Finally, the cells stop to grow at day 6 (Figure 5.14 A). The growth curves of the four different cell lines were similar all along the time course. Therefore, neither the process of selection nor the overexpression of Fra1 had an effect on the growth of the mOBsrsk2-/y.
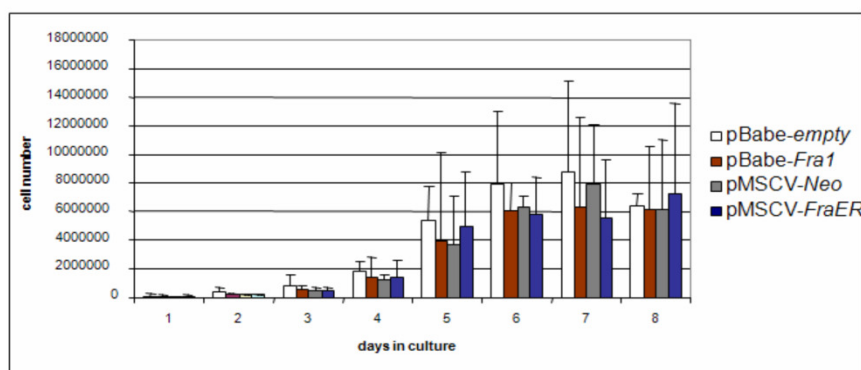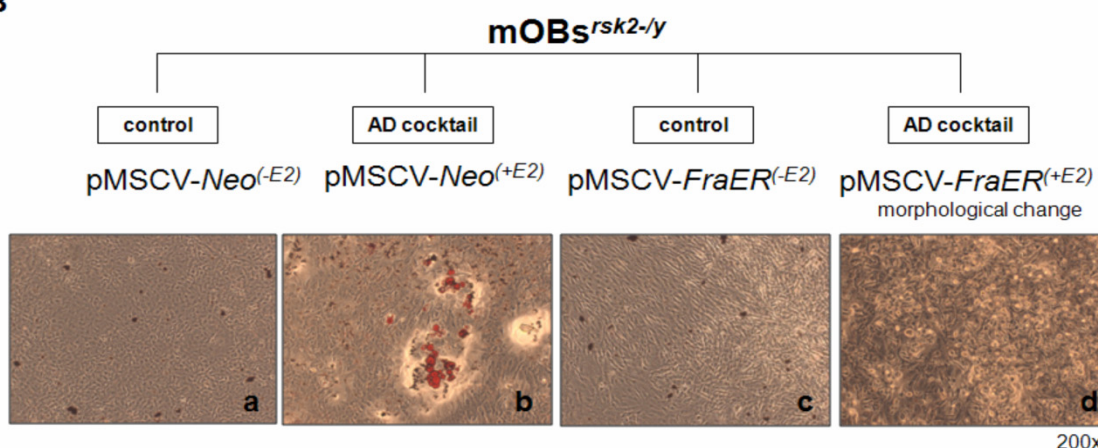
Figure 5.14 Characterisation of Fra1 transfected murine Rsk2-deficient cells

A) mOBsrsk2-/y were infected with different retrovirus vectors and growth were measured; B) Picture of treated or untreated pMSCV-Neo or pMSCV-FraER transfected mOBsrsk2-/y; only transfected mOBsrsk2-/y with pMSCV-FraER and stimulated with 1μM ß-estradiol (+E2) leads to change in the morphology (picture 5.14 B/ d – pMSCV-FraER(+E2)). Cellular lipids were stained with Oil Red O staining, 200x magnification.

The morphology of the cells were analysed to look if Fra1 overexpression has an effect on cell shape. It could be observed, that Fra1 overexpression was leading to changes in the morphology of the mOBs$^{rsk2-/y}$ transfected with pMSCV-*FraER*. When treated with estradiol, the mOBs$^{rsk2-/y}$-pMSCV-*FraER* cells but not the mOBs$^{rsk2-/y}$-pMSCV-*Neo* acquired a longer and thinner shape similar to myocytes. This observation could be made in the absence of adipogenic stimulation. These morphological changes were always connected to Fra1 overexpression since they were not observed in mOBs$^{rsk2-/y}$-pMSCV-*FraER* not stimulated by estradiol (mOBs$^{rsk2-/y}$-pMSCV-*FraER*$^{(-E2)}$ (Figure 5.14 B). The same observation could be made comparing mOBs$^{rsk2-/y}$-pBabe-*empty* to mOBs$^{rsk2-/y}$-pBabe-*Fra1*.

5.4.3.4. In vitro: Effect of pBabe-Fra1 overexpression on mOBsrsk2-/y differentiation – Fra1 is inhibiting adipogenesis

The mOBsrsk2-/y-pBabe-Fra1 cell line and the control cell line mOBsrsk2-/y-pBabe-empty were cultured until confluence and treated every third day without or with Insulin, Dexamethasone and IBMX over 21 days. The cells were fixed and stained with Oil Red O to monitor the efficiency of the differentiation.

No Oil Red O positive colonies were seen in mOBsrsk2-/y-pBabe-empty or mOBsrsk2-/y-pBabe-Fra1 in absence of adipogenic cocktail (Figure 5.15 B/ a and b). Oil Red O positive colonies were seen in mOBsrsk2-/y-pBabe-empty cultured in the presence of the adipogenic cocktail over 21 days (Figure 5.15 B/ c) but not in mOBsrsk2-/y-pBabe-Fra1 cultured in the same condition (Figure 5.15 B/ d).

Thus, Fra1 overexpression was decreasing the capacity of cells to differentiate into adipocytes. These results were comparable to those obtained with ex vivo cultures of Fra1 overexpressing primary osteoblast.
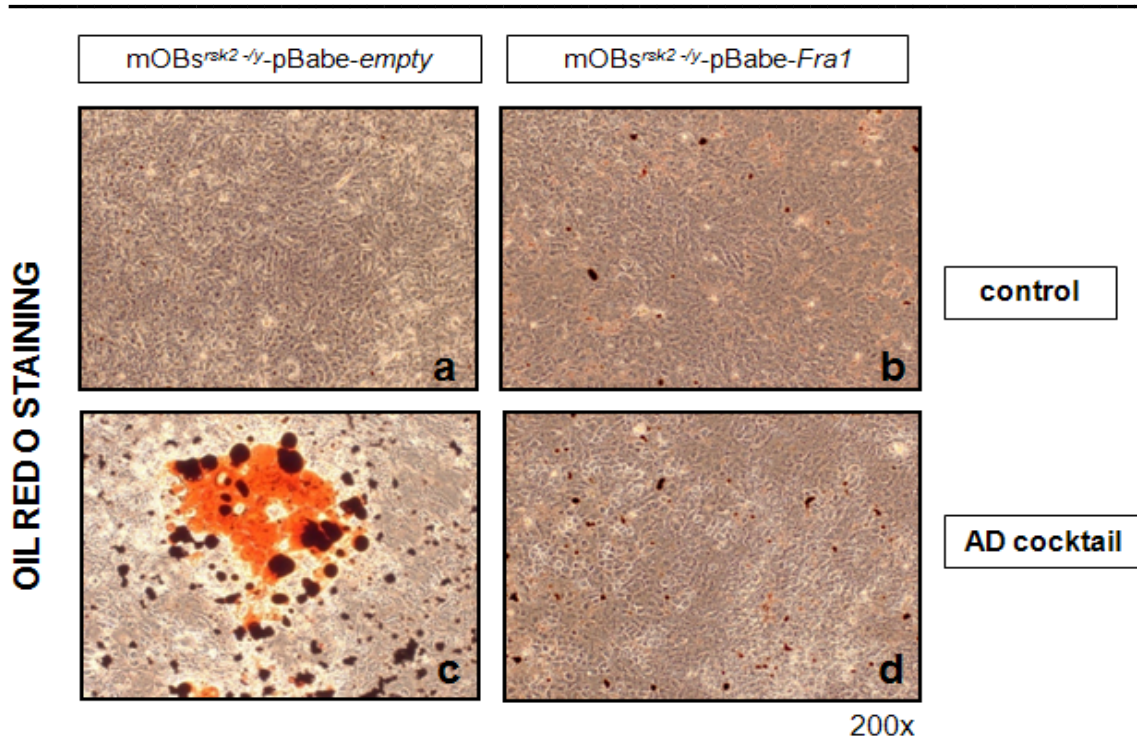
Figure 5.15 Fra1 overexpression blocks triglyceride accumulation in mOBsrsk2-/y cell

Infected mOBsrsk2-/y with pBabe-empty vector (picture 5.15 a and 5.15 c) or pBabe-Fra1 vector (picture 5.15 b and 5.15 d) where cultured over 21 days in absence or presence of Insulin, Dexamethasone and IBMX (AD cocktail), cellular lipid was stained with Oil Red O, 200x magnification.

5.4.3.5. In vitro: Effect of estradiol-induced pMSCV-FraER expression on mOBsrsk2-/y differentiation

Similar experiments were performed using the mOBsrsk2-/y-pMSCV-Neo and mOBsrsk2-/y-pMSCV-FraER cell lines. Again, no Red Oil positive colonies were seen in any of the cultures in the absence of adipogenic cocktail independently of the addition of estradiol (Figure 5.16/ a - d). Red Oil positive colonies were seen in mOBsrsk2-/y-pMSCV-Neo and mOBsrsk2-/y-pMSCV-FraER cultured in the presence of the adipogenic cocktail (Figure 5.16/ e and f).

Addition of estradiol did not affect the formation of adipocytes in mOBsrsk2-/y-pMSCV-Neo culture (Figure 16/ g). Red Oil positive colonies were also seen in mOBsrsk2-/y-pMSCV-FraER cultured in the presence of the adipogenic cocktail (Figure 16/ f) but this effect was totally blocked by addition of estradiol which activated Fra1 (Figure 5.16/ h). Thus, Fra1 overexpression seemed to direct inhibit adipocyte differentiation of mesenchymal progenitors.
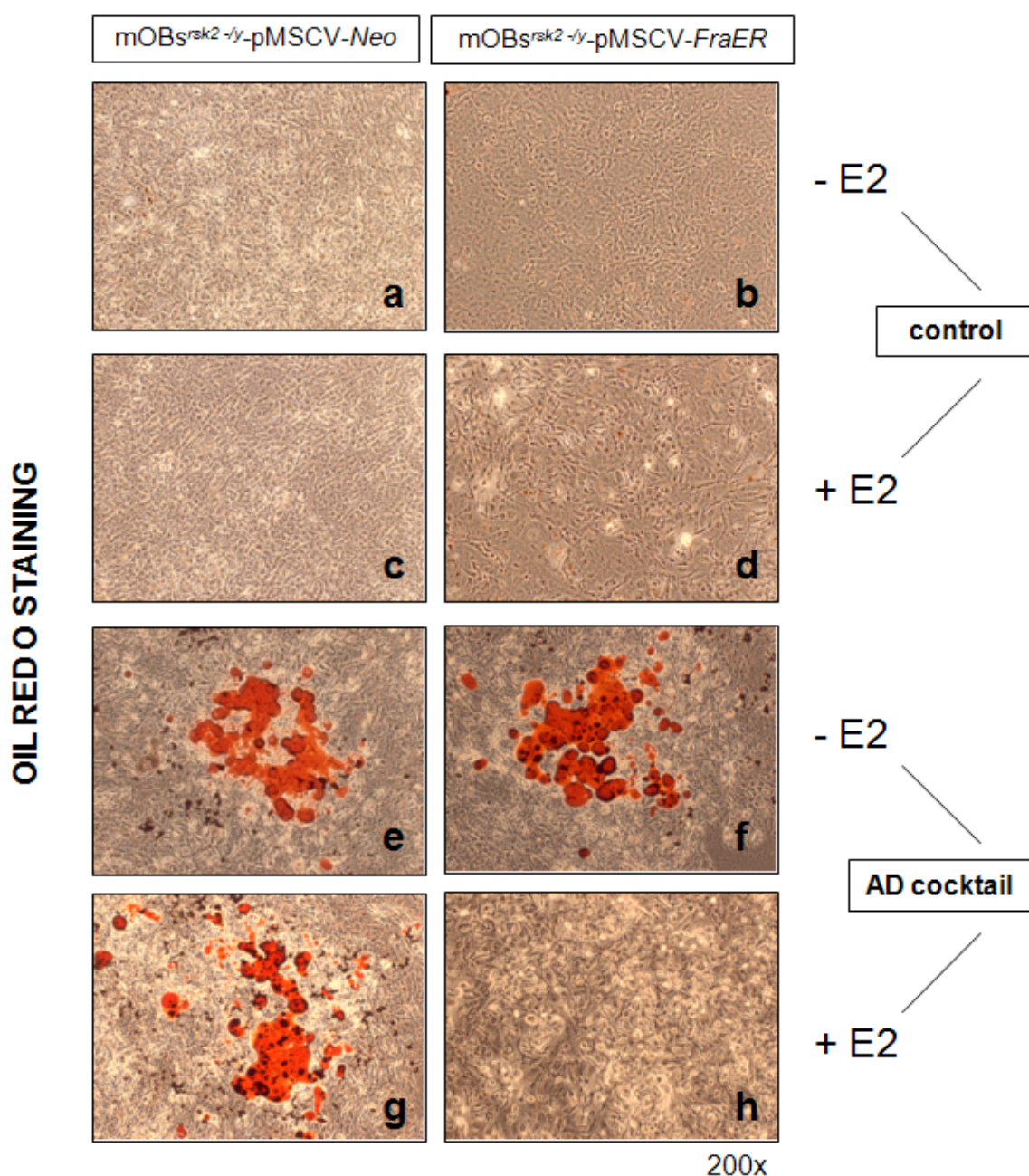
Figure 5.16 Estradiol induced Fra1 overexpression blocks triglyceride accumulation in mOBsrsk2-/y cell infected with pMSCV-FraER

Infected mOBsrsk2-/y with pMSCV-Neo vector (picture 5.31 a, c, e and g) or pMSCV-FraER vector (picture 5.31 b, d, f and h) where stimulated with (+E2) or without (-E2) estradiol over 21 days in absence (control) or presence of Insulin, Dexamethasone and IBMX (AD cocktail). Cellular lipids were stained with Oil Red O, 200x magnification.

_____

To confirm these observations, the level of expression of markers for adipocyte differentiation (C/EBPα, PPARγ and Glut4) as well as markers for osteoblast differentiation (Runx2 and Osx1) or chondrocytes (Sox9) were measured at day 0 and at day 21. All three markers for adipocytes were found to be downregulated in cells overexpressing Fra1; this effect was dependent on Fra1 activation by estradiol in the case of mOBsrsk2-/y-pMSCV-FraER (Figure 5.17).

These data indicated that Fra1 is indeed inhibiting adipocyte differentiation. While no correlation between Fra1 overexpression and the level of Runx2 expression could be established, the adipogenic stimulation combined with Fra1 overexpression was decreasing Osx1 expression (Figure 5.17 B). In these conditions, Sox9 expression was not affected. Thus, Fra1 overexpression seems to specifically block adipogenesis by a mechanism that does involve increased osteoblastogenesis or chondrogenesis.

Next, the expression levels of markers for commitment of mesenchymal cells to osteoblasts (Runx2 and Osx1), as well to chondrocytes (Sox9), or to adipocytes (PPARγ and C/EBPα) were measured in samples isolated at day 0 of the treatment (e.g. when the cells reached confluence) in order to determine whether Fra1 overexpression could affect cell fate decision. Fra1 overexpression did not clearly affect the expression of Runx2, Osx1 or Sox9, but did increase the expression of PPAR and decreased C/EBPα (Figure 5.17 A).

These data indicated that Fra1 overexpression might be inhibiting adipogenesis by directly downregulating C/EBPα, without affecting the other lineage decisions.

A

B
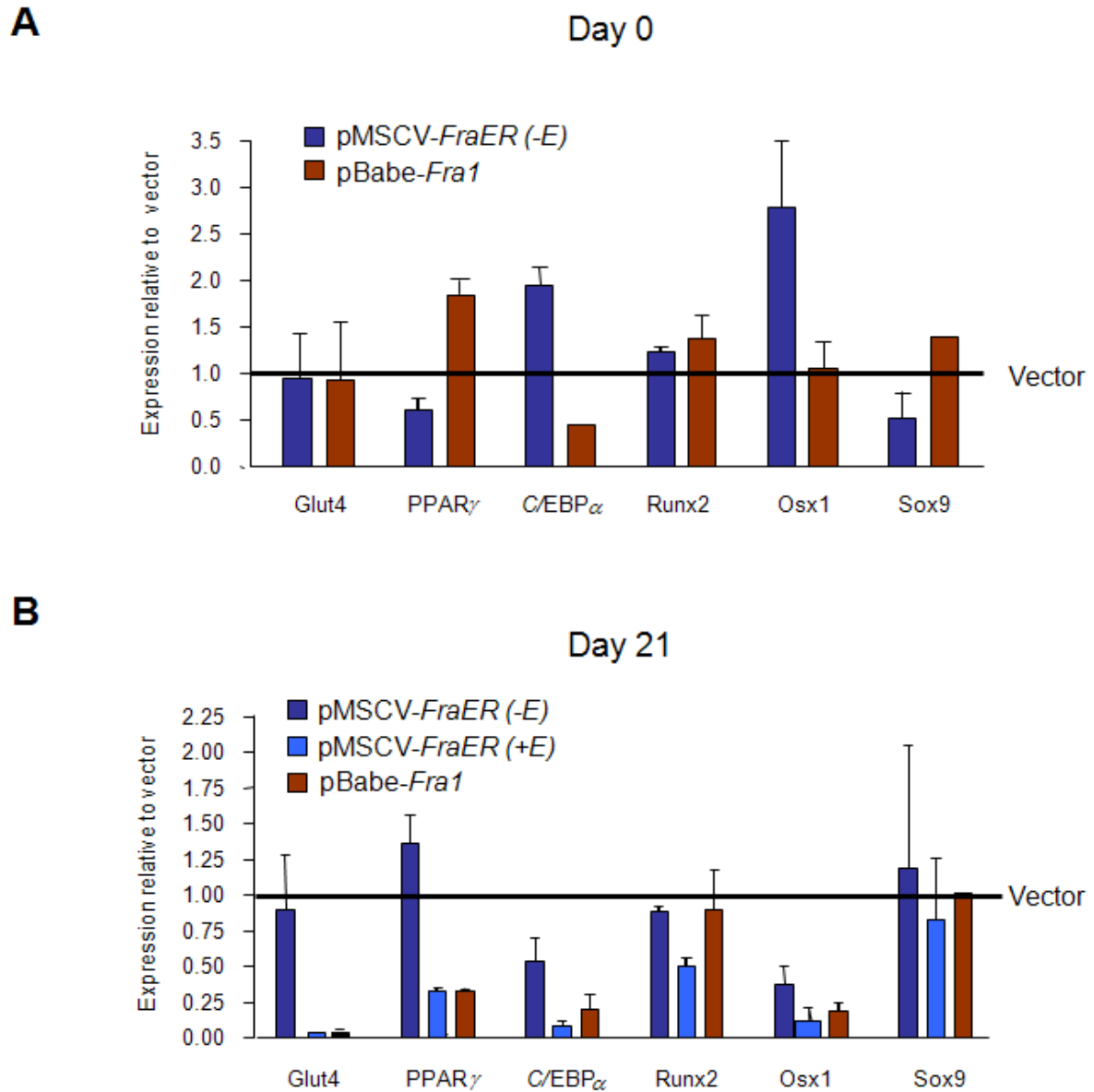
Figure 5.17 Effect of constitutive and induced Fra1 overexpression on mesenchymal cell fate decision (day 0) and on differentiation after 21 days of treatment with adipogenic stimuli

A) Day 0 and B) Day 21 expression of Glut4, PPARγ, C/EBPα, Runx2, Osx1 and Sox9 in Fra1 infected cells relative to the level in vector infected cells measured by PCR ; blue columns: mOBsrsk2-/y infected with pMSCV-FraER (-E2) without Estradiol treatment, light blue columns: mOBsrsk2-/y infected with pMSCV-FraER (+E2) with estradiol treatment, red columns: mOBsrsk2-/y infected with pBabe-Fra1.

5.4.3.6. In vitro: Analysis of the inhibitory mechanism of action of Fra1 on adipogenesis

Adipogenesis in murine osteoblast (mOBsrsk2-/y) was induced in vitro by the stimulation of progenitor cells with cocktail containing Insulin, the glucocorticoid agonist Dexamethasone and IBMX. All three molecules are acting via different pathways.

Insulin is a growth factor which is binding to a surface transmembrane receptor that activates downstream cascades including the PI3K pathway and the MAPK/ ERK pathway. Dexamethasone is binding to a cytosolic steroid receptor, which is then transferred to the nucleus where it can act as a transcription factor. IBMX is a non-specific inhibitor of cAMP and cGMP phosphodiesterases, which leads to an increased cAMP level. This increase activates PKA and contributes to adipogenesis by inducing the expression of CREB protein. Therefore, it was postulated that Fra1 overexpression might interfere with one of this pathways in order to inhibit adipogenesis.

5.4.3.6.1. Fra1 overexpression prevents Dexamethasone-induced growth inhibition

Glucocorticoids are known to block the growth of murine osteoblast cells. Therefore the effect of Dexamethasone on the growth of mOBsrsk2-/y-pBabe-empty and mOBsrsk2-/y-pBabe-Fra1 was compared. The cells were plated in six-well plates, grown with or without addition of 10^{-6} M Dexamethasone for 5 days and counted.

As expected, a 40 % decrease in the number of cells was measured when mOBsrsk2-/y-pBabe-empty were treated with Dexamethasone. The decrease was only of 10 % when mOBsrsk2-/y-pBabe-Fra1 were cultured with the hormone (Figure 5.18 A).

Thus, overexpression of Fra1 was protecting against the effect of glucocorticoids on the growth of the cells.

5.4.3.6.2. The glucocorticoid receptor is downregulated in cells overexpressing Fra1

To gain insight into the mechanism by which Fra1 is protecting the cells against corticoid-induced growth inhibition, the levels of expression of the glucocorticoid receptor in mOBsrsk2-/y-pBabe-empty and mOBsrsk2-/y-pBabe-Fra1 were compared. Western blot analyses were performed to detect the glucocorticoid receptor with an antibody directed against it and β-Actin was used as a loading control. Three different cell extracts were prepared. First, a separation of the cytosolic and nuclear protein fraction (Figure 5.18 B), second using a denaturating buffer (SDS buffer) to prepare total cell extract

(Figure 5.18 C), and third using a non-denaturating buffer (Frakelton) to prepare total extract (Figure 5.18 C). A band with the size of the glucocorticoid receptor was found to be expressed at a lower level in all extracts isolated from mOBsrsk2-/y-pBabe-Fra1 (Figure 5.18 B and C).

Thus, the decreased response to glucocorticoids observed in cells overexpressing Fra1 was likely to be cause by the decreased expression of the glucocorticoid receptor.

A

B

C
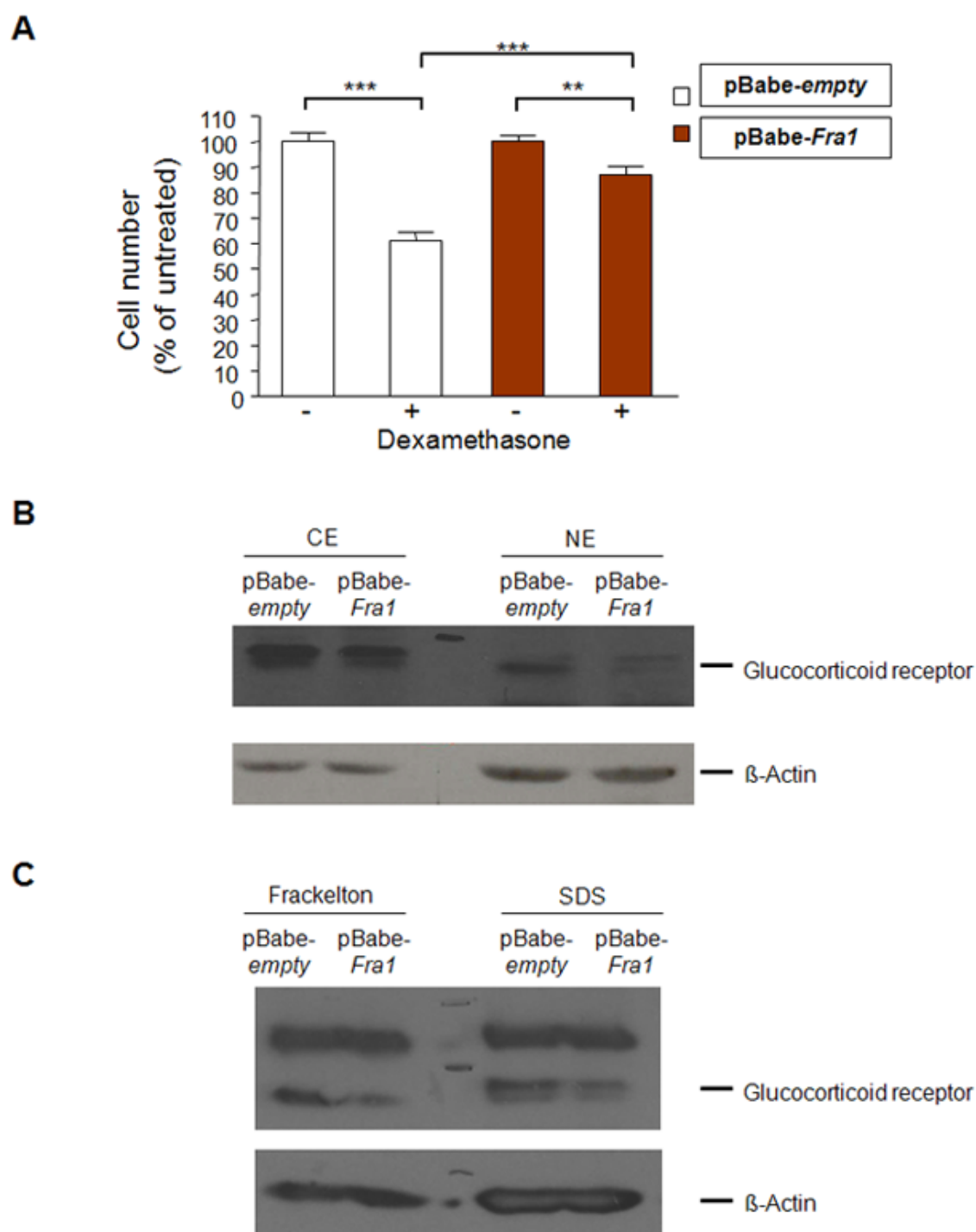
Figure 5.18 Fra1 overexpression prevents Dexamethasone-induced growth inhibition and glucocorticoid receptor is downregulated in cells overexpressing Fra1

A) Reduced sensitivity to Dexamethasone treatment of OBs infected with pBabe-fra1 (Fra-1) compared to OBs infected with pBabe (Vector), treatment with 10μM Dexamethasone (+) and without Dexamethasone (-) statistical significant differences are indicated by asterisks. B) WB analysis of glucocorticoid receptor protein in OBs infected with pBabe-fra1 (Fra-1) and pBabe (Vector), NE= Nuclear extract, CE= Cytosolic extract. C) WB analysis of total amount of glucocorticoid receptor protein. Left: total protein extraction by Frakelton buffer, right: total protein extraction by SDS sample buffer, loading control in both western blots: β-Actin.

5.5   Spleen analyses

The spleen is both, a major lymphoid organ and an efficient blood filtration system. As already described fra1 transgenic mice develop splenomegaly [52]. This was probably due to a bone mass increase, which causes a severe reduction of space in the bone cavity harbouring the bone marrow, the major site of haematopoiesis. The reduction of space in the bone effects the cellular composition in secondary lymphoid organs. To assess whether combined Fra1 overexpression and Rsk2-deficiency not only affects the longitudinal growth of bone [Chapter 5.2.2.] and fat tissue [Chapter 5.3.2.], but also the spleen morphology and function, comparative spleen analyses of wt, rsk2-/y, rsk2-/x, fra1-tg, fra1-tg/rsk2-/y and fra1-tg/rsk2-/x mice were performed.

5.5.1.   Rsk2-deficiency can rescue Fra1 overexpression induced splenomegaly

Representative photographs of spleens isolated from 7 weeks old male wt, rsk2-/y, fra1-tg and fra1-tg/rsk2-/y mice are shown in Figure 5.19 A. Whereas spleens of fra1-tg male mice showed a significant increase of organ size compared to wt mice, no sign of splenomegaly was observed in the case of rsk2-/y and fra1-tg/rsk2-/y mice. However, spleens of male fra1-tg/rsk2-/y mice appeared to be rather anaemic when compared to wt and rsk2-/y spleens, this may indicate a disturbance of the red blood cell compartment in these mice.

In common with the analysis of male mice, female fra1-tg mice showed signs of splenomegaly at both 7 and 18 weeks of age, whereas spleens of rsk2-/x mice were rated normal when compared to wt mice (Figure 5.19 B). In the case of female mice, splenomegaly was additionally observed for 7 weeks old fra1-tg/rsk2-/x mice and occasionally also for 18 weeks old fra1-tg/rsk2-/x mice.
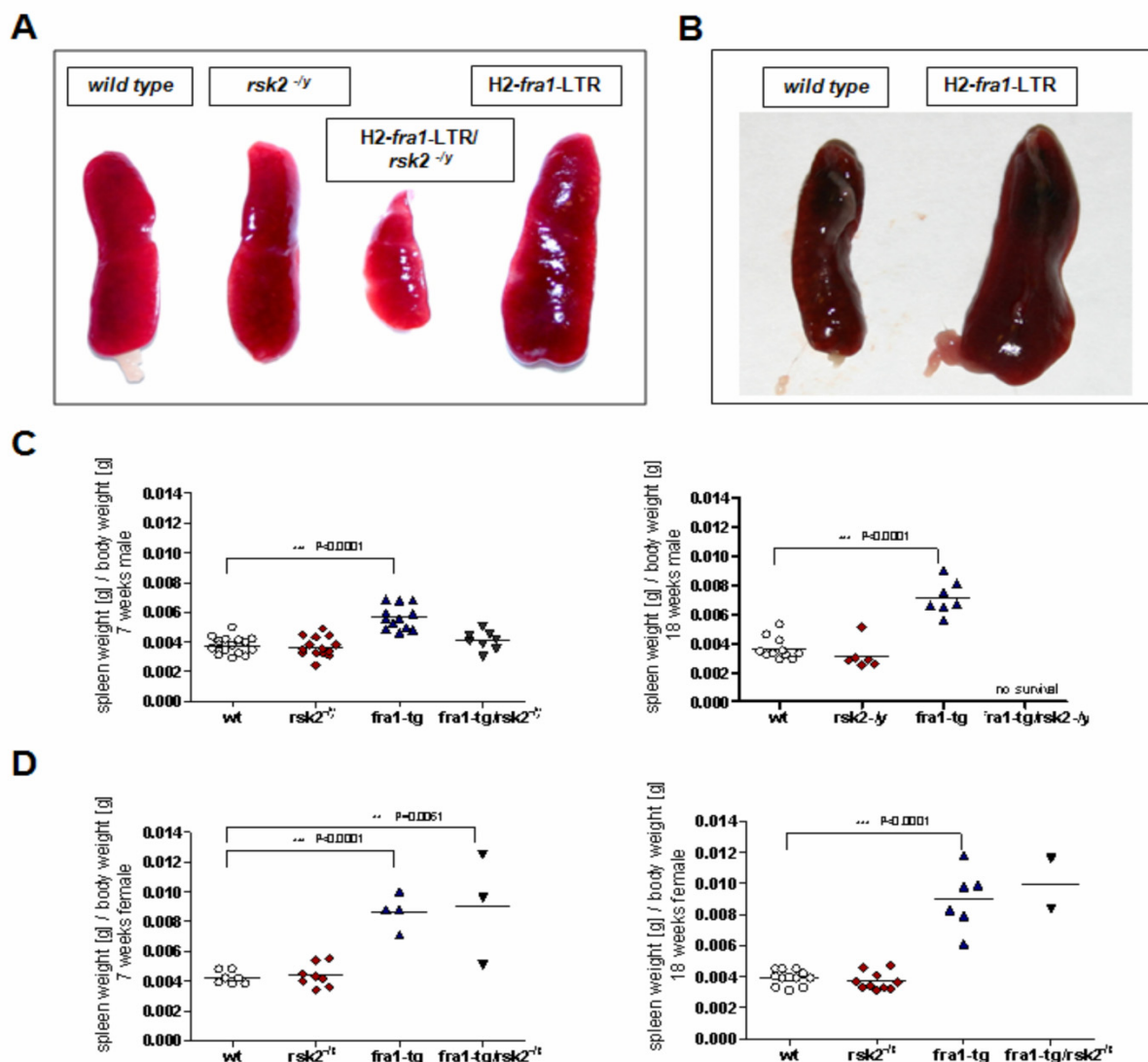
Figure 5.19 Rsk2-deficiency can rescue Fra1-induced splenomegaly

A) Picture of 7 weeks old male rsk2-/y, fra1-tg and fra1-tg/rsk2-/y spleens; B) Picture of 18 weeks old female wt and fra1-tg spleens; C) Ratio between spleen weight and body weight of 7 weeks old and 18 weeks old males wt (7weeks/ n=16; 18weeks/ n=11), rsk2-/y (7weeks/ n=15; 18weeks/ n=6), fra1-tg (7 weeks/ n=12; 18 weeks/ n=7) and fra1-tg/rsk2-/y (7 weeks/ n=8; 18 weeks/ n=0) mice; D) Ratio between fat weight and body weight of 7 weeks old and 18 weeks old females wt (7 weeks/ n=7; 18 weeks/ n=12), rsk2-/x (7 weeks/ n=8; 18 weeks/ n=5), fra1-tg (7 weeks/ n=4; 18 weeks/ n=5) and fra1-tg/rsk2-/x (7 weeks/ n=3; 18 weeks/ n=2) mice. Standard deviations are indicated by error bars. Statistically significant differences are indicated by asterisks.

In order to quantify the degree of organ enlargement, the spleen weight/ body weight ratios were calculated for the same mice as used for the fat pad/ body weight analyses [Chapter 5.3.2]. The median spleen weight/ body weight ratios of 7 weeks old male wt, rsk2-/y and fra1-tg/rsk2-/y mice turned out to be similar. They ranged between 0.0037 and 0.0041 (wt: 0.0038±0.0006; rsk2-/y: 0.0037±0.0007; fra1-tg/rsk2-/y: 0.0041±0.0006; Figure 5.19 C, left panel). Contrary, the median spleen weight/ body

weight ratio of 7 weeks old male fra1-tg mice (fra1-tg: 0.0057±0.0008, ***P<0.0001) was found to be significantly increased when compared to wt mice (Figure 5.19 C, left panel).

The same results were obtained when male mice were analyzed at an age of 18 weeks, except for fra1-tg/rsk2-/y mice that did not survive to this age (wt: 0.0036±0.0008; rsk2-/y: 0.0032±0.0010; fra1-tg: 0.0071±0.0012; Figure 5.19 C, right panel). Apparently, male fra1-tg mice suffer from progressing splenomegaly, since the median spleen weight/ body weight ratio was shown to increase with age (7 weeks: 0.0057±0.0008 vs. 18 weeks: 0.0071±0.0012). The intra-strain variance was constantly low for all tested groups of male mice.

The results obtained through analysis of female mice resembled the findings in male mice in that median spleen weight/ body weight ratios of 7 and 18 weeks old wt and rsk2-/x mice were similar (7 weeks/ wt: 0.0042±0.0004; rsk2-/y: 0.0044±0.0008 and 18 weeks/ wt: 0.0039±0.0005; rsk2-/y: 0.0036±0.0005). On the other hand the ratios of fra1-tg mice were significantly increased (7 weeks/ 0.0087±0.0012, ***P<0.0001; 18 weeks/ 0.0092±0.0021, ***P<0.0001) when compared to wt mice (Figure 5.19 D). Both 7 weeks old and 18 weeks old female fra1-tg/rsk2-/x mice showed significantly increased median spleen weight/ body weight ratios (7 weeks/ 0.0090±0.0038, ***P<0.0001; 18 weeks/ 0.0099) when compared to wt mice (Figure 5.19 D). The median spleen weight/ body weight ratios did neither increase with age in female fra1-tg nor in female fra1-tg/rsk2-/x mice. In addition, the spleen weight/ body weight ratios of 7 weeks old female fra1-tg mice (Figure 5.19 D) were already above the ratios calculated for 18 weeks old male fra1-tg mice (Figure 5.19 C), which may indicate a more severe and faster progression of splenomegaly in the females.

Altogether, these data indicate that Fra1 induced splenomegaly can be counteracted by total rsk2-deficiency such as present in male fra1-tg/rsk2-/y mice but not partial depletion of Rsk2 as existent in the female fra1-tg/rsk2-/x mice.

5.5.2. Rsk2-deficiency cannot rescue the abnormal spleen morphology observed in fra1-tg mice

To investigate whether overexpression of Fra1 and Rsk2-deficiency not only have an impact on the size of the spleen but also affects its structure, various histomorphological analyses were done. At first, spleens were analyzed with respect to segregation of red and white pulp and the overall density of cells within both (of these)

compartments. For this purpose, spleen sections of all mice strains (wt, rsk2-/y, fra1-tg, fra1-tg/rsk2-/y and fra1-tg/rsk2-/x) were subjected to H&E stainings.

Representative series of photomicrographs of H&E stainings obtained at different magnifications are illustrated in Figure 5.20. The H&E staining of wt spleen is shown on Figure 5.20 a – c. A normal spleen structure was observed in rsk2-/y mice (Figure 5.20 d - e), including clear separation of red pulp (arrow) and white pulp regions (asterisk). The erythrocyte-rich red pulp regions were demarcated by intense Eosin staining (pink-red). On the other hand, the lymphocyte-rich areas corresponding to the white pulp were highlighted by distinctive nuclear Hematoxylin staining (blue).

However, clear separation of red and white pulp regions was lost in the case of spleens isolated from fra1-tg (Figure 5.20 i - l) and fra1-tg/rsk2-/y mice (Figure 5.20 m - p). This most likely attributes due to an extension of the lymphocyte compartment and subsequent infiltration of lymphocytes in the red pulp as indicated by diffuse Hematoxylin staining.
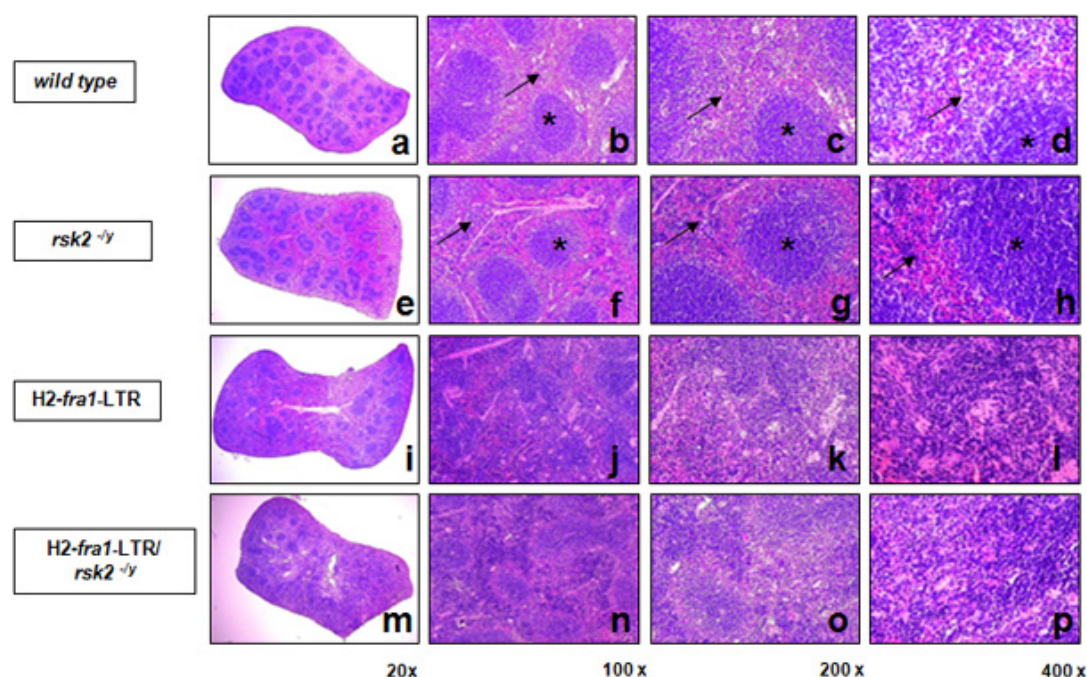
Figure 5.20 Fra1 overexpression induced structure changes in fra1-tg and fra1-tg/rsk2-/y spleens

Hematoxylin and Eosin (H&E) staining of paraffin embedded spleen parenchyma with red and white pulp of 7 weeks old wt (a – d), rsk2-/y (e – f), fra1-tg (i – l) and fra1-tg/rsk2-/y (m – p) mice (microscope magnifications: 20x – 100x – 200x - 400x). The arrow indicates red pulp; the asterisk indicates white pulp. The staining represents means cross section from more than three independent colourings.

5.5.3. Fra1 overexpression causes structural changes of the spleen by inducing connective tissue remodelling

The connective tissue framework of the spleen is formed by a spider-web like network of reticulum fibres that are composed of thin fibrils of Collagen and Elastin. In order to study, if Fra1 overexpression and Rsk2-deficiency also affect the connective tissue remodelling of the spleen, reticulum fibre networks were visualized and analyzed by Mason-Goldner-Tricolor (MGT) stainings.

Representative series of photomicrographs of MGT stainings obtained at different magnifications are illustrated in Figure 5.21. As already shown by H&E staining [Chapter 5.5.2.], wt (Figure 5.21 a - d) and rsk2-/y mice (Figure 5.21 e - h) showing clear separation of red and white pulp regions that are tinged red and yellow in MGT stainings, respectively. In addition, MGT staining revealed normal arrangement of the connective tissue in these mice, in that both the collagen containing splenic capsule and the marginal zone (MZ), that was rich in collagen-containing endothelial/ epithelial cells, could be identified (tinged light-blue in MGT). Likewise, MGT staining indicated the loss of clear red and white pulp segregation in spleens of fra1-tg (Figure 5.21 k – l) and fra1-tg/rsk2-/y mice (Figure 5.21 m – p), which was already a result of the H&E staining [Chapter 5.5.2.]. Moreover, the MGT staining supported the hypothesis that the red pulp was infiltrated by cells from the white pulp in these mice, as the density of erythrocytes seems to be diminished due to intermingling with other cells. Surprisingly, the regions occupied by connective tissue were enlarged in the spleens of fra1-tg and fra1-tg/rsk2-/y mice, a result that might be a sign for commencing fibrosis. Besides being enlarged, the network of reticular fibres in spleens of fra1-tg and fra1-tg/rsk2-/y mice diverged from the normal arrangement of the connective tissue, in that splenic capsules and the MZ could be hardly identified. The network of reticular fibres rather appeared to be loosely dispersed in fra1-tg and fra1-tg/rsk2-/y mice.

Taken together, these data suggest that the observed aberrant morphology of spleens derived from fra1-tg and fra1-tg/rsk2-/y mice might be due to connective tissue remodelling triggered by Fra1 overexpression. Most interestingly, although Rsk2-deficiency was shown to counteract Fra1 induced splenomegaly [Chapter 5.4.1.] it did not rescue spleens from connective tissue remodelling.
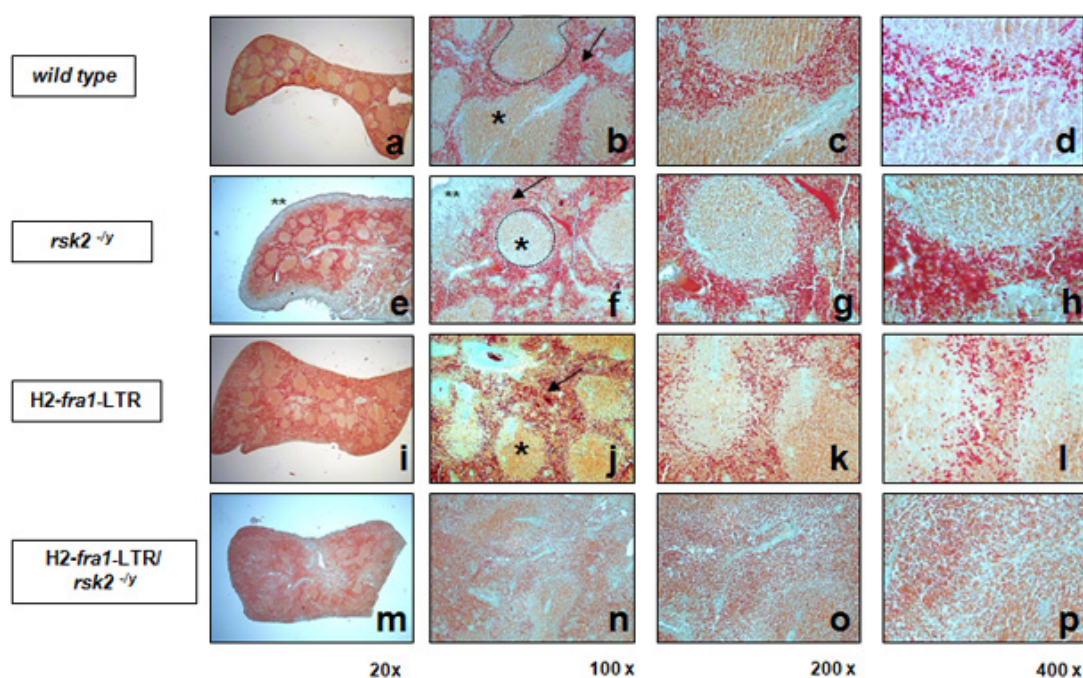
Figure 5.21 Loss of normal spleen structures in Fra1 overexpression spleens

Masson–Goldner-Tricolor (MGT) staining of paraffin embedded spleen parenchyma of 7 weeks old wt, rsk2-/y, fra1-tg and fra1-tg/rsk2-/y mice (microscope magnifications: 20x – 100x – 200x - 400x); one asterisk indicates the white pulp; the arrows indicate the red pulp, two asterisk indicates capsule and point lines indicates marginal zone (MZ) around the red pulp. The staining represents means cross section from more than three independent colourings.

5.5.4. Fra1 overexpression causes changes of the stromal tissue of the splenic white pulp that affect the homing of B cells

H&E and MGT stainings have demonstrated that fra1-tg and fra1-tg/rsk2-/y mice show perturbed morphology of the spleen, particularly regarding its compartmentalization. To assess, whether Fra1 overexpression and Rsk2-deficiency have effects beyond interfering with the basic structure of the spleen as for instance by affecting the cellular composition of white pulp and MZ, spleen sections were additionally immunostained using antibodies against MOMA-1, B220, FDC-M2 and BP-3 (Figure 5.22).

The MOMA-1 antibody stains the ring of metallophilic macrophages (MM) that surrounds the splenic white pulp and forms the inner border of the MZ. Since B220 is expressed on all B cells, resting and activated, it allows the visualization of B cell zones/ follicles and marginal zone (MZ) B cells. The FDC-M2 epitope is constitutively expressed on follicular dendritic cells (FDCs) in primary and secondary B cell follicles and can therefore be used to localize FDC networks. The BP-3 antibody reacts with splenic reticular cells of the white but not red pulp.

Immunostainings of spleen sections derived from wt mice attested normal cellular composition of white pulp regions and the MZ in these mice (Figure 5.22 a - d). Briefly, white pulp regions were shown to comprise marked B cell zones (Figure 5.22 b) that were found in contiguity to FDC-networks (Figure 5.22 c). Furthermore, white pulp regions were both traversed by a network formed by BP-3 positive reticular cells (Figure 5.22 d) and demarcated from the MZ by the ring of MOMA-1 expressing MM (Figure 5.22 a).

In spleens of fra1-tg (Figures 5.22 e - h) and fra1-tg/rsk2-/y mice (Figures 5.22 i - l) white pulp and MZ architecture was found to be altered. Most notably, white pulp regions of fra1-tg and fra1-tg/rsk2-/y mice lack fully developed and compact FDC networks (Figures 5.22 g and k) although, faint FDC-M2 staining was observed at the outer border of white pulp regions. Likewise, the BP-3 staining pattern was different in these mice compared to wt mice in that the BP-3 positive cells were concentrated in ring-like structures that rather seem to overlap with or/ extend into the MZ (Figures 5.22 h and l). MOMA-1 stainings further revealed expanded rings of MM in spleens of fra1-tg and fra1-tg/rsk2-/y mice (Figures 5.22 e and i) when compared to wt mice.

More importantly, the homing and formation of regular B cells to B cell zones was affected in spleens of fra1-tg and fra1-tg/rsk2-/y mice. B cells accumulated forming a ring overlapping with the MZ as indicated by double immunofluorescent stainings of B220 and MOMA-1 (Figures 5.23 f and i). Moreover, the localization of B cells correlated with the staining patterns of BP-3 and FDC-M2 in both fra1-tg and fra1-tg/rsk2-/y spleen sections. Since homing of B cells to B cell zones/ follicles is known to rely on the expression of the chemokine (C-X-C motif) ligand 13 (CXCL-13) by FDCs [344], dislocation of B cells in spleens of fra1-tg and fra1-tg/rsk2-/y mice was likely to be secondary to the changes regarding the stromal tissue of the white pulp (FDC and reticular cells).
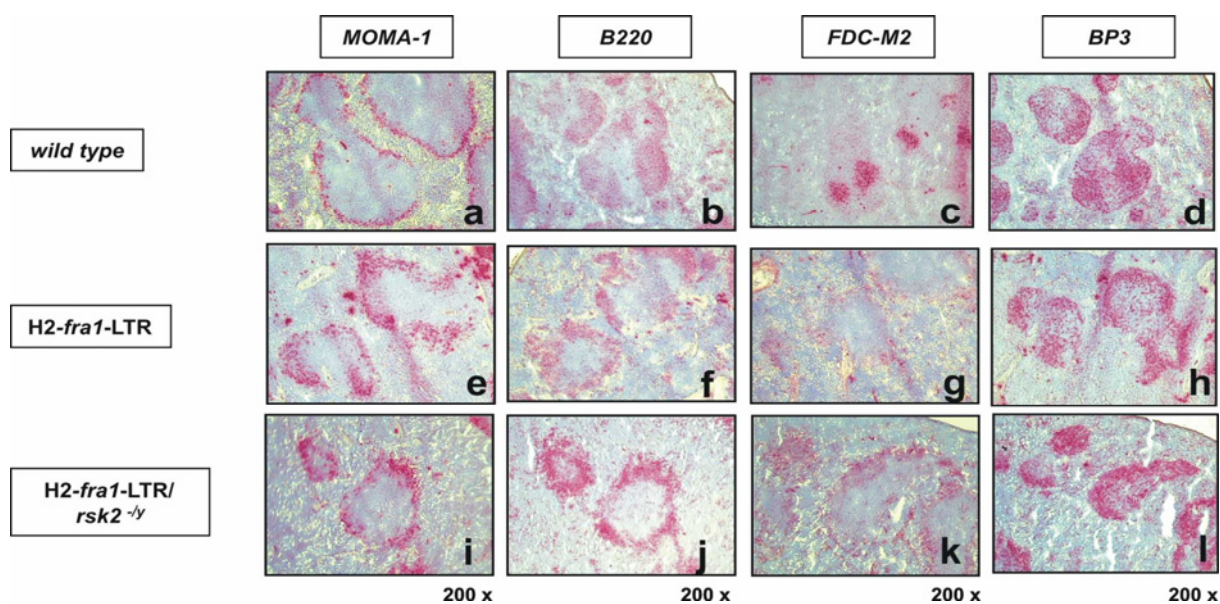
Figure 5.22 Effect of Fra1 overexpression in spleens with different Rsk2 expression

Immunohistochemistry staining of spleen parenchyma of 7 weeks old wt, fra1-tg and fra1-tg/rsk2-/y mice. MOMA-1 for metallophilic macrophages, B220 for B cells follicles, FDC-M2 for follicular dendritic cells clusters, and BP-3 for splenic reticular cells of the white pulp. (Microscope magnifications: 200x). The staining represents means cross section from more than three independent colourings.
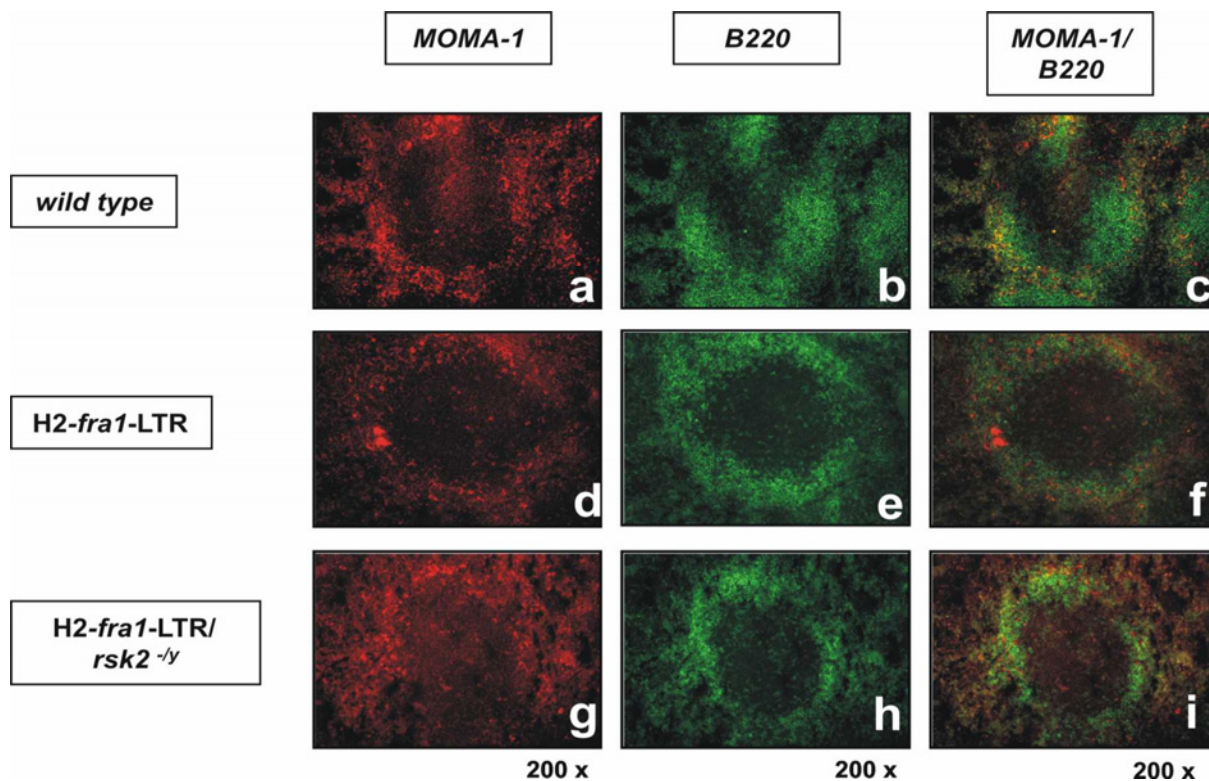
Figure 5.23 B cell accumulations in the splenic marginal zone in Fra1 overexpression spleens

Immunofluorescence staining of spleen parenchyma of 7 weeks old wt, fra1-tg and fra1-tg/rsk2-/y mice. MOMA-1 for metallophilic macrophages, B220 for B cells follicles; MOMA-1/ B220 overlay pictures. (Microscope magnifications: 200x). The staining represents means cross section from more than three independent colourings.

121

5.5.5. Fra1 overexpression induces accumulation of megakaryocytes in the spleen

Megakaryocytes derive from the myeloid lineage of haematopoietic stem cells and are responsible for platelet production. Several severe diseases including thrombocythemia and thrombocytopenia are directly connected to megakaryocytes malfunction [67]. Others like myelofibrosis, osteosclerosis and Hepatitis C are ascribed to increased numbers of megakaryocytes [68, 69, and 70]. Overexpression of Fra1 in mice was previously shown to lead to osteosclerosis of the full skeleton [52]. So far, several results of this study as for instance splenomegaly, reduced density of erythrocytes in the splenic red pulp and changes in the spleen parenchyma suggest that it may be also related to the development of other diseases such as myelofibrosis. Common to the mentioned diseases is that their aetiology is thought to be linked to megakaryocytes development.

To assess, whether the observed abnormalities regarding the spleens of fra1-tg mice also include changes regarding splenic megakaryocytes, additional H&E and Immunostainings were performed on spleen sections derived from paraffin embedded specimens (Figure 5.24). Megakaryocytes were detected by an antibody directed against CD41 in combination with DAPI nuclear counterstained. CD41 is a glycoprotein that is typically expressed on the surface of megakaryocytes.

Megakaryocytes could be identified in spleens of wt, fra1-tg and fra1-tg/rsk2-/y mice by both H&E stainings (Figure 5.24 a - c) and CD41 Immunostainings (Figure 5.24 d - f). However, the stainings collectively pointed at an increased number of megakaryocytes in the spleens of fra1-tg and fra1-tg/rsk2-/y mice. This observation was subsequently verified by statistical counting of CD41 positive megakaryocytes, in that the number of megakaryocytes per observation field (HIM) turned out to be increased about 20- and 28-fold in case of fra1-tg and fra1-tg/rsk2-/y mice, respectively (Table 5.2). According to this, Fra1 overexpression seems to induce the accumulation of megakaryocytes in the spleen through extramedullary haematopoiesis.
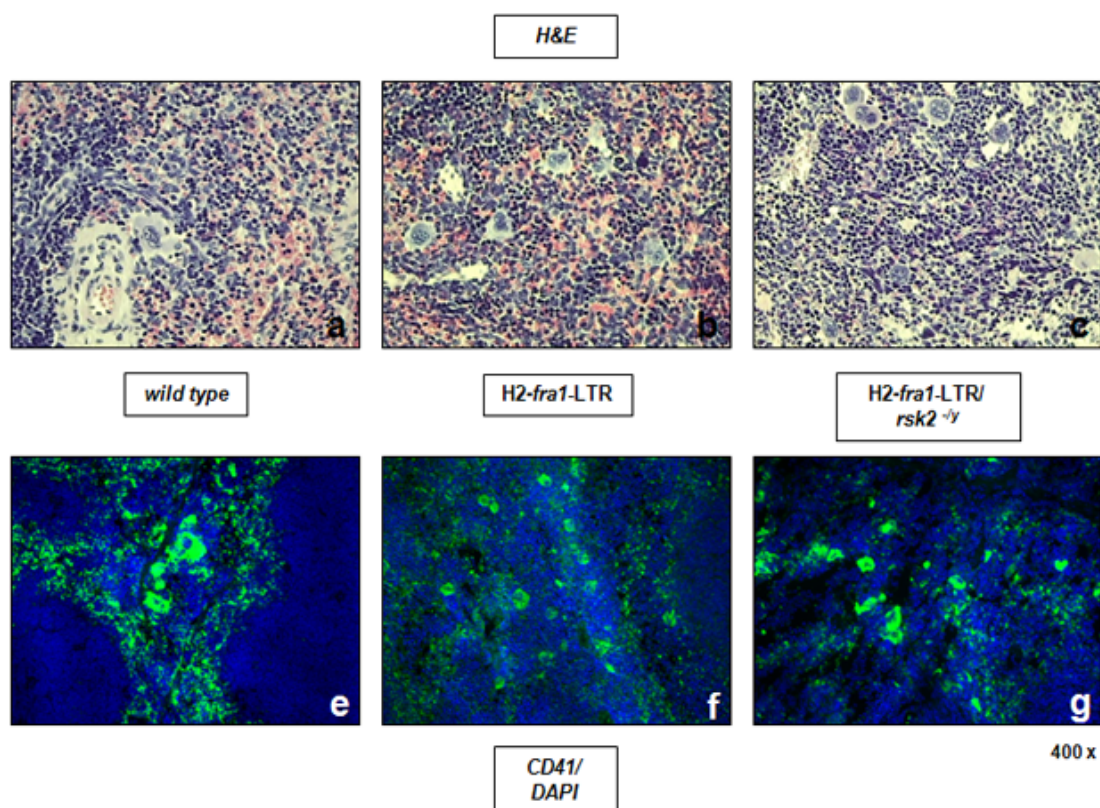
Figure 5.24 Induced megakaryocytes in spleens of Fra1 overexpressing mice

Hematoxylin and Eosin (H&E) staining of paraffin embedded spleen parenchyma of 7 weeks old wt (a), fra1-tg (b) and fra1-tg/rsk2-/y (c) mice (microscope magnifications: 400x) and Immunofluorescence staining of spleen parenchyma of 7 weeks old wt (e), fra1-tg (f) and fra1-tg/rsk2-/y (g) mice. CD41 for platelets or megakaryocytes, DAPI for nucleus, CD41/ DAPI overlay pictures. (Microscope magnifications: 400x). The staining represents means cross section from more than three independent colourings.

Table 5.2 Enumeration of megakaryocytes in wt, fra1-tg and fra1-tg/rsk2-/y spleens

cell density * per HIM **	wild type	fra1- tg	fra1- tg/rsk2-/y
7 weeks Average ± Stdv fold induction	0.32 ± 0.36 0	6.44 ± 0.97 20 fold	9.10 ± 0.71 28 fold

spleen section were counted 5 fields per slide in HIM

* megakaryocytes   ** high image magnification (400x)

5.6   Heart analyses

As shown in fat and spleen analyses, Fra1 overexpression influences cells, which are derived from the mesenchymal lineage. Heart cells or cardiomyocytes are cells, which are coming from the mesenchymal lineage. Therefore, the heart of Fra1 overexpressing mice was analysed.

5.6.1. Deleting of Rsk2 induced heart abnormality in Fra1 overexpressing mice

The heart size of 7 weeks old wt, rsk2-/y, fra1-tg and fra1-tg/rsk2–/y mice are shown in Figure 5.25 A. The wt, rsk2-/y and fra1-tg male hearts were the same in size at age of 7 and 18 weeks. The size of the heart of fra1-tg/rsk2–/y mice at age of 7 weeks appeared to be increased (Figure 5.25 A). Figure 5.26 B is comparing female hearts between the wt, rsk2-/x, fra1-tg mice and the mutated fra1-tg/rsk2-/x female mice at age of 18 week. Only the 18 weeks old mutated fra1-tg/rsk2-/x female mice showed differences in size of the heart.

To quantify a potential heart enlargement the ratio of the heart weight to the body weight were measured for wt, rsk2-deficent, fra1-tg, fra1-tg/rsk2-/y and fra1-tg/rsk2-/x littermates at ages of 7 and 18 weeks. The heart weight/ body weight ratio at age of 7 weeks of wt male and fra1-tg male mice were nearly the same and no significant difference was measured between these two groups (wt: 0.0054±0.0005; fra1-tg: 0.0057±0.0009; Figure 5.25 C, left panel). However, while a significant decrease in the heart weight/ body weight ratio was measured in 7 weeks old rsk2-/y mice (0.0049±0.0006, **P<0.0088), and an increase was measured for fra1-tg/rsk2-/y mice (0.0072±0.0016, ***P<0.0003). Analysis of 18 weeks old male mice did not show any noticeable difference (wt: 0.0050±0.0011; rsk2-/y: 0.0048±0.0005; fra1-tg: 0.0057±0.0009; fra1-tg/rsk2-/y: no survival; Figure 5.25 C, right panel).

When comparing 7 weeks old female littermates no significant difference in their heart weight/ body weight ratio was measured (wt: 0.0052±0.0004; rsk2-/x: 0.0065±0.0029; fra1-tg: 0.0052±0.0011; fra1-tg/rsk2-/x: 0.0059±0.0007; Figure 5.25 D, left panel). However, the ratios were found to be significantly increased in 18 weeks old females overexpressing Fra1 (0.0056±0.0009, ***P=0.0055) and fra1-tg/rsk2-/x mice (0.0062) when compared to wt mice 18 weeks old and rsk2-/x mice 18 weeks old (wt: 0.0047±0.0003; rsk2-/x: 0.0048±0.0004; Figure 5.25 D, right panel).

The analyses of the heart weight/ body weight ratio showed that Fra1 overexpression induce change of the heart in vivo. The differences in the ratio were found to be more pronounced in females than in males. Furthermore, deleting of Rsk2 induced heart abnormalities in Fra1 overexpressing mice.
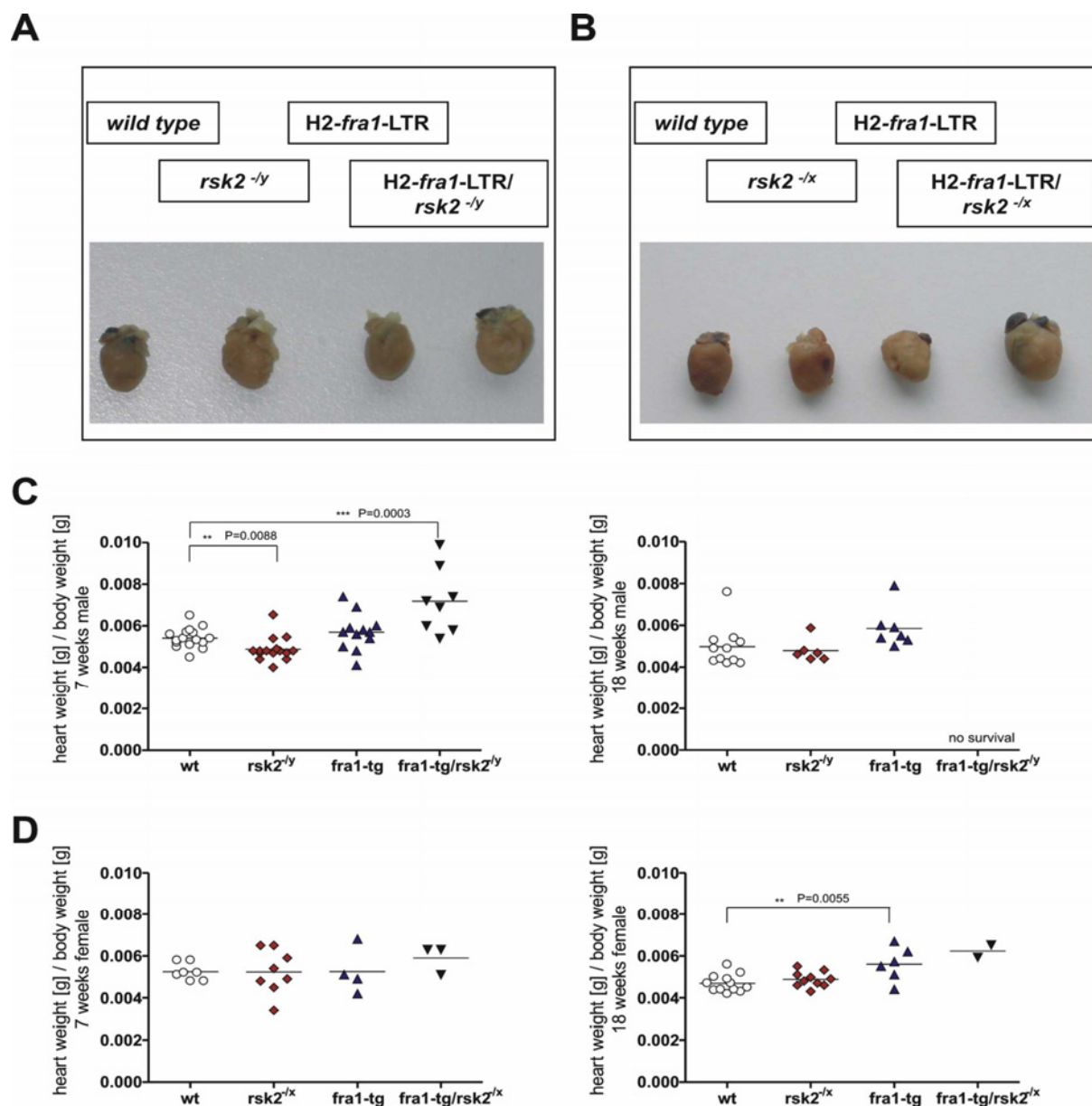
Figure 5.25 Deleting of Rsk2 induced heart abnormality in Fra1 overexpressing mice

A)Picture of 7 weeks old male *wt*, *rsk2*[-/y], *fra1*-tg and *fra1*-tg/*rsk2*[-/y] hearts; **B)** Picture of 18 weeks old female *wt*, *rsk2*[-/x], *fra1*-tg and *fra1*-tg/*rsk2*[-/x] hearts; **C)** Ratio between heart weight and body weight of 7 weeks old and 18 weeks old males *wt* (7weeks/ n=16; 18weeks/ n=11), *rsk2*[-/y] (7weeks/ n=15; 18weeks/ n=6), *fra1*-tg (7 weeks/ n=12; 18 weeks/ n=7) and *fra1*-tg/*rsk2*[-/y] (7 weeks/ n=8; 18 weeks/ n=0) mice; **D)** Ratio between heart weight and body weight of 7 weeks old and 18 weeks old females *wt* (7 weeks/ n=7; 18 weeks/ n=12), *rsk2*[-/x] (7 weeks/ n=8; 18 weeks/ n=5), *fra1*-tg (7 weeks/ n=4; 18 weeks/ n=5) and *fra1*-tg/*rsk2*[-/x] (7 weeks/ n=3; 18 weeks/ n=2) mice. Error bars indicate standard deviations. Asterisks indicate statistically significant differences.

5.6.2.   Fra1 overexpression induced heart fibrosis

125

To look at morphological changes of hearts H&E staining of heart sections were done in 18 weeks old male wt, rsk2-/y and fra1-tg mice and 18 weeks old female fra1-tg/rsk2-/x mice (Figure 5.26). The wt cardiomyocytes were packed into highly-regular arrangements of bundles. Cardiac muscle connects at branching, irregular angles. The cells were connecting net-like and the nucleus lies centrally (Figure 5.26 a & b). When compared to wt, no difference could be detected with this staining in rsk2-/y mice (Figure 5.26 c & d). Visible morphological changes of muscle cells could be seen on H&E stained section of fra1-tg male mice and mutated fra1-tg/rsk2-/x female hearts. Smaller fibrotic cells were detected between the bigger myocardial cells in fra1-tg heart sections (Figure 5.26 e & f) as well as in fra1-tg/rsk2-/x heart sections (Figure 5.26 g & h).
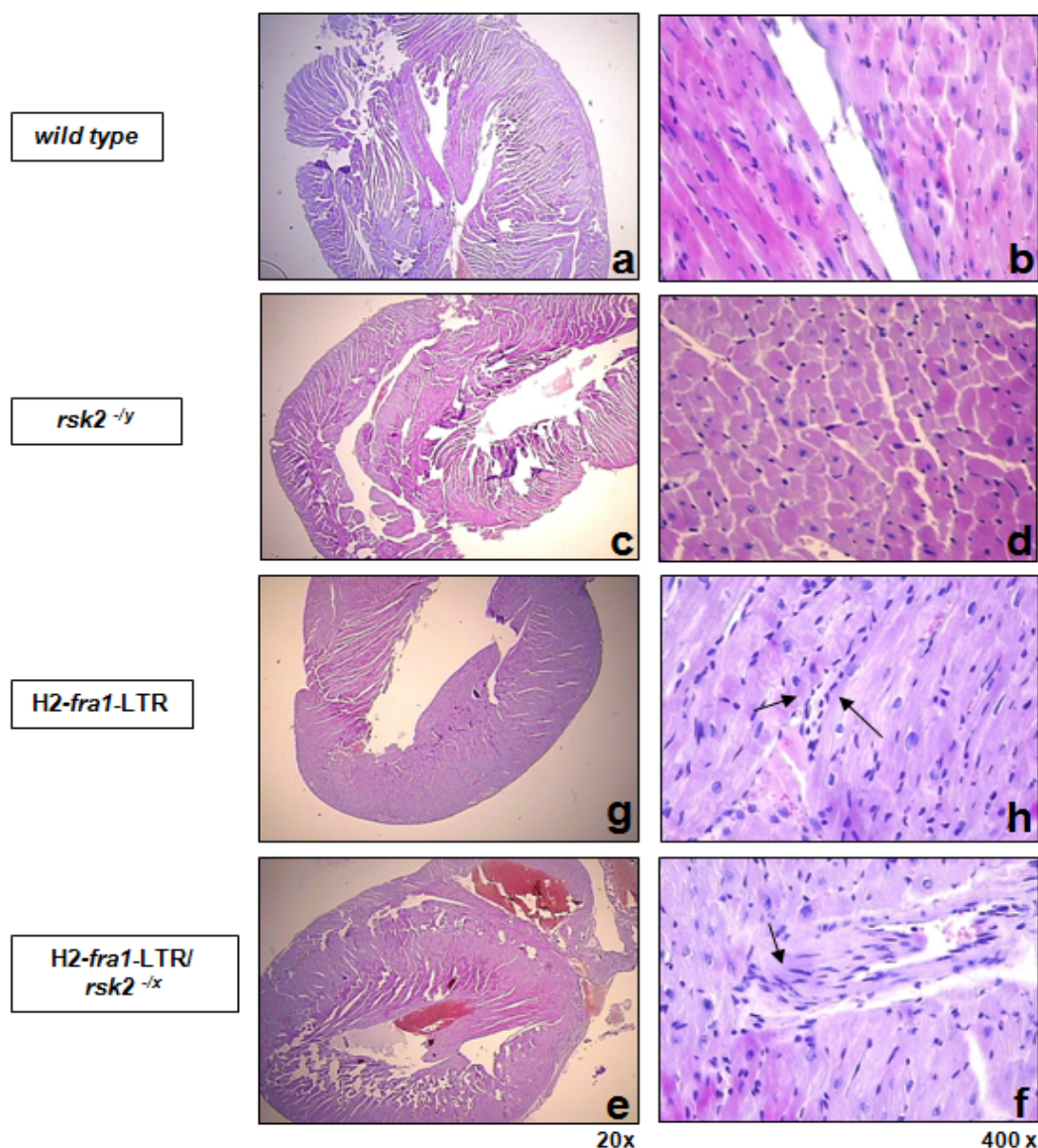
Figure 5.26 Fra1 overexpression induced smaller fibrotic cells between bigger myocardial cells

Hematoxylin and Eosin (H&E) staining of paraffin embedded hearts sections of 18 weeks old wt, rsk2-/y, fra1-tg male mice and fra1-tg/rsk2-/x female mice (phase contrast microscopy: 20x – 400x magnifications) arrow indicate fibrotic cells. The staining represents means cross section from more than three independent colourings.

To identify the smaller cells MGT and EvG staining were performed to look at fibrosis or at the presence of collagen in the tissue off these mice. After staining of wt (Figure 5.27 A/ a - b and 5.27 B/ a - b) male heart sections no morphological alteration was observed. Only pure muscle tissue was found in this staining. Using MGT or EvG staining on sections of 18 weeks old mice, extensive focal interstitial fibrosis were found in fra1-tg heart sections (Figure 5.27 A/ c - d and Figure 5.27 B/ c - d).

Thus, the heart enlargement could be explained by additional collagen producing fibrotic cells between the muscle cells in fra1 transgenic mice.
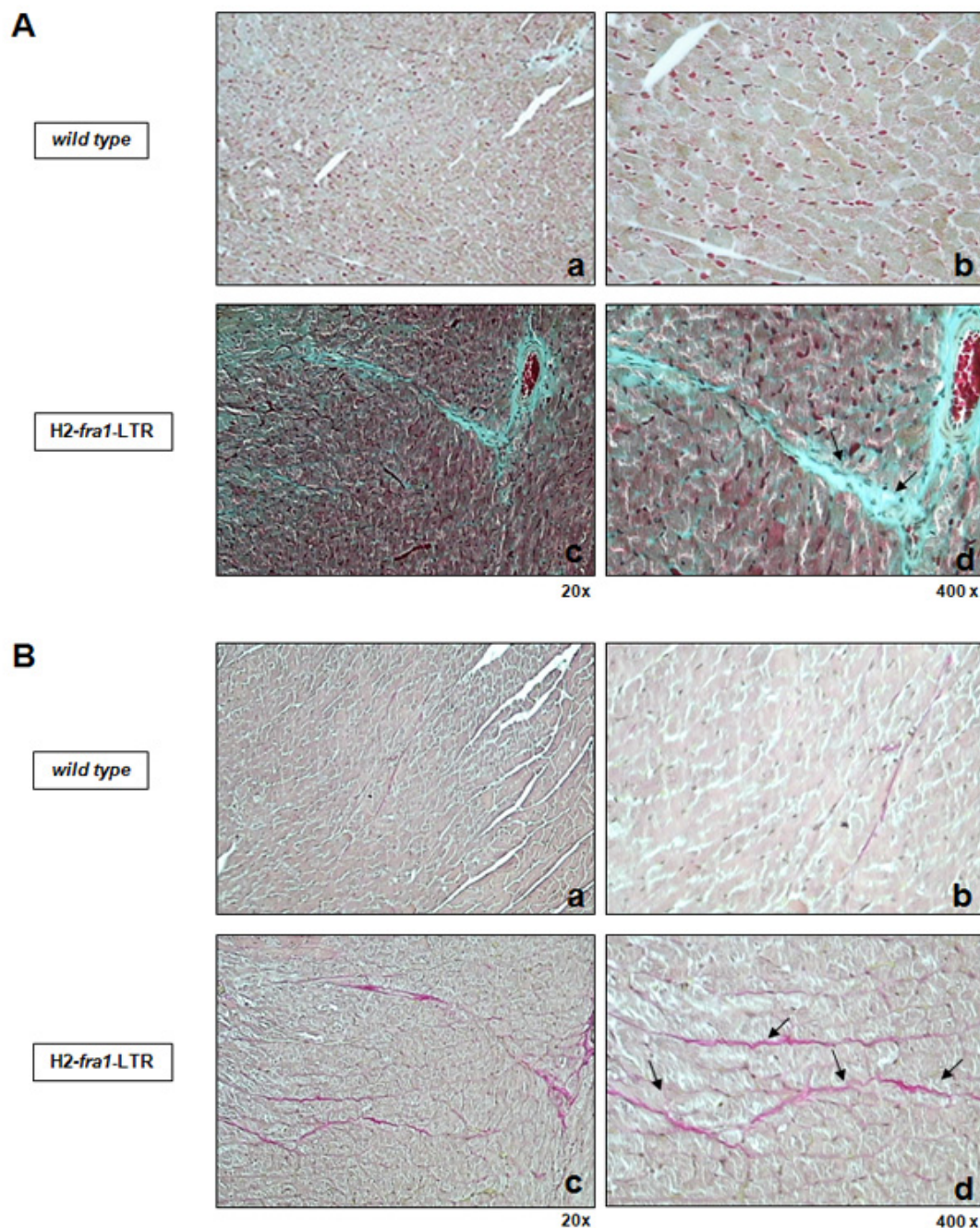
Figure 5.27 Fra1 overexpression increased collagen-inducible tissue in hearts

Masson-Goldner-Tricolor (MGT) staining of paraffin embedded hearts of 18 weeks old wt and fra1-tg male mice; B) Elastica van Gieson (EvG) staining of paraffin embedded hearts of 18 weeks old wt and fra1-tg male mice; phase contrast microscopy: 20x – 400x magnifications; arrow indicate collagen; The staining represents means cross section from more than three independent colourings

5.7 Liver analyses

The liver plays a major role in metabolism. Damages in the liver are often life threatening. Influences of Fra1 overexpression could already show in changes of spleen stoma components, and increased fibrotic cells. By analyzing sections from different littermates the question, arise whether Fra1 could also affect the liver function.

5.7.1. Fra1 overexpression induced fibrosis and inflammation in liver parenchyma

Freshly isolated liver obtained from fra1-tg/rsk2-/x mice were notably paler than the one from wt mice (Figure 5.28) indicating that Fra1 overexpression or Rsk2 deletion could have impaired liver function. Therefore histological analyses of the livers were performed.
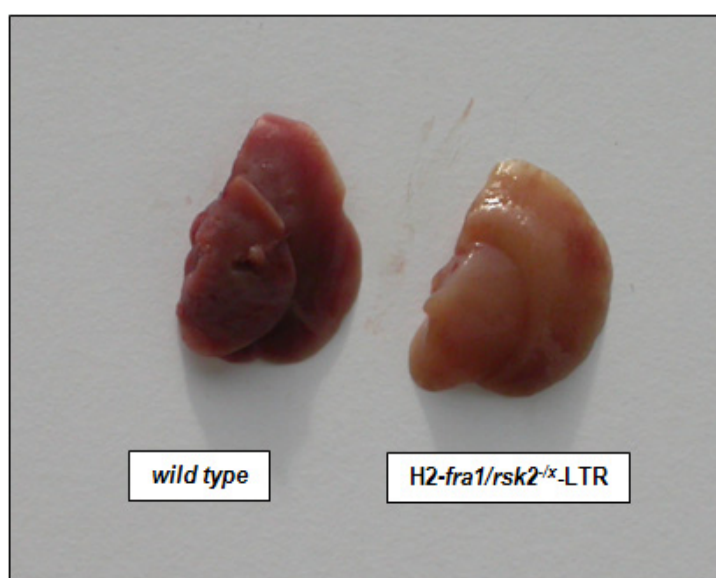
Figure 5.28 Picture of fresh dissect livers of 18 weeks old female wt and fra1-tg/rsk2-/x mice

The paler appearance of the liver can be explained by a disturbance of the blood flow or through a deterioration of the blood transport in the vessels or a disturbance in the liver tissue. Liver fibrosis, for example, results in an excessive deposition of extra cellular matrix in the liver tissue leading to lethality. Histomorphological analyses were done to determine, if the structures of liver tissue between wt and fra1-tg mice are different.
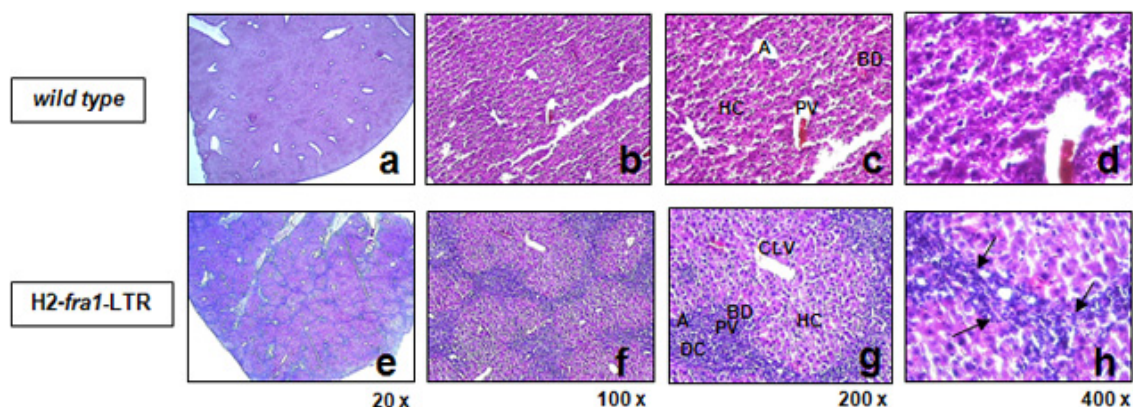
Figure 5.29 Fra1 overexpression induced liver fibrosis

Hematoxylin and Eosin (H&E) staining of paraffin embedded liver sections of 18 weeks old wt and fra1-tg mice; arrow indicate Fra1 induced liver fibrosis; CLV - centrolobular vein, PV - portal vein, A - arteries, BD - bile ducts, HC - hepatocytes, DS - disse space, (phase contrast microscopy: 20x – 100x – 200x - 400x magnifications). The staining represents means cross section from more than three independent colourings.

Figure 5.29 shows wt tissue and fra1-tg tissue of a formalin-fixed paraffin-embedded liver stained through H&E staining. Typical liver structures were seen in wt and fra1-tg sections: a centrolobular vein (CLV), a portal vein (PV), arteries (A), the bile ducts (BD) and numerous hepatocytes (HC). The wt parenchyma was marked by a constant distribution of the H&E colours (Figure 5.30 a – d). The area between endothelial cells of the blood, the bile vessels transport system and the hepatocytes, called disse space (DS) was stained differently in Fra1 overexpressing liver. Fibroblasts, neutrophilic granulocytes macrophages, hepatic stellate cells and lymphoid cells surrounded the fra1-tg disse space. These are cell populations, which are typically associated with inflammation reaction and by replacement of liver tissue by fibrotic scar tissue as well as regenerative nodules, leading to progressive loss of liver function. Hepatic fibrosis, which is characterised by the transformation of normal extra cellular matrix into a reticulated and dense matrix (fibrillar type), was visible in H&E stained fra1-tg liver sections (Figure 5.29 e – h; arrow indicate the fibrotic scar tissue stained dark purple).

Thus, Fra1 overexpression increased fibrotic tissue and plays a role in liver inflammation.

5.7.2. Fra1 overexpression induced accumulation of collagen between hepatocytes and portal triad vessels

To visualise fribroctic tissue in liver, Masson–Goldner-Tricolour (MGT) and Elastica van Gieson (EvG) stainings were done. Both staining methods were used to mark extra cellular matrix like collagen I and III in the liver tissue. Figure 5.30 A shows formalin-fixed paraffin-embedded liver section stained by MGT. On the wt liver section enlarged capillaries are observed between the hepatocytes. These sinusoids are lined by an endothelium (EM). The liver parenchyma was homogenous and erythrocytes were detected in blood vessels (Figure 5.30 A/ a - c).
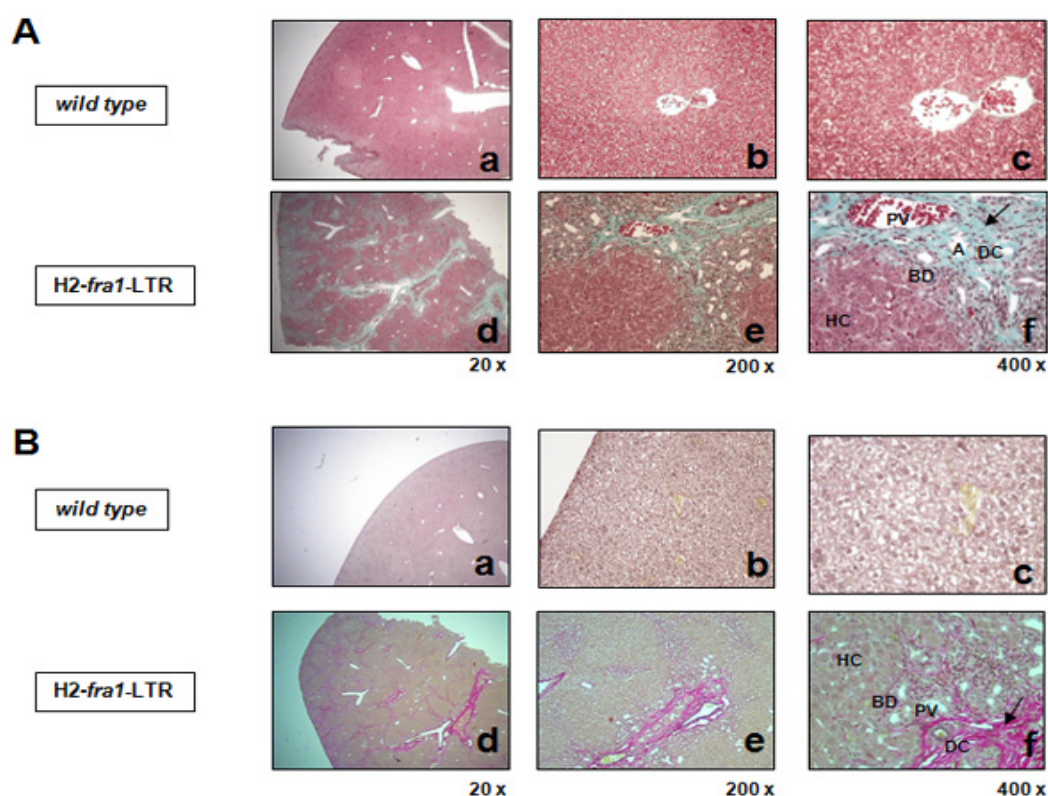
Figure 5.30 Fra1 overexpression in liver induced fibrotic tissue

Masson–Goldner-Tricolor (MGT) staining of paraffin embedded liver sections of wt and fra1-tg mice. B) Elastica van Gieson (EvG) staining of paraffin embedded liver sections of 18 weeks old wt and fra1-tg mice, arrows indicate Fra1 induced connective tissue; PD – portal vein, BD – bile duct, DC – disse space, HC – hepatocytes (phase contrast microscopy: 20x – 200x - 400x magnifications); The staining represents means cross section from more than three independent colourings.

In section of liver from Fra1 overexpressing mice areas between hepatocytes and the portal triad vessels were stained green to blue by MGT staining. This green to blue colour stained extra cellular collagen. Blood vessel (PV) and bile duct (BD) were detected between the collagen deposits. 200 fold magnification showed that the stained areas are located in the disse space (DC) (Figure 5.30 A/ d - f).

Figure 5.30 B shows Elastica van Gieson staining. The wt sections did not show any extra cellular stained matrixes. The liver parenchyma was homogenous with some vessels for blood transport detected (Figure 5.30 B/ a – c). In Fra1 overexpressing liver extra cellular matrix was stained red by EvG staining. Again this collagen was detected in the disse space around the blood vessel and bible duct up to the hepatocytes (Figure 5.30 B/ d – f).

These data show that Fra1 overexpression induced collageneous fibrotic scar tissue between hepatocytes and the portal triad vessels. Furthermore, Fra1 overexpression increased cells, which are typical for inflammation and diseases like primary biliary cirrhosis or primary sclerosing cholangitis.

5.7.3. Fra1 detection in simple cuboidal epithelium cells of portal triad vessels induced cholangitis

To identify the cells which could be responsible for the induced inflammation in fra1-tg mice immunofluorescent staining with Antibody (Ab) for Fra1 where done on liver sections. Figure 5.31 shows in wt and fra1-tg littermates the liver organization of a portal triad: 1) branches of the hepatic artery (A), 2) branches of the hepatic portal vein (PV), 3) small bile ducts (BD) and 4) disse space (DC). Several profiles of bile duct were lined by simple cuboidal epithelium while the blood vessels were lined by endothelium (simple squamous epithelium). Cords of hepatocytes (HC) were also shown in these images. Immunofluorescence staining was done to assess the expression of Fra1 in the liver cells.
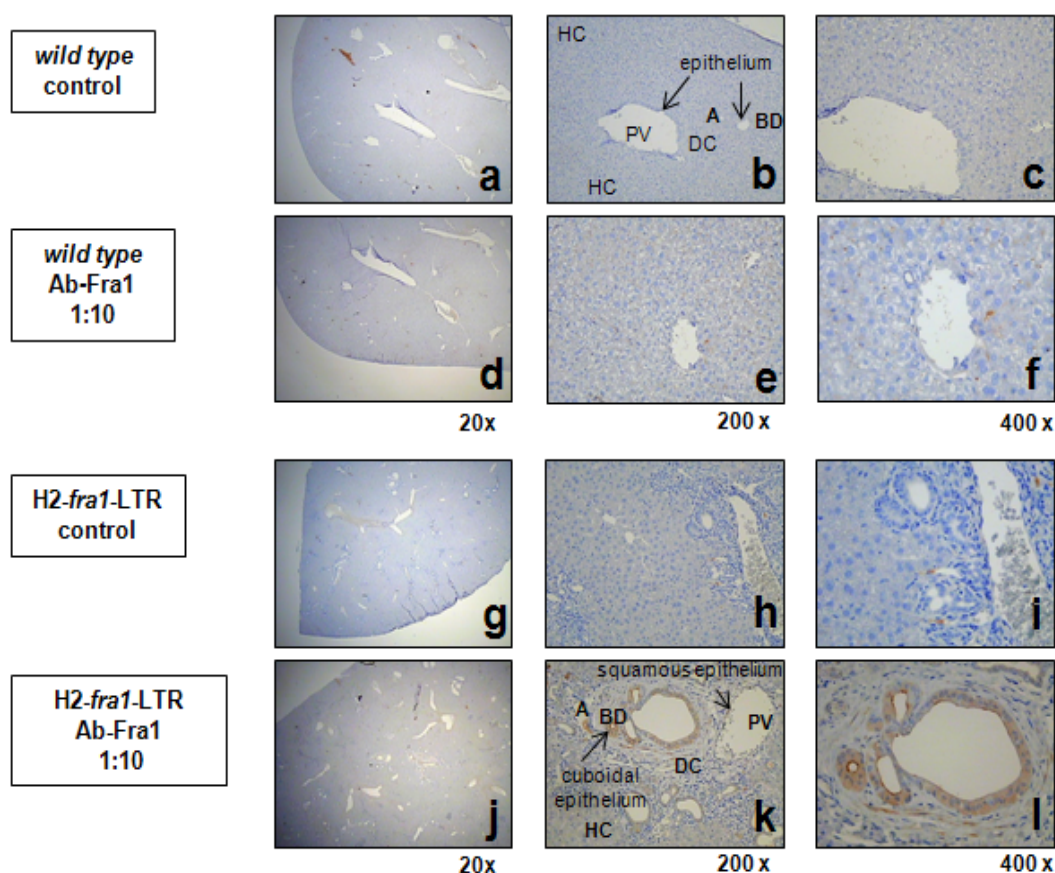
Figure 5.31 Fra1 detection in simple cuboidal epithelium cells of portal triad vessels

Fra1 staining of paraffin embedded liver sections of 18 weeks old wt and fra1-tg mice. PV – portal vein, BD – bile duct, DC – disse space, HC – hepatocytes (phase contrast microscopy: 20x – 200x - 400x magnifications).

Figure 5.31 shows section of liver incubated with Ab-Fra1 (Antibody recognising Fra1). No positive signals were found in control staining (Figure 5.31 a – c) and Ab-Fra1 incubated section of wt liver (Figure 5.31 d – f). However, a specific signal was detected when sections of fra1-tg liver were incubated with Ab-Fra1. High level of expression of Fra1 was detected in simple cuboidal epithelium of the portal triad (Figure 5.31 j – l).

Sustained activation of AP-1 may be a critical factor in determining the outcome of chronical inflammation in liver, and could explain the primary biliary cirrhosis or primary sclerosing cholangitis in fra1-tg mice.

6. Discussion

In the 21th century, the mouse has developed into the premier mammalian model system for genetic research. Scientists from a wide range of biomedical fields have gravitated to the mouse because of its close genetic and physiological similarities to humans, as well as the ease with which its genome can be manipulated and analysed. Although yeasts, worms and flies are excellent models for studying the cell cycle and many developmental processes, mice are far better tools for probing the skeletal, immune, cardiovascular, metabolic, nervous and other complex physiological systems that mammals share. Like humans and many other mammals, mice naturally develop diseases that affect these systems, including osteosclerosis, splenomegaly, heart and liver failure, diabetes or lipodystrophy. In addition, certain diseases that afflict humans but normally do not strike mice, such as cystic fibrosis or Alzheimer's, can be induced by manipulating the mouse genome and environment. Adding to the mouse's appeal as a model for biomedical research is the animals relatively low cost of maintenance and its ability to quickly multiply, reproducing as often as every nine weeks. Mouse models currently available for genetic research include thousands of unique inbred strains and genetically engineered mutants.

One of the topic biomedical research areas is bone development. With knockout (KO) and transgenic (tg) mice it was possible to study the function of genes in skeletal environment [106]. One major emphasis is the genetic analysis of the transcription factor AP-1 complex with regard to its role in normal and pathological bone and also organ development. Scientists also made important contributions in defining the role of AP-1 proteins in developmental processes, e.g. at bone or liver biology and tumor formation.

6.1 AP-1 family member Fra1 regulates bone and fat differentiation and the role of the kinase Rsk2

6.1.1. Fos-related protein-1 (Fra1) and Rsk2 act independently on bone formation

The growth and the maintenance of the skeleton is depend on the coordinated function of osteoblasts and osteoclasts, the two principal cell types of bone tissue [79, 106]. Osteoblasts, which like adipocytes, chondrocytes and myocytes derive from mesenchymal progenitors, produce the extracellular matrix of the bone that later undergoes mineralisation. In contrast, osteoclasts belong to the monocyte/ macrophage

lineage and they reduce bone mass by resorbing the mineralized extracellular matrix. Genetic studies have shown that components of the transcription factor AP-1, mainly members of the Fos family such as c-Fos and Fra1, have important functions in both of these cell types [13, 106].

Transgenic mice expressing c-Fos develop osteosarcoma through transformation of the osteoblast lineage. This phenotype is specific for c-Fos, because mice expressing c-Jun, JunB or FosB do not develop a bone phenotype despite high transgene expression in bone tissue [28]. In contrast, mice lacking c-Fos develop osteopetrosis due to an early differentiation block in the osteoclast lineage [29]. This differentiation block is rescued by Fra1, a Fos-related protein-1 encoded by the c-Fos target gene Fosl1 (referred to as Fra1) [34, 103]. Owing to a lack of transactivation domains, Fra1 has reduced transforming potentials compared with c-Fos [51]. In agreement, ectopic Fra1 in a broad range of organ, e.g. bone and fat tissue resulted in the development of a progressive increase in bone mass leading to osteosclerosis of the entire skeleton. The phenotype was due to a cell-autonomous increase in the number of mature osteoblasts in vivo [52]. Moreover, osteoblast differentiation, but not proliferation, was enhanced and osteoclastogenesis was also elevated in vitro. These data indicated that, unlike c-Fos, which causes osteosarcoma, Fra1 specifically enhances bone formation, which may be exploited to stimulate bone formation in pathological conditions. A similar skeletal phenotype was described in transgenic mice expressing another Fos protein deltaFosB (ΔFosB) [103]. ΔFosB is a naturally occurring truncated form of FosB that lacks the C-terminal transactivation domain, and its overexpression gives a strikingly similar osteosclerotic phenotype. Again, the increased bone mass appears to be the result of increased osteoblast differentiation, rather than proliferation, and leads to significant increases in bone formation rates and increased radio density of bone tissues throughout the entire skeleton [51, 103]. These results add Fra1 and ΔFosB to a growing list of proteins implicated in regulating the bone balance. The models are interesting as they involve increased bone formation, compared with the more commonly observed defects in bone resorption.

How can the specificity of action of the various Fos members be explained? Being transcription factors, they simply may be regulating different set of genes. In agreement with this hypothesis, the analysis using mouse embryonic fibroblast indicated that Fra1 can switch on some but not all the c-Fos target genes in response to serum stimulation [102]. Fra1 and ΔFosB proteins are small Fos proteins that in contrary to c-Fos are lacking detectable transactivation domains, these differences may explain the difference in the pattern of regulated genes. It remains to be seen which AP-1 target genes are involved

in osteoblast differentiation and transformation or in other mesenchymal derived cells. A second possibility is a consequence of the heterodimeric structure of AP-1. Indeed, it is accepted that the transcriptional potential may depend on their heterodimerizing partners, their co-activators. Finally, being intensively regulated by post-transcriptional modification, phosphorylation through different kinases, e.g. ERK, JNK and p38 may explain the phenotypic differences. Two phosphorylation sites located on the C-terminal domain of c-Fos have been shown to regulate its transforming activity in vitro [18, 298]. These sites, serine 362 and 374 are respectively phosphorylated by Rsk2 and ERK. It was shown that mice lacking Rsk2 developed a progressive skeletal disease, osteopenia due to impaired osteoblast function and normal osteoclast differentiation. The phenotype was associated with decreased expression of Phex, an endopeptidase regulating bone mineralisation. This defect was probably not mediated by Rsk2-dependent phosphorylation of c-Fos on serine 362 in the C-terminus as shown by lack of phenotype affecting the osteoblast lineage in mice lacking c-Fos. However, in the absence of Rsk2, c-Fos–dependent osteosarcoma formation was impaired. The lack of c-Fos phosphorylation leads to reduced c-Fos protein levels, which are thought to be responsible for decreased proliferation and increased apoptosis of transformed osteoblasts. Therefore, Rsk2-dependent stabilisation of c-Fos was essential for osteosarcoma formation in mice [19]. Interestingly, mice lacking Rsk2 or lacking Fra1 are both osteopenic due to decreased bone formation by osteoblasts suggesting that Fra1 function in bone could have been regulated by phosphorylation and stabilisation by Rsk2 [19, 52].

This study investigated this hypothesis by generating mice overexpressing Fra1 but lacking Rsk2. The results showed that inactivation of Rsk2 did not rescue the osteosclerosis induced by Fra1 overexpression. In addition, the mineralisation defect caused by downregulation of Phex observed in Rsk2-deficient mice was also not corrected by Fra1 overexpression. In contrary, the volume of non-mineralised bone matrix was found increased in the double mutant mice. These data indicate that both proteins are acting independently on bone formation. They also indicate that, while Fra1 is mainly regulating bone matrix deposition. Rsk2 is involved in its mineralisation [19, 50 and 52]. These data are in agreement with the role previously proposed for Fra1 in bone [50]. Fra1 not being downstream of Rsk2 in bone. A study by Elefteriou et al., 2006 demonstrated that the mineralisation activity of Rsk2 is most likely mediated via the phosphorylation of ATF4 [227].

6.1.2. Fos-related protein-1 (Fra1) and Rsk2 reduce white adiposite tissue (WAT)

Previous studies already showed that inactivation of Fra1, resulted in embryonic lethality around day 10 of development because of defects in the placenta [51]. The labyrinth layer of mutant placentas was reduced in size and was largely avascular suggesting that the invasion of allantoic vessels into the chorionic plate was impaired in the absence of Fra1. The development of mutant fetuses could be rescued up to birth by providing wild type extra-embryonic tissues using tetraploid blastocyst injection [228]. Moreover, the lethality of Fra1-deficient mice was fully rescued by the ectopic expression of Fra1 from transgenic mice demonstrating that AP1/ Fra1 activity during development does not have to be tightly regulated. These rescued mice still developed osteosclerosis, which was indistinguishable from the disease observed in the fra1 transgenic mice. These data suggested that Fra1 was dispensable for the differentiation of most, if not all, cell lineages in the fetus [51, 228]. However, my observations that fra1-tg mice lacking Rsk2 are more severely growth retarded than the parental lines still indicated that both proteins may act together in tissues other than bone.

A similar osteosclerotic phenotype was observed in transgenic mice expressing ΔFosB in osteoblasts, interestingly these mice also showed reduced white adipose tissue (WAT) that has not been reported in Fra1 transgenic mice [64, 52]. A mild lipodystrophy has been described in one of the mouse line lacking Rsk2 [230]. My data did not confirm these observations. Whether the differences could be due to differences in the diet given to the mice remain to be tested. Nevertheless, I now uncovered that fra1 transgenic mice also developed a severe progressive lipodystrophy that was enhanced by deleting Rsk2. Histological analysis as well as the analysis of fat specific genes expression indicated that the phenotype was associated with decreased maturation of the adipocytes. Alterations of cell volume participate in the machinery regulating cell proliferation and apoptotic cell death. Deranged cell volume regulation significantly contributes to the pathophysiology of several disorders such as liver insufficiency, diabetic ketoacidosis, hypercatabolism, fibrosing disease, sickle cell anaemia, and infection.

6.1.3. Fos-related protein-1 (Fra1) and Rsk2 regulate body growth, body weight and lifespan

The first hints for metabolic disruptions were noted when the various genotypes were analysed by medallion frequency. Later, metabolism disturbances became more evident when the body growth, body weight and lifespan were analysed. The fra1-tg

male and female offspring were mildly reduced in their birthrate, but mice carrying the double mutation, fra1-tg/rsk2-/y or fra1-tg/rsk2-/x, were born with a pronounced decreased frequency. Furthermore, the fra1-tg/rsk2-/y mice had a drastic reduction of their lifespan and were severely growth-retarded along their life. Their weight was reduced up to 50 % compared to wt and Rsk2-deficient littermates at 7 weeks of age. In contrary to previously published data [230, 305] no significant difference was found between the body weights of wt and rsk2-/y mice, whereas a mild reduction in the body weight was already observed in the fra1-tg mice confirming previously published data [19, 52] . In addition, the lifespan of fra1-tg mice was also reduced although to a lesser extend. Thus, it appeared that Rsk2 inactivation amplified the effects of Fra1 overexpression on the survival and the growth of mice.

The p90 ribosomal S6 kinase (Rsk), a cytosolic substrate for the extracellular signal-regulated kinase (ERK), is involved in transcriptional regulation, and one isoform (Rsk2) has been implicated in the activation of glycogen synthase by Insulin. To determine Rsk2 function in vivo, mice lacking a functional Rsk2 gene were generated by Dufresne and colleagues and studied in response to Insulin and exercise, two potent stimulators of the ERK cascade in skeletal muscle [229]. Rsk2 knockout mice weighed 10 % less and were 14 % shorter than wt mice. They also showed impaired learning and coordination. Dufresne's conclusions were that Rsk2 likely played a major role in feedback inhibition of the ERK pathway in skeletal muscle. Furthermore, Rsk2 was not required for activation of muscle glycogen synthase by Insulin but may indirectly modulate muscle glycogen synthesis activity and/ or glycogen content by other mechanisms. In 2003 the group published in more detail how Rsk2 can influence the mice body [230]. They showed that Rsk2-deficiency in mice resulted in reduced body weight, largely because of a specific loss of WAT. Furthermore, the mice were resistant to development of obesity and hyperleptinemia when fed a high fat diet (HFD). The Rsk2 KO mice were mildly diabetic and Insulin resistant and have fatty livers. Dufresne´s group speculated that the dysregulation of glucose homeostasis was secondary to loss of fat tissue because administration of recombinant leptin, a fat-derived hormone, normalises glucose and Insulin parameters [229, 230]. This conclusion was consistent with other reports about the Insulin-sensitising effects of leptin in both normal mice and mice with partial or total lipodystrophy that were hypoleptinemic and severely Insulin resistant [231, 232, and 233]. But it was also possible that altered expression of other adipocyte-derived factors involved in the regulation of Insulin sensitivity, including adiponectin and tumor necrosis factor alpha (TNF-α) may play a role in the decreased Insulin sensitivity in the Rsk2-deficient mice [234, 235, and 236]. Although they did find several phenotypic similarities

to the rare cases of humans lacking functional Rsk2 proteins, the lean and diabetic phenotypes of the Rsk2 KO mice have not been reported in Coffin–Lowry syndrome (CLS). These differences therefore appear species dependent, and possible explanations include differential tissue distribution of Rsk2 and/ or differential compensatory mechanisms between humans and mice, including upregulation of other Rsk family members, e.g. Rsk1, Rsk3 or Rsk4.

In contrast to these data, I could not see any difference between the wt and rsk2-/y in growth, in weight, even a specific loss of WAT or decreased adipocyte cell size with age as observed in Fra1 overexpressing mice. However, I showed here that the Fra1-anti-adipogenic effect can be amplified by Rsk2-deficiency in vivo. The data clearly demonstrating that Rsk2 is require for proper adipocytes differentiation in case of Fra1 overexpression. Although all mice were backcrossed onto a similar background, the C57/Bl6 background for more than nine generations. I cannot exclude that differences in feeding and the environment of the mice contribute to the difference in the phenotype, but all animals were housed with food and water available ad libitum, in a light- and temperature-controlled environment.

6.1.4. Consequence of lipodystrophy and mechanisms of action of Fra1 in fat

In contrast to Dufresne and colleagues, two studies by Moitra (1998) and Shimomura (1999) similar to our in vivo (WAT) and ex vivo (mPOB) findings have been published [237, 238]. Moitra and colleagues generated a transgenic mouse with no white fat. These mice expressed a dominant-negative protein, termed A-ZIP/F, under the control of the adipose-specific aP2 enhancer/ promoter. The aP2 belongs to a large family of intracellular lipid carrier proteins that includes adipocytes, liver, intestine, kidney, and heart fatty acid-binding proteins, as well as myelin P2, and the cellular retinol- and retinoic acid-binding proteins. The precise function of aP2 is believed to play a role in fatty acid transport or protection against the detergent-like effects of fatty acids [239]. The adipocyte P2 gene has served as a model for differentiation-dependent gene expression in this cell type. The gene was transcriptionally activated during adipocyte differentiation [240, 241]. Several cis- and trans-acting regulatory components of the gene have been identified, including an AP-1 sequence at -120, where Moitra and colleagues have identified sequence-specific interactions between Fos-containing protein complexes and DNA [242, 243]. In addition, a binding site for the CAAT/enhancer-binding protein (C/EBP) located 140 base pairs upstream of the start of transcription, has been described [244, 245]. The differentiation dependence and tissue specificity of the aP2 gene and its relatively

high level of expression appear to be determined by a potent fat-specific enhancer located 5.4 kilo bases upstream of the start of transcription, which functions in both cultured adipocytes and transgenic mice [246, 247]. A binding site for a member of the nuclear factor 1 family (NF1) and several other nuclear factors play an important role in this enhancer [247]. The aP2 protein prevents the DNA binding of bZIP transcription factors of both the C/EBP and AP-1 family members. Moitra´s A-ZIP/F-1 transgenic mice had 99 % less white adipose tissue and dramatically reduced amounts of brown adipose tissue, which was inactive. They were initially growth-delayed. The mice ate, drunk, and urinated copiously, had decreased fecundity and premature death. The physiological consequences of having no white fat tissue were profound. The liver was engorged with lipid, and the internal organs were enlarged. Furthermore, the mice were diabetic, with reduced leptin (20-fold) and elevated serum glucose (3-fold), Insulin (50- to 400-fold), free fatty acids (2-fold), and triglycerides (3- to 5-fold).

The second study was published by Shimomura and colleagues [238]. They produced transgenic mice that overexpressed nSREBP-1c in adipose tissue under the control of the adipocyte-specific aP2 enhancer/ promoter. These mice exhibited many of the features of lipodystrophy. The white fat failed to differentiate fully, and the size of white fat depots was markedly decreased. The mice had disordered differentiation of adipose tissue. Levels of mRNA encoding adipocyte differentiation markers (C/EBPα and PPARγ) were reduced, but levels of Pref-1 were increased. A marked Insulin resistance with 60-fold elevation in plasma Insulin was observed. In diabetes mellitus with elevated blood glucose levels (>300 mg/dl) failed to decline when Insulin was injected. Fatty liver from birth and elevated plasma triglyceride levels later in life.

However, when comparison these two mice models with the fra1-tg and fra1-tg/rsk2-/y mice, there are common characteristics. In fra1-tg/rsk2-/y mice the white fat failed to differentiate to 100 %. The adult fra1-tg mice contain decreased WAT (fat pad) and the size of white fat depots was markedly decreased. The fra1-tg WAT expressed exogenous and endogenous Fra1. In the wt fat pad only small amount of endogenous Fra1 was detectable. Detailed mRNA analyses of fra1-tg WAT showed significant reduction of adipocyte markers, such as PPARγ, C/EBPα, Glut4, and aP2. WAT growth and differentiation is known to be regulated by sequence-specific DNA binding proteins of C/EBP bZIP families. Furthermore, AP-1 factors promoted precursor cells proliferation [242, 248]. C/EBP factors mediate adipocyte differentiation via a sequential pattern of expression beginning with C/EBP and C/EBPβ and followed by C/EBPα [249]. The Fra1 protein contains a basic leucine zipper region, which can heterodimerize with either Jun or C/EBP family members. We do not know today, which of these families is critical for

the phenotype observed in fra1-tg mice. The use of established preadipose cell lines (e.g. the 3T3-L1, 3T3-F442A, Ob17 lines or our own mOBrsk2-/y-pBabe-fra1 and mOBrsk2-/y-pMSCV-FraER) may allow answering this question. Indeed, when appropriately induced in culture, these cells undergo differentiation and acquire the biochemical and morphological phenotype of adipocytes [250, 251, 252, and 253]. Their differentiation can be induced by adding Insulin, glucocorticoid, and an agent that increases intracellular cAMP level (IBMX). The adipocyte differentiation program is regulated by transcriptional activators such as CCAAT/enhancer binding protein alpha (C/EBPα), peroxisomal proliferator activated receptor gamma (PPARγ), and transcriptional repressors such as preadipocyte factor-1 (Pref-1), originally identified in mouse 3T3-L1 preadipocytes, and known to play a key role in inhibiting the adipose conversion. These transcription factors coordinate the expression of genes involved in creating and maintaining the adipocyte phenotype including the Insulin-responsive glucose transporter (Glut4), and the fatty acid binding protein (aP2). I could not detect in my in vivo and ex vivo studies enhanced levels of Pref-1 in adipocytes. Indeed, Pref-1 was abundantly expressed in fra1-tg preadipocytes, and its expression was downregulated during adipocyte differentiation. In agreement, adipogenesis was not completely blocked in fra1-tg mice but the cell size and their maturation was effected as shown by the downregulation of adipocyte differentiation markers, e.g. C/EPBα, PPARγ, Glut4 and aP2.

Furthermore, the CAAT/enhancer-binding protein (C/EBP) family of transcription factors plays a major role in the regulation of adipocyte differentiation. These factors are proteins of the bZIP class, with a basic domain that mediates DNA binding and a leucine zipper dimerization domain [254]. Two members of this family, C/EBPβ and C/EBPδ likely play a role early in differentiation. Their expression is induced shortly after initiation of the differentiation program and decreases in the terminal phase [255]. Two of the agents employed to induce differentiation, IBMX and glucocorticoid, appeared to be directly responsible for the induction of C/EBPβ and C/EBPδ respectively. Conditional ectopic expression of C/EBPβ in NIH-3T3 fibroblasts led to commitment of these cells to the adipose lineage [256, 257, and 258]. Treatment with Dexamethasone, fetal bovine serum, and Insulin led to differentiation of these cells into adipocytes and induction of PPARγ. Peroxisome proliferator activated receptors (PPARs) are a class of nuclear hormone receptors, originally identified based on their activation by agents that induce peroxisome proliferation. Evidence has accumulated over the past few years, which suggested that this group of transcription factors plays a role in adipocyte differentiation. Activators of

PPARs promoted adipose differentiation of preadipocytes, myoblasts and the multipotent C3H10T cells, and ectopic expression of certain PPARs in the presence of such activators can induce differentiation of NIH-3T3 fibroblasts. Members of the PPAR family bind as heterodimeric complexes with the retinoid X receptors (RXRs) to PPAR response elements (PPRE/ DR-1; direct repeats of the sequence RGGTCA separated by one base) [259]. Such elements have been identified in a number of adipocyte genes, including the adipocyte fatty acid–binding protein aP2 [260]. Studies by Liao and colleagues (2007) showed that PPAR action was mediated by both Glut4 and Glut1 [261]. Interestingly, PPARγ-depleted cells displayed enhanced inflammatory responses to TNF-α stimulation, consistent with a chronic anti-inflammatory effect of endogenous PPARγ. The strong effect of PPAR in promoting adipocyte differentiation is consistent with its abundant and specific expression in adipose tissue. The transactivation potential of all the PPARs is stimulated synergistically by Insulin [262, 263]. Insulin stimulation is dependent on the RAF/MAP/ERK/p90 ribosomal S6 kinase (Rsk2) kinase cascade pathway but has not been demonstrated to require direct phosphorylation of PPAR by Rsk2 kinase. MAP kinase phosphorylates a consensus MAP kinase site in the N-terminal region of PPAR in response to various growth factors that are known to block differentiation, leading to inhibition of PPAR transactivation [264]. Mutation of this site does not abolish Insulin stimulation but does block the inhibitory effects of growth factors on PPAR transactivation and promotion of adipocyte differentiation [264, 265]. How Rsk2 regulating adipogenesis is remain to be analysed, but our data indicate that Fra1 overexpression negatively controls adipocyte differentiation by downregulating PPARγ and C/EBPα, and consequently their known target genes Glut4 and aP2.

6.1.5. Fra1 downregulate the glucocorticoid receptor (GR)

Adipocyte differentiation can be induced by adding Insulin, Dexamethasone, and an agent that increases intracellular cAMP level like IBMX. I already could show that ex vivo Fra1 overexpressing cells less differentiated to adipocytes compared to wt cells. Moreover, adipocyte differentiation markers such as C/EBPα and PPARγ, as well as Glut4 and aP2 were decreased in vivo (WAT) and ex vivo (mPOBfra1-tg). Additional adipocyte differentiation experiments with retroviral vectors encoding for a constitutive or an inducible form of Fra1 have shown that Fra1 overexpression was directly responsible for the inhibition of adipogenesis. All these data clearly demonstrated that Fra1, in addition to promoting osteoblast differentiation was decreasing adipocytes differentiation in a cell autonomous manner. This phenotype was similar to the one described for the

transgenic mice overexpressing another Fos-related protein: ΔFosB [65, 66, and 103]. In the case of ΔFosB, the increased osteoblastogenesis has been shown to be independent on the decreased adipogenesis. The independence of the bone and the fat phenotype in ΔFosB transgenic mice was shown by osteoblast specific overexpression of ΔFosB using the ostreocalcin (OG2) promoter. These mice developed osteosclerosis without any evidence of lipodystrophy. All ex vivo and in vitro analyses converged to a Fra1-mediated downregulation of one of the key transcription factors controlling adipocyte differentiation, namely C/EBPα. So far, adipocytes differentiation is understood as follow. Adipogenic stimulation by Insulin, IBMX and the corticosteroid agonist Dexamethasone activates C/EBPβ and C/EBPδ both known to upregulate C/EBPα that in turn switch on PPARγ transcription. Finally, PPARγ activation upregulates C/EBPα establishing a positive regulatory loop [139, 141 and 160]. A connection between corticosteroid and C/EBPα in the regulation of adipogenesis has been demonstrated. Binding of Dexamethasone to the glucocorticoid receptor was shown to stimulate C/EBPα synthesis and thereby adipogenesis [266]. In the GR pathway, the receptor interacts with its steroid hormone ligand in the cytoplasm and undergoes an allosteric change that enables the hormone receptor complex to bind a specific DNA-responsive element (glucocorticoid responsive element [GRE]) and modulate transcription [267]. Regulation of physiological processes by glucocorticoids is achieved by ligand binding to the GR and subsequent modulation of gene expression. GR modulation of gene expression can occur by either direct DNA binding or by protein-protein interaction with other transcription factors, revealing the in vivo relevance of GR activities that are independent of DNA binding [268]. Studies in humans have observed GR polymorphisms associated with high blood pressure, increased visceral fat, variations in tissue-specific steroid sensitivity, and alterations in Insulin sensitivity and BMI [269, 270, 271, and 272]. There is evidence that GR in the nervous system can affect energy balance [273], but recent studies also suggest that central GR and the peripheral GR in adipose tissue can contribute to abdominal obesity [274]. The ability of glucocorticoids (GCs) to regulate cell proliferation plays an important role in their therapeutic use. The canonical Wnt pathway, which promotes the proliferation of many cancers and differentiated tissues, is an emerging target for the actions of GCs, albeit existing links between these signaling pathways are indirect. By screening known Wnt target genes for their ability to respond differently to GCs in cells whose proliferation is either positively or negatively regulated by GCs, scientists identified c-myc, c-Jun, and cyclin D1, which encode rate-limiting factors for G(1) progression of the cell cycle. In other cell system, activation of C/EPBα was shown to be involved corticosteroid-induced

growth arrest [275]. Interestingly, it has been found, that mesenchymal cells overexpressing Fra1 were expressing lower level of the glucocorticoid receptor and were protected against corticosteroid-induced growth arrest. Glucocorticoids are known to inhibit bone formation most likely by decreasing the proliferation of the osteoblastic cells and by increasing the apoptosis of mature osteoblasts [276]. Therefore, downregulation of the glucocorticoid receptor might be one of the mechanisms by which Fra1 is inducing bone formation. In conclusion, I demonstrated that, in addition to promoting osteogenesis, Fra1 is blocking adipogenesis by directly inhibiting adipocyte differentiation. The mechanism seems to involve the downregulation of the glucocorticoid receptor that results in a decreased expression of C/EPBα (Figure 6.1).
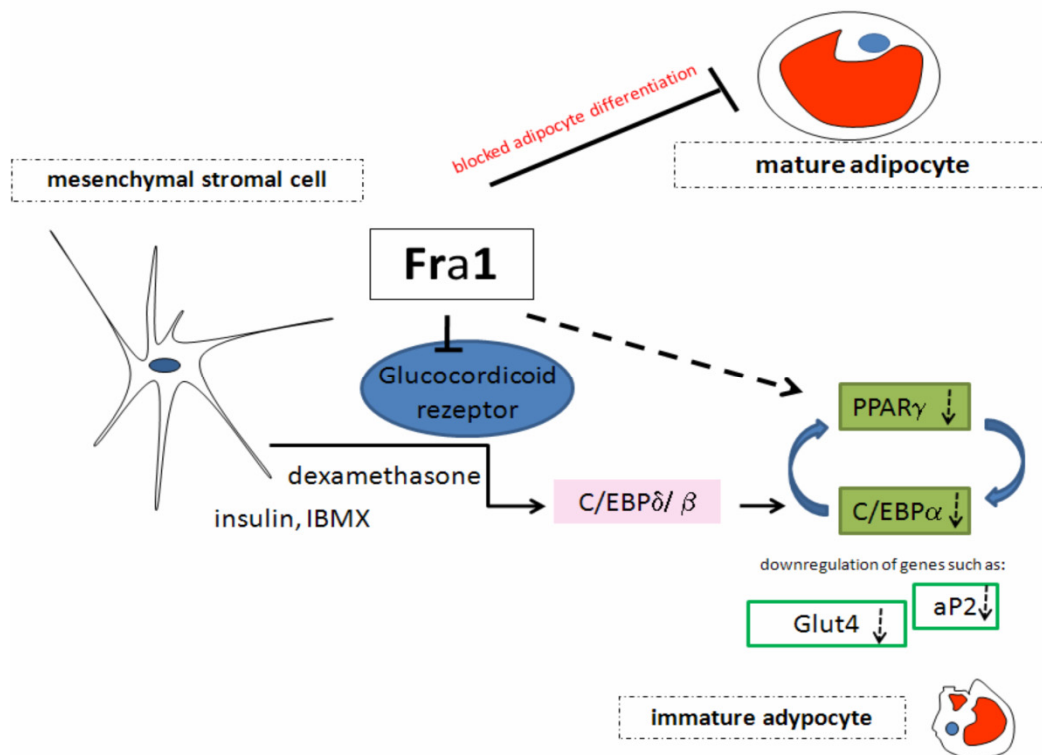
Figure 6.1 Fra1 downregulates important adipocytes differentiation markers

6.1.6. Connection between fat metabolism and immune diseases such as diabetes and ketoacidosis

Many diseases have multifactorial origins. The Fra1 overexpressing phenotype includes poor fertility (observation experience), splenomegaly (spleen weight/ body weight ratio analysis), lipodystrophy (Red O Oil staining), and early death (survival analysis). The phenotype is may be attributed to the lack of WAT, disrupting energy

storage and communication among the tissues of the body, including signals from both WAT and the rest of the body to WAT. Without WAT, to take up and store free fatty acids/ triglycerides, derived mainly from diet and hepatic production, blood levels become elevated. Increased circulating free fatty acids have been proposed to cause increased blood glucose via the glucose-fatty acid cycle, in which muscle uses free fatty acids as a fuel in preference to glucose [277, 278]. The resulting increased blood glucose levels, in turn, lead to more Insulin secretion and pancreatic islet -cell hypertrophy and hyperplasia. Free fatty acids, known ligands for transcription factors, might also cause Insulin resistance via transcriptional mechanisms. The resulting extraordinarily high Insulin levels are sufficient for cross-talk activation of IGF-1 receptors [279]. IGF-1 receptor stimulation could explain the enlarged organs and continued adult growth of the fra1-tg mice. However, fatty liver could not be observed in fra1-tg ever fra1-tg/rsk2-/y mice. In contrast to the A-ZIP/F-1 and nSREBP-1c mice, liver of fra1-tg and fra1-tg/rsk2-/y mice were anaemic and Red Oil staining of liver sections did not showed any accumulation of fatty acids/ triglycerides.

Fatty acids play a critical role in both normal metabolism and certain metabolic diseases. They serve as the primary energy source for skeletal muscle and also represent the major carrier of metabolic energy, which is ultimately stored in adipose cells in periods of nutritional abundance. In fasted states, fatty acids are exported from fat at an elevated rate to spare glucose, e.g. for the brain or other ATP-energy using processes. This major glucose-utilizing tissue can also adapt to a prolonged fast to utilize ketone bodies derived from fatty acids by oxidation in the liver. In addition to these obviously beneficial functions of fatty acids, they also are an integral part of certain pathological conditions. In poorly treated diabetic states, as well as I suppose it in the fra1-tg and more in the fra1-tg/rsk2-/y mice, fatty acids can reach extremely high levels and cause significant medical problems. Data have suggested that elevated levels of fatty acids themselves (which frequently occur in both obese and diabetic individuals) might play a role in the generation of an Insulin-resistant state [280, 281]. One disease could explain the non-fatty liver, the decreased differentiation/ maturation of adipocytes or increased lipolysis in existing adipocytes, the reduced lifespan, and the prematurely death in our mice models of Fra1 overexpression. These conditions are known as ketoacidosis. Insulin-deficiency leaves the muscle, fat, and liver cells unable to use glucose (sugar) in the blood as fuel. Other hormones such as glucagon, growth hormone, and adrenaline cause fat to break down within the cells of these tissues into glucose and fatty acids. These fatty acids are converted to ketones by a process called oxidation. The body is literally consuming muscle, fat, and liver cells for fuel. Diabetic

ketoacidosis (DKA) is a state of inadequate Insulin levels resulting in high blood sugar and accumulation of organic acids and ketones in the blood [282, 283, 284, and 285]. It is also common in DKA to have severe dehydration and significant alterations of the body's blood chemistry. DKA is usually seen in humans who have type 1 (Insulin-dependent) diabetes. Most often, these are diabetics younger than 25 years, but the condition may occur in diabetics of any age. Males and females are equally affected. DKA is characterized by hyperglycemia, acidosis, and high levels of circulating ketone bodies. The pathogenesis of DKA is mainly due to acidosis. Excessive production of ketone bodies lowers the pH of the blood; a blood pH below 6.7 is incompatible with life. Onset of DKA may be fairly rapid, often within 24 hours. A key component of DKA is that there is no or very little circulating Insulin so it occurs mainly (but not exclusively) in type 1 diabetes (because type 1 diabetes is characterized by a lack of Insulin production in the pancreas). It is much less common in type 2 diabetes that is closely related to cell insensitivity to Insulin, not shortage or absence of Insulin. Some type 2 diabetics have lost their own Insulin production and must take external Insulin; they have some susceptibility to DKA. Although glucagon plays a role as an antagonistic hormone to Insulin when there are low blood glucose levels, mainly by stimulating the process of glycogenolysis in hepatocytes (liver cells), Insulin is the most important hormone with the most widespread effects throughout the body. Its presence or absence can by itself regulate most of DKA's pathological effects; notably, it has a short half-life in the blood of only a few minutes (typically about six), short time is needed between cessation of Insulin release internally and the reduction of Insulin levels in the blood. Most cells in the body are sensitive to one or more of Insulin's effects; the main exception being erythrocytes, neurons, hepatocytes, some intestinal tissue, and pancreatic beta-cells which do not require Insulin to absorb glucose from the blood. The difference is due to different glucose transporter (Glut) proteins. Most cells contain only Glut4 proteins which move to the cell surface membrane when stimulated by a second messenger cascade initiated by Insulin, thus enabling uptake of glucose. Conversely, when Insulin concentrations are low, these transporters dissociate from the cell membrane and so prevent uptake of glucose. Other effects of Insulin include stimulation of the formation of glycogen from glucose and inhibition of glycogenolysis; stimulation of fatty acid (FA) production from stored lipids and inhibition of FA release into the blood; stimulation of FA uptake and storage; inhibition of protein catabolism and of gluconeogenesis, in which glucose is synthesized (mostly from some amino acid types, released by protein catabolism). A lack of Insulin therefore has significant effects, all of which contribute to

increasing blood glucose levels, to increased fat metabolism and protein degradation. Fat metabolism is one of the underlying causes of DKA.

6.1.7. Are Fra1 overexpressing mice a model for lipoatrophic diabetes?

The Fra1 overexpressing phenotype was similar to that of humans with severe lipoatrophic diabetes (total lipodystrophy, the Seip-Berardinelli syndrome, ketoacidosis). The human lipodystrophies are a heterogenous group of disorders characterized by decreased fat mass, Insulin resistance, and elevated triglycerides [284, 286]. Both genetic and acquired forms (presumably autoimmune) are known. Lipodystrophic diabetes was recently recognized as a complication of protease inhibitor treatment of HIV infection [285]. The similarities of our own phenotype and lipoatrophic diabetes include cardiovascular disease and splenomegaly. Humans with severe lipoatrophic diabetes often die from complications of diabetes. Fra1 overexpressing mice also die prematurely, possibly as a result of high glucose causing a hyperosmolar state (hypothetical). In addition to the similarities above, both lipoatrophic humans and fra1-tg mice have an increased metabolic rate, which attribute to their splenomegaly. Fra1-tg lipoatrophic diabetes is a consequence of the absence of fat, suggesting that a lack of fat is causative for the human disease. Lipodystrophy is paradoxical, with the lack of fat causing diabetes. The usual scenario is that obesity causes type 2 diabetes. Thus it is important to examine the similarities between lipoatrophic and type 2 diabetes. As postulated above, increased free fatty acids may cause lipoatrophic diabetes and a role for free fatty acids has also been proposed in type 2 diabetes [289]. Alternatively, lack of WAT in fra1-tg mice may cause diabetes by a different mechanism from that which occurs in obese mice. Lack of adipose tissue in Fra1 overexpression mice could also causes leptin deficiency. Low leptin levels contribute to the Insulin resistance, since leptin-deficient ob/ob mice are diabetic [290]. Leptin also increases muscle glucose utilization, enhances Insulin's inhibition of hepatic glucose production, and is required for sexual maturation and fertility [291, 292, and 293]. Other lean mouse models exist, but none of the previous models and my own model (fra1-tg/rsk2-/y) produced viable mice lacking WAT throughout development, suggesting that WAT is essential for life.

6.2 Fra1´s immune modulation role in the spleen

The largest secondary lymphatic organ of mammals derived from mesenchyme is the spleen. This organ is located on the left side of the abdomen and has a role initially in blood and then immune system development. The spleen's haematopoietic function (blood cell formation) is lost with embryonic development and lymphoid precursor cells migrate into the developing organ. After birth the bone marrow haematopoietic microenvironment occupies the medullary cavities of bones throughout the skeleton and provides support for haematopoiesis and immune cells development. The work on c-Fos by Erwin Wagner and co-workers identified this proto-oncogene, as a primary factor which directs effect cell differentiation along the osteoclast/ macrophage lineages, and thus regulates bone remodelling [19, 29, 34, 34, 44, 45 and 48]. Their studies support a link between skeletogenesis, marrow formation and haematopoiesis, and may help to delineate mechanisms underlying the oncogenic transformation of skeletal and haematopoietic. Furthermore, Jochum and colleagues showed that overexpression of Fra1 in mice results in an elevation in the number of mature osteoblasts, and the supra-physiological bone formation without increased bone resorption resulting in osteosclerosis [52]. Moreover, splenomegaly in fra1 transgenic mice was observed.

6.2.1. Fra1 overexpression induce splenomegaly but not in the absence of Rsk2

As already previously described, fra1 transgenic mice develop in addition to osteosclerosis splenomegaly [52]. This may be due to a bone mass increase, which causes a severe reduction of space in the bone cavity harbouring the bone marrow, the major site of haematopoiesis. In this study I showed that the fra1-tg/rsk2-/y mice developed a comparable Fra1 increase in bone mass with a severe reduction of space in the bone cavity, which causes osteosclerosis. Surprisingly the fra1-tg/rsk2-/y mice did not show any visible spleen enlargement compare to Fra1 overexpression mice. In order to quantify the degree of organ enlargement, spleen weight/ body weight ratios were calculated for al phenotype. Summarised, the data indicate that Fra1 overexpression induced splenomegaly can be counteracted by total Rsk2-deficiency but not following partial depletion of Rsk2 (such in fra1-tg/rsk2-/x spleens). However, spleens of male fra1-tg/rsk2-/y mice appeared to be rather anaemic when compared to wt and rsk2-/y spleens.

Not much is known about the role of Rsk2 in spleen morphology or function. The family of the 90 kDa ribosomal S6 kinases have multiple cellular functions [296]. They are

involved in the phosphorylation of histone H3 and remodelling of chromatin in response to epidermal growth factor (EGF) and can regulate gene expression by phosphorylation of transcription factors, including c-Fos [18, 297, and 298], cAMP-response element-binding protein (CREB) [299, 300 and 301], CREB-binding protein [302, 303], Estrogen receptor [304], ATF4 [35], NFATc4 [305] and NF-κB/IκBα[306, 307]. p90Rsk2 was also reported to phosphorylate the p34cdc2 inhibitory kinase Myt1 in frog oocytes, leading to activation of the cyclin-dependent kinase p34cdc2 that then promotes cell-cycle progression of oocytes through the G2/M phase of meiosis [308]. Phosphorylation of the proapoptotic protein, Bcl-XL/Bcl-2–associated death promoter (Bad) by p90Rsk2 suppresses Bad-mediated apoptosis in neurons [309]. In addition, phosphorylation of the Ras GTP/ GDP-exchange factor, SOS, by p90Rsk2 in response to EGF may be involved in negative feedback regulation of the MAP kinase signalling pathway [310]. Furthermore, Rsk2 appears to play an essential role in T-cell activation at least for cellular growth/ survival [311]. Finally, loss-of-function mutations of p90Rsk2 in humans cause the Coffin-Lowry syndrome, an X-linked form of mental retardation that is associated with delayed bone age, delayed closure of fontanelles, and a short stature [312, 313, and 314]. Although, Rsk2 plays a major role in the cell communication. The results in this study do not provide clear information about a possible "spleen-dwarfism-syndrome" in fra1-tg/rsk2-/y mice which would be caused by the absence of phosphorylation of Fra1 by Rsk2.

6.2.2. Fra1 overexpression affects the red pulp, white pulp and marginal zone compartimentalization

I investigate whether the consequence of the reduction the bone marrow space on the cellular composition and organization of the one secondary lymphoid: the spleen. For this purpose, spleen sections of all mice strains were subjected to Hematoxylin & Eosin staining. I demonstrated that a clear separation of red and white pulp regions was lost in the spleens isolated from fra1-tg and fra1-tg/rsk2-/y mice. In control (wt) mice the spleen was normally divided into two types of pulp which correspond to the two most important functional roles of the spleen – the red pulp and the white pulp. The splenic red pulp is characterized by a specialized network of open sinuses that facilitates mechanical filtration of the blood and removes unwanted materials from the blood, including senescent red blood cells (erythrocytes). Due to the high abundance of erythrocytes, it is macroscopically tinged red - to which the red pulp owes its name. Reticular fibers crosslink to form a fine meshwork (reticulum) in the red pulp (splenic cords). This network is composed of type I and III collagen and acts as a supporting mesh in soft

tissues [315]. The red pulp was separated from the white pulp by the so-called marginal zone (MZ). It is composed of cells derived primarily from the myeloid compartment of bone marrow like specialized macrophages, dendritic cells and a particular subset of B lymphocytes [316]. Within the marginal zone, the blood leaks from the terminal arterioles into the open sinuses resulting in a slow-down of the blood flow. This facilitates the marginal zone, in particular its residing macrophages. Finally, the white pulp of the spleen was organized around a central arteriole and is demarcated from the surrounding red pulp by the marginal sinus defining the marginal zone. The red pulp was intermingled with white pulp cords that lack erythrocytes but instead mostly consist of white blood cells such as lymphocytes (B and T cells), macrophages and dendritic cells (FDC). Within the white pulp, B and T lymphocytes accumulate in well separated compartments. Whereas T lymphocytes are located within the periarteriolar sheaths (PALS) surrounding the incoming central arterioles, B lymphocytes reside in adjacent B cell follicles [317, 318, 319, and 320].

In this study the clear separation of red and white pulp regions in Fra1 overexpressing mice was lost due to an extension of the lymphocyte compartment and subsequent infiltration of lymphocytes in the red pulp as indicated by diffuse Hematoxylin staining. Furthermore, the H&E staining let me suppose that the connective tissue framework of the spleen, which is formed by a spider-web like network of reticulum fibres and composed of thin fibrils of collagen and elastin was modified in Fra1 overexpressing mice and fra1-tg mice lacking Rsk2.

In order to answer the question whether Fra1 overexpression and Rsk2-deficiency may also affect connective tissue remodelling of the spleen, reticulum fiber networks were visualized and analysed by Mason-Goldner-Tricolor (MGT) staining. Using a combination of three different staining solutions, muscle fibers, collagenous fibers, fibrin and erythrocytes can be selectively visualized. The original methods were primarily used to differentiate collagenous and muscle fibers. The stains used have different molecular sizes and enable the individual tissues to be stained differentially. As already shown by H&E staining, wt and rsk2-/y mice show clear separation of red and white pulp regions that are tinged red and yellow in MGT staining, respectively. In addition, MGT staining revealed normal arrangement of connective tissue in these mice - both the collagen containing splenic capsule and the marginal zone (MZ) that is rich in collagen-containing endothelial/ epithelial cells could be identified. Likewise, MGT staining showed the loss of clear red and white pulp segregation in spleens of fra1-tg and fra1-tg/rsk2-/y mice already noticed by H&E staining. Moreover, the MGT staining supported the hypothesis that the red pulp was infiltrated by cells from the white pulp in these mice, as the density

of erythrocytes seems to be diminished due to intermingling with other cells. Strikingly, the regions occupied by connective tissue are enlarged in spleens of fra1-tg and fra1-tg/rsk2-/y mice, a finding that might point at commencing fibrosis. Besides being enlarged, the network of reticular fibres in spleens of fra1-tg and fra1-tg/rsk2-/y mice diverged from the normal arrangement of connective tissue. Here, the splenic capsules and the MZ could be hardly identified. The network of reticular fibres appeared to be rather loosely dispersed in fra1-tg and fra1-tg/rsk2-/y mice. Histological evaluation including H&E staining as well as MGT staining did indicate a Fra1-related increase of connective tissue formation or fibrosis. Altogether, these data could be signs of systemic or organ-specific inflammation.

6.2.3. Fra1 overexpression causes changes in marginal zone compartimentalization, affects FDC network, B cell homing and formation of B cell zones

Like NF-κB, AP-1 is minimally activated by physiological stimuli, but is dramatically activated by many pathophysiological stimuli, including LPS, cytokines, and reactive oxygen species [321]. AP-1 is a ubiquitous regulatory protein complex that interacts with AP-1 binding sites of target genes to regulate transcription under pathophysiological conditions. Members of the mitogen-activated protein kinase (MAPK) family, c-Jun N-terminal kinase (JNK) and p38 MAPK are important in the regulation of AP-1 to mediate expression of inducible genes. The inducible transcription factor AP-1 appears to play key roles in the transcription of a number of inflammatory genes strongly involved in the pathophysiology of T and B cell related diseases or systematic inflammatory response syndrome (SIRS), including sepsis. For example, the promoter regions of ICAM-1 and COX-2 genes contain several putative AP-1 binding sites, suggesting that initiation of the signal pathway for activation of AP-1 leads to the induction of these genes [322, 323]. The spleen functions as a blood-filtering system that is capable of removing particulate matter such as bacteria from the circulation [324]. It also functions as a lymphatic organ and facilitates the generation of immune responses to blood-borne Ags [325]. There are three segregated areas of the spleen: the white pulp, the red pulp, and the marginal zone (MZ) [326]. The MZ forms a distinctive border between the red and white pulp and is the entry point for blood entering the splenic circulation. In addition to trafficking leukocytes, four types of cells are constitutively present in the MZ of murine spleen: MZ B cells, MZ dendritic cells, MZ macrophages (MZMs), and marginal metallophilic macrophages (MMMs). MMMs are located on the inner border of the MZ

directly adjacent to the white pulp, whereas MZM are located on the outer border of the splenic MZ, at the border with the red pulp.

MMMs are not considered to be highly phagocytic, but are essential for the initiation of an immune response to T-dependent particulate Ags and T-independent type 2 Ags [327, 328, and 329]. MMMs are capable of migrating from the MZ, into a developing germinal center during the course of an immune response, suggesting that MMMs are involved in the transport of unprocessed Ag from the MZ into the B cell follicles, and are thus thought to be important in the generation of immune responses [330, 331]. Because spleen inflammation induces spleen injury, I assessed the degree of spleen injury and the inflammatory response in wt, fra1-tg and fra1-tg/rsk2-/y mice. To analyse an inflammation I focused my research on cell markers which are responsible for spleen injury.

Many markers are known to describe the B cell compartments of the white pulp. MOMA-1 is a useful marker for the identification of macrophage subpopulations, mostly characterised by a high level of non-specific esterase expression [332]. The marginal metallophilic macrophages are recognized by using either the MOMA-1 mAb or the marginal zone macrophages were identified using the ERTR-9 mAb. Double immunocytochemical staining of spleen sections clearly revealed the two distinct macrophage populations of the marginal zone, with metallophilic macrophages (MMMs) forming a continuous layer outlining the white pulp area and marginal zone macrophages (MZMs) scattered outside this layer. In addition, MOMA-1 detects macrophages at inflammatory sites. In this study immunostainings of spleen sections derived from wt mice attested normal cellular composition (white pulp regions, MZ) but this was not observed for Fra1 overexpressing spleen sections.

B220, a B cell marker in mice, is expressed by B cells that do not express the memory B cell marker CD 27 [333, 334, and 335]. In reactive lymphoid tissues, B220 is expressed by B cells occupying the mantle zones and by a subpopulation of germinal center cells, but, in contrast, marginal zone B cells in the spleen do not express B220. Furthermore, B cell lymphoproliferative disorders are positive for B220, including most cases of marginal zone lymphoma, follicular lymphoma, and lymphoplasmacytic lymphoma. In contrast, all cases of precursor B lymphoblastic leukemia/ lymphoma, mantle cell lymphoma, and chronic lymphocytic leukemia/ small lymphocytic lymphoma are negative for B220 [336]. B220 is expressed in a select subset of normal, reactive B cells in a pattern that is consistent with a marker of naive B cells. However, this restricted expression pattern is not seen in B cell lymphoproliferative disorders. Discordance between the B220 expression patterns of normal mantle and marginal zone B cells and

their respective neoplastic counterparts may aid in the distinction between normal and neoplastic proliferations at these anatomical sites. The BP-3 antigen expression by B lineage cells extends from the earliest detectable progenitors in the bone marrow to immature B cells in the periphery [337]. A discrete subpopulation of reticular cells in the peripheral lymphoid organs also expresses the BP-3 antigen [338]. The splenic BP-3 positive reticular cells are confined to the white pulp areas and their expression of the BP-3 antigen begins when the neonatal spleen becomes a secondary tymphoid organ, thus raising the possibility that the BP-3 molecule could be involved in lymphocyte-stroma interactions. In contrast to the pattern of BP-3 antigen expression by lymphoid cell lineages, BP-3 antigen expression on myeloid cells increases as a function of maturation.

A marker for follicular dendritic cells (FDCs) is named FDC-M2 [339, 340]. FDCs are cells of the immune system found in B cell follicles. They are probably not of haematopoietic origin, but simply look similar to true dendritic cells. They share their appearance and function with the other types of dendritic cells and assist in B cell maturation by the presentation of intact antigen to the B cells and induce class switching and proliferation. FDC-M2 is localized on FDCs, independently of the presence of germinal centers (GC). The GC was first described in 1884 by Walther Flemming, who observed a site of large lymphocytes undergoing mitosis in the follicles of lymph nodes and other secondary lymphoid organs and proposed this site to be a major source of all lymphocytes in the body. Today, the GC is now known to be associated with T cell dependent immune responses, and experimental evidence indicates that it is the main site in which high-affinity antibody-secreting plasma cells and memory B cells are generated.

Furthermore, the MZ, which surrounds B cell follicles in the spleen, contains a specialized subset of B cells. MZ B cells participate in T cell independent (TI) "innatelike" immune response to microbial pathogens, and can rapidly proliferate and differentiate into IgM or even switch to other isotype-secreting plasma cells, producing the bulk of the primary antibody response [341, 342, and 343]. TI responses do not generate memory B cells, consistent with a relatively short-lived antibody production. MZ B cells can be viewed as a bridge between the innate and adaptive immune responses to pathogens invading the host and barrier between red and white pulp.

In this study the H&E and MGT stainings have demonstrated that fra1-tg and fra1-tg/rsk2-/y mice have disturbed morphology of the spleen, particularly regarding its compartmentalisation. Immunostainings of spleen sections derived from wt mice revealed normal cellular composition of white pulp regions and the MZ in these mice.

Briefly, white pulp regions were shown to comprise marked B cell zones that were found in contiguity to FDC-networks. Furthermore, white pulp regions were both traversed by a network formed by BP-3 positive reticular cells and demarcated from the MZ by the ring of MOMA-1 expressing MM. In spleens of fra1-tg and fra1-tg/rsk2-/y mice white pulp and MZ architecture was found to be altered. Most notably, white pulp regions of fra1-tg and fra1-tg/rsk2-/y mice were not fully developed and lacked compact FDC networks although, faint FDC-M2 staining was observed at the outer border of white pulp regions. Likewise, the BP-3 staining pattern was different in these mice compared to wt mice in that the BP-3 positive cells were concentrated in ring-like structures that rather seem to overlap with or/ extend into the MZ. MOMA-1 staining further revealed the expanded rings of MMs in spleens of fra1-tg and fra1-tg/rsk2-/y mice when compared to wt mice. More importantly, regular B cell homing and formation of B cell zones were strikingly affected in spleens of fra1-tg and fra1-tg/rsk2-/y mice. Accumulated B cells formed a ring overlapping with the MZ as indicated by double immunofluorescent stainings of B220 and MOMA-1. Moreover, the localisation of B cells correlated with the staining patterns of BP-3 and FDC-M2. Since homing of B cells to B cell zones/ follicles is known to rely on the expression of the chemokine (C-X-C motif) ligand 13 (CXCL-13) by FDCs [344], dislocation of B cells in spleens of fra1-tg and fra1-tg/rsk2-/y mice is likely to be secondary to the changes regarding the stromal tissue of the white pulp (FDC and reticular cells). Taken together, these data showing a total disorganisation of an immune defence organ, in this case the spleen, in fra1-tg mice and fra1-tg/rsk2-/y mice, allow me to assume that the AP-1 member Fra1 plays an pivotal role in the immune modulation.

6.2.4. Fra1 overexpression influences the myeloid cells lineages

While the bone marrow is the primary site of haematopoiesis in the adult, up until the fifth month of gestation, the spleen has important haematopoietic functions. After birth, no significant haematopoietic function is left in the spleen except in some haematological disorders which affect mostly the myeloid stem cells and also lymphoid stem cell.

The myelodysplastic/ myeloproliferative diseases (MDS/ MPD) are clonal myeloid disorders that possess both dysplastic and proliferative features but are not properly classified as either myelodysplastic syndromes (MDS) or chronic myeloproliferative disorders (CMPD). The prefix "myelo-" refers to marrow. Bone marrow, known as a reddish substance in the middle of some bones, produces blood cells. In the myeloproliferative diseases, the body makes too many blood cells. Blood contains red

blood cells to carry oxygen, white blood cells to fight infections, and platelets to initiate blood clotting. Myeloproliferative diseases develop when a myeloid progenitor cell becomes overactive (e.g. chronic myelocytic leukemia, thrombocythemia, myelofibrosis). The abnormal progenitor cell continues to make normal blood cells, but makes too many of them. This excess of blood cells results in varying symptoms, depending on the progenitor cell involved. Other problems develop when some of the abnormal myeloid progenitor cells travel to the spleen, liver, or lymph nodes and begin making blood cells there. Most often, they migrate to the spleen. An enlarged spleen can crowd other organs in the abdomen and cause discomfort or digestive troubles. It is also susceptible to painful damage by blocking arteries. Massively swollen spleens can use large amounts of energy and cause muscle wasting and weight loss. Splenomegaly is usually associated with increased workload (such as in haemolytic anaemia), which suggests that it is a response to hyperfunction and is associated with any disease process that involves abnormal red blood cells being destroyed in the spleen. Other common causes include congestion due to portal hypertension and infiltration by leukaemia and lymphomas. In the later stages of myeloproliferative diseases, the bone marrow can become scarred. This may leave no space for progenitor cells. As a result, blood cell production can drop to dangerously low levels. The abnormal progenitor cells may also mutate and develop into leukaemia (B and T cell leukaemia). These two serious complications are rare in some myeloproliferative diseases but very common in others.

In this report, I have provided evidence that Fra1 could mediates its immune modulatory effect (increased megakaryocytes) by downregulation of C/EBPα (as shown for mPOBfra1-tg and mOBfra1-tg). C/EBPα is a key regulator of early myeloid development [345, 346]. Mice lacking C/EBPα have reduced granulocytes and monocytes. C/EBPα increases monocytic lineage commitment from bipotential myeloid progenitors. In addition to C/EBPα, AP-1 proteins also have the capacity to induce monocytic maturation. The initial suggestion that AP-1 proteins favor monocytic development comes from the finding that c-Jun or c-Fos can induce monocytic differentiation when expressed in myeloid cell lines and from the observation that phorbol esters rapidly induce AP-1 proteins and direct myeloid cell maturation to monocytes [347, 348, and 349]. C/EBPalpha:c-Jun or C/EBPalpha:c-Fos leucine zipper heterodimers induce monopoiesis more potently than C/EBPalpha or c-Jun homodimers or c-Fos:c-Jun heterodimers. C/EBPs and NF-kappaB cooperatively regulate numerous genes during the inflammatory response. The C/EBPα basic region interacts with NF-kappaB p50, but

not p65, to induce Bcl-2, and this interaction may be relevant to myeloid cell survival and development [350, 351, 352 and 353].

Overexpression of Fra1 in mice was previously shown to lead to osteosclerosis of the full skeleton [52]. Thus far, several findings of this study as for instance splenomegaly, reduced density of erythrocytes in the splenic red pulp and changes in the spleen parenchyma suggest that it may be also related to the development of other diseases such as myelofibrosis. A common feature of these diseases is that their aetiology is thought to be linked to megakaryocytes development. Megakaryocytes derive from the myeloid lineage of haematopoietic stem cells and are responsible for platelet production. Several severe diseases including thrombocythemia and thrombocytopenia are directly attributable to megakaryocytes malfunction [354, 355]. Others like myelofibrosis, osteosclerosis and Hepatitis C are ascribed to increased numbers of megakaryocytes [356, 357, and 358]. To assess, whether the observed abnormalities regarding the spleens of fra1-tg mice also include changes regarding splenic megakaryocytes, additional H&E and immunostainings were performed on spleen sections. Megakaryocytes were detected by an antibody directed against CD41 in combination with DAPI nuclear counterstained. CD41 is a glycoprotein that is typically expressed on the surface of megakaryocytes [354]. In this study megakaryocytes could be identified in spleens of wt, fra1-tg and fra1-tg/rsk2-/y mice by both H&E staining and CD41 immunostaining. However, the staining collectively implied an increased number of megakaryocytes in the spleens of fra1-tg and fra1-tg/rsk2-/y mice. This observation was subsequently verified by statistical counting of CD41 positive megakaryocytes, in which the number of megakaryocytes per observation field turned out to be increased about 20- and 28-fold in case of fra1-tg and fra1-tg/rsk2-/y mice, respectively. Based on this observation, Fra1 overexpression seems to modulate the immune system trough differentiation defects of haemapoetic stem cell line. Moreover, the Bethesda proposal for the classification of non-lymphoid haematopoietic neoplasms in mice provides precise criteria for accurate diagnosis [359]. The disease that developed most often in fra1 transgenic and fra1-tg/rsk2-/y mice meets several of the criteria that define a non-lymphoid leukaemia. The disease diffusely involved haematopoietic tissues with an increase in myeloid cells in the spleen, and was accompanied by anemia and megakaryocytopenia. Altogether, these criteria would define the disease as a potential myeloproliferative disease–like myeloid leukemia.

6.3   Fra1´s immune modulation role in heart

The heart is a specialised muscle that contracts regularly and continuously, pumping blood to the body and the lungs. The function of the right side of the heart is to collect de-oxygenated blood, in the right atrium, from the body and pump it, via the right ventricle, into the lungs (pulmonary circulation) so that carbon dioxide can be dropped off and oxygen picked up (gas exchange). The left side collects oxygenated blood from the lungs into the left atrium. From the left atrium the blood moves to the left ventricle which pumps it out to the body. On both sides, the lower ventricles are thicker and stronger than the upper atria. The muscle wall surrounding the left ventricle is thicker than the wall surrounding the right ventricle due to the higher force needed to pump the blood through the systemic circulation.

The most common cause of heart disease is a narrowing of or blockage in the coronary arteries supplying blood to the heart muscle itself (coronary artery disease). Some heart diseases are present at birth (congenital heart disease). Other causes include hypertension, abnormal heart valve function, abnormal heart rhythm and weakening of the heart's pumping ability caused by infection or toxins. Diseases such as hypertension and heart failure can cause fibrosis, a hardening or stiffening of the heart tissue. This condition arises when heart cells called cardiac fibroblasts are activated. These cells secrete collagen, a protein that provides structural support for the heart and an enlargement. Cardiac fibroblasts are recognized as the cell type primarily responsible for homeostatic maintenance of extracellular matrix (ECM) in the normal heart. Myocytes are surrounded by a basement membrane whose principal structural component is non-filamentous type IV collagen. Collagen fibrils composed primarily of collagen I with smaller amounts of collagen III are arranged in successive layers of organization [360].

6.3.1. Heart abnormality in Fra1 overexpressing mice and fra1-tg mice lacking Rsk2

In this study, experiments including heart weight to body weight analysis were carried out to explain the observed heart enlargement. Furthermore, stainings (H&E, MGT and EvG) were performed in order to get hinds about the cell environment and to find out the cells, which are responsible for the induced fibrotic tissue. However, the in vivo role of Fra1 and Rsk2 in heart physiology remains unknown. In contrast, Fra1 conditional knockout mice have a normal hypertrophic response, whereas hearts from fra1 transgenic mice decompensate prematurely [51, 52, and 361]. Moreover, fra1-tg as well

fra1-tg/rsk2-/y mice developed reduced body size and body weight, had defects in fat pad development, became splenomegaly, and died earlier.

Importantly, it could be shown that the analyses of heart weight/ body weight ratio of Fra1 overexpression mice induced change of the heart in vivo. The difference in these heart enlargements was found to be more pronounced in females than in males. Furthermore, deletion of Rsk2 induced heart abnormalities in Fra1 overexpression mice as well. There are already conflicting data regarding Fra1 expression could influence heart development and function. Bergman et al., 2003 demonstrated that defined members of the Fos and Jun transcription-factor families specifically regulate genes, like MMP-2, under conditions relevant to critical pathophysiological processes for heart failure [362]. Moreover, it has been reported that Fra1seems to regulate the cardiac hypertrophy gene ANF [363]]. How Fra1 modulates genes through which the pool of active cardiac fibroblasts is expanded remains to be explained.

6.3.2. Fra1 overexpression changes the cellular environment of the heart

This study sought to elucidate Fra1 overexpression can activate cardiac fibroblasts or myofibroblast. However, the nonmyocyte cell populations of the heart are increasingly appreciated to contribute to the performance of the normal and failing heart. In particular, cardiac fibroblasts have been recognized to constitute the major nonmyocyte cell type of the heart numerically and to contribute importantly to multiple aspects of myocardial function and pathophysiology. Myofibroblasts have been described as a specialized phenotype of activated fibroblasts [360]. These cells have big spindle-shape nucleus, express contractile proteins, including smooth muscle α-actin, vimentin, and desmin; effectively contract collagen gels in vitro; and are postulated to be important for wound closure and structural integrity of healing scars. In addition to normal wound healing, myofibroblasts are associated with hypertrophic fibrotic scars in injury models from multiple organ systems, and differentiation to the myofibroblast phenotype is strongly promoted by the fibrogenic growth factor TGFβ. Myofibroblast apoptosis has been associated with progression of granulomatous tissue to a mature scar, whereas failure of myocyte apoptosis has been suggested to drive the progression to fibrosis. Cardiac myofibroblasts were shown to persist in mature infarct scars.

In this report, I have provided evidence that Fra1 overexpression mediate immune modulatory effects by induction of cell population, such as myofibroblast. The histopathology analyses revealed difference in the cell environment of the heart. Firstly, the heart size of adult fra1-tg and fra1-tg/rsk2–/y mice was markedly increased, which

was confirmed by the increased heart-to-body weight ratios in fra1-tg and fra1-tg/rsk2–/y mice compared to mice with all other genotypes. Secondly, the histological H&E analyses showed induction of cells with smaller spindle-shape nucleus in sections of fra1-tg mice.

6.3.3. Fra1 overexpression induces heart fibrosis

Histologically, hypertensive myocardial fibrosis is defined through following characteristics: an initial excessive deposition of type III collagen fibers, followed by type I as the process progresses; the fibers are arranged as bundles lining the interstices and around the intramyocardial vessels; fiber accumulation is mostly limited to the left ventricle but sometimes also present in the other cardiac chambers; the amount of fiber accumulation is inversely related to the number of cardiomyocytes and directly related to their degree of hypertrophy [364, 365, and 366]. The histological analysis of mice section showed visible morphological changes of muscle cells on H&E stained section of fra1-tg male mice. Smaller fibrotic cells were detected between the bigger myocardial cells in fra1-tg heart sections. Furthermore, to identify these smaller cells MGT and EvG stainings were performed. Staining of wt male heart sections showed no morphological alteration. Only pure muscle tissue was found in this staining. Using MGT or EvG staining on sections of 18 weeks old mice, extensive focal interstitial fibrosis were found in fra1-tg heart sections. Finally, the heart enlargement could be explained by additional collagen producing fibrotic cells between the muscle cells in fra1 transgenic mice.

6.4 Fra1´s immune modulation role in liver

The liver plays a major role in metabolism, digestion, detoxification and elimination of substances from the body. The liver is the principal metabolic factory in the body: it is supplied with molecules derived from food by the intestine, which it then modifies to various extents; it breaks down ammonia to produce urea and supplies the body with the sugar (glucose) it needs, together with many other essential substances, including the blood coagulation factors that protect us from haemorrhage. The production of the bile acts as a detergent to facilitate the digestion of fat. The liver is also involved in hormone production and storage of Vitamin A.

Branches of the portal vein, the hepatic artery and the bile ducts run embedded in connective tissue along the longitudinal axis in between adjacent lobules in the portal

spaces. There are three to six portal spaces per lobule each containing one branch of the portal vein, the hepatic artery and a bile duct forming the portal triad. The branch of the portal vein is characterized by the largest lumen, whereas the branch of the bile duct can be distinguished by its cuboidal epithelium. In addition, lymph vessels are found in the portal spaces. The vessels send distributing branches along the periphery of each lobule. Inlet venues and arterioles branch from these and spill their blood into sinusoids. The sinusoids drain into the central vein. From the bile canaliculi located in between the plates of hepatocytes bile drains into the branches of the bile ducts. The individual lobules function in parallel with one another, not in series. Thus, if the vascular supply or drainage for one lobular unit is damaged the adjacent units will continue to function. However, at last serious malfunctions of the liver can lead to a decrease of the synthesis function, the decontamination function and to the increase of the portal pressure.

6.4.1. Fra1 overexpression induces anaemia in liver and Fra1 overexpressing mice develope a typical autoimmune liver disease

The first signs that Fra1 overexpression can also influence an organ like the liver have been observed in the livers from Fra1 overexpression mice lacking Rsk2. Their livers showed evidence for an anaemic character. Actually, anaemia goes mostly undetected, and symptoms can be vague. Very severe anaemia prompts the body to compensate by increasing cardiac output, and failed to heart failure. Through comparison of the different mice phenotypes the liver of Fra1 overexpressing mice looks pale-faced than wt. The change of color may be caused by anaemia. A disturbance of the blood flow or anaemia can be caused through a deterioration of the blood transport in the vessels or also by disturbance in the tissue.

There are five different types of liver injuries are known. Hepatitis implies injury to liver characterised by presence of inflammatory cells in the liver tissue [367, 368, 369, and 370]. The condition can be self limiting, healing on its own or can progress to scarring (cicatrisation) of liver. There are several forms of viral hepatitis; A, B, C, D, E, F and more recently G. Hepatitis B and hepatitis C are the most significant. Acute hepatitis is when it lasts less than 6 months and chronic hepatitis is when it persists longer. A group of viruses known as the hepatitis viruses cause most liver damages worldwide. The diseases can also be due to toxins (notably alcohol), other infections or from autoimmune process. It may run a subclinical course when the affected person may not feel ill. The patient becomes unwell and symptomatic when the disease impairs liver

functions that include among other things, screening of harmful substances, regulation of blood composition and production of bile to help digestion.

The second form of liver disease is cirrhosis [371, 372, 373, 374 and 375]. This term means that the liver has been damaged more severely, its normal architecture is disturbed, there is an increase in scar tissue and the liver mass is often reduced. Cirrhosis may be the consequence of long-standing injury from alcohol, certain viruses, bile duct injury or metabolic disorders including lipid metabolism distributions. Pimary biliary cirrhosis (PBC) is an autoimmune disease of unknown etiology leading to progressive destruction of intrahepatic bile duct, with cholestasis, cirrhosis, and eventually liver failure. Epidemiological data indicate that environmental factors trigger autoimmunity in genetically susceptible individuals, although no definitive association of PBC with specific genes has been found. In addition, no convincing explanation has been provided for the strong female predominance observed in the prevalence of PBC. It would suggested that the enhanced monosomy X in peripheral white blood cells, and particularly in lymphocytes, of affected women might play a role in the induction of PBC. The major paradox of PBC is that the damage is highly localized and targets biliary epithelium cells (BECs) lining only the small and medium-sized intrahepatic bile ducts (and the salivary gland epithelial cells in patients with also Sjogren's syndrome) despite the ubiquitous expression of the autoantigens. The epithelium of affected bile ducts presents a distinct morphology when compared to their larger counterparts also presenting different reactivity patterns when challenged with proinflammatory cytokines.

Thirdly, the liver can be affected by infiltrations from many different substances. The most common is fat which often occurs in patients who are overweight and in diabetics. Tumours that spread from other parts of the body often invade the liver. At this stage cancer is usually wide spread [376, 377 and 378].

Fourthly, certain disorders effect the circulation in the liver such as heart failure, or vascular shock [379, 380]. Finally many liver disorders result from abnormalities in the bile ducts both within and outside the liver that drain bile into the intestine. These disorders may occur secondary to gall stone or pancreatic disorders, from autoimmune damage of the bile duct tissue (Primary Biliary Cirrhosis, Sclerosing Cholangitis) or to tumours of the biliary ducts.

In this study, I hypothized the existence of a connection between the lipodystrophy and the anaemic liver in fra1-tg/rsk2-/x and in Fra1 overexpressing animals. Due to limited material only fra1-tg and wt livers were histologically analysed. The typical liver structures were observed in wt and fra1-tg sections: a centrolobular vein, a portal vein, arteries, the bile ducts and numerous hepatocytes. The wt parenchyma

was marked by a steady distribution of the H&E colors. However, the disse space was stained differently in Fra1 overexpressing liver and was surrounded by fibroblasts, neutrophilic granulocytes macrophages, hepatic stellate cells and lymphoid cells. These cell populations are typically associated with inflammation reaction and by replacement of liver tissue by fibrotic scar tissue, leading to progressive loss of liver function.

A special role in liver inflammations is played by hepatic stellate cells [381, 382 and 383]. In vitro studies performed in the early 1980s clearly demonstrated that the collagen found in cultures of primary hepatocytes was due to contaminating HSCs within the cell monolayers [384]. Further studies confirmed that cultured HSCs synthesize and secrete large amounts of collagen and other ECM proteins, whereas other cells types (i.e. hepatocytes, sinusoidal endothelial cells) only secrete modest amounts of these proteins. Studies using immunocytochemistry and in situ hybridization identified collagen expression in damaged livers in activated HSCs rather than in parenchymal cells. Studies in rat HSCs showed that quiescent HSCs express low levels of messenger RNA (mRNA) encoding procollagen I and III, whereas HSCs activated both in culture or in vivo show a marked up-regulation of these genes and secrete large amounts of collagen. A dramatic increase in the mRNA stability of pro-collagen in activated HSCs plays an important role in its increased gene expression [385, 386]. HSCs isolated from fibrogenic livers markedly overexpress genes encoding ECM proteins, which is not observed in other hepatic cell types [387]. Studies assessing both experimental models of liver fibrosis and human fibrogenesis have demonstrated a positive correlation between the degree of fibrosis and the accumulation of activated HSCs in the damaged liver [388, 389]. Substances that inhibit the activation or proliferation of HSCs also attenuate the progression of hepatic fibrosis in experimental models of chronic liver injury [390, 391]. Hepatic stellate cells (HSCs) are vitamin A-storing pericytes in the subendothelial space of the liver. Upon injury to the liver, HSCs become transdifferentiated into myofibroblastic cells to participate in wound healing [392]. This transdifferentiation is characterized by reduced vitamin A content, increased cell proliferation and migration, enhanced matrix protein expression, and induced expression of α-smooth muscle actin [393]. This response of HSCs constitutes the normal, reparative homeostatic response of the liver to injury. However, dysregulation of HSCs leads to excessive accumulation of extracellular matrices, resulting in liver fibrosis and cirrhosis. Investigative effort has been made to characterize transcriptional regulation that underlies HSCs transdifferentiation. Such examples include identification of Kruppel-like factor 6, a differentially expressed zinc finger protein in activated HSCs in vitro and in vivo. This transcription factor binds to the GC box sites of TGFβ1, TGFβ receptor type I and II, urokinase-type plasminogen

activator, and α1 (I) procollagen and induces transcription of these fibrogenic genes [394, 395]. The myofibroblastic phenotype seen in activated HSCs is best characterized by induction of α-smooth muscle actin that is mediated by c-Myb binding to an E-box element in its promoter [396]. The significance of this mode of regulation is supported by the demonstration of prevention of the myofibroblastic phenotypic switch by the treatment of HSCs with antisense oligonucleotides for c-Myb. Sustained NF-κB activation confers activated HSCs their proliferative and antiapoptotic status that may be important in progressive liver fibrogenesis [397]. NF-κB may also mediate inflammatory responses by HSCs via induction of chemokines and adhesion molecules [398, 399]. Increased AP-1 activity is essential for induction of matrix metalloproteinase, tissue inhibitor of matrix metalloproteinase-1, and interleukin-6 gene transcription in activated HSCs, where JunD was shown to play a pivotal role [400]. During liver fibrogenesis profound changes occur in the normal liver extracellular matrix most notably an accumulation of interstitial collagens type I and III. It is well recognised that perisinusoidal hepatic stellate cells, which become activated to α-smooth muscle actin (α-SMA)-positive myofibroblastic phenotype following liver injury, are major producers of this neomatrix of fibrosis. In vitro studies suggest that the accumulation of interstitial collagens affects the proliferation, survival and biosynthetic activities of liver cells including endothelial cells, hepatocytes and HSCs. There is increasing awareness that key facets of HSCs biology are regulated by their pericellular ECM.

To analyse whether the fra1-tg disse space, which was surrounded by hepatic stellate cells, fibroblasts, macrophages and lymphoid cells, is replaced by fibrotic scar tissue (ECM), Masson–Goldner-Tricolour (MGT) and Elastica van Gieson (EvG) stainings were done. Both staining methods were used to mark extracellular matrices like collagen I and III in the liver tissue. Finally, the results showed clear fibrotic tissues. In section of liver from Fra1 overexpression mice areas between hepatocytes and the portal triad vessels were stained green to blue by MGT staining. This green to blue colour stained extracellular collagen (ECM). Blood vessel (PV) and bile duct (BD) were detected between the collagen deposits. Moreover, the Elastica van Gieson staining did not show any extracellularly stained matrix in wt sections. The liver parenchyma was homogenous with some vessels for blood transport detected. In Fra1 overexpression liver extracellular matrix was stained red by EvG staining. Again, this collagen was detected in the subendothelial space or disse space - around the blood vessel and bible duct up to the hepatocytes. It is known that ECM can directly influence the function of surrounding cells through interaction with cell surface receptors, including integrins and nonintegrin matrix receptors (such as discoidin domain receptor 2). ECM can also indirectly affect cell

function via release of soluble cytokines, which in turn are controlled by local metalloproteinases. As already described the HSCs are the primary source of ECM fibrotic liver and these cells are resident perisinusoidal cells in the subendothelial space between hepatocytes and sinusoidal endothelial cells called disse space. These data showed that in Fra1 overexpressing mice extracellular matrix is induced between hepatocytes and the portal triad vessels and cells which are typical for inflammation and diseases like fibroses/ cirrhosis in liver tissue are activated.

To understand why HSCs could be activated through Fra1 overexpression topical mental attempts are discussed in the following: Are there any connections between the metabolic syndrome (Lipodystrophy) and the fibroses? Which local problems could still be a cause of the activation on HSCs? A complexity in the understanding of HSCs differentiation is underscored by different cellular phenotypes that are expressed by HSCs. In addition to the myofibroblastic phenotype, HSCs also express MyoD, the myogenic transcription factor specific for skeletal muscle [401]. Neuronal markers such as GFAP, N-CAM, nestin, and synaptophysin are also expressed in HSCs, suggesting the neural phenotype and that N-CAM and nestin are induced in activated HSCs [402, 403, and 404]. Activated HSCs express leptin, an adipocyte-specific gene, raising an intriguing possibility that HSCs may also share the adipocytic phenotype [405]. In fact, the quiescent HSCs is laden with lipids including triglycerides, cholesterol, and phospholipids in addition to retinyl esters [406, 407]. In support of this notion, PPARγ, one of the key transcription factors for adipocyte differentiation, is expressed in the quiescent HSCs, and its expression and activity decrease in HSCs activation in vitro and in vivo [408, 409, 410, and 411]. Further, the treatment of culture-activated HSCs with the natural or synthetic ligands for PPARγ suppresses many functional parameters of the cell activation, including cell proliferation, expression of collagen, TGFβ, α-smooth muscle actin, monocyte chemotactic protein-1 genes, and chemotaxis [412]. More importantly, the treatment of the animal models of liver fibrosis with the PPARγ ligands ameliorates not only induction of fibrosis but also progression of preexisting fibrosis. It may not be also forgotten that the liver is the major target organ of glucocorticoid action where it modulates a large number of metabolic functions. Their genomic action is mediated by an intracellular receptor, the glucocorticoid receptor (GR), which belongs to the steroid receptor family. The hormone receptor complex regulates expression of target genes via binding to glucocorticoid response elements (GRE) of certain promoter regions. Corticosteroids are common prescribed antiphlogistic steroids which were used in several therapies, e.g. chronic active liver disease and it is supposed that mineralcorticoid antagonists are candidates for antifibrogenic drugs [412, 413]. TGFβ, a key

factor in activation of hepatic stellate cells (HSCs), induces production of extracellular matrix, this being a prerequisite for the development of liver fibrosis. Glucocorticoid s and their receptors may provide a crosstalk with the TGFβ-Smad signalling pathway by antagonizing TGFβ effects. Dexamethasone treatment reduces TGFβ mRNA transcription in a time-dependent manner. Activated HSCs produce TGFβ and secrete it into the cell culture medium. After Dexamethasone treatment, TGFβ secretion is reduced [414]. Finally there is a high likelihood that MSC could differentiate into hepatic stellate that are cells of mesenchymal origin [415, 416]. The data about the Fra1-induced lipodystrophy through a PPARγ-decreased effect and downregulation of the glucocorticoid receptor might be one of the mechanisms that provide further evidence that the Fra1 overexpression affects also HSCs. Thus, these findings support the hypothesis that the maintenance of the quiescent state of HSCs requires PPARγ and depletion of this adipogenic transcription factor underlies activation of HSCs.

6.4.2. High Fra1 expression can be localized in simple cuboidal epithelium cells of portal triad vessels of fra1-tg mice

To identify the cells which could be responsible for the induced inflammation/ (activation of HSCs) in fra1-tg mice, immunofluorescent staining with Antibody (Ab) for Fra1 was done on liver sections. No positive signals were found in control staining and Ab-Fra1 incubated section of wt liver. However, a specific signal was detected when sections of fra1-tg liver were incubated with Ab-Fra1. High expression level of Fra1 was detected in simple cuboidal epithelium of the portal triad. Simple cuboidal epithelium, as their name implies, are roughly square or cuboidal in shape. Each cell has a spherical nucleus in the centre. Cuboidal epithelium is found in glands and in the lining of the kidney tubules as well as in the ducts of the glands. They also constitute the germinal epithelium which produces the egg cells in the female ovary and the sperm cells in the male testes.

One hypothesis was that a sustained activation of AP-1 may be a critical factor in determining the outcome a chronical inflammation in liver and this could explain the primary biliary cirrhosis in fra1-tg mice. Primary biliary cirrhosis (PBC) is one of the most common forms of chronic cholestatic liver disease. PBC is a disorder primarily involving the smallest bile duct branches. The liver parenchyma, including hepatocytes, is involved by chronic inflammatory and biliary obstructive processes often leading to ascending cholangitis, biliary degenerative changes, fibrosis and cirrhosis [417, 418]. It has classically been assumed that the liver parenchyma and sinusoids are involved only as a secondary

response to the cholestatic process and those changes in these "extraductular" sites are not seen as critical primary events. However, researcher recently surveyed the perisinusoidal spaces (disse space) in PBC [419] and described a significant increase in the number of macrovesicular hepatic stellate cells in patients. The pathogenesis of this abnormality and its significance remains unclear. The importance of cytokines in chronic inflammation may be related also to the hepatocyte apoptosis triggered by natural substances such as chemokines and other endogenous molecules and foreign toxins [420]. Cytokines implicated in fibrogenesis (i.e. TGFβ) and those involved in the initiation of inflammation (i.e. interferon gamma, interleukin-1 and tumor necrosis factor-a TNF-β) also stimulated recognition of apoptotic neutrophil. Endotoxin and IL1β up regulate the mannose receptor expression of liver cells and consequently the phagocytic activity of sinusoidal cells. The importance of the phagocytosis of dying cells as a process in itself is important especially in inflammation [421]. The recognition and ingestion of apoptotic cells by Kupffer cells and by other liver cells shows clearly those human liver macrophages are active participants in the removal of apoptotic cells and that this removal is efficient in inflammatory/ immune response.

Taken together Fra1 overexpressing mice suffer from liver injuries like fibrosis through activation of HSCs, possibly due to the close relationship to MSCs and there downregulation of the GR and PPARγ by Fra1. Moreover, the high level of Fra1 expression in simple cuboidal epithelium of the portal could induce an inflammation which is responsible for (auto)immune diseases like primary biliary cirrhosis, primary sclerosing cholangitis or autoimmune hepatitis.

References

1. Bohmann D, Admon A, Turner DR and Tjian R, Transcriptional regulation by the AP-1 family of enhancer-binding proteins: a nuclear target for signal transduction. Cold Spring Harb Symp Quant Biol, 1988, 53: 695-700.

2. Curran T and Franza BR Jr, Fos and Jun: the AP-1 connection. Cell, 1988, 55(3): 395-7.

3. Angel P, Imagawa M, Chiu R, Stein B, Imbra RJ, Rahmsdorf HJ, Jonat C, Herrlich P and Karin M, Oncogene jun encodes a sequence-specific trans-activator similar to AP-1. 1987, Cell, 49: 729-739.

4. Angel P and Karin M, The role of Jun, Fos and the AP-1 complex in cell-proliferation and transformation. Cancer, 1991, 129-157.

5. Hai T and Hartman MG, The molecular biology and nomenclature of the activating transcription factor/cAMP responsive element binding family of transcription factors: activating transcription factor proteins and homeostasis. Gene, 2001, 273(1): 1-11.

6. Herdegen T and Leah JD, Inducible and constitutive transcription factors in the mammalian nervous system: control of gene expression by Jun, Fos and Krox, and CREB/ATF proteins. Brain Res Brain Res Rev, 1998, 28(3): 370-490.

7. O'Shea EK, Rutkowski R and Kim PS, Mechanism of specificity in the Fos-Jun oncoprotein heterodimer. Cell, 1992, 68(4): 699-708.

8. Kovary K and Bravo R, Expression of different Jun and Fos proteins during the G0-to-G1 transition in mouse fibroblasts: in vitro and in vivo associations. Mol Cell Biol, 1991, 11(5): 2451-9.

9. Kovary K and Bravo R, The jun and fos protein families are both required for cell cycle progression in fibroblasts. Mol Cell Biol, 1991, 11(9): 4466-72.

10. Perkins KK, Dailey GM and Tjian R, Novel Jun- and Fos-related proteins in Drosophila are functionally homologous to enhancer factor AP-1. EMBO J, 1988, 7(13): 4265-73.

11. Perkins KK, Admon A, Patel N and Tjian R, The Drosophila Fos-related AP-1 protein is a developmentally regulated transcription factor. Genes Dev, 1990, 4(5): 822-34.

12. Kockel L, Homsy JG and Bohmann D, Drosophila AP-1: lessons from an invertebrate. Oncogene, 2001, 20(19): 2347-64.

13. Wagner EF, AP-1 - Introductory remarks. Oncogene, 2001, 20(19): 2334-5.

14. Chinenov Y and Kerppola TK, Close encounters of many kinds: Fos–Jun interactions that mediate transcription regulatory specificity. Oncogene, 2001, 20: 2438–2452.

15. Eferl R and Wagner EF, AP-1: a double-edged sword in tumorigenesis. Nat Rev, 2003, Cancer 3: 859–868.

16. Pulverer BJ, Kyriakis JM, Avruch J, Nikolakaki E and Woodgett JR, Phosphorylation of c-jun mediated by MAP kinases. Nature, 1991, 353: 670.

17. Smeal T, Binetruy B, Mercola DA, Birrer M and Karin M, Oncogenic and transcriptional cooperation with Ha-Ras requires phosphorylation of c-Jun on serines 63 and 73. Nature, 199, 354: 494.

18. Chen RH, Juo PC, Curran T and Blenis J, Phosphorylation of c-Fos at the C-terminus enhances its transforming activity. Oncogene, 1996, 12: 1493–1502.

19. David JP, Mehic D, Bakiri L, Schilling AF, Mandic V, Priemel M, Idarraga MH, Reschke MO, Hoffmann O, Amling M and Wagner EF, Essential role of RSK2 in c-Fos-dependent osteosarcoma development. J Clin Invest, 2005, 115(3): 664-72.

20. Molven A, Houge G and Berger R, Chromosomal assignment of the human gene encoding the Fos-related antigen-2 (FRA2) to chromosome 2p22-p23. Genomics, 1996, 38(1): 72-5.

21. Rauscher FJ 3rd, Voulalas PJ, Franza BR Jr and Curran T, Fos and Jun bind cooperatively to the AP-1 site: reconstitution in vitro. Genes Dev., 1988, 2(12B): 1687-99.

22. Curran T, Peters G, Van Beveren C, Teich NM and Verma IM, FBJ murine osteosarcoma virus: identification and molecular cloning of biologically active proviral DNA. J Virol, 1982, 44(2): 674-82.

23. Greenberg ME and Ziff EB, Stimulation of 3T3 cells induces transcription of the c-fos proto-oncogene. Nature, 1984, 311(5985): 433-8.

24. Piechaczyk M and Blanchard JM, c-fos proto-oncogene regulation and function. Crit Rev Oncol Hematol, 1994, 17(2): 93-131.

25. Murphy LO, Smith S, Chen RH, Fingar DC and Blenis J, Molecular interpretation of ERK signal duration by immediate early gene products. Nat Cell Biol, 2002, 4(8): 556-64.

26. Bossis G, Ferrara P, Acquaviva C, Jariel-Encontre I and Piechaczyk M, c-Fos proto-oncoprotein is degraded by the proteasome independently of its own ubiquitinylation in vivo. Mol Cell Biol, 2003, 23(20): 7425-36.

27. Shaulian E and Karin M, AP-1 in cell proliferation and survival. Oncogene, 2001, 20(19): 2390-400.

28. Johnson RS, Spiegelman BM, Papaioannou V.Pleiotropic effects of a null mutation in the c-fos proto-oncogene. Cell, 1992, 71(4):5 77-86.

29. Wang ZQ, Ovitt C, Grigoriadis AE, Möhle-Steinlein U, Rüther U and Wagner EF, Bone and haematopoietic defects in mice lacking c-fos. Nature, 1992, 360(6406): 741-5.

30. Dony C and Gruss P, Proto-oncogene c-fos expression in growth regions of fetal bone and mesodermal web tissue. Nature, 1987, 328(6132): 711-4.

31. Caubet JF, c-fos proto-oncogene expression in the nervous system during mouse development. Mol Cell Biol, 1989, 9(5): 2269-72.

32. Alitalo R, Partanen J, Pertovaara L, Hölttä E, Sistonen L, Andersson L and Alitalo K, Increased erythroid potentiating activity/tissue inhibitor of metalloproteinases and jun/fos transcription factor complex characterize tumor promoter-induced megakaryoblastic differentiation of K562 leukemia cells. Blood, 1990, 75(10): 1974-82.

33. Smeyne RJ, Curran T and Morgan JI, Temporal and spatial expression of a fos-lacZ transgene in the developing nervous system. Brain Res Mol Brain Res, 1992, 16(1-2): 158-62.

34. Grigoriadis AE, Schellander K, Wang ZQ and Wagner EF, Osteoblasts are target cells for transformation in c-fos transgenic mice. J Cell Biol, 1993, 122(3): 685-701.

35. Yang X, Matsuda K, Bialek P, Jacquot S, Masuoka HC, Schinke T, Li L, Brancorsini S, Sassone-Corsi P, Townes TM, Hanauer A and Karsenty G, ATF4 is a substrate of RSK2 and an essential regulator of osteoblast biology; implication for Coffin-Lowry Syndrome. Cell. 2004 Apr 30;117(3):387-98.

36. Young MR, Nair R, Bucheimer N, Tulsian P, Brown N, Chapp C, Hsu TC and Colburn NH, Transactivation of Fra-1 and consequent activation of AP-1 occur extracellular signal-regulated kinase dependently. Mol Cell Biol. 2002 Jan;22(2):587-98.

37. Casalino L, De Cesare D and Verde P, Accumulation of Fra-1 in ras-transformed cells depends on both transcriptional autoregulation and MEK-dependent posttranslational stabilization. Mol Cell Biol. 2003 Jun;23(12):4401-15.

38. Welter JF and Eckert RL, Differential expression of the fos and jun family members c-fos, fosB, Fra-1, Fra-2, c-jun, junB and junD during human epidermal keratinocyte differentiation. Oncogene, 1995, 11(12): 2681-7.

39. Yoshioka K, Deng T, Cavigelli M and Karin M, Antitumor promotion by phenolic antioxidants: inhibition of AP-1 activity through induction of Fra expression. Proc Natl Acad Sci, 1995, 92(11): 4972-6.

40. Schreiber M, Poirier C, Franchi A, Kurzbauer R, Guenet JL, Carle GF and Wagner EF, Structure and chromosomal assignment of the mouse fra-1 gene, and its exclusion as a candidate gene for oc (osteosclerosis). Oncogene, 1997, 15(10): 1171-8.

41. Kakumoto K, Sasai K, Sukezane T, Oneyama C, Ishimaru S, Shibutani K, Mizushima H, Mekada E, Hanafusa H and Akagi T, FRA1 is a determinant for the difference in RAS-induced transformation between human and rat fibroblasts. Proc Natl Acad Sci, 2006, 103(14): 5490-5.

42. Shirsat NV and Shaikh SA, Overexpression of the immediate early gene fra-1 inhibits proliferation, induces apoptosis, and reduces tumourigenicity of c6 glioma cells. Exp Cell Res, 2003, 291(1): 91-100.

43. Vallone D, Battista S, Pierantoni GM, Fedele M, Casalino L, Santoro M, Viglietto G, Fusco A and Verde P, Neoplastic transformation of rat thyroid cells requires the junB and fra-1 gene induction which is dependent on the HMGI-C gene product. EMBO J, 1997, 16(17): 5310-21.

44. Brüsselbach S, Möhle-Steinlein U, Wang ZQ, Schreiber M, Lucibello FC, Müller R and Wagner EF, Cell proliferation and cell cycle progression are not impaired in fibroblasts and ES cells lacking c-Fos. Oncogene, 1995, 10(1): 79-86.

45. Matsuo K, Owens JM, Tonko M, Elliott C, Chambers TJ and Wagner EF, Fosl1 is a transcriptional target of c-Fos during osteoclast differentiation. Nat Genet, 2000, 24(2): 184-7.

46. Mechta F, Lallemand D, Pfarr CM and Yaniv M. Transformation by ras modifies AP1 composition and activity. Oncogene, 1997, 14(7): 837-47.

47. Kustikova O, Kramerov D, Grigorian M, Berezin V, Bock E, Lukanidin E and Tulchinsky E, Fra-1 induces morphological transformation and increases in vitro invasiveness and motility of epithelioid adenocarcinoma cells. Mol Cell Biol, 1998,18(12): 7095-105.

48. Matsuo K, Owens JM, Tonko M, Elliott C, Chambers TJ and Wagner EF, Fosl1 is a transcriptional target of c-Fos during osteoclast differentiation. Nat Genet, 2000, 24(2): 184-7.

49. Tallquist MD, Soriano P and Klinghoffer RA, Growth factor signaling pathways in vascular development. Oncogene, 1999, 18(55): 7917-32.

50. Eferl R, Hoebertz A, Schilling AF, Rath M, Karreth F, Kenner L, Amling M and Wagner EF, The Fos-related antigen Fra-1 is an activator of bone matrix formation. EMBO J, 2004, 23(14): 2789-99.

51. Schreiber M, Wang ZQ, Jochum W, Fetka I, Elliott C and Wagner EF, Placental vascularisation requires the AP-1 component fra1. Development, 2000, 127(22): 4937-48.

52. Jochum W, David JP, Elliott C, Wutz A, Plenk H Jr, Matsuo K and Wagner EF, Increased bone formation and osteosclerosis in mice overexpressing the transcription factor Fra-1. Nat Med, 2000, 6(9): 980-4.

53. Nishina H, Sato H, Suzuki T, Sato M and Iba H, Isolation and characterization of fra-2, an additional member of the fos gene family. Proc Natl Acad Sci U S A, 1990, 87(9): 3619-23.

54. Matsui M, Tokuhara M, Konuma Y, Nomura N and Ishizaki R, Isolation of human fos-related genes and their expression during monocyte-macrophage differentiation. Oncogene, 1990, 5(3): 249-55.

55. Foletta VC, Sonobe MH, Suzuki T, Endo T, Iba H and Cohen DR, Cloning and characterisation of the mouse fra-2 gene. Oncogene, 1994, 9(11): 3305-11.

56. Carrasco D and Bravo R, Tissue-specific expression of the fos-related transcription factor fra-2 during mouse development. Oncogene, 1995, 10(6): 1069-79.

57. McHenry JZ, Leon A, Matthaei KI and Cohen DR, Overexpression of fra-2 in transgenic mice perturbs normal eye development. Oncogene, 1998, 17(9): 1131-40.

58. Karreth F, Hoebertz A, Scheuch H, Eferl R and Wagner EF. The AP1 transcription factor Fra2 is required for efficient cartilage development. Development, 2004, 131(22): 5717-25.

59. Zerial M, Toschi L, Ryseck RP, Schuermann M, Müller R and Bravo R, The product of a novel growth factor activated gene, fos B, interacts with JUN proteins enhancing their DNA binding activity. EMBO J, 1989, 8(3): 805-13.

60. Gruda MC, van Amsterdam J, Rizzo CA, Durham SK, Lira S and Bravo R. Expression of FosB during mouse development: normal development of FosB knockout mice. Oncogene, 1996, 12(10): 2177-85.

61. Brown JR, Ye H, Bronson RT, Dikkes P and Greenberg ME, A defect in nurturing in mice lacking the immediate early gene fosB. Cell, 1996, 86(2): 297-309.

62. Alibhai IN, Green TA, Potashkin JA and Nestler EJ, Regulation of fosB and ΔfosB mRNA expression: In vivo and in vitro studies Brain Res, 2007, 1143: 22-33.

63. Nakabeppu Y and Nathans D, A naturally occurring truncated form of FosB that inhibits Fos/Jun transcriptional activity. Cell, 1991, 64(4): 751-9.

64. Yen J, Wisdom RM, Tratner I and Verma IM, An alternative spliced form of FosB is a negative regulator of transcriptional activation and transformation by Fos proteins. Proc Natl Acad Sci U S A, 1991, 88(12): 5077-81.

65. Kveiborg M, Sabatakos G, Chiusaroli R, Wu M, Philbrick WM, Horne WC and Baron R, DeltaFosB induces osteosclerosis and decreases adipogenesis by two independent cell-autonomous mechanisms. Mol Cell Biol, 2004, 24(7): 2820-30.

66. Kveiborg M, Chiusaroli R, Sims NA, Wu M, Sabatakos G, Horne WC and Baron R, The increased bone mass in deltaFosB transgenic mice is independent of circulating leptin levels. Endocrinology, 2002, 143(11): 4304-9.

67. Friedenstein AJ, Piatetzky-Shapiro II and Petrakova KV, Osteogenesis in transplants of bone marrow cells. J Embryol Exp Morphol, 1966,16: 381–390.

68. Friedenstein AJ, Chailakhjan RK and Lalykina KS, The development of fibroblast colonies in monolayer cultures of guinea-pig bone marrow and spleen cells. Cell Tissue Kinet, 1970, 3: 393–403.

69. Owen M, Marrow derived stromal stem cells. J Cell Science Supp, 1988, 10: 63–76.

70. Becker AJ, McCulloch EA and Till JE, Cytological demonstration of the clonal nature of spleen colonies derived from transplanted mouse marrow cells. Nature, 1963, 197: 452-4.

71. Siminovitch L, McCulloch EA and Till JE, The distribution of colony-forming cells among spleen colonies. Journal of Cellular and Comparative Physiology, 1963, 62: 327-36.

72. Friedenstein AJ, Deriglasova UF, Kulagina NN, Panasuk AF, Rudakowa SF, Luria EA and Ruadkow IA, Precursors for fibroblasts in different populations of hematopoietic cells as detected by the in vitro colony assay method. Exp Hemato, 1974, 2(2): 83-92.

73. Friedenstein AJ, Gorskaja JF and Kulagina NN, Fibroblast precursors in normal and irradiated mouse hematopoietic organs. Exp Hematol, 1976, 4(5): 267-74.

74. http://en.wikipedia.org/wiki/Mesenchymal_stem_cell#_note-0#note-02007

75. Bensidhoum M, Chapel A, Francois S, Demarquay C, Mazurier C, Fouillard L, Bouchet S, Bertho JM, Gourmelon P, Aigueperse J, Charbord P, Gorin NC, Thierry D and Lopez M, Homing of in vitro expanded Stro-1- or Stro-1+ human mesenchymal stem cells into the NOD/SCID mouse and their role in supporting human CD34 cell engraftment. Blood, 2004, 103: 3313–3319.

76. Gronthos S, Zannettino AC, Hay SJ, Shi S, Graves SE, Kortesidis A and Simmons PJ, Molecular and cellular characterisation of highly purified stromal stem cells derived from human bone marrow. J Cell Sci, 2003, 116(9): 1827-35.

77. Javazon EH, Beggs KJ and Flake AW, Mesenchymal stem cells: paradoxes of passaging. Exp Hematol, 2004, 32: 414–425.

78. Karihaloo A, Nickel C and Cantley LG, Signals which build a tubule. Nephron Exp Nephrol, 2005, 100(1): 40-5.

79. Wagner EF und Karsenty G, Genetic control of skeletal development. Curr Opin Genet Dev, 2001, 11(5): 527-32.

80. Caetano-Lopes J, Canhão H and Fonseca JE. Osteoblasts and bone formation. Acta Reumatol Port, 2007, 32(2): 103-10.

81. Nakashima K and de Crombrugghe B, Transcriptional mechanisms in osteoblast differentiation and bone formation. Trends in Genetics, 2003, 8: 458-466.

82. Bielby R, Jones E and McGonagle D, The role of mesenchymal stem cells in maintenance and repair of bone. Injury, 2007, 38(Suppl 1): S26-32.

83. Ducy P, Amling M, Takeda S, Priemel M, Schilling AF, Beil FT, Shen J, Vinson C, Rueger JM and Karsenty G, Leptin inhibits bone formation through a hypothalamic relay: A central control of bone mass. Cell, 2000, 100(2): 197–207.

84. Cohen MM, The new bone biology: Pathologic, molecular and clinical correlates. Am J Med Genet, 2006, 140(23): 2646–2706.

85. Bae SC, Yamaguchi-Iwai YE, Maruyama M, Inuzuka M, Kagoshima H, Shigesadam M, Satake M and Ito Y, Isolation of PEBP2αB cDNA representing the mouse homolog of human acute myeloid leukemia gene, AML1. Oncogene, 1993, 8: 809–814.

86. Bae SC, Takahashi E, Zhang W, Ogawa E, Shigesada K, Namba Y, Satake M and Ito Y, Cloning, mapping and expression of PEBP2αC, a third gene encoding the mammalian Runt domain. Gene, 1995, 159: 245–248.

87. Ogawa E, Maruyama M, Kagoshima H, Inuzuka M, Lu J, Satake M, Shigesada K and Ito Y, PEBP2/PEA2 represents a new family of transcription factor homologous to the products of the Drosophila runt and the human AML1 gene. Proc Natl Acad Sci, 1993, 90: 6859–6863.

88. Kania MA, Bonner AS, Duffy JP and Gergen JP, The Drosophila segmentation gene runt encodes a novel nuclear regulatory protein that is also expressed in the developing nervous system. Genes Dev, 1990, 4: 1701–1713.

89. Ogawa E, Inuzaka M, Maruyama M, Satake M, Naito-Fujimoto M, Ito Y and Shigesada K, Molecular cloning and characterization of PEBP2β, the heterodimeric partner of a novel Drosophila runt-related DNA binding protein PEBP2α. Virology, 1993, 194: 314–331.

90. Wang S, Wang Q, Crute BE, Melnikova IN, Keller SR and Speck NA, Cloning and characterization of subunits of the T-cell receptor and murine leukemia virus enhancer core-binding factor. Mol Cell Biol, 1993, 13: 3324–3339.

91. Kamachi Y, Ogawa E, Asano M, Ishida S, Murakami Y, Satake M, Ito Y and Shigesada K, Purification of a mouse nuclear factor that binds to both the A and B cores of the polyomavirus enhancer. J. Virol. 1990, 64: 4808–4819.

92. Wang S and Speck NA, Purification of core-binding factor, a protein that binds the conserved core site in murine leukemia virus enhancers. Mol Cell Biol, 1992, 12: 89–102.

93. Geoffroy C, Ducy P and Karsenty G, A PEBP2α/AML-1-related factor increases osteocalcin promoter activity through its binding to an osteoblast-specific cis-acting element. J Biol Chem, 1995, 270: 30973–30979.

94. Merriman HL, van Wijnen AJ, Hiebert S, Bidwell JP, Fey E, Lian J, Stein J and Stein GS, The tissue-specific nuclear matrix protein, NMP-2, is a member of the AML/CBF/PEBP2/Runt domain transcription factor family: interaction with the osteocalcin gene promoter. Biochemistry, 1995, 34: 13125–13132.

95. Banerjee C, Hiebert SW, Stein JL, Lian JB and Stein GS, An AML-1 consensus sequence binds an osteoblast-specific complex and transcriptionally activates the osteocalcin gene. Proc Natl Acad Sci, 1996, 93: 4968–4973.

96. Komori T, Yagi H, Nomura S, Yamaguchi A, Sasaki K, Deguchi K, Shimizu Y, Bronson R, Gao Y and Inada M, Targeted disruption of Cbfa1 results in a complete lack of bone formation owing to maturational arrest of osteoblasts. Cell, 1997, 89: 755-764.

97. Otto F, Thornell AP, Crompton T, Denzel A, Gilmour KC, Rosewell IR, Stamp GW, Beddington RS, Mundlos S, Olsen BR, Selby PB and Owen MJ, Cbfa1, a candidate gene for cleidocranial dysplasia syndrome, is essential for osteoblast differentiation and bone development. Cell, 1997, 89(5): 677-80.

98. Nakashima K, Zhou X, Kunkel G, Zhang Z, Deng JM, Behringer R and deCrombrugghe B. The novel zinc finger-containing transcription factor Osterix is required for osteoblast differentiation and bone formation. Cell, 2002, 108: 17–29.

99. Milona MA, Gough JE and Edgar AJ, Expression of alternatively spliced isoforms of human Sp7 in osteoblast-like cells. BMC Genomics, 2003, 4(1): 43.

100. Tai G, Polak J M, Bishop A E, Christodoulou I and Buttery L D, Differentiation of osteoblasts from murine embryonic stem cells by overexpression of the transcriptional factor osterix. Tissue Eng, 2004,10: 1456–1466.

101. Ducy P, Zhang R, Geoffroy V, Ridall AL and Karsenty G, Osf2/Cbfa1: a transcriptional activator of osteoblast differentiation. Cell, 1997, 89: 747–754.

102. Fleischmann A, Hafezi F, Elliott C, Remé CE, Rüther U and Wagner EF, Fra-1 replaces c-Fos-dependent functions in mice. Genes Dev. 2000 Nov 1;14(21):2695-700.

103. Sabatakos G, Sims NA, Chen J, Aoki K, Kelz MB, Amling M, Bouali Y, Mukhopadhyay K, Ford K, Nestler EJ and Baron R, Overexpression of DeltaFosB transcription factor(s) increases bone formation and inhibits adipogenesis. Nat Med, 2000, 9: 970-990.

104. Grigoriadis AE, Schellander K, Wang ZQ and Wagner EF, Osteoblasts are target cells for transformation in c-fos transgenic mice. J Cell Biol, 1993, 122(3): 685-701.

105. Zelzer E and Olsen BR, The genetic basis for skeletal diseases. Nature, 2003, 423: 343–348.

106. Karsenty G and Wagner EF, Reaching a genetic and molecular understanding of skeletal development, Dev Cell, 2002, 2: 389–406.

107. You J, Reilly GC, Zhen X, Yellowley CE, Chen Q, Donahue HJ and Jacobs CR, Osteopontin gene regulation by oscillatory fluid flow via intracellular calcium mobilization and activation of mitogen-activated protein kinase in MC3T3-E1 osteoblasts. J Biol Chem, 2001, 276: 13365–13371.

108. Haroon ZA, Lai TS, Hettasch JM, Lindberg RA, Dewhirst MW and Greenberg CS, Tissue transglutaminase is expressed as a host response to tumor invasion and inhibits tumor growth. Lab Invest, 1999, 79: 1679–1686.

109. Nakajima M, Negishi Y, Tanaka H and Kawashima K, p21(Cip-1/SDI-1/WAF-1) expression via the mitogen-activated protein kinase signaling pathway in Insulin-induced chondrogenic differentiation of ATDC5 cells. Biochem Biophys Res Commun, 2004, 320: 1069–1075.

110. Akiyama T, Miyazaki T, Bouillet P, Nakamura K, Strasser A and Tanaka S, In vitro and in vivo assays for osteoclast apoptosis. Biol Proced Online, 2005,7: 48-59.

111. Lefebvre V, Li P and de Crombrugghe B, A new long form of Sox5 (L-Sox5), Sox6 and Sox9 are coexpressed in chondrogenesis and cooperatively activate the type II collagen gene. EMBO J, 1998,17: 5718–33.

112. DeLise AM, Fischer L and Tuan RS, Cellular interactions and signaling in cartilage development. Osteoarthritis Cartilage, 2000, 8(5): 309-34.

113. Flier JS, The adipocyte: storage depot or node on the energy information superhighway? Cell, 1995, 80:15–18.

114. Cornelius P, MacDougald OA and Lane MD, Regulation of adipocyte development. Annu Rev Nutr, 1994, 14: 99–129.

115. MacDougald OA and Lane MD, Transcription regulation of gene expression during adipocyte differentiation. Annu Rev Biochem, 1995, 64: 345–373.

116. Ringold GM, Chapman AB, Knight DM, Navre M and Torti FM, Hormonal control of adipocyte differentiation and adipocyte gene expression. Recent Prog Horm Res, 1988, 44: 115–140.

117. Spiegelman BM, Regulation of gene expression in the adipocyte: implications for obesity and proto-oncogene function. Trends Genet, 1988,4: 203–207.

118. Spiegelman BM, Choy L, Hotamisligil GS, Graves RA and Tontonoz P, Regulation of adipocyte gene expression in differentiation and syndromes of obesity/diabetes. J Biol Chem, 1993, 268: 6823–6826.

119. Vasseur-Cognet M and Lane MD, Trans-acting factors involved in adipogenic differentiation. Curr Opin Genet Dev, 1993, 3: 238–245.

120. Smas CM and Sul HS, Pref-1, a protein containing EGF-like repeats, inhibits adipocyte differentiation. Cell, 1993, 73: 725–734.

121. Smas CM, Green D and Sul HS, Structural characterization and alternate splicing of the gene encoding the preadipocyte EGF-like protein Pref-1. Biochemistry, 1994, 33: 9257–9265.

122. Chawla A, Schwarz EJ, Dimaculangan DD and Lazar MA, Peroxisome proliferator-activated receptor (PPAR) γ: adipose-predominant expression and induction early in adipocyte differentiation. Endocrinology, 1994, 135: 798–800.

123. Tontonoz P, Hu E, Devine J, Beale EG and Spiegelman B, PPARγ2 regulates adipose expression of the phosphoenolpyruvate carboxykinase gene. Mol Cell Biol 1995, 15: 351–357.

124. Green H and Kehinde O, Subline of mouse 3T3 cells that accumulate lipid. Cell, 1974, 1: 113–116.

125. Green H and Kehinde O, Spontaneous heritable changes leading to increased adipose conversion in 3T3 cells. Cell, 1974, 3: 127–133.

126. Landschulz WH, Johnson PF, Adashi EY, Graves BJ and McKnight SL, Isolation of a recombinant copy of the gene encoding C/EBP. Genes Dev, 1988 2: 786–800.

127. Landschulz WH, Johnson PF and McKnight SL, The DNA binding domain of the rat liver nuclear protein C/EBP is bipartite. Science, 1989, 243: 1681–1688.

128. Akira S, Isshiki H, Sugita T, Tanabe O, Kinoshita S, Nishio Y, Nakajima T, Hirano T and Kishimoto T, A nuclear factor for IL-6 expression (NF-IL6) is a member of a C/EBP family. EMBO J, 1990, 9(6): 1897-906.

129. Chang CJ, Chen TT, Lei HY, Chen DS and Lee SC, Molecular cloning of a transcription factor, AGP/EBP that belongs to members of the C/EBP family. Mol Cell Biol, 1990, 10(12): 6642-53.

130. Descombes P, Chojkier M, Lichtsteiner S, Falvey E and Schibler U, LAP, a novel member of the C/EBP gene family, encodes a liver-enriched transcriptional activator protein. Genes Dev, 1990, 4(9): 1541-51.

131. Poli V, Mancini FP and Cortese R, IL-6DBP, a nuclear protein involved in interleukin-6 signal transduction, defines a new family of leucine zipper proteins related to C/EBP. Cell, 1990, 63(3): 643-53.

132. Cao Z, Umek RM and McKnight SL, Regulated expression of three C/EBP isoforms during adipose conversion of 3T3-L1 cells. Genes Dev, 1991, 5(9): 1538-52.

133. Williams SC, Cantwell CA and Johnson PF, A family of C/EBP-related proteins capable of forming covalently linked leucine zipper dimers in vitro. Genes Dev, 1991, 5(9): 1553-67.

134. Kageyama R, Sasai Y and Nakanishi S, Molecular characterization of transcription factors that bind to the cAMP responsive region of the substance P precursor gene. cDNA cloning of a novel C/EBP-related factor. J Biol Chem, 1991, 266(23): 15525-31.

135. Tang QQ, Jiang MS and Lane MD, Repression of transcription mediated by dual elements in the CCAAT/enhancer binding protein alpha gene. Proc Natl Acad Sci, 1997, 94(25): 13571-5.

136. Yeh WC, Cao Z, Classon M and McKnight SL, Cascade regulation of terminal adipocyte differentiation by three members of the C/EBP family of leucine zipper proteins. Genes Dev, 1995, 9(2): 168-81.

137. Tanaka T, Yoshida N, Kishimoto T and Akira S, Defective adipocyte differentiation in mice lacking the C/EBPbeta and/or C/EBPdelta gene. EMBO J, 1997, 16: 7432-7443.

138. Tang Q Q, Otto T C and Lane M D, CCAAT/enhancer-binding protein beta is required for mitotic clonal expansion during adipogenesis. Proc Natl Acad Sci, 2003, 100: 850-855.

139. Wu Z, Xie Y, Bucher N L and Farmer SR, Conditional ectopic expression of C/EBP beta in NIH-3T3 cells induces PPAR gamma and stimulates adipogenesis. Genes Dev, 1995, 9: 2350-2363.

140. Rosen ED, Hsu C H, Wang X, Sakai S, Freeman M W, Gonzalez FJ and Spiegelman B M, C/EBPalpha induces adipogenesis through PPARgamma: a unified pathway. Genes Dev, 2002, 16: 22-26.

141. Wu Z, Bucher NL and Farmer SR, Induction of peroxisome proliferator-activated receptor γ during the conversion of 3T3 fibroblasts into adipocytes is mediated by C/EBPβ, C/EBPδ, and glucocorticoids. Mol Cell Biol, 1996, 16: 4128-4136.

142. Wu Z, Puigserver P and Spiegelman B M, Transcriptional activation of adipogenesis. Curr Opin Cell Biol, 1999, 11: 689-694.

143. Wu Z, Rosen ED, Brun R, Hauser S, Adelmant G, Troy AE, McKeon C, Darlington GJ and Spiegelman BM, Cross-regulation of C/EBP alpha and PPAR gamma controls the transcriptional pathway of adipogenesis and Insulin sensitivity. Mol Cell,1999, 3: 151-158.

144. Herrera R, Ro HS, Robinson GS, Xanthopoulos KG and Spiegelman BM, A direct role for C/EBP and the AP-I-binding site in gene expression linked to adipocyte differentiation. Mol Cell Biol, 1989, 9(12): 5331-5339.

145. Bernlohr DA, Angus CW, Lane MD, Bolanowski MA and Kelly TJ, Expression of specific mRNA during adipose differentiation: identification of an mRNA encoding a homologue of myelin P2 protein. Proc Natl Acad Sci, 1984, 81: 5468-5472.

146. Cook KS, Hunt CR and Spiegelman BM, Developmentally regulated mRNA in 3T3-adipocytes: analysis of transcriptional control. J Cell Biol, 1985,100: 514-520.

147. Spiegehnan BM, Regulation of gene expression in the adipocyte: implications for obesity and proto-oncogene function.Trends Genet, 1988, 4: 203-207.

148. Spiegelman BM, Frank M and Green H, Molecular cloning of mRNA from 3T3-adipocytes. Regulation of mRNA content for glycerophosphate dehydrogenase and other differentiation dependent proteins during adipocyte development. J Biol Chem, 1983, 258: 10083-10089.

149. Bell GI, Kayano T and Buse JB, Molecular biology of mammalian glucose transporters. Diabetes Care, 1990, 13: 198–208.

150. Mueckler M, Family of glucose-transporter genes: implications for glucose homeostasis and diabetes. Diabetes, 1990, 39: 6–11.

151. Kahn BB, Charron MJ, Lodish HF, Cushman SW and Flier JS, Differential regulation of two glucose transporters in adipose cells from diabetic and Insulin-treated diabetic rats. J Clin Invest, 1989, 84: 404–411.

152. Toker A and Cantley LC, Signalling through the lipid products of phosphoinositide-3-OH kinase. Nature, 1997, 387(6634): 673-6.

153. Vanhaesebroeck B, Leevers SJ, Panayotou G and Waterfield MD, Phosphoinositide 3-kinases: a conserved family of signal transducers. Trends Biochem Sci, 1997, 22(7): 267-72.

154. Pearson GF, Robinson, TB, Gibson BE, Karandikar M, Berman K and Cobb MH, Mitogen-activated protein (MAP) kinase pathways: regulation and physiological functions. Endocr Rev, 2001, 22: 153-183.

155. Yang L and Baker NE, Cell cycle withdrawal, progression, and cell survival regulation by EGFR and its effectors in the differentiating Drosophila eye. Dev Cell, 2003, 4: 359-369.

156. Lin AW, Barradas M, Stone JC, van Aelst L, Serrano M and Lowe SW, Premature senescence involving p53 and p16 is activated in response to constitutive MEK/MAPK mitogenic signaling. Genes Dev, 1998, 12: 3008-3019.

157. Pages G, Lenormand P, L'Allemain G, Chambard JC, Meloche S and Pouyssegur J, Mitogen-activated protein kinases p42mapk and p44mapk are required for fibroblast proliferation. Proc Natl Acad Sci, 1993, 90: 8319-8323.

158. White MA, Nicolette C, Minden A, Polverino A, van Aelst L, Karin M and Wigler MH, Multiple Ras functions can contribute to mammalian cell transformation. Cell, 1995, 80: 533-541.

159. Zhu J, Woods D, McMahon M and Bishop JM, Senescence of human fibroblasts induced by oncogenic Raf. Genes Dev, 1998, 12: 2997-3007.

160. Prusty D, Park BH, Davis KE and Farmer SR, Activation of MEK/ERK signalingpromotes adipogenesis by enhancing peroxisome proliferator-activated receptor gamma (PPARgamma) and C/EBPalpha gene expression during the differentiation of 3T3-L1 preadipocytes. J Biol Chem, 2002, 277: 46226-46232.

161. Sale EM, Atkinson PG and Sale GJ, Requirement of MAP kinase for differentiation of fibroblasts to adipocytes, for Insulin activation of p90 S6 kinase and for Insulin or serum stimulation of DNA synthesis. EMBO J, 1995, 14: 674-684.

162. Tang QQ, Otto TC and Lane MD, Mitotic clonal expansion: a synchronous process required for adipogenesis. Proc Natl Acad Sci, 2003, 100: 44-49.

163. Font de Mora J, Porras A, Ahn N and Santos E, Mitogen-activated protein kinase activation is not necessary for, but antagonizes, 3T3-L1 adipocytic differentiation. Mol Cell Biol, 1997,17: 6068-6075.

164. Hu E, Kim JB, Sarraf P and Spiegelman BM, Inhibition of adipogenesis through MAP kinase-mediated phosphorylation of PPARgamma. Science, 1996, 274: 2100-2103.

165. Cinti S, Frederich RC, Zingaretti MC, Dematteis R, Flier JS and Lowell BB, Immunohistochemical localization of leptin and uncoupling protein in white and brown adipose tissue. Endocrinology, 1997, 138: 797–804.

166. Thomas T, Burguera B, Melton LJ, Atkinson EJ, Riggs BL and Khosla S, Relationship of serum leptin levels with body composition, sex steroid, and Insulin levels in men and women. Metabolism, 2000, 49: 1278–1284.

167. Yu WH, Kimura M, Walczewska A, Karanth S and McCann SM, Role of leptin in hypothalamic-pituitary function. Proc Natl Acad Sci, 1997, 94: 1023–1028.

168. Flier JS, Leptin expression and action: new experimental paradigms. Proc Natl Acad Sci, 1997, 94: 4242–4245.

169. Weintraub H, Dwarki VJ, Verma I, Davis R, Hollenberg S, Snider L, Lassar A and Tapscott SJ, Muscle-specific transcriptional activation by MyoD. Genes Dev, 1991, 5(8): 1377-86.

170. Emerson CP, Myogenesis and developmental control genes. Curr Opin Cell Biol, 1990, 2(6): 1065-75.

171. Arnold HH and Braun T, The role of Myf-5 in somitogenesis and the development of skeletal muscles in vertebrates. J Cell Sci, 1993, 104(Pt 4): 957-60.

172. Marieb EN, Human Anatomy & Physiology, 1998, 4th ed. Menlo Park, California: Benjamin/Cummings Science Publishing.

173. Netter FH, Musculoskeletal system: anatomy, physiology, and metabolic disorders. 1987, New Jersey: Ciba-Geigy Corporation.

174. Tortora GJ, Principles of Human Anatomy. 19895th ed. New York: Harper & Row, Publishers

175. http://en.wikipedia.org/wiki/Bone

176. Wada T, Nakashima T, Hiroshi N and Penninger JM, RANKL-RANK signaling in osteoclastogenesis and bone disease. Trends Mol Med, 2006, 12(1): 17-25.

177. Theill LE, Boyle WJ and Penninger JM. RANK-L and RANK: T cells, bone loss, and mammalian evolution. Annu Rev Immunol, 2002, 20: 795-823.

178. Kong YY and Penninger JM, Molecular control of bone remodeling and osteoporosis.Exp Gerontol, 2000, 35(8): 947-56.

179. Heller-Steinberg M, Ground substance, bone salts, and cellular activity in bone 201 formation and destruction. Am J Anat, 1951,89: 347–379.

180. Belanger LF, Osteocytic osteolysis. Calcif Tissue Res, 1969, 4: 1–12.

181. van der Plas EMA, Feijen JH, de Boer AH, Wiltink A, Alblas MJ, de Leij L and Nijweide PJ, Characteristics and properties of osteocytes in culture. J Bone Miner Res, 1994, 9: 1697–1704.

182. Heuck F, Comparative investigations of the function of osteocytes in bone resorption. Calcif Tissue Res, 1970, Suppl: 148–149.

183. Lanyon LE, Osteocytes, strain detection, bone modeling and remodeling. Calcif Tissue Int, 1993, 53: S102–106.

184. Kurihara N, The origin of osteoclasts. Bull Kanagawa Dent Coll, 1990, 18(2): 161-4.

185. Hattersley G, Kerby JA and Chambers TJ, Identification of osteoclast precursors in multilineage hemopoietic colonies. Endocrinology, 199, 128(1): 259-62.

186. Teitelbaum SL, Tondravi MM and Ross FP, Osteoclast biology. Osteoporosis, 1996, 61-94.

187. Bellido T, Regulation of interleukin-6, osteoclastogenesis, and bone mass by androgens. The role of the androgen receptor. J Clin Invest, 1995, 95: 2886-2895.

188. Girasole G, Jilka RL, Passeri G, Boswell S, Boder G, Williams DC and Manolanas SC, 17-Estradiol inhibits interleukin-6 production by bone marrow derived stromal cells and osteoblasts in vitro: A potential mechanism for the anti-osteoporotic effect of estrogens. J Clin Invest, 1992, 89: 883-891.

189. Hattersley G, Kirby JA and Chambers TJ, Identification of osteoclast precursors in multilineage hematopoietic colonies. Endocrinology, 1991, 128: 259-262.

190. Jilka RL, Increased osteoclast development after estrogen loss: Mediation by interleukin-6. Science, 1992, 257: 88-91.

191. Kurihara N, Chenu C, Miller M, Civin C and Roodman GD, Identification of 214 committed mononuclear precursors for osteoclast-like cells in long-term human marrow cultures. Endocrinology, 1990, 126: 2733-2741.

192. Matsuzaki K, Osteoclast differentiation factor (ODF) induces osteoclast-like cell formation in human peripheral blood mononuclear cell cultures. Biochem Biophys Res Commun, 1998, 246: 199-204.

193. Shevde NK, Bendixen AC, Dienger KM and Pike JW, Estrogens suppress RANK ligand-induced osteoclast differentiation via a stromal cell independent mechanism involving c-Jun repression. Proc Natl Acad Sci, 2000, 97: 7829-7834.

194. Tondravi MM, McKercher SR, Anderson K, Erdmann JM, Quiroz M, Maki R and Teitelbaum SL, Osteopetrosis in mice lacking haematopoietic transcription factor PU.1. Nature, 1997, 386: 81-84.

195. Tsukii K, Osteoclast differentiation factor mediates an essential signal for bone resorption induced by 1 alpha, 25-dihydroxyvitamin D3, prostaglandin E2, or parathyroid hormone in the microenvironment of bone. Biochem Biophys Res Commun, 1998, 246: 337-341.

196. Erlebacher A, Filvaroff EH, Gitelman SE and Derynck R, Toward a molecular understanding of skeletal development. Cell, 1995, 80(3): 371-8.

197. Cohn MJ and Tickle C, Limbs: a model for pattern formation within the vertebrate body plan. Trends Genet, 1996, 12(7): 253-7.

198. Reichenberger E, Aigner T, von der Mark K, Stöss H and Bertling W, In situ hybridization studies on the expression of type X collagen in fetal human cartilage. Dev Biol, 1991, 148(2): 562-72.

199. Shapiro IM, Adams CS, Freeman T and Srinivas V, Fate of the hypertrophic chondrocyte: microenvironmental perspectives on apoptosis and survival in the epiphyseal growth plate. Birth Defects Res C Embryo Today, 2005, 75(4): 330-9.

200. Gerber HP, Vu TH, Ryan AM, Kowalski J, Werb Z and Ferrara N, VEGF couples hypertrophic cartilage remodeling, ossification and angiogenesis during endochondral bone formation. Nat Med, 1999, 5(6): 623-8.

201. van der Eerden BC, Karperien M and Wit JM, Systemic and local regulation of the growth plate. Endocr Rev, 2003, 24(6): 782-801.

202. Abad V, Meyers JL, Weise M, Gafni RI, Barnes KM, Nilsson O, Bacher JD and Baron J, The role of the resting zone in growth plate chondrogenesis. Endocrinology, 2002, 143(5): 1851-7.

203. Rosen ED and MacDougald OA, Adipocyte differentiation from the inside out. Nat Rev Mol Cell Biol, 2006, 7(12): 885-96.

205. McNamara JP, Adipose tissue metabolism during lactation: where do we go from here? Proc Nutr Soc, 1997, 56(1A): 149-67.

206. Considine RV and Caro JF, Leptin and the regulation of body weight. Int J Biochem Cell Biol, 1997, 29(11): 1255-72.

207. O'Donnell CP, Tankersley CG, Polotsky VP, Schwartz AR, Smith PL, Leptin, obesity, and respiratory function. Respir Physiol, 2000, 119(2-3): 163-70.

208. Kennedy GC, The role of depot fat in the hypothalamic control of food intake in the rat. Proc R Soc Lond B Biol Sci, 1953, 140(901): 578-96.

209. Trayhurn P, Hoggard N, Mercer JG and Rayner DV, Hormonal and neuroendocrine regulation of energy balance--the role of leptin. Arch Tierernahr, 1998, 51(2-3): 177-85.

210. Pittenger MF, Mackay AM, Beck SC, Jaiswal RK, Douglas R, Mosca JD, Moorman MA, Simonetti DW, Craig S and Marshak DR, Multilineage potential of adult human mesenchymal stem cells. Science, 1999, 284: 143-147.

211. Bennett JH, Joyner CJ, Triffitt JT and Owen ME, Adipocytic cells cultured from marrow have osteogenic potential. J. Cell Sci, 1991, 99: 131-139.

212. Nuttall ME, Patton AJ, Olivera DL, Nadeau DP and Gowen M, Human trabecular bone cells are able to express both osteoblastic and adipocytic phenotype: implications for osteopenic disorders. J Bone Miner Res, 1998, 13: 371-382.

213. Park SR, Oreffo RO and Triffitt JT, Interconversion potential of cloned human marrow adipocytes in vitro. Bone, 1999, 24: 549-554.

214. Beresford JN, Bennett JH, Devlin C, Leboy PS and Owen ME, Evidence for an inverse relationship between the differentiation of adipocytic and osteogenic cells in rat marrow stromal cell cultures. J Cell Sci, 1992, 102: 341-351.

215. Meunier P, Aaron J, Edouard C and Vignon G, Osteoporosis and the replacement of cell populations of the marrow by adipose tissue. A quantitative study of 84 iliac bone biopsies. Clin Orthop, 1971, 80: 147-154.

216. Burkhardt R, Changes in trabecular bone, hematopoiesis and bone marrow vessels in aplastic anemia, primary osteoporosis, and old age: a comparative histomorphometric study. Bone, 1987, 8: 157-164.

217. Rozman C, Age-related variations of fat tissue fraction in normal human bone marrow depend on both size and number of adipocytes: a stereological study. Exp Hematol,1989,17: 34-37.

218. Rosen ED, Walkey CJ, Puigserver P and Spiegelman BM, Transcriptional regulation of adipogenesis. Genes Dev, 2000, 14: 1293-1307.

219. Tontonoz P, Hu E and Spiegelman BM, Stimulation of adipogenesis in fibroblasts by PPARgamma2, a lipid-activated transcription factor. Cell, 1994, 79: 1147-1156.

220. Barak Y, Nelson MC, Ong ES, Jones YZ, Ruiz-Lozano P, Chien KR, Koder A and Evans RM, PPARgamma is required for placental, cardiac, and adipose tissue development. Mol Cell, 1999, 4(4): 585-95.

221. Kubota N, Terauchi Y, Miki H, Tamemoto H, Yamauchi T, Komeda K, Satoh S, Nakano R, Ishii C, Sugiyama T, Eto K, Tsubamoto Y, Okuno A, Murakami K, Sekihara H, Hasegawa G, Naito M, Toyoshima Y, Tanaka S, Shiota K, Kitamura T, Fujita T, Ezaki O, Aizawa S and Kadowaki T, PPARgamma mediates high-fat diet-induced adipocyte hypertrophy and Insulin resistance. Mol Cell, 1999, 4(4): 597-609.

222. Rosen ED, PPARgamma is required for the differentiation of adipose tissue in vivo and in vitro. Mol Cell, 1999, 4: 611-617.

223. Mallamaci F, Tripepi G and Zoccali C, Leptin in end stage renal disease (ESRD): a link between fat mass, bone and the cardiovascular system. J Nephrol, 2005, 18(4): 464-8.

224. Karsenty G, Convergence between bone and energy homeostases: leptin regulation of bone mass. Cell Metab, 2006, 4(5): 341-8.

225. Thomas T, The complex effects of leptin on bone metabolism through multiple pathways. Curr Opin Pharmacol. 2004, 4(3): 295-300.

226. Hong JH, Hwang ES, McManus MT, Amsterdam A, Tian Y, Kalmukova R, Mueller E, Benjamin T, Spiegelman BM, Sharp PA, Hopkins N and Yaffe MB, TAZ, a transcriptional modulator of mesenchymal stem cell differentiation. Science, 2005, 309(5737): 1074-8.

227. Elefteriou F, Benson MD, Sowa H, Starbuck M, Liu X, Ron D, Parada LF, Karsenty G. ATF4 mediation of NF1 functions in osteoblast reveals a nutritional basis for congenital skeletal dysplasiae. Cell Metab. 2006 Dec;4(6):419-20.

228. Wang ZQ, Kiefer F, Urbánek P, Wagner EF. Generation of completely embryonic stem cell-derived mutant mice using tetraploid blastocyst injection. Mech Dev. 1997 Mar;62(2):137–145.

229. Dufresne SD, Bjørbaek C, El-Haschimi K, Zhao Y, Aschenbach WG, Moller DE, Goodyear LJ. Altered extracellular signal-regulated kinase signaling and glycogen metabolism in skeletal muscle from p90 ribosomal S6 kinase 2 knockout mice. Mol Cell Biol. 2001 Jan;21(1):81-7.

230. El-Haschimi K, Dufresne SD, Hirshman MF, Flier JS, Goodyear LJ, Bjørbaek C. Insulin resistance and lipodystrophy in mice lacking ribosomal S6 kinase 2. Diabetes. 2003 Jun; 52(6):1340-6.

231. Barzilai N, She L, Liu L, Wang J, Hu M, Vuguin P, Rossetti L: Decreased visceral adiposity accounts for leptin effect on hepatic but not peripheral Insulin action. Am J Physiol, 1999, 277: E291 –E298.

232. Yaspelkis BB 3rd, Ansari L, Ramey EL, Holland GJ, Loy SF: Chronic leptin administration increases Insulin-stimulated skeletal muscle glucose uptake and transport. Metabolism, 1999, 48:671 –676.

233. Shimomura I, Hammer RE, Ikemoto S, Brown MS, Goldstein JL: Leptin reverses Insulin resistance and diabetes mellitus in mice with congenital lipodystrophy. Nature, 1999, 401 :73 –76.

234. Yamauchi T, Kamon J, Minokoshi Y, Ito Y, Waki H, Uchida S, Yamashita S, Noda M, Kita S, Ueki K, Eto K, Akanuma Y, Froguel P, Foufelle F, Ferre P, Carling D, Kimura S, Nagai R, Kahn BB and Kadowaki T, Adiponectin stimulates glucose utilization and fatty-acid oxidation by activating AMP-activated protein kinase. Nat Med, 2002, 11 :1288–1295.

235. Stefan N and Stumvoll M, Adiponectin: its role in metabolism and beyond. Horm Metab Res, 2002, 34:469 –474.

236. Barth N, Langmann T, Scholmerich J, Schmitz G and Schaffler A, Identification of regulatory elements in human adipose most abundant gene transcript-1 (apM-1) promoter: role of SP1/SP3 and TNF-alpha as regulatory pathways. Diabetologia, 2002, 45 :1425 –1433.

237. Moitra J, Mason MM, Olive M, Krylov D, Gavrilova O, Marcus-Samuels B, Feigenbaum L, Lee E, Aoyama T, Eckhaus M, Reitman ML and Vinson C. Life without white fat: a transgenic mouse. Genes Dev, 1998, 12(20):3168-81.

238. Shimomura I, Hammer RE, Richardson JA, Ikemoto S, Bashmakov Y, Goldstein JL and Brown MS, Insulin resistance and diabetes mellitus in transgenic mice expressing nuclear SREBP-1c in adipose tissue: model for congenital generalized lipodystrophy. Genes Dev, 1998, 12(20): 3182-94.

239. Gavrilova O, Marcus-Samuels B, Leon LR, Vinson C and Reitman ML: Leptin and diabetes in lipoatrophic mice. Nature, 2000, 403: 850 –851.

240. Matarese V, Stone RL, Waggoner DW and Bernlohr DA.Intracellular fatty acid trafficking and the role of cytosolic lipid binding proteins. Prog Lipid Res, 1989, 28(4): 245-72.

241. Cook KS, Hunt CR and Spiegelman BM, Developmentally regulated mRNAs in 3T3-adipocytes: analysis of transcriptional control.J Cell Biol, 1985, 100(2): 514-20.

242. Bernlohr DA, Bolanowski MA, Kelly TJ Jr and Lane MD, Evidence for an increase in transcription of specific mRNAs during differentiation of 3T3-L1 preadipocytes. J Biol Chem, 1985, 260(9): 5563-7.

243. Distel RJ, Ro KS, Rosen BS, Groves D and Spiegelman BM, Nucleoprotein complexes that regulate gene expression in adipocyte differentiation: Direct participation of c-*fos*. Cell, 1987, 49: 835–844.

244. Rauscher FJ, Sambucetti LC, Curran T, Distel RJ and Spiegelman BM, Common DNA binding site for *fos* protein complexes and transcription factor AP-1. Cell, 1988, 52: 471–480.

245. Christy RJ, Yang VW, Ntambi JM, Geiman DE, Landschultz WH, Friedman AD, Nakabeppu Y, Kelly TJ and Lane MD, Differentiation-induced gene expression in 3T3-L1 preadipocytes: CCAAT/enhancer binding protein interacts with and activates the promoter of adipocyte-specific genes. Genes Dev, 1989, 3: 1323–1335.

246. Herrera R, Ro HS, Robinson GS, Xanthopoulos KG and Spiegelman BM, A direct role for C/EBP and the AP-I-binding site in gene expression linked to adipocyte differentiation. Mol Cell Biol, 1989, 9(12): 5331-9.

247. Rossum SR, Graves RA, Greenstein A, Platt KA, Shyu HL, Mellovitz B, Spiegelman BM, A fat-specific enhancer is the primary determinant of gene expression for adipocyte P2 in vivo. Proc Natl Acad Sci U S A, 1990, 87(24): 9590-4.

248. Graves RA, Tontonoz P, Ross SR, Spiegelman BM. Identification of a potent adipocyte-specific enhancer: involvement of an NF-1-like factor. Genes Dev, 1991, 5(3): 428-37.

249. Stephens JM and Pekala PH, Transcriptional repression of the C/EBP-alpha and GLUT4 genes in 3T3-L1 adipocytes by tumor necrosis factor-alpha. Regulations is coordinate and independent of protein synthesis. J Biol Chem, 1992, 5;267(19):13580-4.

251. Mandrup, S and MD, Lane. Regulating adipogenesis, J. Biol. Chem, 1997, 272: 5367-5370.

252. Green H and Kehinde O, Sublines of mouse 3T3 cells that accumulate lipids. Cell, 1974, 1: 113–116.

253. Cornelius P, MacDougald OA and Lane MD, Regulation of adipocyte development. Annu Rev Nutr, 1994, 14: 99-129.

254. Mandrup S and Lane MD, Regulating adipogenesis. J Biol Chem, 1997, 272(9): 5367-70.

255. Hurst H, Transcription factors 1: bZIP proteins. Protein Profile, 1994, 1: 123.

256. Cao Z, Umek RM and McKnight SL, Regulated expression of three C/EBP isoforms during adipose conversion of 3T3-L1 cells. Genes Dev, 1991, 5: 1538– 52.

257. Yeh W-C, Cao Z, Classon M and McKnight SL, Cascade regulation of terminal adipocyte differentiation by three members of the C/EBP family of leucine zipper proteins. Genes Dev, 1995, 9(2): 168– 81.

258. Wu Z, Xie Y, Bucher NL and Farmer SR, Conditional ectopic expression of C/EBP beta in NIH-3T3 cells induces PPAR gamma and stimulates adipogenesis. Genes Dev, 1995, 9: 2350– 63.

259. Brun RP, Tontonoz P, Forman BM, Ellis R and Jasmine C, Differential activation of adipogensis by multiple PPAR isoforms. Genes Dev, 1996, 10: 974– 84.

260. Tontonoz P, Hu E, Graves RA, Budavari AI and Spiegelman BM, mPPARγ2: tissue-specific regulator of an adipocyte enhancer. Genes Dev, 1994a, 8: 1224– 34.

261. Liao W, Nguyen MT, Yoshizaki T, Favelyukis S, Patsouris D, Imamura T, Verma IM and Olefsky JM, Suppression of PPAR-gamma attenuates Insulin-stimulated glucose uptake by affecting both GLUT1 and GLUT4 in 3T3-L1 adipocytes. Am J Physiol Endocrinol Metab, 2007,;293(1):E219-27.

262. Zhang B, Berger J, Zhou G, Elbrecht A and Biswas S, Insulin- and mitogen-activated protein kinase-mediated phosphorylation and activation of peroxisome proliferator-activated receptor gamma. J. Biol. Chem, 1996a, 271: 31771– 74.

263. Shalev A, Siegrist-Kaiser CA, Yen PM, Wahli W and Burger AGC, The peroxisome proliferator-activated receptor alpha is a phosphoprotein: regulation by Insulin. Endocrinology, 1996, 137: 4499– 502.

264. Hu E, Kim J, Sarraf P and Spiegelman B, Inhibition of adipogenesis through MAP kinase-mediated phosphorylation of PPAR gamma. Science, 1996, 274: 2100–3.

265. Zhang B, Graziano MP, Doebber TW, Leibowitz MD and White CS, Down-regulation of the expression of the obese gene by an antidiabetic thiazolidinedione in Zucker diabetic fatty rats and db/db mice. J. Biol. Chem, 1996, 271: 9455–59.

266. Wiper-Bergeron N, Wu D, Pope L, Schild-Poulter C and Haché RJ, Stimulation of preadipocyte differentiation by steroid through targeting of an HDAC1 complex. EMBO J, 2003, 22(9): 2135-45.

267. Beato, M, Herrlich, P and Schutz, G, Steroid hormone receptors: many actors in search of a plot. Cel, 1995, 83: 851-857.

268. Reichardt HM and Schutz G, Glucocorticoid signaling: multiple variations of a common theme. Mol Cell Endocrinol, 1998, 146: 1-6.

269. Dobson MG, Redfern CP, Unwin N and Weaver JU, The N363S polymorphism of the glucocorticoid receptor: potential contribution to central obesity in men and lack of association with other risk factors for coronary heart disease and diabetes mellitus J Clin Endocrinol Metab, 2001, 86: 2270-2274.

270. Ukkola O and Bouchard C, Clustering of metabolic abnormalities in obese individuals: the role of genetic factors. Ann Med, 2001, 33: 79-90.

271. Rosmond R, Bouchard C and Björntorp P, Tsp509I polymorphism in exon 2 of the glucocorticoid receptor gene in relation to obesity and cortisol secretion: cohort study. BMJ, 2001, 322: 652-653.

272. Golub MS, The adrenal and the metabolic syndrome. Curr Hypertens Rep, 2001, 3: 117-120.

273. Kellendonk C, Eiden S and Kret, O, Inactivation of the GR in the nervous system affects energy accumulation. Endocrinology, 2002, 143: 2333-2340.

274. Ljung T, Ottosson M and Ahlberg AC, Central and peripheral glucocorticoid receptor function in abdominal obesity. J Endocrinol Invest, 2002, 25: 229-235.

275. Cram EJ, Ramos RA, Wang EC, Cha HH, Nishio Y and Firestone GL, Role of the CCAAT/Enhancer Binding Protein-alpha Transcription Factor in the Glucocorticoid Stimulation of p21$^{waf1/cip1}$ Gene Promoter Activity in Growth-arrested Rat Hepatoma Cells, JBC, 1998, 4: 2008-2014.

276. Canalis E and Delany AM, Mechanisms of glucocorticoid action in bone. Ann N Y Acad Sci, 2002, 966: 73-81.

277. Randle, P.J., P.B. Garland, C.N. Hales, and E.A. Hewsholme. 1963. The glucose fatty-acid cycle, its role in Insulin sensitivity and the metabolic disturbances of diabetes mellitus. Lancet 1: 785-789.

279. Smith, P.J., L.S. Wise, R. Berkowitz, C. Wan, and C.S. Rubin. 1988. Insulin-like growth factor-I is an essential regulator of the differentiation of 3T3-L1 adipocytes. J. Biol. Chem. 263: 9402-9408.

280. Grunfeld C, Baird K, Van Obberghen E, Kahn CR. Glucocorticoid-induced Insulin resistance in vitro: evidence for both receptor and postreceptor defects. Endocrinology, 1981 Nov; 109(5):1723-30.

281. Svedberg J, Björntorp P, Smith U, Lönnroth P. Free-fatty acid inhibition of Insulin binding, degradation, and action in isolated rat hepatocytes. Diabetes, 1990, 39(5): 570-4.

282. Kitabchi AE, Umpierrez G, Fisher JN, Murphy MB and Stentz F, THIRTY YEARS OF PERSONAL EXPERIENCE IN HYPERGLYCEMIC CRISES: DIABETIC KETOACIDOSIS, AND HYPERGLYCEMIC HYPEROSMOLAR STATE. J Clin Endocrinol Metab, 2008, Feb 12.

283. Robbins DC, Sims EA. Recurrent ketoacidosis in acquired, total lipodystrophy (lipoatrophic diabetes). Diabetes Care. 1984 Jul-Aug;7(4):381-5

284. Brüning JC, Winnay J, Bonner-Weir S, Taylor SI, Accili D and Kahn CR, Development of a Novel Polygenic Model of NIDDM in Mice Heterozygous for IR and IRS-1 Null Alleles. Cell Press, 1997, 88: 561-572.

285. Kitabchi AE and Umpierrez GE. Changes in serum leptin in lean and obese subjects with acute hyperglycemic crises. J Clin Endocrinol Metab, 2003, 88(6): 2593-6.

286. Robbins DC and Sims EA, Recurrent ketoacidosis in acquired, total lipodystrophy (lipoatrophic diabetes). Diabetes Care, 1984, 7(4): 381-5.

289. Foster DW 1994. The lipodystrophies and other rare disorders of adipose tissue. In Harrison's principles of internal medicine (ed. K.J. Isselbacher, E. Braunwald, J.D. Wilson, J.B. Martin, A.S. Fauci and D.L. Kasper), pp. 2131-2136. McGraw-Hill, New York, NY.

290. Seip M and Trygstad O, Generalized lipodystrophy, congenital and acquired (lipoatrophy). Acta Paediatr, 1996, 413: 2-28.

291. Carr A, Samaras K, Chisholm DJ and Cooper DA, Pathogenesis of HIV-1-protease inhibitor-associated peripheral lipodystrophy, hyperlipidaemia, and Insulin resistance. Lancet, 1998, 351: 1881-1883.

292. Coleman DL, Obese and diabetes: Two mutant genes causing diabetes-obesity syndromes in mice. Diabetologia, 1978, 14: 141-148.

293. Kamohara S, Burcelin R, Halaas JL, Friedman JM and Charron MJ, Acute stimulation of glucose metabolism in mice by leptin treatment. Nature, 1997, 389: 374-377.

294. Rossetti L, Mallillon D, Barzilai N, Vuguin P, Chen W, Hawkins M, Wu J and Wang J, Short term effect of leptin on hepatic gluconeogenesis and in vivo Insulin action. J. Biol. Chem, 1997, 272: 27758-27763,

295. Chehab F, Lim ME and Lu R, Correction of the sterility defect in homozygous obese female mice by treatment with the human recombinant leptin. Nat. Genet, 1996, 12: 318-320.

296. Frödin M and Gammeltoft S. Role and regulation of 90 kDa ribosomal S6 kinase (RSK) in signal transduction. Mol Cell Endocrinol, 1999, 151(1-2): 65-77.

297. Sassone-Corsi P, Mizzen CA and Cheung P, Requirement of Rsk-2 for epidermal growth factor-activated phosphorylation of histone H3. Science, 1999, 285: 886–891.

298. Chen RH, Abate C and Blenis J. Phosphorylation of the c-Fos transrepression domain by mitogen-activated protein kinase and 90-kDa ribosomal S6 kinase. Proc Natl Acad Sci U S A 1993; 90:10952–10956.

299. Xing J, Ginty DD and Greenberg ME. Coupling of the RAS-MAPK pathway to gene activation by RSK2, a growth factor-regulated CREB kinase. Science, 1996, 273:959–963.

300. De Cesare D, Jacquot S, Hanauer A and Sassone-Corsi P. Rsk-2 activity is necessary for epidermal growth factor-induced phosphorylation of CREB protein and transcription of c-fos gene. Proc Natl Acad Sci U S A, 1998, 95: 12202–12207.

301. Merienne K, Pannetier S, Harel-Bellan A and Sassone-Corsi P. Mitogen-regulated RSK2-CBP interaction controls their kinase and acetylase activities. Mol Cell Biol, 2001, 21:7089–7096.

302. Nakajima T, Fukamizu A and Takahashi J, The signal-dependent coactivator CBP is a nuclear target for pp90RSK. Cell, 1996; 86:465–474.

303. Buck M, Poli V, Hunter T and Chojkier M. C/EBPbeta phosphorylation by RSK creates a functional XEXD caspase inhibitory box critical for cell survival. Mol Cell, 2001, 8:807–816.

304. Joel PB, Smith J, Sturgill TW, Fisher TL, Blenis J and Lannigan DA. pp90rsk1 regulates estrogen receptor-mediated transcription through phosphorylation of Ser-167. Mol Cell Biol, 1998, 18:1978–1984.

305. Yang TT, Xiong Q, Graef IA, Crabtree GR and Chow CW. Recruitment of the extracellular signal-regulated kinase/ribosomal S6 kinase signaling pathway to the NFATc4 transcription activation complex. Mol Cell Biol, 2005, 25:907–920.

306. Ghoda L, Lin X and Greene WC. The 90-kDa ribosomal S6 kinase (pp90rsk) phosphorylates the N-terminal regulatory domain of IkappaBalpha and stimulates its degradation in vitro. J Biol Chem, 1997, 272: 21281–21288.

307. Schouten GJ, Vertegaal AC, Whiteside ST, et al. IkappaB alpha is a target for the mitogen-activated 90 kDa ribosomal S6 kinase. EMBO J 1997; 16:3133–3144.

308. Palmer A, Gavin A Cand Nebreda AR, A link between MAP kinase and p34(cdc2)/cyclin B during oocyte maturation: p90(rsk) phosphorylates and inactivates the p34(cdc2) inhibitory kinase Myt1. EMBO J, 1998, 17: 5037–5047.

309. Bonni A, Brunet A, West AE, Datta SR, Takasu MA and Greenberg ME. Cell survival promoted by the Ras-MAPK signaling pathway by transcription-dependent and -independent mechanisms, Science, 1999, 286: 1358–1362.

310. Douville E and Downward J, EGF induced SOS phosphorylation in PC12 cells involves P90 RSK-2. Oncogene, 1997, 15: 373–383.

311. Lin JX, Spolski R and Leonard WJ, Critical role for Rsk2 in T-lymphocyte activation. Blood, 2008, 111(2): 525-33.

312. Trivier E, De Cesare D and Jacquot S, Mutations in the kinase Rsk-2 associated with Coffin-Lowry syndrome. Nature, 1996, 384: 567–570.

313. Coffin R, Phillips JL, Staples WI and Spector S, Treatment of lead encephalopathy in children. J Pediatr, 1966, 69: 198–206.

314. Lowry B, Miller JR, Fraser FC. A new dominant gene mental retardation syndrome: association with small stature, tapering fingers, characteristic facies, and possible hydrocephalus. Am J Dis Child, 1971, 121: 496–500.

315. Satoh T, Takeda R, Oikawa H and Satodate R, Immunohistochemical and structural characteristics of the reticular framework of the white pulp and marginal zone in the human spleen. Anat Rec,1997, ,249(4): 486-94.

316. Brendolan A, Rosado MM, Carsetti R, Selleri L and Dear TN, Development and function of the mammalian spleen Bioessays, 2007, 29(2): 166-77.

317. Banks TA, Rouse BT, Kerley MK, Blair PJ, Godfrey VL, Kuklin NA, Bouley DM, Kanangat TS and Mucenski ML, Lymphotoxin-alpha-deficient mice. Effects on secondary lymphoid organ development and humoral immune responsiveness. J Immunol, 1995, 155(4): 1685–93.

318. Kim J, Kammertoens T, Janke M, Schmetzer O, Qin Z, Berek C and Blankenstein T, Establishment of early lymphoid organ infrastructure in transplanted tumors mediated by local production of lymphotoxin alpha and in the combined absence of functional B and T cells. J Immunol, 2004, 172(7): 4037–47.

319. Gonzalez F, Mackay JL, Browning M, Kosco-Vilbois H and Noelle RJ, The sequential role of lymphotoxin and B cells in the development of splenic follicles. J Exp Med, 1998, 187(7):997–1007.

320. Ngo VN, Cornall RJ and Cyster JG, Splenic T zone development is B cell dependent. J Exp Med, 2001, 194(11): 1649–60.

320. Adcock IM, Transcription factors as activators of gene transcription: AP-1 and NF-kappa B. Monaldi Arch Chest Di1. 1997, 52(2): 178-86.

322. Voraberger G, Schäfer R and Stratowa C, Cloning of the human gene for intercellular adhesion molecule 1 and analysis of its 5'-regulatory region. Induction by cytokines and phorbol ester. J Immunol, 1991, 147(8): 2777-86.

323. Ogasawara A, Arakawa T, Kaneda T, Takuma T, Sato T, Kaneko H, Kumegawa M and Hakeda Y, Fluid shear stress-induced cyclooxygenase-2 expression is mediated by C/EBP beta, cAMP-response element-binding protein, and AP-1 in osteoblastic MC3T3-E1 cells. J Biol Chem, 2001, 276(10): 7048-54.

324 Spencer RP and Pearson HA, The spleen as a hematological organ. Semin. Nucl. Med, 1975, 5: 95-102.

325. Wennberg E and Weiss L, The structure of the spleen and hemolysis. Annu. Rev. Med, 1969, 20: 29-40.

326. Kraal G, Cells in the marginal zone of the spleen. In International Review of Cytology, 1992, 132: 31-74.

327. Delemarre FG, Kors N and van Rooijen N, Elimination of spleen and of lymph node macrophages and its difference in the effect on the immune response to particulate antigens. Immunobiology, 1990, 182: 70-78.

328. Buiting AM, De Rover Z, Kraal G, van Rooijen N, Humoral immune responses against particulate bacterial antigens are dependent on marginal metallophilic macrophages in the spleen. Scand. J. Immunol, 1996, 43: 398-405.

329. Kraal G, Ter Hart H, Meelhuizen C, Venneker G and Claassen E, Marginal zone macrophages and their role in the immune response against T-independent type 2 antigens: modulation of the cells with specific antibody. Eur. J. Immunol, 1989, 19: 675-680.

330. Groeneveld PH, Erich T and Kraal G, The differential effects of bacterial lipopolysaccharide (LPS) on splenic non-lymphoid cells demonstrated by monoclonal antibodies. Immunology, 1986, 58: 285-290.

331. Mueller CG, Cremer I, Paulet PE, Niida S, Maeda N, Lebeque S, Fridman WH and Sautes-Fridman C, Mannose receptor ligand-positive cells express the metalloprotease decysin in the B cell follicle. J. Immunol, 2001, 167: 5052-5060.

332. Kraal G and Janse M, Marginal metallophilic cells of the mouse spleen identified by a monoclonal antibody. Immunology, 1989, 58: 665-669.

333. Braford D, Flint AJ and Tonks NK, Crystal structure of human phosphotase 1B. Science, 1994,253(5152): 1373.

334. Kung C, Pingel JT, Heikinheimo M, Klemola T, Varkila K, Yoo LI, Vuopala K, Poyhonen M, Rogers M, Speck SH, Chatilla TA and TM Matthews, Mutations in the tyrosine phosphatase CD45 gene in a child with severe combined immunodeficiency disease. Nat Med, 2000, 6(3): 343-5.

335. Virts E, Barritt D, Siden E and William RA, Murine mast cells and monocytes express distinctive sets of CD45 isoforms. Immunology, 1997, 34(16-17): 1119-1197.

336. Rodig A, Shahsafaei BLi and Dorfman D, The CD45 isoform B220 identifies select subsets of human B cells and B-cell lymphoproliferative disorders. Human Pathology, 2005, 1: 51-57.

337. Dong C, Wang J, Neame P and Cooper MD, The murine BP-3 gene encodes a relative of the CD38/NAD glycohydrolase family. International Immunology, 9: 1353-1360.

338. McNagny KM, Bucy RP and Cooper MD, Reticular cells in peripheral lymphoid tissues express the phosphatidylinositol-linked BP-3 antigen. Eur J Immunol, 1991, 21(2): 509-15.

339. Balogh P, Aydar Y, Tew JG, Szakal AK, Ontogeny of the follicular dendritic cell phenotype and function in the postnatal murine spleen. Cell Immunol, 2001, 214(1): 45-53.

340. Taylor PR, Pickering MC, Kosco-Vilbois MH, Walport MJ, Botto M, Gordon S and Martinez-Pomares L, The follicular dendritic cell restricted epitope, FDC-M2, is complement C4; localization of immune complexes in mouse tissues. Eur J Immunol, 2002, 32(7): 1888-96.

341. Cariappa A and Pillai S, Antigen-dependent B-cell development. Curr Opin Immunol, 2002, 14: 241-249.

342. Weller S, Reynaud CA and Weill JC. Splenic marginal zone B cells in humans: where do they mutate their Ig receptor? Eur J Immunol, 2005, 35: 2789-2792.

343. Felipe Suarez, Olivier Lortholary, Olivier Hermine, and Marc Lecuit Infection-associated lymphomas derived from marginal zone B cells: a model of antigen-driven lymphoproliferation. Blood, 2006, 8: 3034-3044.

344. Ansel KM, Ngo VN, Hyman PL, Luther SA, Förster R, Sedgwick JD, Browning JL, Lipp M and Cyster JG, A chemokine-driven positive feedback loop organizes lymphoid follicles. Nature, 2000, 406(6793): 309-14.

345. Smith ML, Cavenagh JD, Lister TA and Fitzgibbon J, Mutation of CEBPA in familial acute myeloid leukemia. N Engl J Med, 2004, 351: 2403−2407.

346. Radomska HS, Huettner CS, Zhang P, Cheng T, Scadden DT and Tenen DG, CCAAT/enhancer binding protein alpha is a regulatory switch sufficient for induction of granulocytic development from bipotential myeloid progenitors. Mol Cell Biol, 1998, 18: 4301−4314.

347. Lord A, Abdollahi B, Hoffman-Liebermann L and Liebermann DA, Proto-oncogenes of the fos/jun family of transcription factors are positive regulators of myeloid differentiation. Mol. Cell. Biol, 1993, 841–851.

348. Szabo E, Preis LH and Birrer MJ, Constitutive c-Jun expression induces partial macrophage differentiation in U-937 cells. Cell Growth Differ, 1993, 5: 439–446.

349. Li J, King I and Sartorelli AC, Differentiation of WEHI-3B D+ myelomonocytic leukemia cells induced by ectopic expression of the protooncogene c-Jun, Cell Growth Differ, 1994, 5: 743–751.

350. Xia C, Cheshire JK, Patel H and Woo P, Cross-talk between transcription factors NF-κB and C/EBP in the transcriptional regulation of genes. Int. J. Biochem. Cell Biol, 1997, 29: 1525–1539.

351. Stein PC, Cogswell V and Baldwin AS Jr, Functional and physical association between NF-κB and C/EBP family members: a Rel domain–bZIP interaction, Mol. Cell. Biol, 1993, 13: 3964–3974.

352. Paz-Priel I, Cai DH and Wang D, C/EBPα and C/EBPα myeloid oncoproteins induce Bcl-2 via interaction of their basic regions with NF-κB p50, Mol. Cancer Res, 2005, 3: 585–596.

353. Sha C, Liou HC, Tuomanen EI and Baltimore D, Targeted disruption of the p50 subunit of NF-κB leads to multifocal defects in immune responses, Cell, 1995, 80: 321–330.

354. Chagraoui H, Wendling F and Vainchenker W. Pathogenesis of myelofibrosis with myeloid metaplasia: Insight from mouse models. Best Pract Res Clin Haematol, 2006, 19(3): 399-412.

355. Nurden AT, Phillips DR and George JN, Platelet membrane glycoproteins: historical perspectives. J Thromb Haemost, 2006, 4(1): 3-9.

356. Reilly JT, Pathogenesis of idiopathic myelofibrosis: present status and future directions. Br J Haematol, 1994, 88(1): 1-8.

357. Mesa RA, Barosi G, Cervantes F, Reilly JT and Tefferi A. Myelofibrosis with myeloid metaplasia: disease overview and non-transplant treatment options. Best Pract Res Clin Haematol, 2006, 19(3): 495-517.

358. Cadieux C, Fournier S, Peterson AC, Bédard C, Bedell BJ and Nepveu A, Transgenic Mice Expressing the p75 CCAAT-Displacement Protein/Cut Homeobox Isoform Develop a Myeloproliferative Disease–Like Myeloid Leukemia Cancer Research, 2006, 66: 9492-9501.

359. Kogan SC, Ward JM and Anver MR, Bethesda proposals for classification of nonlymphoid hematopoietic neoplasms in mice. Blood, 2002,100: 238–45.

360. Brown RD, Ambler SK, Mitchell MD and Long CS. The cardiac fibroblast: therapeutic target in myocardial remodeling and failure. Annu Rev Pharmacol Toxicol, 2005, 45: 657-87.

361. Ricci R, Eriksson U, Oudit GY, Eferl R, Akhmedov A, Sumara I, Sumara G, Kassiri Z, David JP, Bakiri L, Sasse B, Idarraga I, Rath M, Kurz D, Theussl HC, Perriard JC, Backx P, Penninger JM and Wagner EF, Distinct functions of junD in cardiac hypertrophy and heart failure. Genes & Development, 2005, 19: 208-213.

362. Bergman MR, Cheng S, Honbo N, Piacentini L, Karliner JS and Lovett DH, A functional activating protein 1 (AP-1) site regulates matrix metalloproteinase 2 (MMP-2) transcription by cardiac cells through interactions with JunB-Fra1 and JunB-FosB heterodimers. Biochem J, 2003, 369(Pt 3): 485-96.

363. Kovacic-Milivojevic B and Gardner DG, Fra-1, a Fos gene family member that activates atrial natriuretic peptide gene transcription. Hypertension, 1995, 25(4 Pt 2): 679-82.

364. Olivetti G, Melissari M, Balbi T, Quaini F, Cigola E, Sonnenblick EH and Anversa P, Myocyte cellular hypertrophy is responsible for ventricular remodelling in the hypertrophied heart of middle aged individuals in the absence of cardiac failure. Cardiovasc Res, 1994, 28(8): 1199-208.

365. Sun Y and Weber KT, Animal models of cardiac fibrosis. Methods Mol Med, 2005, 117: 273-90.

366. Pardo Mindán FJ and Panizo A, Alterations in the extracellular matrix of the myocardium in essential hypertension Eur Heart J, 1993, 14: 12-4.

367. Müller C, The hepatitis alphabet--hepatitis A-G and TTV. Wien Klin Wochenschr, 1999, 111(12): 461-8.

368. Smithson JE and Neuberger JM. Acute liver failure. Overview. Eur J Gastroenterol Hepatol, 1999, 11(9): 943-7.

369. Issa IA and Mourad FH, Hepatitis A: an updated overview. J Med Liban, 2001, 49(2): 61-5.

370. Higuchi H and Gores GJ, Mechanisms of liver injury: an overview. Curr Mol Med, 2003, 3(6): 483-90.

371. Kisseleva T, Brenner DA.Mechanisms of fibrogenesis. Exp Biol Med (Maywood), 2008, 233(2): 109-22.

372. Miller KB, Sepersky RA, Brown KM, Goldberg MJ, Kaplan MM. Genetic abnormalities of immunoregulation in primary biliary cirrhosis. Am J Med, 1983, 75(1): 75-80.

373. Kouroumalis E and Notas G, Pathogenesis of primary biliary cirrhosis: a unifying model. World J Gastroenterol, 2006, 12(15): 2320-7.

374. Shimoda S, Harada K, Niiro H, Yoshizumi T, Soejima Y, Taketomi A, Maehara Y, Tsuneyama K, Nakamura M, Komori A, Migita K, Nakanuma Y, Ishibashi H, Selmi C and Gershwin ME, Biliary epithelial cells and primary biliary cirrhosis: The role of liver-infiltrating mononuclear cells. Hepatology, 2008, 7.

375. Selmi C, Invernizzi P, Zuin M, Podda M, Seldin MF and Gershwin ME, Genes and (auto)immunity in primary biliary cirrhosis. Genes Immun, 2005, 6(7): 543-56.

376. Qureshi K and Abrams GA. Metabolic liver disease of obesity and role of adipose tissue in the pathogenesis of nonalcoholic fatty liver disease. World J Gastroenterol, 2007, 13(26): 3540-53.

377. Kallwitz ER, McLachlan A and Cotler SJ, Role of peroxisome proliferators-activated receptors in the pathogenesis and treatment of nonalcoholic fatty liver disease. World J Gastroenterol, 2008, 14(1): 22-8.

378. Mensink RP, Plat J and Schrauwen P, Diet and nonalcoholic fatty liver disease. Curr Opin Lipidol, 2008, 19(1):25-9.

379. Malnick S, Melzer E, Sokolowski N and Basevitz A, The involvement of the liver in systemic diseases. J Clin Gastroenterol, 2008, 42(1): 69-80.

380. Lee RF, Glenn TK and Lee SS. Cardiac dysfunction in cirrhosis. Best Pract Res Clin Gastroenterol, 2007, 21(1): 125-40.

381. Moreira RK, Hepatic stellate cells and liver fibrosis. Arch Pathol Lab Med, 2007, 131(11): 1728-34.

382. Herrmann J, Gressner AM, Weiskirchen R. Immortal hepatic stellate cell lines: useful tools to study hepatic stellate cell biology and function? J Cell Mol Med, 2007, 11(4): 704-22.

383. Hinz B, Phan SH, Thannickal VJ, Galli A, Bochaton-Piallat ML and Gabbiani G. The myofibroblast: one function, multiple origins. Am J Pathol, 2007, 170(6): 1807-16.

384. Maher JJ, Bissell DM, Friedman S and Roll FJ. Collagen measured in primary cultures of normal rat hepatocytes derives from lipocytes within the monolayer. J Clin Invest, 1988, 82: 450-459.

385. Maher JJ, Zia S and Tzagarakis C. Acetaldehyde-induced stimulation of collagen synthesis and gene expression is dependent on conditions of cell culture: studies with rat lipocytes and fibroblasts. Alcohol Clin Exp Res, 1994, 18: 403-409.

386. Stefanovic B, Hellerbrand C and Holcik M, Posttranscriptional regulation of collagen alpha1(I) mRNA in hepatic stellate cells. Mol Cell Biol, 1997, 17: 5201-5209.

387. Milani S, Herbst H and Schuppan D, Cellular sources of extracellular matrix proteins in normal and fibrotic liver. Studies of gene expression by in situ hybridization. J Hepatol, 1995, 22: 71-76.

388. Ballardini G, Degli Esposti S and Bianchi FB, Correlation between Ito cells and fibrogenesis in an experimental model of hepatic fibrosis. A sequential stereological study. Liver, 1983, 3: 58-63.

389. Knittel T, Kobold D and Piscaglia F, Localization of liver myofibroblasts and hepatic stellate cells in normal and diseased rat livers: distinct roles of (myo-)fibroblast subpopulations in hepatic tissue repair. Histochem Cell Biol, 1999, 112: 387-401.

390. Baroni GS, D'Ambrosio L and Curto P, Interferon gamma decreases hepatic stellate cell activation and extracellular matrix deposition in rat liver fibrosis. Hepatology, 1996, 23: 1189-1199.

391. Bruck R, Genina O and Aeed H, Halofuginone to prevent and treat thioacetamide-induced liver fibrosis in rats. Hepatology, 2001, 33: 379-386.

392. Lieber CS. Prevention and treatment of liver fibrosis based on pathogenesis. Alcohol Clin Exp Res, 1999,23: 944-999.

393. Hautekeete M L and Geerts A, The hepatic stellate (Ito) cell: its role in human liver disease. Virchows Arch, 1997, 430(3): 295-207.

394. Kim Y, Ratziu V, Cho SG, Lalazar A, Theiss G, Dang Q, Kim S J and Friedman S L, Transcriptional activation of transforming growth factor beta1 and its receptors by the Kruppel-like factor Zf9/core promoter-binding protein and Sp1. Potential mechanisms for autocrine fibrogenesis in response to injury. J Biol Chem, 1998, 273(50): 33750-8.

395. Kojima S, Hayashi S, Shimokado K, Suzuki Y, Shimada J, Crippa M P and Friedman S L, Transcriptional activation of urokinase by the Krüppel-like factor Zf9/COPEB activates latent TGF-beta1 in vascular endothelial cells. Blood, 2000, 95: 1309-1316.

396. Buck M, Kim DJ, Houglum K, Hassanein T and Chojkier M, c-Myb modulates transcription of the alpha-smooth muscle actin gene in activated hepatic stellate cells. Am. J. Physiol, 2000, 278: G321-G328.

397. Lang A, Schoonhoven R, Tuvia S, Brenner DA and Rippe RA, Nuclear factor kappaB in proliferation, activation, and apoptosis in rat hepatic stellate cells. J. Hepatol, 2000, 33: 49-58.

398. Hellerbrand C, Jobin C, Licato LL, Sartor RB and Brenner DA, Cytokines induce NF-kappaB in activated but not in quiescent rat hepatic stellate cells. Am. J. Physiol, 1998, 275: G269-G278.

399. Knittel T, Dinter C, Kobold D, Neubauer K, Mehde M, Eichhorst S and Ramadori G, Expression and regulation of cell adhesion molecules by hepatic stellate cells (HSC) of rat liver: involvement of HSC in recruitment of inflammatory cells during hepatic tissue repair.) Am. J. Pathol, 1999, 154: 153-167.

400. Smart DE, Vincent KJ, Arthur MJ, Eickelberg O, Castellazzi M, Mann J and Mann DA, JunD Regulates Transcription of the Tissue Inhibitor of Metalloproteinases-1 and Interleukin-6 Genes in Activated Hepatic Stellate Cells˙ J. Biol. Chem, 2001, 276: 24414-24421.

401. Vincent KJ, Jones E, Arthur MJ, Smart DE, Trim J, Wright MC and Mann DA, Regulation of E-box DNA binding during in vivo and in vitro activation of rat and human hepatic stellate cells. Gut, 2001, 49: 713-71.

402. Neubauer K, Knittel T, Aurisch S, Fellmer P and Ramadori G. Glial fibrillary acidic protein-a cell type specific marker for Ito cells in vivo and in vitro. J. Hepatol, 1996, 24: 719-730.

403. Niki T, Pekny M, Hellemans K, Bleser PD, Berg KV, Vaeyens F, Quartier E, Schuit F and Geerts A, Class VI intermediate filament protein nestin is induced during activation of rat hepatic stellate cells. Hepatology, 1999, 29: 520-527.

404. Cassiman D, van Pelt J, De Vos R, Van Lommel F, Desmet V, Yap SH and Roskams T, Synaptophysin: A novel marker for human and rat hepatic stellate cells. Am. J. Pathol, 1999, 155: 1831-1839.

405. Potter JJ, Womack L, Mezey E and Anania FA, Transdifferentiation of rat hepatic stellate cells results in leptin expression. Biochem. Biophys. Res. Commun, 1998, 244: 178-182.

406. Yamada M, Blaner WS, Soprano DR, Dixon JL, Kjeldbye HM and Goodman DS, Biochemical characteristics of isolated rat liver stellate cells. Hepatology, 1987, 7: 1224-1229.

407. Spiegelman BM and Flier JS, Adipogenesis and obesity: rounding out the big picture. Cell, 1996, 87: 377-389.

408. Miyahara T, Schrum L, Rippe R, Xiong S, Yee HF, Motomura K, Anania FA, Willson TM and Tsukamoto H, Peroxisome Proliferator-activated Receptors and Hepatic Stellate Cell Activation, J. Biol. Chem, 2000, 275: 35715-35722.

409. Galli A, Crabb DW, Ceni E, Salzano R, Mello T, Svegliati-Baroni G, Ridolfi F, Trozzi L, Surrenti C and Casini A, Antidiabetic thiazolidinediones inhibit collagen synthesis and hepatic stellate cell activation in vivo and in vitro. Gastroenterology, 2002, 122: 1924-1940.

410. Marra F, Efsen E, Romanelli R G, Caligiuri A, Pastacaldi S, Batignani G, Bonacchi A, Caporale R, Laffi G, Pinzani M and Gentilini P, Ligands of peroxisome proliferator-activated receptor gamma modulate profibrogenic and proinflammatory actions in hepatic stellate cells. Gastroenterology, 2000, 119: 466-478.

411. Chawla A, Barak Y, Nagy L, Liao D, Tontonoz P and Evans RM, PPAR-gamma dependent and independent effects on macrophage-gene expression in lipid metabolism and inflammation. Nat. Med, 2001, 7: 48-52.

412. Bolkenius U, Glucocorticoids decrease the bioavailability of TGF-beta which leads to a reduced TGF-beta signaling in hepatic stellate cells. Biochem Biophys Res Commun. 2004, 325(4): 1264-70.

413. Wickert L, Abiaka M, Bolkenius U, Gressner AM.Corticosteroids stimulate selectively transforming growth factor (TGF)-beta receptor type III expression in transdifferentiating hepatic stellate cells. J Hepatol. 2004, 40(1): 69-76.

414. Raddatz D, Henneken M, Armbrust T and Ramadori G, Subcellular distribution of glucocorticoid receptor in cultured rat and human liver-derived cells and cell lines: influence of Dexamethasone. Hepatology, 1996, 24(4): 928-33.

415. Imasawa T, Utsunomiya Y, Kawamura T, Zhong Y, Nagasawa R, Okabe M, Maruyama N, Hosoya T and Ohno T, The potential of bone marrow-derived cells to differentiate to glomerular mesangial cells. J Am Soc Nephrol, 2001, 12(7): 1401-9.

416. Ito T, Bone marrow is a reservoir of repopulating mesangial cells during glomerular remodeling. J Am Soc Nephrol 2001, 12: 2625.

417. LaRusso F, Wiesner RH, Ludwig J and MacCarty RL, Primary sclerosing cholangitis. New Engl J Med, 1984, 310: 899–903.

418. Ludwig J, Barham SS, LaRusso F, Elveback LR, Wiesner RH and McCall JT, Morphologic features of chronic hepatitis associated with primary sclerosing cholangitis and chronic ulcerative colitis. Hepatology, 1981, 1: 632–639.

419. Andus T, Bauer J and Gerok W, Effects of cytokines on the liver. Hepatology, 1991, 13: 364–375

420. Pessayre D, Feldmann G, Haouzi D, Fau D, Moreau A and Neuman MG. Hepatocyte apoptosis triggered by natural substances (cytokines and other endogenous molecules and foreign toxins). In: Cameron RG, Fauer G, editors. Apoptosis and its modulation by drugs. Handbook of Experimental Pharmacology. Heidelberg: Springer-Verlag, 1999, 69–108.

421. Neuman MG, Cytokines and inflamed liver. Clin and Investigative Med, 1998, 23: 1–6.

Danksagung

Mein Dank geht an alle, die zum Gelingen dieser Arbeit beigetragen haben.

Für die Hilfe und Unterstützung, die ich im Laufe der Zeit am DRFZ erhalten haben, besonders aber bei Matthias Megges und Anne Reichhardt möchte ich mich ganz recht herzlich bedanken.

Herrn Dr. Jean-Pierre David danke ich im Besonderen für die Überlassung des Themas, sein ständiges Interesse, die interessanten Anregung sowie der hervorragenden fachlichen Betreuung.

Mein besonderer Dank gilt Prof. Michael Amling, Dr. Arndt Schilling, Prof. Roland Lauster, Dr. Rudolf Manz, Prof. Harald Saumweber, Prof. Thomas Börner, Prof. Achim Leutz und Prof. Wolfgang Lockau.

Zuletzt möchte ich mich ganz lieb bei Thordis, Nicole, Luzie, Gudrun, Herbert, Manuela, Petra, Kilian, Tanja, Sören, Martina, Marco, Gordon, Atijeh, Verena, Helmi, Dale, Farah, Claudia, Renate, Steffanie, Gretel, Jörg und Sabine für den Beistand bedanken, sowie bei meinen Eltern.

Danke.

Anhang

Veröffentlichungen/ Full Paper

Driessler F., Sabat R., Asadullah K. and Schottelius A., 2004. Molecular Mechanisms of Interleukin-10-mediated Inhibition of NF-κB Activity: A Role for p50. Clinical Experimental Immunology

Gehaltene Vorträge/ Talks

Driessler F., Sabat R., Asadullah K. and Schottelius A., 2001. A Role for p50 in the Molecular Mechanisms of Interleukin-10 to inhibit NF-κB Activity. 3rd International Workshop on IL-10 and related molecules. Berlin, Germany, April 4th to 7th 2001

Driessler F., Sabat R., Asadullah K. and Schottelius A., 2001. Molecular Mechanisms of Interleukin-10 to regulate the Transcriptionfactor NF-κB. International Symposium. NF-κB: Regulation, Gene Expression and Disease. Gent, Belgium, July 4th to 8th 2001

Driessler F., Sabat R., Asadullah K. and Schottelius A., 2003. Interleukin-10 increases the homodimer p50/p50 to inhibit NF-κB Activity. 30. Jahrestagung der ADF, Frankfurt am Main, Germany, February 27th to March 1th 2003

Driessler F., Megges M., Reichardt A., Schilling A., Amling M and David J.-P., 2008. AP-1 function in mesenchymal cell fate decision: The role of Ribosomal S6 Kinase and Fra1. Osteologie 2008. Hannover, Germany, April 2th to 5th 2008

Poster/ Abstracts

Driessler F., Sabat R., Asadullah K. and Schottelius A., 2001. Molecular Mechanisms of Interleukin-10 to regulate the Transcriptionfactor NF-κB. International Symposium. NF-κB: Regulation, Gene Expression and Disease. Gent, Belgium, July 4th to 8th 2001

Driessler F., Megges M., Reichardt A., Schilling A., Amling M and David J.-P., 2007. AP-1 function in mesenchymal cell fate decision: The role of Ribosomal S6 Kinase and Fra1. 2rd European Summer School of Advanced Immunology. Sardinia, April 16th to 21th 2007

Auszeichnungen/ Scholarship

04/ 07   Fellowship Summer School 2007 (ENII-MUGEN)
                The European Network of Immunology Institutes

Selbständigkeitserklärung

Hiermit versichere ich, dass ich die vorliegende Dissertation selbständig verfasst und keine anderen als die angegebenen Quellen und Hilfsmittel verwendet habe.

Berlin, April 2008   Frank Drießler